

**Cytochrome P450_{cam} (CYP101A1) Mutants to Study
Dehalogenation of Endosulfan: A Persistent Organic
Pollutant, and Oxidation of β -phellandrene:
A Monoterpene**

by
Abdul Rehman

MSc, University of Newcastle upon Tyne, 2010

Thesis Submitted in Partial Fulfillment of the
Requirements for the Degree of
Doctor of Philosophy

in the
Department of Chemistry
Faculty of Science

© Abdul Rehman 2021
SIMON FRASER UNIVERSITY
Summer 2021

Copyright in this work rests with the author. Please ensure that any reproduction or re-use is done in accordance with the relevant national copyright legislation.

Declaration of Committee

Name: Abdul Rehman

Degree: Doctor of Philosophy

Thesis title: Cytochrome P450_{cam} (CYP101A1) Mutants to Study Dehalogenation of Endosulfan: A Persistent Organic Pollutant, and Oxidation of β -phellandrene: A Monoterpene

Committee: **Chair: Corina Andreoiu**
Associate Professor, Chemistry

Erika Plettner
Supervisor
Professor, Chemistry

Andrew J. Bennet
Committee Member
Professor, Chemistry

Peter D. Wilson
Committee Member
Associate Professor, Chemistry

Jeffrey J. Warren
Examiner
Associate Professor, Chemistry

Kirsten Wolthers
External Examiner
Associate Professor, Biochemistry and Molecular Biology, Chemistry
The University of British Columbia

Abstract

Cytochrome P450_{cam} (CYP101A1) from the soil bacterium *Pseudomonas putida* oxidizes camphor regio- and stereoselectively at the 5-position, to give 5-exo-hydroxycamphor. In order to alter the substrate range of P450_{cam}, it has to be mutated. Previously, we have randomly mutated P450_{cam} and selected seven mutants on the bicyclic polychlorinated pollutant endosulfan (ES). Endosulfan is a pesticide and is a persistent organic pollutant (POP). Endosulfan diol (ES diol), which is the major hydrolysis product of endosulfan in the environment, is also persistent in the environment, along with endosulfan itself. Here, we describe the activity of the P450_{cam} mutants towards biodegradation of endosulfan diol. The P450_{cam} mutants convert these substrates to substituted *ortho*-quinones, which we detected using 4-aminoantipyrine (4-AAP) in the assays. Here, we have studied the dehalogenation of endosulfan diol catalyzed by the endosulfan – selected P450_{cam} mutants, using *in vitro* kinetics, chloride release assays and ¹³C labeled endosulfan diol. *ES7* (V247F/D297N/K314E) was found to be the most active mutant, significantly more active than the wild type (WT) towards biodegradation of ES diol. On average ~ 5.2 Cl⁻ ions are released per aromatic product detected upon turnover of ES diol. Based on these findings, we propose a mechanism that begins with the epoxidation of the ES-substrate's double bond on the norbornene system, proceeds with elimination of six chloride ions and loss of the bridge as CO₂, to furnish the *ortho*-quinone.

The monoterpene β-phellandrene is released by certain species of pine when placed under stress. Due to the limited supply of β-phellandrene available from natural sources, here we describe a short synthesis of racemic β-phellandrene from readily available β-pinene. Furthermore, oxidized monoterpenes are known to be released by plants and to function as attractants or repellents of insects, so it is of interest to find ways of selectively oxidizing β-phellandrene. The compound was found to be a substrate for WT-P450_{cam} and the *ES7* mutant. In *in vitro* assays with the cytochrome P450_{cam}, β-phellandrene was hydroxylated.

Keywords: Cytochrome P450_{cam} CYP101A1; endosulfan biodegradation; persistent organic pollutant; β-phellandrene; monoterpene; enzyme kinetics

Dedication

*I dedicate my dissertation work
to my lovely parents
for their love, endless support and encouragement.*

Acknowledgements

I wish to express my deepest gratitude to my senior supervisor Dr. Erika Plettner for her support, advice, guidance, and encouragement in my research without which the goals of this study would not have been realized. I am thankful to her for trusting me and giving enormous opportunities to learn and grow professionally. I truly appreciate the confidence she showed in me.

I extend my gratitude to my supervisory committee, Dr. Peter Wilson and Dr. Andrew Bennet for their support and guidance throughout my research study. I deeply appreciate the time and their effort in the improvement of my work.

I would like to thank Professor Robert Young for allowing me to use LC-MS instrument and Dr. Gang Chen for training me to the LC-MS. I also want to extend my thank you to Colin Zhang and Eric Ye for NMR services, and Fred Chin for technical support. I would also like to acknowledge Nathalie Fournier, Amber Schroeder and Jen Jackson for their continuous assistance.

I am thankful to past graduate student Dr. Brinda Prasad for the training and assistance. I am also thankful to Dr. Mailyn Terrado for thoughtful comments and suggestions during my PhD. I would like to acknowledge Priyadarshini Balaraman for constructing and providing me the plasmid for His₆-tagged proteins. I would like to thank Soniya Dawdani and Govardhana Pinnelli for motivational support to progress in my research work. I express my gratitude to past and present members of Plattner lab: Ashna Aulakh, Dr. Arasakumar Thangaraj, Dr. Jorge Macias, Jurgen Sanes, Nicole Gkaleni, Shaima Kammonah, and Shubha Srivastava for all the help, their support and friendship.

Lastly, I am thankful for the support and love from friends and family members. I am grateful to my parents, Ghulam Rabbani and Murtaza Bibi for their continuous support, love, understanding, and encouragement, which inspired me to keep going and complete my goals. I would like to thank my wife and son for their love, support and understanding especially on my most struggling days, and motivating me to complete my research work.

I would like to acknowledge the financial support from NSERC and Simon Fraser University in the form of teaching assistantship, research assistantship and graduate fellowship.

Table of Contents

Declaration of Committee	ii
Abstract	iii
Dedication	iv
Acknowledgements	v
Table of Contents	vi
List of Tables	x
List of Figures	xi
List of Schemes	xvii
List of Acronyms	xviii
Chapter 1. Introduction	1
1.1. Cytochrome P450	1
1.1.1. Nomenclature of Cytochromes P450	2
1.1.2. Classes of cytochrome P450	3
Class I	4
Class II	5
Class III	8
Class IV	8
Class V	8
Class VI	9
Class VII	9
Class VIII	9
Class IX	10
Class X	10
1.1.3. Type of reactions catalyzed by cytochromes P450	11
Hydroxylation of aliphatic carbon (C–H bond)	11
Alkene epoxidation	12
Arene epoxidation and hydride (H ⁻) shift	13
Dealkylation of heteroatoms	13
Dehydrogenation of saturated alkanes	14
Baeyer-Villiger oxidation	15
Sulfoxidation by P450s	16
Dehalogenation	16
1.1.4. Catalytic cycle of cytochromes P450 and role of redox partners	17
Uncoupling reactions of P450s	21
Artificial shunting to generate Compound-I	22
1.1.5. Oxidation of (+)-D-camphor by cytochrome P450 _{cam} : regio- and stereoselectivity	22
Cytochrome P450 _{cam} structure	23
(+)-D-Camphor oxidation by cytochrome P450 _{cam}	30
1.1.6. Engineered P450 _{cam} and range of substrates	32

P450 _{cam} mutations and substrate selectivity	33
1.1.7. Method of enzyme mutations – Random or Targeted Approach	37
Site-directed mutagenesis.....	37
Random mutagenesis	37
1.2. Endosulfan: a polychlorinated persistent organic pollutant.....	38
1.2.1. Endosulfan and its use	39
1.2.2. Endosulfan toxicity.....	40
1.2.3. Endosulfan: a persistent organic pollutant (POP).....	40
1.2.4. Degradation of endosulfan in nature and known metabolites	41
1.3. β -Phellandrene: a monoterpene	43
1.3.1. Terpenes and type of terpenes	43
1.3.2. β -Phellandrene and trees under attack by bark beetles	46
1.3.3. Oxidized monoterpenes.....	47
1.4. Objectives of my thesis.....	49
1.5. Thesis layout	50
Chapter 2. Materials and methods	51
2.1. Endosulfan diol biodegradation.....	52
2.1.1. Synthesis of substrates and standards	52
Preparation of endosulfan lactone (ES lactone, 15).....	52
Synthesis of endosulfan diol (ES diol, 14)	53
Synthesis of ¹³ C labeled ES diol.....	53
Synthesis of 5,6-dimethoxy-2-benzofuran-1(3H)-one (23).....	54
Synthesis of 5,6-dihydroxy-2-benzofuran-1(3H)-one (24).....	55
Preparation of the 4-aminoantipyrine (4-AAP) adduct of compound (25).....	55
2.1.2. Molecular biology methods	56
Transformation of P450 _{cam} mutants into an E. coli strain that co-expresses putidaredoxin (PdX) and putidaredoxin reductase (PdR).....	56
Expression of P450 _{cam} mutants and WT in E. coli with PdR and PdX and production of lysates.....	56
Site-directed mutations of WT P450 _{cam} for His ₆ – tagged P450 _{cam} mutant protein expression	57
WT P450 _{cam} and P450 _{cam} mutants (His ₆ tagged) protein expression and purification	58
2.1.3. Assays and spectroscopy of P450 enzymes.....	59
Analysis of protein samples for P450 concentration	59
Steady-state kinetic assays for endosulfan diol (ES diol 14) with the crude lysates of P450 _{cam} mutant(s) using 4-aminoantipyrine (4-AAP) coupled assay with horseradish peroxidase (HRP) and H ₂ O ₂	59
Titration of endosulfan diol (ES diol, 14) and (+)-camphor (10) with the purified P450 _{cam} mutant(s) and dissociation constant (K _d).....	60
Chloride release from endosulfan diol with a NADH regeneration system and chloride release detection by chloride electrode.....	60
Chloride release from endosulfan diol with m-CPBA as a shunt and chloride release detection by a chloride selective electrode	61

Extraction and identification of products; assays with ¹³ C labeled substrate (¹³ C-ES diol)	61
2.1.4. <i>In silico</i> docking studies	62
2.2. β-phellandrene oxidation.....	64
2.2.1. Synthesis of racemic β-phellandrene (22).....	64
Synthesis of (+)-nopinone (27) from (-)-β-pinene (21)	64
Synthesis of racemic cryptone (28) from (+)-nopinone (27)	65
Synthesis of β-phellandrene (22) from cryptone (28).....	66
2.2.2. Enzymatic Assays	66
WT P450 _{cam} and ES7 mutant (His ₆ tagged) protein expression and purification	66
Titration of β-phellandrene with the purified WT P450 _{cam} or ES7 mutant, and dissociation constant (K _d).....	67
In-vitro assays of β-phellandrene oxidation using WT or ES7 P450 _{cam} with m-CPBA as a shunt	67
2.2.3. <i>In silico</i> docking studies	68
Chapter 3. Endosulfan diol degradation by P450_{cam} mutants.....	69
3.1. Results	69
3.1.1. Mutants obtained.....	69
3.1.2. Coupled assay optimization	69
3.1.3. Initial screen with crude lysates	71
3.1.4. His ₆ -tagged P450s: stability and kinetics	74
3.1.5. Steady-state kinetic assay using redox partners vs. using only <i>m</i> -CPBA (shunt) 75	75
3.1.6. Ligand binding and dissociation constant (K _d) using selected purified mutants and WT-P450 _{cam}	76
3.1.7. Chloride release with purified WT-P450 _{cam} and <i>ES7</i> mutants.....	78
3.1.8. Isolation of products using purified WT-P450 _{cam} and <i>ES7</i> mutant.....	79
3.1.9. Results from product isolation and ¹³ C NMR study	80
3.1.10. <i>In-silico</i> docking studies	81
ES1 mutant and ES diol (14).....	88
ES2 mutant and ES diol (14).....	90
ES3 mutant and ES diol (14).....	92
ES4 mutant and ES diol (14).....	94
ES5 mutant and ES diol (14).....	96
ES6 mutant and ES diol (14).....	98
ES7 mutant and ES diol (14).....	100
IND1 mutant and ES diol (14)	102
K314E mutant and ES diol (14).....	104
WT-P450 _{cam} and ES diol (14)	106
3.2. Discussion.....	108
3.2.1. Proposed mechanism of dehalogenation.....	108
3.2.2. Effects of mutation in ES variants of P450 _{cam}	110
3.3. Conclusion.....	114

Chapter 4. Oxidation of β-phellandrene by WT-P450_{cam} and ES7 mutant.....	116
4.1. Results	116
4.1.1. Synthesis of β -phellandrene	116
Oxidation of β -pinene to synthesize (+)-nopinone (27)	116
Ring opening of (+)-nopinone using AlCl ₃ to give (\pm)-cryptone (28)	117
Wittig reaction of (\pm)-cryptone (28) to give (\pm)- β -phellandrene (22)	118
4.1.2. Enzymatic assays.....	118
Ligand binding and dissociation constant (K _d) using purified WT-P450 _{cam} and the ES7 mutant	118
In-vitro assay of β -phellandrene oxidation using WT P450 _{cam} with <i>m</i> -CPBA as a shunt.....	120
In-vitro assay of β -phellandrene oxidation using ES7 P450 _{cam} mutant with <i>m</i> -CPBA as a shunt	122
Fragmentation pattern in mass spectrum and expected oxidation products of β -phellandrene	125
4.1.3. <i>In-silico</i> docking studies using MOE	131
4.2. Discussion	137
4.2.1. Short synthesis racemic β -phellandrene	137
4.2.2. Oxidation of β -phellandrene (22) by WT-P450 _{cam} and ES7 mutant using <i>m</i> -CPBA as a shunt	138
4.3. Conclusion.....	141
Chapter 5. Future work	143
5.1. Endosulfan and related substrates	143
5.2. Oxidation of β -phellandrene by P450 _{cam}	144
References.....	146
Appendix A. Chapter 3 supplementary information	183
Appendix B. Chapter 4 supplementary information	207
Oxidation of β -pinene to nopinone using KMnO ₄	207

List of Tables

Table 1.1	Hydroxylation of aliphatic carbon (C–H bond)	12
Table 1.2	Epoxidation of carbon-carbon π bonds (C=C bond)	13
Table 1.3	Demethylation and dehydrogenation reaction catalyzed by P450s.....	14
Table 1.4	Baeyer-Villiger oxidation, sulfoxidation and dehalogenation by P450s ...	16
Table 1.5	Amino acid residues and their effect on P450 _{cam} catalytic activity.....	29
Table 1.6	Selected P450 _{cam} mutants with modified aromatic compounds as substrates	35
Table 1.7	Selected P450 _{cam} mutants with modified alkanes and terpenes as substrates	36
Table 1.8	Selected P450 _{cam} mutants with modified chlorinated compounds as substrates	37
Table 1.9	Examples of oxidized monoterpenes and non-terpene compounds, and their significance	48
Table 3.1	Mutations of P450 _{cam} discovered previously by selection of a SeSaM library on minimal media containing endosulfan (13) and <i>m</i> -CPBA	69
Table 3.2	Kinetic data of ES diol (14) with WT-P450 _{cam} and mutants (using crude lysate)	72
Table 3.3	Kinetic data of ES diol (14) with purified WT-P450 _{cam} and mutants.....	75
Table 3.4	Dissociation constant measured using Camphor (10) and ES diol (14) with purified WT P450 _{cam} and mutants	76
Table 3.5	Ratio of chloride released to quinone (4-AAP coupled) formed in assay with <i>m</i> -CPBA as shunt	79
Table 3.6	Metabolites detected from <i>ES7</i> using ES diol (14).....	80
Table 4.1	Synthesis of (+)-Nopinone (27) using different oxidizing agents/conditions	117
Table 4.2	Ring opening of nopinone (27) and product ratio over time	118
Table 4.3	Dissociation constant measured using β -phellandrene (22) with purified WT P450 _{cam} and <i>ES7</i> mutant	120
Table 4.4	Syntheses of cryptone (28) reported previously	138
Table 4.5	Example of monoterpene oxidation catalyzed by WT-P450 _{cam}	140

List of Figures

Figure 1.1	Type- <i>b</i> heme (protoporphyrin IX) showing iron atom (Fe ^{III}) coordinated to thiolate of cysteine residue in P450s.	2
Figure 1.2	Schematic outline of different P450 systems. (Ia) Class I, bacterial system; (Ib) class I, mitochondrial system; (II) class II microsomal system; (III) class III, bacterial system (example P450 _{cin} , CYP176A1); (IV) class IV, bacterial thermophilic system; (V) class V, bacterial [Fdx]–[P450] fusion system; (VI) class VI, bacterial [Fldx]–[P450] fusion system; (VII) class VII, bacterial [PFOR]–[P450] fusion system; (VIII) class VIII, bacterial [CPR]–[P450] fusion system; (IX) class IX, soluble eukaryotic (P450 _{nor}); (X) independent eukaryotic system (example P450TxA).....	7
Figure 1.3	Schematic representation of the catalytic cycle cytochrome P450. Species 1 – 9 are parts of the catalytic cycle. Substrate is represented here as RH, the bold horizontal lines on either side of Fe represent the porphyrin moiety and electrons (e ⁻) are supplied from the redox partner PdX. Path “d” shows direct formation of high-valent compound I (Cpd-I) by oxidant such as <i>m</i> -CPBA. Path “a”, “b” and “c” show uncoupling reactions, wherein superoxide (a), hydrogen peroxide (b) or water are released and the substrate is not oxidized.....	19
Figure 1.4	Electron transfer from NADH to P450 _{cam} via putidaredoxin reductase (PdR) and putidaredoxin (PdX); a class I cytochrome P450 system.	20
Figure 1.5	The possible mechanism of epoxidation by Compound-0 (A) and Compound-I (B) of P450.	21
Figure 1.6	The possible mechanism of formation of Compound-0 (when R=H) and compound-1 by cleavage of O–O bond using peroxy acid or peroxide. ...	22
Figure 1.7	Structure of camphor-bound CYP101A1 (PDB entry 3L63, (Lee et al., 2010)). Secondary structures are labeled as described by Pochapsky (Pochapsky & Pochapsky, 2019). Heme is shown as sticks (green) and substrate <i>d</i> -camphor in grey. (A) Top view (distal), (B) side view of P450 _{cam}	24
Figure 1.8	Amino acid sequence of cytochrome P450 _{cam} with different helices (A – L) shown in different colors (Pochapsky et al., 2003). C357 shown in blue at the N-terminus of Helix L.	25
Figure 1.9	H-bonding by D251 and T251 (in helix-I, backbone ribbon is shown in yellow color) through a water network and Heme–Fe–O ₂ complex in P450 _{cam} (proposed H-bonds are shown as yellow dotted lines). Camphor is shown in grey color, heme in green color and Y96 in cyan color (PDB 2A1M, (Nagano & Poulos, 2005)).	27
Figure 1.10	Superimposed structures of the open (PDB entry 3L62 cyan color) and the closed (PDB entry 3L63, yellow color) forms of P450 _{cam} , camphor in color red (Lee et al., 2010).	28
Figure 1.11	Oxidation of camphor by P450 _{cam} : formation of 5- <i>exo</i> -hydroxycamphor (11) and 5-ketocamphor (12).....	30

Figure 1.12	The hydrogen bonding between camphor (grey in color) and Tyrosine-96 (Y96, shown in green color) present in Helix B' (proposed H-bonds are shown as yellow dotted lines). (PDB 3L63, (Lee et al., 2010)).....	31
Figure 1.13	Amino acid residues around camphor in the binding pocket of P450 _{cam} . Y96 makes an H-bond with the carbonyl group of camphor (PDB 3L63, visualized using Molecular Operating Environment-MOE). Residues shown in purple are polar while residues in green are nonpolar. Residues and ligand atoms with light blue clouds are exposed to the solvent environment.	32
Figure 1.14	"Side-on" view of the cytochrome P450 _{cam} active site. Residues in Tier 1, shown in yellow, are positioned near the heme (T101, L244, G248, V295, and D297). Tier 2, shaded light gray, form the upper region of the binding pocket (F87, Y96, V247, I395, and V396), and Tier 3, shown in green, form the top region of the binding pocket (M184, and T185) (Bell et al., 2003; Loida & Sligar, 1993). Camphor is shown in light blue and heme is shown in green. (PDB 3L63).	34
Figure 1.15	Endosulfan and other selected chlorinated compounds	39
Figure 1.16	Structures of the endosulfan (ES) diastereoisomers, known as α – endosulfan and β – endosulfan.....	40
Figure 1.17	Known endosulfan metabolites found in the environment. (Note that they all have the hexachloronorborene moiety intact).	42
Figure 1.18	Building blocks of terpenes: isoprene, isopentenyl and dimethylallyl pyrophosphate.	44
Figure 1.19	Examples of terpenes: (A) monoterpenes, (B) other terpenes: sesquiterpene, diterpene, sesterterpene, triterpene and tetraterpenes...	45
Figure 1.20	β -phellandrene enantiomers, and other monoterpenes.	47
Figure 1.21	Examples of monoterpenes used in flavors, fragrances or medicines. ...	49
Figure 2.1	List of endosulfan and metabolites used as ligands for <i>in silico</i> docking studies.	63
Figure 2.2	Carbon number assigned to endosulfan ligands used to calculate the distance to the heme-iron in MOE docking studies.....	64
Figure 2.3	Enantiomers of β -phellandrene used as ligands in MOE docking studies.	68
Figure 2.4	Carbon number assigned to ligands (β -phellandrene) used to calculate the distance to the heme-iron in MOE docking studies.	68
Figure 3.1	Degradation of ES diol (14) by P450 _{cam} mutants and detection of the metabolites in a coupled assay with 4-aminoantipyrine (4-AAP, 26), a system used to detect quinones.	70
Figure 3.2	<i>ES7</i> and ES diol (14) assay optimization (A) net absorbance at 506 nm using α -ES (13) and ES diol (14) during 5 days assay, (B) net absorbance at 506 nm using α -ES (13) and ES diol (14) after 5 days assay, (C) total absorbance at different concentrations of ES diol (14) using <i>ES7</i> in the coupled assay, (D) total absorbance with <i>ES7</i> and using different concentrations of ES diol (14).	71

Figure 3.3	Allosteric sigmoidal kinetics of ES diol (14) with WT-P450 _{cam} and mutants (using crude lysate).	73
Figure 3.4	Steady state kinetic assays of <i>ES7</i> using ES diol (14). (A) using redox partners (PdX and PdR) and NADH, and (B) using <i>m</i> -CPBA as a shunt.	75
Figure 3.5	Titration of wild-type (WT) P450 _{cam} (top) and mutant <i>ES7</i> (bottom) with camphor (10) (left set of graphs) or ES diol (14) (right set of graphs). The spectra (top set of graphs for each enzyme) show the blue shift in the Soret band as substrate is titrated into the enzyme preparation. The isotherms (lower set of graphs for each enzyme) depict the change in the Soret band (the increase in absorption at the blue-shifted wavelength relative to the decrease in absorption of the original Soret band).	77
Figure 3.6	Chloride release using ES diol (14) and <i>m</i> -CPBA, with WT-P450 _{cam} (ES diol 14, 300 μ M), <i>ES7</i> (¹³ C-ES diol 14, 300 μ M), <i>ES7</i> (ES diol 14, 300 μ M) and No P450 _{cam} control.	78
Figure 3.7	¹³ C NMR spectra. Blue: spectrum of dihydroxy phthalide (5,6-dihydroxy-2-benzofuran-1(3H)-one, 24). Comparison of extracts from assays with ¹³ C-ES diol (green) and ES diol (14) (brown) with <i>ES7</i> (using <i>m</i> -CPBA).....	81
Figure 3.8	Schematic representation of orientation of ES diol (14) found in <i>in silico</i> docking studies using MOE. (A) C1 and C2 are closer to heme-Fe, (B) C3 and C4 are closer to heme-Fe (The heme-Fe is represented as “-Fe”).	82
Figure 3.9	Average distances of C1, C2, C3 and C4 from heme-Fe in WT-P450 _{cam} , K314E, <i>ES1-7</i> and <i>IND1</i> mutants. (A) α -ES (13A), (B) β -ES (13B), (C) ES diol (14), (D) ES lactone (15A), (E) ES lactone (15B), (F) ES ether (16), (G) ES sulfate (20), and (H) carbon numbers assigned to endosulfan bicyclic core for the purpose of this discussion.	83
Figure 3.10	Selected poses of ES diol (14) positioned above the heme in the active sites of WT-P450 _{cam} and mutants (selected based on Equation 3.1).	84
Figure 3.11	Comparison of the calculated “ <i>x</i> ”-value with kinetic data of WT-P450 _{cam} and mutants (crude lysate). (A) k_{cat} vs. “ <i>x</i> ”-value, (B) K_M vs. “ <i>x</i> ”-value, (C) k_{cat}/K_M vs. “ <i>x</i> ”-value.	86
Figure 3.12	Different substrates and calculated “ <i>x</i> ”-values from the selected poses in WT-P450 _{cam} and mutants in MOE docking (see Figure 2.1 for list of substrates).	87
Figure 3.13	The <i>in silico</i> molecular docking results of <i>ES1</i> (T56A/N116H/D297N) and ES diol (14). (A) P450 is shown in cyan color, heme in yellow color, mutations are shown in green colored spheres, and ES diol in pink color. (B) Orientation of ES diol (14) in active site (proposed H-bonds are shown as yellow dotted lines).	89
Figure 3.14	The <i>in silico</i> molecular docking results of <i>ES2</i> (F292S/A296V/K314E/P321T) and ES diol (14). (A) P450 is shown in cyan color, heme in yellow color, mutations are shown in red colored spheres, and ES diol in pink color. (B) Orientation of ES diol (14) in active site (proposed H-bonds are shown as yellow dotted lines).	91
Figure 3.15	The <i>in silico</i> molecular docking results of <i>ES3</i> (Q108R/R290Q/I318N) and ES diol (14). (A) P450 is shown in cyan color, heme in yellow color, mutations are shown in blue colored spheres, and ES diol in pink color.	

	(B) Orientation of ES diol (14) in active site (proposed H-bonds are shown as yellow dotted lines).....	93
Figure 3.16	The <i>in silico</i> molecular docking results of ES4 (S221R/I281N) and ES diol (14). (A) P450 is shown in cyan color, heme in yellow color, mutations are shown in yellow colored spheres, and ES diol in pink color. (B) Orientation of ES diol (14) in active site (proposed H-bonds are shown as yellow dotted lines).....	95
Figure 3.17	The <i>in silico</i> molecular docking results of ES5 (A296P) and ES diol (14). (A) P450 is shown in cyan color, heme in yellow color, mutation is shown in magenta colored spheres, and ES diol in pink color. (B) Orientation of ES diol (14) in active site (proposed H-bonds are shown as yellow dotted lines).	97
Figure 3.18	The <i>in silico</i> molecular docking results of ES6 (G120S) and ES diol (14). (A) P450 is shown in cyan color, heme in yellow color, mutation is shown in magenta colored spheres, and ES diol in pink color. (B) Orientation of ES diol (14) in active site (proposed H-bonds are shown as yellow dotted lines).	99
Figure 3.19	The <i>in silico</i> molecular docking results of ES7 (V247F/D297N/K314E) and ES diol (14). (A) P450 is shown in cyan color, heme in yellow color, mutations are shown in white colored spheres, and ES diol in pink color. (B) Orientation of ES diol (14) in active site (proposed H-bonds are shown as yellow dotted lines).	101
Figure 3.20	The <i>in silico</i> molecular docking results of IND1 (E156G/V247F/V253G/F256S) and ES diol (14). (A) P450 is shown in cyan color, heme in yellow color, mutations are shown in wheat colored spheres, and ES diol in pink color. (B) Orientation of ES diol (14) in active site (proposed H-bonds are shown as yellow dotted lines).	103
Figure 3.21	The <i>in silico</i> molecular docking results of K314E and ES diol (14). (A) P450 is shown in cyan color, heme in yellow color, mutation is shown in light blue colored spheres, and ES diol in pink color. (B) Orientation of ES diol (14) in active site (proposed H-bonds are shown as yellow dotted lines).	105
Figure 3.22	The <i>in silico</i> molecular docking results of WT-P450 _{cam} and ES diol (14). (A) P450 is shown in cyan color, heme is in yellow color, and ES diol in pink color. (B) Orientation of ES diol (14) in active site (proposed H-bonds are shown as yellow dotted lines).....	107
Figure 3.23	Proposed mechanism of degradation of ES diol (14) by P450 _{cam} mutants, such as ES7. The proposed route accounts for the loss of 6 Cl ⁻ ions from the ES diol core structure and of the bridge as CO ₂	108
Figure 3.24	Superimposed structures of WT-P450 _{cam} and mutants (ES diol is not shown). P450 is shown in light blue color, heme in yellow color, and mutated residues are identified with the residue number. Residues are colored: ES1 in green, ES2 in blue, ES3 in magenta, ES4 in yellow, ES5 in orange, ES6 in wheat, ES7 in purple blue, IND1 in light green, K314E in pink and WT in red.	112
Figure 4.1	Ring opening of (+)-nopinone (27) to cryptone (28) catalyzed by Lewis acid (AlCl ₃).	117

Figure 4.2	<p>Titration of wild-type (WT) (left set of graphs) P450_{cam} and mutant <i>ES7</i> (right set of graphs) with β-phellandrene (22). The spectra (top set of graphs for each enzyme) show the blue shift in the Soret band as substrate is titrated into the enzyme preparation. The isotherms (lower set of graphs for each enzyme) depict the change in the Soret band (the increase in absorption at the blue-shifted wavelength relative to the decrease in absorption of the original Soret band). 119</p>
Figure 4.3	<p>GC-MS analysis of extracts from the <i>in-vitro</i> assay using WT-P450_{cam}, <i>m</i>-CPBA and β-phellandrene. (A) Gas chromatograms: Control – no P450_{cam} using <i>m</i>-CPBA and β-phellandrene only, control – no substrate using WT-P450_{cam} and <i>m</i>-CPBA only, and treatment experiments using WT-P450_{cam}, <i>m</i>-CPBA and β-phellandrene. Peaks belonging to epoxidized products with retention times 10.5, 10.5, 10.8 and 11.0 min are represented by a 'star'. (B) Mass spectrum of the new peak at 9.3 minutes from treatment-A using WT-P450_{cam}. 121</p>
Figure 4.4	<p>Area of the peaks at different retention time from <i>in-vitro</i> assay of β-phellandrene oxidation using WT-P450_{cam} and <i>m</i>-CPBA. 122</p>
Figure 4.5	<p>GC-MS analysis of extracts from the <i>in-vitro</i> assay using <i>ES7</i>-P450_{cam}, <i>m</i>-CPBA and β-phellandrene. (A) Gas chromatograms: Control – no P450_{cam} using <i>m</i>-CPBA and β-phellandrene only, control – no substrate using <i>ES7</i>-P450_{cam} and <i>m</i>-CPBA only, and treatment experiments using <i>ES7</i>-P450_{cam}, <i>m</i>-CPBA and β-phellandrene. Peaks belonging to epoxidized products with retention time 10.5, 10.5, 10.8 and 11.0 min are represented by a 'star'. (B) Mass spectrum of new peak at 9.3 minutes from treatment-A using <i>ES7</i>-P450_{cam}. 123</p>
Figure 4.6	<p>Area of the peaks at different retention time from <i>in-vitro</i> assay of β-phellandrene oxidation using <i>ES7</i>-P450_{cam} and <i>m</i>-CPBA. 124</p>
Figure 4.7	<p>Comparing the catalytic activity: peak areas of the peak (152 <i>m/z</i>, with retention time at 9.3 minutes) from the <i>in-vitro</i> assay of β-phellandrene oxidation using WT-P450_{cam} and <i>ES7</i> mutants. 125</p>
Figure 4.8	<p>Possible oxidized products of β-phellandrene catalyzed by P450_{cam}. ... 126</p>
Figure 4.9	<p>Analysis of mass spectrum of β-phellandrene (22): (A) mass spectrum (electron impact (EI) ionization), (B) possible fragmentations of β-phellandrene (22) from EI. 127</p>
Figure 4.10	<p>Mass spectrum of the peak (retention time 9.3 minutes) of oxidized β-phellandrene product and fragmented ion peaks. 128</p>
Figure 4.11	<p>Expected fragmentation of β-phellandrene oxidized product 38 in mass spectrum (EI). 129</p>
Figure 4.12	<p>Expected fragmentation of β-phellandrene oxidized product 39 in mass spectrum (EI). 130</p>
Figure 4.13	<p>Expected fragmentation of β-phellandrene oxidized product 40 in mass spectrum (EI). 131</p>
Figure 4.14	<p>Selected poses of (-)-<i>R</i>-β-phellandrene (22a, left side, shown in magenta) and (+)-<i>S</i>-β-phellandrene (22b, right side, shown in orange) positioned above the heme (shown in yellow color) in the active sites of the <i>ES7</i> mutant and WT-P450_{cam}. 132</p>

Figure 4.15	<i>In-silico</i> docking studies, (A) carbon numbers assigned to β -phellandrene (22), and (B) minimum distances of C4, C5 and C6 from heme-Fe in WT-P450 _{cam} (left), and in the ES7 mutant (right) in selected poses. 133
Figure 4.16	Enantiomers of β -phellandrene (22) with prochiral CH ₂ groups shown. 134
Figure 4.17	The <i>in silico</i> molecular docking results of ES7 (V247F/D297N/K314E) and superimposed poses of (-)- <i>R</i> - β -phellandrene (22a, shown in green) and (+)- <i>S</i> - β -phellandrene (22b, shown in orange): (A) P450 is shown in cyan, heme in yellow, mutations are shown in white colored spheres, (B) Orientation of (-)- <i>R</i> - β -phellandrene (22a, shown in green, H _R on prochiral C4 indicated by (*)) and (+)- <i>S</i> - β -phellandrene (22b, shown in orange, H _R on prochiral C4 indicated by (**)) in the active site. 135
Figure 4.18	The <i>in silico</i> molecular docking results of WT-P450 _{cam} and superimposed poses of (-)- <i>R</i> - β -phellandrene (22a, shown in green) and (+)- <i>S</i> - β -phellandrene (22b, shown in orange): (A) P450 is shown in cyan, heme in yellow, (B) Orientation of (-)- <i>R</i> - β -phellandrene (22a, shown in green, H _R on prochiral C4 indicated by (*)) and (+)- <i>S</i> - β -phellandrene (22b, shown in orange, H _R on prochiral C4 indicated by (**)) in the active-site (residues shown in white sticks were found to be mutated in ES7 mutant). 136
Figure 5.1	Endosulfan (ES, 13) and other related polychlorinated organic compounds. 144

List of Schemes

Scheme 1.1	Oxidation of non-activated C-H bond by cytochrome P450	1
Scheme 4.1	Synthesis of β -phellandrene from β -pinene.....	116

List of Acronyms

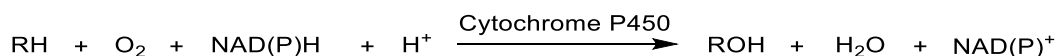
4-AAP	4-Aminoantipyrine
Cpd I	Compound I
Cpd II	Compound II
CPR	Cytochrome P450 reductase
DDT	Dichlorodiphenyltrichloroethane
DMSO	Dimethyl sulfoxide
<i>E. coli</i>	<i>Escherichia coli</i>
EDTA	Ethylenediaminetetraacetic acid
EI	Electron impact
ES	Endosulfan
EtOAc	Ethyl acetate
FAD	Flavin adenine dinucleotide
Fld	FMN-containing flavodoxin
FMN	Flavin mononucleotide
GC-MS	Gas chromatography – mass spectrometry
HCH	Hexachlorocyclohexane
HPLC	High performance liquid chromatography
HRP	Horseradish peroxidase
IPTG	Isopropyl β -D-1-thiogalactopyranoside
LB media	Lauria Bertani media
<i>m</i> -CPBA	<i>meta</i> -chloroperbenzoic acid
MOE	Molecular operating environment
MWCO	Molecular weight cut-off
NAD ⁺	Nicotinamide adenine dinucleotide (oxidized)
NADH	Nicotinamide adenine dinucleotide (reduced)
NMR	Nuclear magnetic resonance
OFOR	2-oxoacid ferredoxin oxidoreductase
<i>P. putida</i>	<i>Pseudomonas putida</i>
Page	Polyacrylamide gel electrophoresis
PDB	Protein data bank
PdR	Putidaredoxin reductase
PdX	Putidaredoxin

PFOR	Phthalate-family oxygenase reductase
PMSF	Phenylmethylsulfonyl fluoride
POP	Persistent organic pollutant
ppm	Parts per million
RPM	Rounds per minute
SDS	Sodium dodecyl sulphate
SeSaM	Sequence saturated mutagenesis
TLC	Thin Layer Chromatography
WT	Wild-type

Chapter 1. Introduction

1.1. Cytochrome P450

Cytochromes P450 (P450s, CYPs) are a family of heme containing enzymes which catalyze a variety of oxidative reactions against wide range of substrates (Cryle & Voss, 2006; Guengerich, 2001; Lee et al., 2013; Meyer et al., 2014; Roberts & Jones, 2010; Sono et al., 1996). These enzymes are called monooxygenases as they activate molecular oxygen, incorporate one oxygen atom into an organic substrate, while they use the other oxygen atom for the production of a water molecule (Denisov et al., 2005). During the catalytic activity of P450s, the electrons are transferred via a NAD(P)H (nicotinamide adenine dinucleotide) – driven redox partner system (Girvan & Munro, 2016). The most remarkable reaction catalyzed by cytochromes P450, is the activation of a C-H bond resulting in hydroxylation of the substrate molecule (Scheme 1.1).



Scheme 1.1 Oxidation of non-activated C-H bond by cytochrome P450

The iron of heme (type-*b* heme or protoporphyrin IX, Figure 1.1) present in the active site, is coordinated to the thiolate of a conserved cysteine residue in P450s (Hannemann et al., 2007). The terminology “cytochrome P450” is derived from the characteristic spectral properties associated with this thiolate axial ligand, displaying typical absorption spectra at 450 nm when the reduced form of this type-*b* heme (Fe^{+2}) is bound to carbon monoxide (CO): cytochrome stands for hemeprotein, P for pigment and 450 reflects the 450 nm absorption of the reduced CO complex (Klingenberg, 1958; Omura & Sato, 1962, 1964). The initial experimental evidence related to cytochromes P450 was reported in 1950s using liver microsomal systems to oxidize xenobiotic compounds (Axelrod, 1955; Brodie et al., 1955). Since then, cytochromes P450 have been found in genomes across biological kingdoms (Nelson, 2018; Sigel et al., 2007). In humans, cytochromes P450 play important roles in metabolism of endogenous and xenobiotic compounds (such as drugs) (Pikuleva, 2006; Rendic & Guengerich, 2015; Zanger & Schwab, 2013). In plants, their role is crucial in synthesizing natural compounds

for the plant's defense mechanism (Irmisch et al., 2014; Keeling & Bohlmann, 2006; Neilson et al., 2013; Shang & Huang, 2020). In bacteria, cytochromes P450 play significant roles in the degradation of organic compounds, to use them as a carbon source (Grogan et al., 1993; Meharena et al., 2008) and in the production of antibiotic and antifungal compounds (Beilen et al., 2005; Fjærvik & Zotchev, 2005).

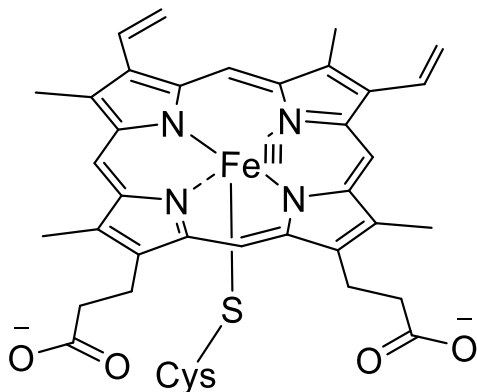


Figure 1.1 Type-*b* heme (protoporphyrin IX) showing iron atom (Fe^{III}) coordinated to thiolate of cysteine residue in P450s.

1.1.1. Nomenclature of Cytochromes P450

Cytochromes P450 are found throughout nature, catalyzing diverse types of reactions such as hydroxylation (Benveniste et al., 1982; Gelb, Heimbrook, et al., 1982; Girhard et al., 2010; Groves et al., 1978; Maier et al., 2001), epoxidation (Chiu et al., 2019; Gelb et al., 1982; Hagmann & Grisebach, 1984; Jin et al., 2003; Lin et al., 2014; Ruettinger & Fulco, 1981; Sauveplane et al., 2009), O-, and N-dealkylations (Lee et al., 2013; Meyer et al., 2014; Roberts & Jones, 2010; Smith & Mortimer, 1985), sulfoxidation (Baclocchi et al., 1997; Watanabe et al., 1982), and others. With the increasing number of cytochromes P450 identified in all biological kingdoms, and with many individual P450s involved in multiple reactions, classification of these enzymes is challenging. Therefore, a systematic nomenclature has been developed based on sequence identity and phylogenetic relationship (Nelson et al., 1996). According to this system, members under the same family share more than 40% of sequence identity while members in the same subfamily share more than 55% sequence identity (Nelson, 2018; Nelson et al., 1996). Each

Cytochrome P450 gene of a superfamily is named with an abbreviated CYP followed by a number representing the family (CYP1, CYP2, CYP101 and others), a letter representing the subfamily and a number for the individual gene (for example CYP101A1 for P450_{cam}, CYP102A1 for P450-BM3) (Nelson et al., 1996; Ortiz de Montellano, 2015). Over 300,000 cytochrome P450 genes have been collected in a database by Dr. Nelson, of which, nomenclature has been assigned to more than 41,000 cytochromes P450 categorized in 2252 families (Nelson, 2018).

1.1.2. Classes of cytochrome P450

Cytochromes P450 catalyse a vast number of reactions in nature. During their catalytic activity, electrons are sourced from nicotinamide adenine dinucleotide phosphate (NADPH), or nicotinamide adenine dinucleotide (NADH) for reductive cleavage of oxygen (O₂) bound to heme-Fe resulting in insertion of one oxygen atom into the substrate at the final stage, hence these enzymes are called monooxygenase. Most of the cytochromes P450 interact with one or more redox partners for the transfer of electrons from NAD(P)H. For example, the membrane bound adrenal mitochondrial P450s use adrenodoxin reductase (flavin adenine dinucleotide (FAD) containing) and adrenodoxin (2Fe-2S containing) for electron transfer from NAD(P)H (Ohashi & Omura, 1978; Omura et al., 1966), while the liver microsomal P450s use FAD and FMN (flavin mononucleotide) containing reductase for transfer of electrons from NAD(P)H (Black & Coon, 1982; Iyanagi & Mason, 1973). The first bacterial cytochrome P450 to be isolated came from *Pseudomonas putida* (P450_{cam}, CYP101A1). This enzyme catalyzes NADH-dependent oxidation of camphor (Bradshaw et al., 1959; Hedegaard & Gunsalus, 1965). The cytochrome P450_{cam} requires a soluble P450 reductase system comprised of putidaredoxin reductase (FAD containing, PdR) and putidaredoxin (2Fe-2S containing, PdX) similar to mitochondrial ones (Katagiri et al., 1968). Later, the first self-sufficient, P450-reductase fusion in a single polypeptide chain, the cytochrome P450BM3 (CYP102) was found in *Bacillus megaterium* (Narhi & Fulco, 1986, 1987).

With the increasing numbers of cytochromes P450 that have been found, different types of these redox partners and electron transfer systems have been discovered. Most of the cytochromes P450 belong to two main classes: the mitochondrial/ bacterial type and the microsomal type. In addition, with consideration of the protein components

involved in electron transfer reactions, cytochromes P450 have been divided into the following classes by Hannemann et al. (Hannemann et al., 2007).

Class I

Class I P450s are found in bacteria and in the membrane of mitochondria in eukaryotes. This class of cytochromes P450 has three separate protein components: (1) the cytochrome P450, (2) a flavin adenine dinucleotide (FAD) containing reductase, which accepts electrons from NAD(P)H or NADH and reduces the second component of the system, (3) an iron-sulfur protein (2Fe-2S, ferredoxin), which shuttles the electron from the flavoprotein to the cytochrome P450 to reduce heme-iron at two points in the catalytic cycle. All these three proteins are soluble proteins, in the case of bacteria (Figure 1.2, **la**). In eukaryotes, ferredoxin reductase and cytochrome P450 are both membrane bound to the inner membrane of mitochondria, while the ferredoxin component is soluble in the mitochondrial matrix (Figure 1.2, **lb**) (Hannemann et al., 2007). Plants and fungi have many microsomal cytochromes P450 (class II, see below), however, no mitochondrial P450 has been reported (Omura & Gotoh, 2017).

Most of the bacterial cytochromes P450 use nicotinamide adenine dinucleotide (NADH) as a source of electrons. Ferredoxin reductase (FAD containing) and ferredoxin (2Fe-2S containing) transfer the electron to cytochrome P450 (Bernhardt, 2006; Poulos, 2014). However, in a few bacterial species, ferredoxin contain other types of iron-sulfur clusters such as 3Fe-4S or 4Fe-4S (Duée et al., 1994; Mutter et al., 2019). Bacterial cytochromes P450 play important roles in catabolism of organic compounds used as carbon sources by these bacteria (Grogan et al., 1993; Katagiri et al., 1968), production of antifungal and antibiotic compounds (Beilen et al., 2005; Fjærvik & Zotchev, 2005), and metabolism of xenobiotics (Taylor et al., 1999). Cytochrome P450_{cam} (CYP101A1), which was isolated from the soil bacterium *Pseudomonas putida*, is class I cytochrome P450. The flavoprotein – putidaredoxin reductase (FAD containing, PdR) and putidaredoxin (iron-sulfur cluster (2Fe-2S) containing, PdX) are involved in transferring two electrons one at a time to the cytochrome P450_{cam}. *Pseudomonas putida* uses D-camphor as a carbon source. Cytochrome P450_{cam} catalyzes the first step of D-camphor breakdown, producing 5-exo-hydroxycamphor. This process was demonstrated to be both regio- and stereoselective (Katagiri et al., 1968; Poulos, 2014). The structure of cytochrome P450_{cam} was the first cytochrome P450 structure to be determined using X-ray crystallography.

Later, the structures of P450_{cam} redox partner proteins, putidaredoxin (PdX) and putidaredoxin reductase (PdR) were also obtained (Haniu et al., 1982; Poulos et al., 1985; Sevrioukova et al., 2003, 2004). Other bacterial cytochromes P450 that belong to class I include: CYP105A1 (P450_{SU-I}) from *Streptomyces griseolus* (which can hydroxylate Vitamin D₃) (Sawada et al., 2004) and CYP107H (P450_{Biol}) from *Bacillus subtilis* (involves in oxidation of a fatty acid during biotin synthesis) (Green et al., 2001).

Mitochondrial cytochromes P450 play important roles in the biosynthesis of vitamin D and steroid hormones. The adrenal cytochromes P450 use iron-sulfur (2Fe-2S) containing ferredoxin and FAD-containing, NADPH-dependant ferredoxin reductase, referred as adrenodoxin (AdX) and adrenodoxin reductase (AdR) respectively, to transfer electrons from NADPH. Examples of class I enzymes include CYP11A1 (cytochrome P450_{SCC}, which is involved in the biosynthesis of pregnenolone by side-chain cleavage of a cholesterol molecule), CYP11B1 (11-deoxycortisol oxidation to cortisol), CYP11B2 (Corticosterone 18-hydroxylation), CYP24A1 (25-hydroxyvitamin D₃ 24-hydroxylation), CYP27A1 (Sterol 27-hydroxylation), and CYP27B1 (Vitamin D₃ 1-hydroxylation) (Bernhardt, 2006; Guengerich, 2015).

Though bacterial and mitochondrial cytochromes P450 have similar protein components, there are considerable differences in these proteins. For example, CYP101A1 and CYP11A1 are not able to substitute their respective ferredoxin proteins in order to perform the catalysis (Schiffler & Bernhardt, 2003).

Class II

Class II cytochromes P450 are membrane bound proteins found in the endoplasmic reticulum (ER) of eukaryotes. The NADPH-dependent cytochrome P450 reductase (CPR), which contains both FAD and FMN domains, transfers the electrons from NADPH to cytochrome P450 (Figure 1.2, II). Cytochrome P450 reductase (CPR) has an N-terminal FMN-containing domain similar to bacterial flavodoxin, and a C-terminal domain with FAD-containing ferredoxin NADP⁺ reductase and NADH-cytochrome *b5* reductase (Porter & Kasper, 1986).

Class II cytochromes P450 are the most common ones in eukaryotes. In mammals, they are involved in a variety of catalytic reactions including oxidative metabolism of steroids (CYP1B1, CYP7A1, CYP39A1, CYP51A1), fatty acids (CYP2J2, CYP4A11,

CYP4B1), vitamins (CYP2R1, CYP26A1, CYP26B1), as well as exogenous compounds such as therapeutic drugs and environmental toxins (CYP1A1, CYP1A2, CYP2A6, CYP2B6, CYP2C8, CYP3A5, CYP3A7) (Guengerich, 2015). In plants, class II cytochromes P450 play role in secondary metabolism as well as synthesis of different compounds (phytoalexins) for their defence mechanism, fatty acids, pigments and hormones (Mizutani & Sato, 2011; Schuler, 2015). Fungal cytochromes P450 play role in synthesis of mycotoxin and detoxification of phytoalexins (Hannemann et al., 2007; Schuler & Werck-Reichhart, 2003). Cytochromes P450 in insect play important tasks from synthesis degradation of ecdysteroids (arthropod steroid hormones) (Kayser et al., 1997), pheromones (Ahmad et al., 1987) and juvenile hormones (Sutherland et al., 2000) to metabolism of foreign chemicals (Andersen et al., 1994; Stevens et al., 2000).

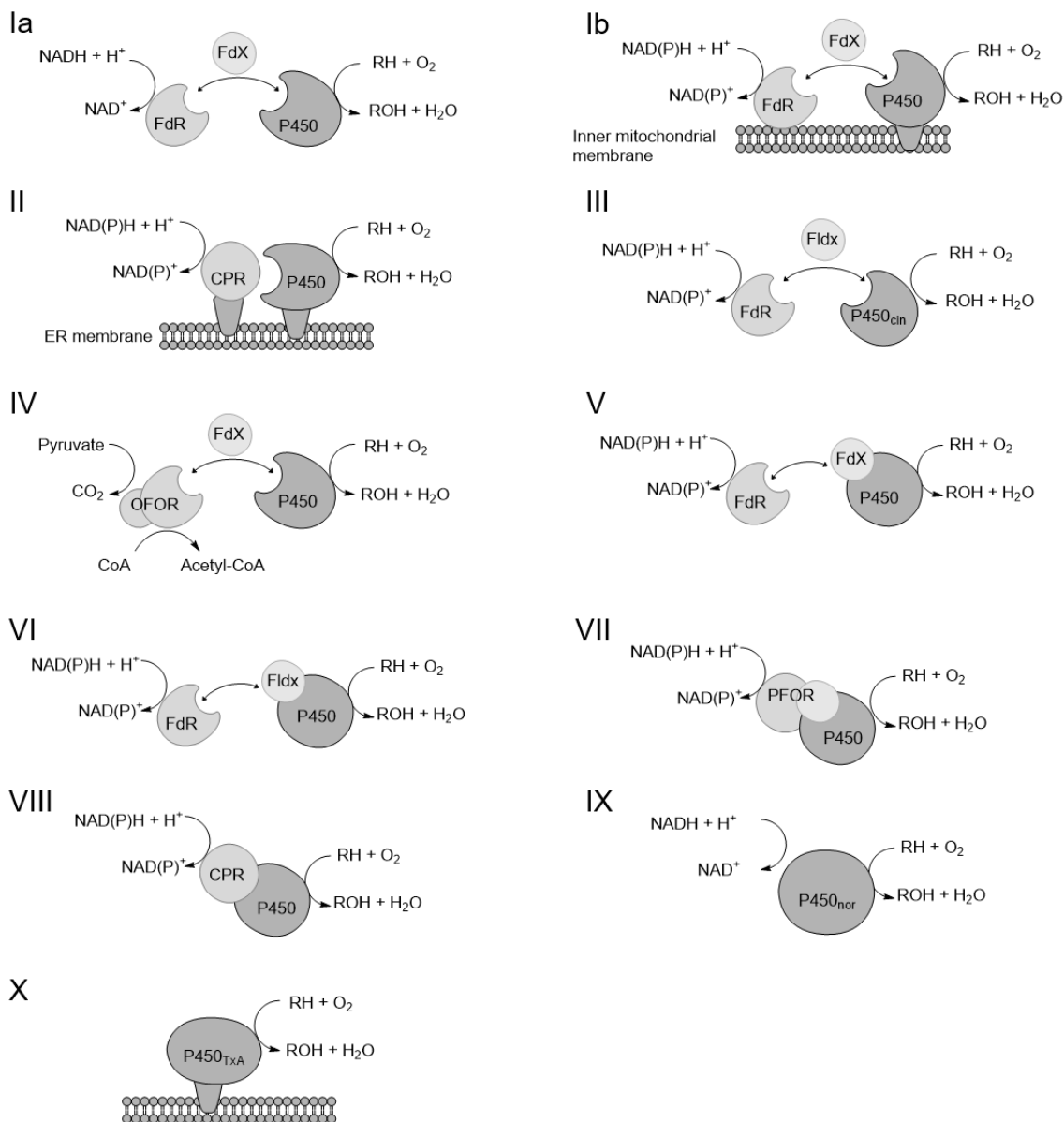


Figure 1.2 Schematic outline of different P450 systems. (Ia) Class I, bacterial system; (Ib) class I, mitochondrial system; (II) class II microsomal system; (III) class III, bacterial system (example P450_{cin}, CYP176A1); (IV) class IV, bacterial thermophilic system; (V) class V, bacterial [Fdx]-[P450] fusion system; (VI) class VI, bacterial [Fldx]-[P450] fusion system; (VII) class VII, bacterial [PFOR]-[P450] fusion system; (VIII) class VIII, bacterial [CPR]-[P450] fusion system; (IX) class IX, soluble eukaryotic (P450_{nor}); (X) independent eukaryotic system (example P450_{TxA}).

Abbreviated protein components contain following redox centers: Fdx (iron-sulfur-cluster); FdR, Ferredoxin reductase (FAD); CPR, cytochrome P450 reductase (FAD, FMN); Fldx, Flavodoxin (FMN); OFOR, 2-oxoacid:ferredoxin oxidoreductase; PFOR, phthalate-family oxygenase reductase.

Class III

One example of the novel class III cytochrome P450 is CYP176A1 (P450_{cin}), which was isolated in 2002 from *Citrobacter braakii*, a gram-negative bacterium. It resembles the class I bacterial cytochrome P450 system in terms of having three-components: a FAD-containing ferredoxin/ flavodoxin reductase which transfers the electrons from NAD(P)H to the second redox protein, and the protein then transfer the electrons to cytochrome P450. This second mediator protein is suggested to be a flavodoxin (flavin containing redoxin) referred as cindoxin (Figure 1.2, III) (Hawkes et al., 2002; Meharena et al., 2004). While most other bacterial and mitochondrial cytochromes P450 in class I have iron-sulfur containing ferredoxin proteins, in this class the transfer involves only flavoproteins. In comparison to Class II cytochromes P450 (microsomal), where both FAD and FMN-containing components are fused together, this novel cytochrome P450 uses two separate FAD-containing flavodoxin reductase and FMN-containing flavodoxin. Thus, cytochrome P450_{cin} was the first example to use FMN-containing flavodoxin (Meharena et al., 2004). Cytochrome P450_{cin} (CYP176A1) oxidizes cineol, a monoterpene which is used as carbon source by *Citrobacter braakii* (Hannemann et al., 2007).

Class IV

Members of class IV are cytochromes P450 from thermophilic organisms. CYP119 was the first member of this class, isolated from acidothermophilic archaeon *Sulfolobus acidocaldarius* (Rabe et al., 2008; Wright et al., 1996), shows stability at high temperature and pressure ($T_M = 91^\circ\text{C}$, up to 200 MPa) (Chang & Loew, 2000; Koo et al., 2000; McLean et al., 1998; Park et al., 2002). CYP119 has two potential redox partners: a ferredoxin and a non-NAD(P)H-dependent 2-oxoacid:ferredoxin oxidoreductase (OFOR). The systems from *S. tokodaii* and *S. solfataricus* have shown efficient redox chain (Figure 1.2, IV) (Fukuda et al., 2001; Nishida & Ortiz de Montellano, 2005; Puchkaev & Ortiz de Montellano, 2005). CYP119A1 (*S. acidocaldarius*), Cytochrome P450_{ST} (CYP119A2, *S. tokodaii*) and CYP175A1 (*Thermus thermophilus*) are three examples of P450s in this class (Nishida & Ortiz de Montellano, 2005; Oku et al., 2004; Puchkaev & Ortiz de Montellano, 2005; Rabe et al., 2008; Yano et al., 2003).

Class V

The first example of a class V cytochrome P450 is CYP51 (MC-CYP51FX) from *Methylococcus capsulatus*. This cytochrome P450 is fused to an iron-sulfur (3Fe-4S)

containing ferredoxin, via an alanine rich linker at the C-terminus of the cytochrome P450, which makes it different from class I bacterial cytochromes P450. The electrons are transferred from NADPH dependent ferredoxin reductase (Figure 1.2, **V**). Using the redox partners, the cytochrome P450 (MCCYP51FX) catalyzes 14 α -demethylation of sterols (Hannemann et al., 2007; Jackson et al., 2002).

Class VI

The class VI cytochrome P450 system comprises an NAD(P)H dependent FAD-containing flavodoxin reductase and flavodoxin (FMN, Fldx) – P450 – fusion protein, which makes it different from other cytochrome P450 classes (Class III and Class V) (Figure 1.2, **VI**) (Seth-Smith et al., 2002). The example of class VI P450s is the cytochrome P450 from *Rhodococcus rhodochrous* strain 11Y (Xp1A), where the cytochrome P450 is fused with flavodoxin with its N-terminus. This cytochrome P450 could be responsible for the degradation of military grade explosive hexahydro-1,3,5-trinitro-1,3,5-triazole (RDX) (Hannemann et al., 2007; Rylott et al., 2006; Seth-Smith et al., 2002).

Class VII

In this class, also from bacteria, a cytochrome P450 is fused to a phthalate-family dioxygenase reductase domain (PFOR), which makes it a unique cytochrome P450 system (Figure 1.2, **VII**). CYP116B2 (P450RhF) from *Rhodococcus sp.* strain NCIMB 9784 is an example of class VII. The P450RhF reductase part shows three distinct functional parts: a NADH binding, a FMN-binding domain and a ferredoxin (2Fe-2S) domain. The C-terminal reductase domain and N-terminal cytochrome P450 domain are separated by 16 amino acids (Roberts et al., 2002). This NADH-utilizing system resembles the family of phthalate oxygenase reductase enzymes, where electrons are transferred from an electron donor via FMN and the iron-sulfur [2Fe-2S] reductase domain to cytochrome P450 domain. P450RhF is capable of utilizing both NADH as well as NADPH for electron source (Hannemann et al., 2007; Hunter et al., 2005; Roberts et al., 2002, 2003).

Class VIII

Class VIII cytochromes P450 are another example of catalytically self-sufficient monooxygenases. In a single polypeptide chain, the P450 domain is fused to a eukaryotic-like diflavin reductase partner – cytochrome P450 reductase (CPR) (Figure 1.2, **VIII**). Example of this class is cytochrome P450BM3 (CYP102A1) from a soil bacterium *Bacillus*

megatarium, which catalyses the hydroxylation of fatty acids (Miura & Fulco, 1974; Narhi & Fulco, 1986). The N-terminus of the cytochrome P450 domain is fused via a short protein linker to its NADPH cytochrome P450 – reductase. The reductase domain contains 1 equivalent of each FMN and FAD, which makes it resemble mammalian cytochromes P450 (Narhi & Fulco, 1987). Electrons are transferred one at a time from primary electron donor (NADPH) via FAD and FMN to cytochrome P450 (Narhi & Fulco, 1987; Ost et al., 2003).

Two other examples of class VIII cytochromes P450 are CYP102A2 and CYP102A3 from *B. subtilis*. CYP102A2 and CYP102A3 are also involved in the hydroxylation of unsaturated and branched fatty acids (Gustafsson et al., 2004). CYP505A1 (P450foxy) isolated from *Fusarium oxysporum* also resembles CYP102A1, and involves in hydroxylation of fatty acids (Hannemann et al., 2007; Nakayama et al., 1996).

Class IX

This class of cytochrome P450 is a totally different case among heme-thiolate proteins. An example is nitric oxide reductase (P450_{nor}, CYP55I which was isolated from a fungus *Fusarium oxysporum* (Kizawa et al., 1991). This cytochrome P450 catalyzes the unique reduction of nitric oxide (NO) using NADH only without using any other redox partner to produce nitrous oxide (N₂O) and a water molecule from two molecules of nitric oxide (Figure 1.2, IX). Under low oxygen conditions, CYP55 plays an important role in denitrification (Daiber et al., 2005; Hannemann et al., 2007; Takaya et al., 1999).

Class X

Cytochromes P450 of Class X do not require separate redox partners or a primary source of electrons such as NAD(P)H. These cytochromes P450 accept acyl hydroperoxides as a substrate and use an independent intermolecular oxygen transfer system to oxidise the substrate. Allene oxide synthase (AOS, CYP74A), hydroperoxide lyase (HPL, CYP74B and CYP74C) and divinyl ether synthase (DES, CYP74D) from the CYP74 family are examples of plant-based cytochrome P450s present in membranes of chloroplasts (Figure 1.2, X) (Froehlich et al., 2001; Itoh & Howe, 2001; Shibata et al., 1995). These cytochromes P450 are involved in the synthesis of oxylipins (oxygenated fatty acids) which are important in signalling pathways in plants (Froehlich et al., 2001).

Other examples of class X are prostacyclin synthase which catalyzes the synthesis of prostacyclin from isomerization of prostaglandin H₂ (PGH₂), and thromboxane synthase (TXAS, CYP5A1) which is involved in the synthesis of thromboxane A₂ from prostaglandin H₂ (Hannemann et al., 2007; Haurand & Ullrich, 1985; Hecker & Ullrich, 1989; Wu & Liou, 2005).

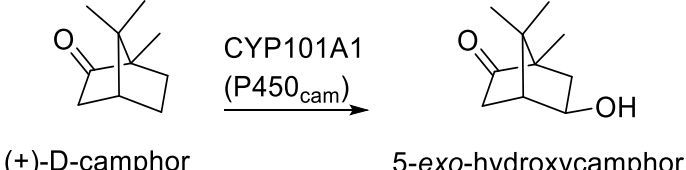
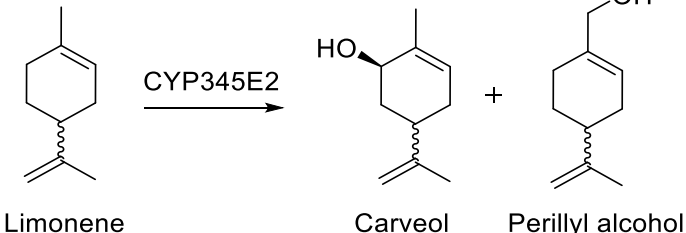
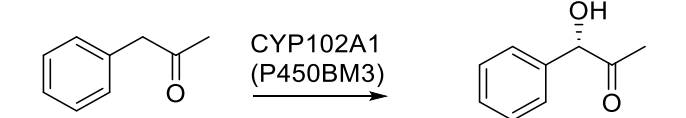
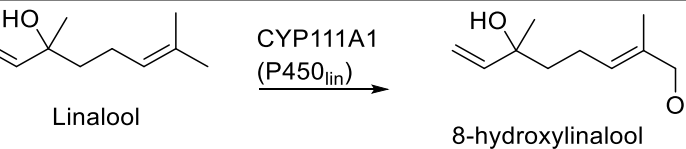
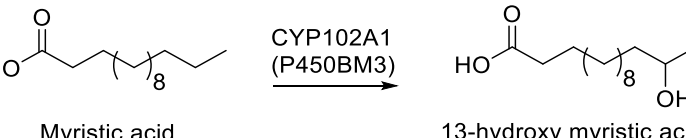
1.1.3. Type of reactions catalyzed by cytochromes P450

Cytochromes P450 activate molecular oxygen, to incorporate one oxygen atom into an organic substrate and use the other oxygen atom for the production of a water molecule (Denisov et al., 2005). There are a variety of oxidation reactions catalysed by cytochromes P450 including hydroxylation of aliphatic carbon (C–H bond), epoxidation of alkenes (C=C bond), O-, and N-dealkylations, sulfoxidation and many others.

Hydroxylation of aliphatic carbon (C–H bond)

The most common reaction catalyzed by cytochromes P450 is the hydroxylation of hydrocarbons. During this reaction, a C–H bond in the substrate is broken, and an oxygen atom is inserted to produce an alcohol (C–O–H) (Scheme 1.1). The C–H bond dissociation energies of primary, secondary, tertiary, benzylic or allylic carbon are between 88-105 kcal/mol (Blanksby & Ellison, 2003). Cleavage of these type of C–H bond and their oxidation reactions are catalyzed by P450s very effectively (Benveniste et al., 1982; Gelb et al., 1982; Groves et al., 1978; Maier et al., 2001). For regio- and stereoselectivity of oxidation reactions catalyzed by P450s, steric hinderance and orientation of the molecule in the substrate binding pocket of P450s above the heme moiety are important (Ortiz de Montellano, 2015). Examples of hydroxylation reactions are the oxidation of D-(+)-camphor, limonene, linalool and myristic acid by CYP101A1, CYP345E, CYP111A1 and CYP102A1 respectively (Table 1.1).

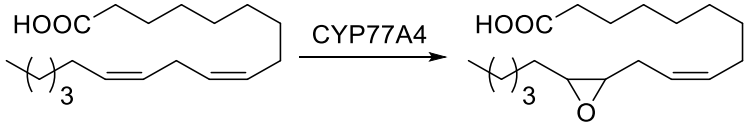
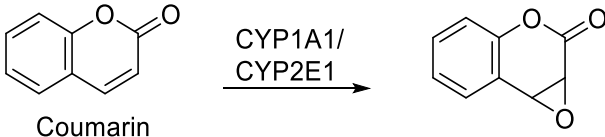
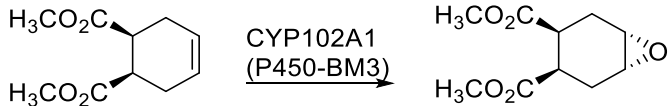
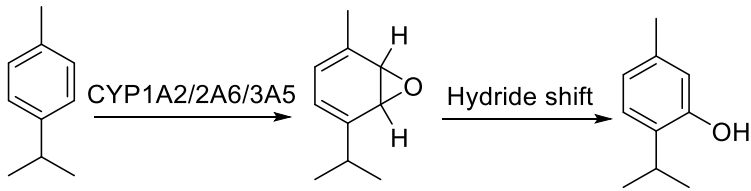
Table 1.1 Hydroxylation of aliphatic carbon (C–H bond)

Entry	Reported reactions by P450s	Reference
1	 <p>(+)-D-camphor 5-exo-hydroxycamphor</p>	(Gelb et al., 1982; Prasad et al., 2011)
2	 <p>Limonene Carveol Perillyl alcohol</p>	(Keeling et al., 2013)
3	 <p>CYP102A1 (P450BM3)</p>	(Agudo et al., 2015)
4	 <p>Linalool 8-hydroxylinalool</p>	(Ullah et al., 1990)
5	 <p>Myristic acid 13-hydroxy myristic acid</p>	(Narhi & Fulco, 1986)

Alkene epoxidation

The insertion of an oxygen atom into carbon-carbon π bond of an alkene by cytochrome P450 results in epoxide formation (Chiu et al., 2019; Gelb et al., 1982; Hagmann & Grisebach, 1984; Jin et al., 2003; Lin et al., 2014; Ruettinger & Fulco, 1981; Sauveplane et al., 2009). The alkene stereochemistry is retained due to concerted mechanism of oxygen insertion by P450s. For example, *cis* alkene gives *cis*-epoxide (Table 1.2).

Table 1.2 Epoxidation of carbon-carbon π bonds (C=C bond)

Entry	Reported reactions by P450s	Reference
1	Epoxidation of alkene  Linoleic acid	(Sauveplane et al., 2009)
2	Epoxidation of alkene  Coumarin	(Born et al., 2002)
3	Epoxidation of alkene 	(Ilie et al., 2015)
4	Epoxidation of arene and hydride (H) shift 	(Meesters et al., 2009)

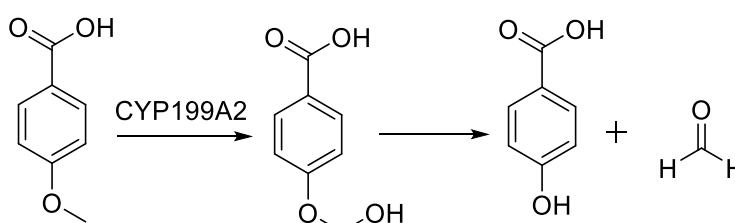
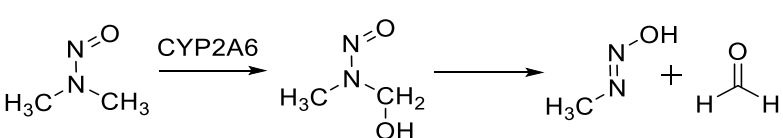
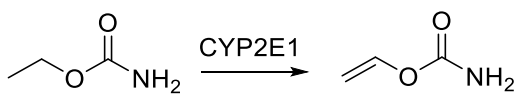
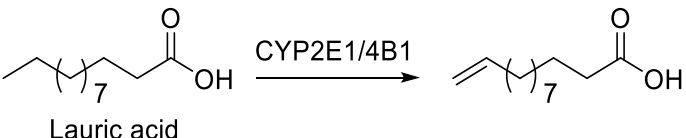
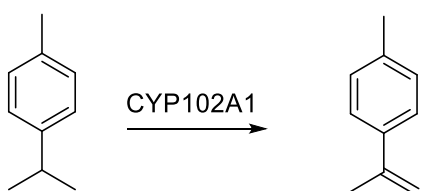
Arene epoxidation and hydride (H) shift

The epoxidation of *p*-cymene is catalysed by three different cytochromes P450 (CYP1A2, 2A6 and 3A5), and the resulting intermediate undergoes a hydride shift (an intramolecular 1,2-hydride migration to restore the aromatic system) to yield thymol (Table 1.2, entry 4) (Meesters et al., 2009).

Dealkylation of heteroatoms

Substrates that contain a heteroatom (N, O) attached to an alkyl group, have shown to undergo dealkylation upon oxidation by cytochrome P450. Such an oxidation reaction results in a dealkylated heteroatom-containing compound and an aldehyde (Table 1.3, entry 1 and 2) (Bell et al., 2008; Chowdhury et al., 2010; Meyer et al., 2014; Miwa et al., 1980; Nordblom et al., 1976; Smith & Mortimer, 1985).

Table 1.3 Demethylation and dehydrogenation reaction catalyzed by P450s

Entry	Reported reactions by P450s	Reference
1	O-dealkylation	(Bell et al., 2008)
	 <p>The reaction shows 4-methoxybenzoic acid reacting with CYP199A2 to form 4-hydroxybenzoic acid and formaldehyde (HCHO).</p>	
2	N-dealkylation	(Chowdhury et al., 2010)
	 <p>The reaction shows N,N-dimethyl-N-nitrosamine reacting with CYP2A6 to form N-hydroxy-N-nitrosamine and formaldehyde (HCHO).</p>	
3	Dehydrogenation	(Guengerich & Kim, 1991)
	 <p>The reaction shows ethyl carbamate reacting with CYP2E1 to form vinyl carbamate.</p>	
4	Dehydrogenation	(Guan et al., 1998)
	 <p>The reaction shows lauric acid reacting with CYP2E1/4B1 to form 13-oxo-12-oxoheptadecanoic acid. The starting material is labeled "Lauric acid".</p>	
5	Dehydrogenation/ dehydration	(Whitehouse et al., 2008)
	 <p>The reaction shows 4-isopropylphenol reacting with CYP102A1 to form 4-isopropylstyrene.</p>	

Dehydrogenation of saturated alkanes

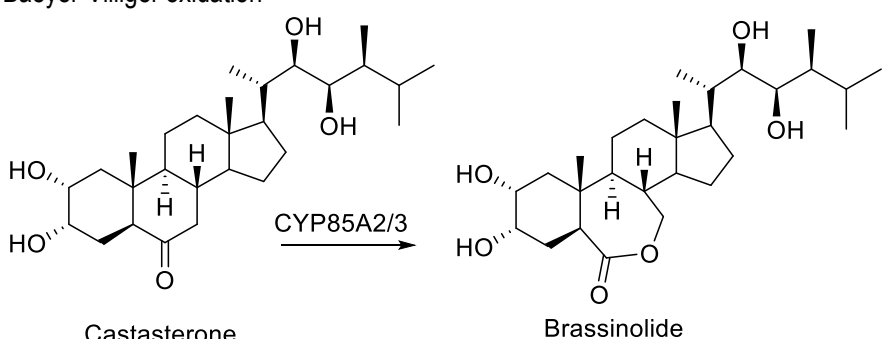
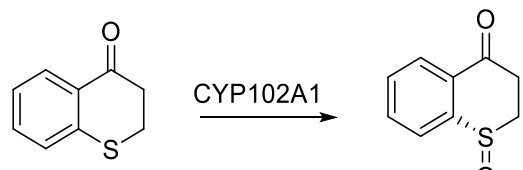
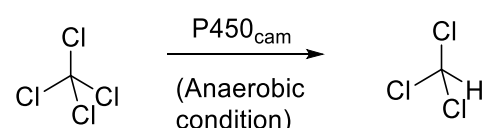
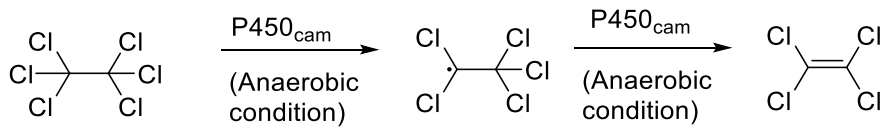
Cytochromes P450 are known for hydroxylation of alkanes. On the other hand, desaturation (dehydrogenation) reactions catalyzed by P450s are also reported (Di Nardo et al., 2007; Guengerich & Böcker, 1988; Ji et al., 2015). Ethyl carbamate is converted to vinyl carbamate by CYP2E1 (Guengerich & Kim, 1991). CYP2E1 and CYP4B1 catalyze the desaturation reaction of lauric acid, with the removal of hydrogen at the ω -1 position to produce a terminally unsaturated fatty acid (Table 1.3, entry 4) (Guan et al., 1998). The

possible dehydration of P450 catalyzed hydroxylated products has also been reported (Table 1.3, entry 5) (Whitehouse et al., 2008).

Baeyer-Villiger oxidation

The oxidation reaction of a ketone to an ester by inserting an oxygen atom into the carbon-carbon bond is referred as Bayer-Villiger oxidation. An example of a P450-catalyzed Baeyer-Villiger oxidation is the conversion of castasterone to brassinolide in the plant *Arabidopsis thaliana* catalyzed by CYP85A2. In tomato, the same oxidation is catalyzed by CYP85A3 (Table 1.4). Brassinolide plays role in plant growth (Kim et al., 2005; Nomura et al., 2005).

Table 1.4 Baeyer-Villiger oxidation, sulfoxidation and dehalogenation by P450s

Entry	Reported reactions by P450s	Reference
1	Baeyer-Villiger oxidation  Castasterone $\xrightarrow{\text{CYP85A2/3}}$ Brassinolide	(Kim et al., 2005; Nomura et al., 2005)
2	Sulfoxidation  <chem>O=C1C=CC=C1S1</chem> $\xrightarrow{\text{CYP102A1}}$ <chem>O=S1C=CC=C1</chem>	(Wang et al., 2017)
3	Dehalogenation  <chem>ClC(Cl)(Cl)Cl</chem> $\xrightarrow[\text{(Anaerobic condition)}]{\text{P450}_{\text{cam}}}$ <chem>ClC(Cl)Cl</chem>	(Castro et al., 1985)
4	Dehalogenation  <chem>ClC(Cl)(Cl)C(Cl)Cl</chem> $\xrightarrow[\text{(Anaerobic condition)}]{\text{P450}_{\text{cam}}}$ <chem>ClC(Cl)=CCl</chem>	(Li & Wackett, 1993; Walsh et al., 2000)

Sulfoxidation by P450s

Oxidation of a sulfur atom in a sulfur containing compound can be catalyzed by P450 to produce a sulfoxide product. CYP102A1 catalyzes the enantioselective sulfur oxidation in 1-thiochroman-4-ones (Table 1.4, entry 2) (Wang et al., 2017; Watanabe et al., 1982, 1982).

Dehalogenation

The reductive dehalogenation of carbon tetrachloride to trichloromethane was shown to be catalyzed by CYP101A1 (P450_{cam}) under anaerobic conditions. The enzyme

was also shown to convert hexachloroethane to tetrachloroethane by a two electron reduction under anaerobic conditions (Castro et al., 1985; Li & Wackett, 1993; Walsh et al., 2000). Dehalogenation of tetrachloroethene to trichloroacetaldehyde was shown to be catalyzed by CYP1A2 under aerobic conditions (Table 1.4) (Yanagita et al., 1997).

1.1.4. Catalytic cycle of cytochromes P450 and role of redox partners

All members of the P450 super-family that are monooxygenases operate by the same catalytic cycle, which involves the reduction of dioxygen (O_2) and the insertion of one oxygen atom into substrate along with reduction of the other oxygen to water (Figure 1.3). However, there are subtle differences in specificity with which these enzymes bind with their substrate(s) or redox partner, or in the efficiency with which they utilize atmospheric O_2 and electrons, in order to complete the oxidation of substrate in the catalytic cycle (Ortiz de Montellano, 2015). CYP101A1 ($P450_{cam}$), being the first P450 to be isolated and characterized structurally, has been studied intensively as a model of P450 catalysis (Poulos et al., 1982, 1985). Thus, the catalytic cycle of this enzyme is presented here.

In the resting state of the enzyme, a water molecule occupies the active site as a sixth ligand on the axial position of the heme-iron (Fe^{III}) opposite to the cysteine thiolate, making it hexacoordinated (Figure 1.3, **1**). In this state, the Fe^{III} is predominantly low spin. The binding of a substrate (D-camphor) displaces the axial water molecule from the active site and makes heme-iron (Fe^{III}) pentacoordinated (Figure 1.3, **2**). This displacement of water by D-camphor results in transition of the ferric iron (Fe^{III}) from low spin ($S = 1/2$) to high spin ($S = 5/2$) (Primo et al., 1992; Sligar, 1976) and in a change in the redox potential of ferric iron from -303 mV to -173 mV. This enables putidaredoxin (PdX, redox potential -240 mV) to bind and transfer the first electron to $P450_{cam}$ to produce ferrous iron (Fe^{II}) (Figure 1.3, **3**). Thus, one of two electrons from NADH is transferred to P450 via putidaredoxin reductase (FMN containing, PdR) and putidaredoxin (2Fe-2S containing, PdX), to $P450_{cam}$ (Figure 1.4) (Pochapsky & Pochapsky, 2019).

The reduced heme-iron accepts and ligates to molecular oxygen (O_2) to form a ferric superoxo species (**4**), which gives a ferric peroxo complex (**5**) upon transfer of a second electron from reduced PdX. A proton transfer to peroxo species (**5**) makes the hydroperoxo species, also known as Compound-0 (Cpd-0, Figure 1.3, **6**). Asp251 and

Thr252 in P450_{cam} play key roles in the efficient delivery of protons to the distal oxygen of the peroxo (**5**) and hydroperoxo (**6**) complexes, through a water network (Schlichting et al., 2000; Vidakovic et al., 1998). Transfer of a second proton to the distal oxygen atom of Compound-0 (**6**), results in cleavage of O–O bond and departure of a water molecule, forming Fe^{IV}-oxo-porphyrin cation radical species known as Compound-I (Cpd-I, Figure 1.3, **7**) (Harris & Loew, 1998; Sligar, 2010). The cysteine-thiolate ligand of heme-iron plays an important role in cytochromes P450 during O–O cleavage to form compound-I (**7**) (Dawson et al., 1976; Murugan & Mazumdar, 2005; Sono et al., 1982).

Compound-I either abstracts a hydrogen atom and forms a carbon radical (**8**) or else forms a sigma complex with substrate to give hydroxylated product. The hydrogen abstraction mechanism is referred as “oxygen-rebound”. The product is released and replaced by a water molecule giving Fe^{III}-hexacoordinated species (Figure 1.3, **1**) (Cook et al., 2016; Davydov et al., 2001; Rittle & Green, 2010).

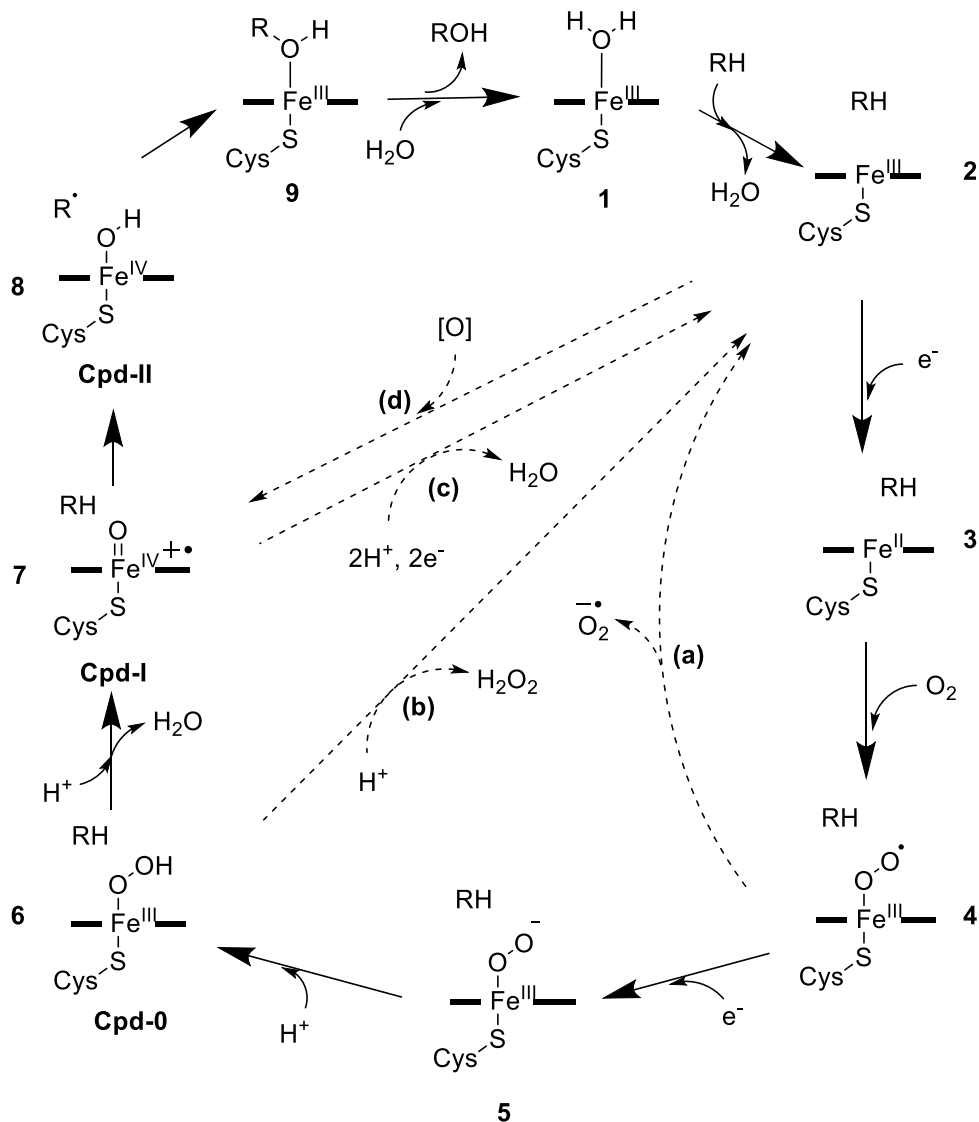


Figure 1.3 Schematic representation of the catalytic cycle cytochrome P450. Species 1 – 9 are parts of the catalytic cycle. Substrate is represented here as RH, the bold horizontal lines on either side of Fe represent the porphyrin moiety and electrons (e⁻) are supplied from the redox partner PdX. Path “d” shows direct formation of high-valent compound I (Cpd-I) by oxidant such as *m*-CPBA. Path “a”, “b” and “c” show uncoupling reactions, wherein superoxide (a), hydrogen peroxide (b) or water are released and the substrate is not oxidized.

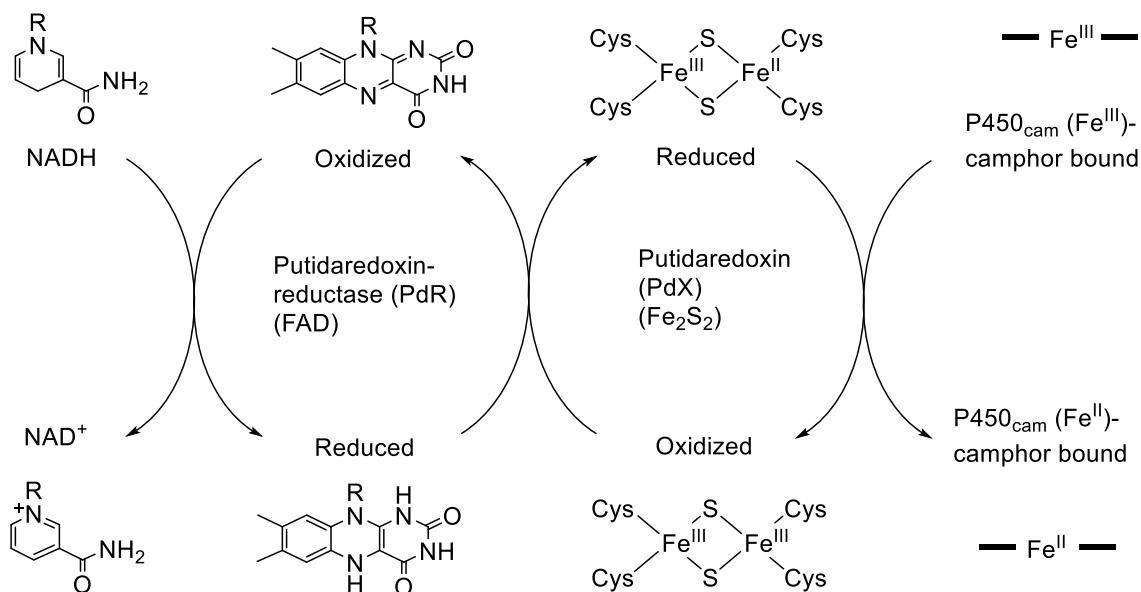


Figure 1.4 Electron transfer from NADH to P450_{cam} via putidaredoxin reductase (PdR) and putidaredoxin (PdX); a class I cytochrome P450 system.

Compound-I can be generated from the resting state of the enzyme (Fe^{III}) using peroxide or peroxy acids such as *m*-chlorobenzoic acid (*m*-CPBA) (Figure 1.3, path 'd') (Egawa et al., 1994; Spolidak et al., 2006). It is compound-I (**7**) which is used to rationalize most of the reactions catalyzed by P450s (Sono et al., 1996). Compound-I is reported to show hydroxylation of alkanes and epoxidation of C=C bond in alkenes when *m*-CPBA is used to get Compound-I (Guengerich et al., 2016; Lonsdale et al., 2010; Rittle & Green, 2010; Spolidak et al., 2006). However, compound-0, the iron (Fe^{III})-peroxo species (**6**) has also been reported to catalyze the epoxidation or oxidation reactions (Figure 1.5) (Jin et al., 2003; Kim et al., 2005).

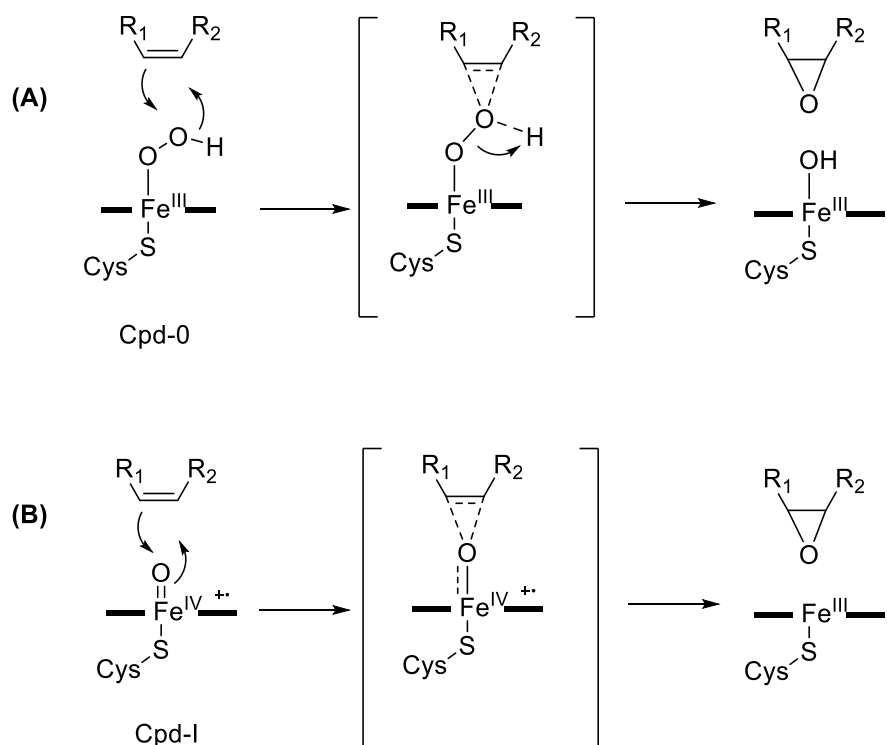


Figure 1.5 The possible mechanism of epoxidation by Compound-0 (A) and Compound-I (B) of P450.

Uncoupling reactions of P450s

During catalytic cycle, once molecular oxygen (O_2) is bound to heme-iron, dissociation can occur which will result in stopping of the catalytic cycle, thus, making the enzyme unsuccessful in catalyzing oxidation of the substrate. This is referred as “uncoupling”. Uncoupling can occur in three ways, (1) iron (Fe^{III})-superoxo species (**4**) can give superoxide radical (path **a**, one electron uncoupling), (2) iron (Fe^{III})-hydroperoxy compound-0 (**6**) gets protonated and hydrogen peroxide is released (path **b**, two electron-uncoupling), and (3) compound-I can also give uncoupling of iron-oxo ($Fe^{IV}=O$, **7**) upon double protonation and double reduction to give a water molecule (path **c**), taking the enzyme back to its resting state heme- Fe^{III} (Figure 1.3). The coupling efficiency of a P450 is important in determining the rate of catalysis of the enzyme (Altarsha et al., 2010; Davydov et al., 1999; Yoshioka et al., 2000).

Artificial shunting to generate Compound-I

Compound-I (**7**) can be generated from the resting state heme-iron (Fe^{III}) by using peroxides or peroxy acids, such as *m*-chlorobenzoic acid (*m*-CPBA) (Prasad et al., 2011), iodosobenzene (Gelb, Heimbrook, et al., 1982), cumene hydroperoxide and *p*-nitroperbenzoic acid (Nordblom et al., 1976) and others. (Figure 1.3, path 'd') (Egawa et al., 1994; Spolitak et al., 2006). In the usual catalytic cycle of P450, 2 electrons and 2 protons are required to make compound-I (**7**) from resting state enzyme (Fe^{III}). As peroxy acids or peroxides have two electrons and a proton on the dioxygen moiety, the enzyme heme-iron (Fe^{III}) rearranges the proton from the proximal oxygen atom to the distal one to facilitate the hydrolytic cleavage of the O–O bond, creating compound-I (Figure 1.6) (Ortiz de Montellano, 2015).

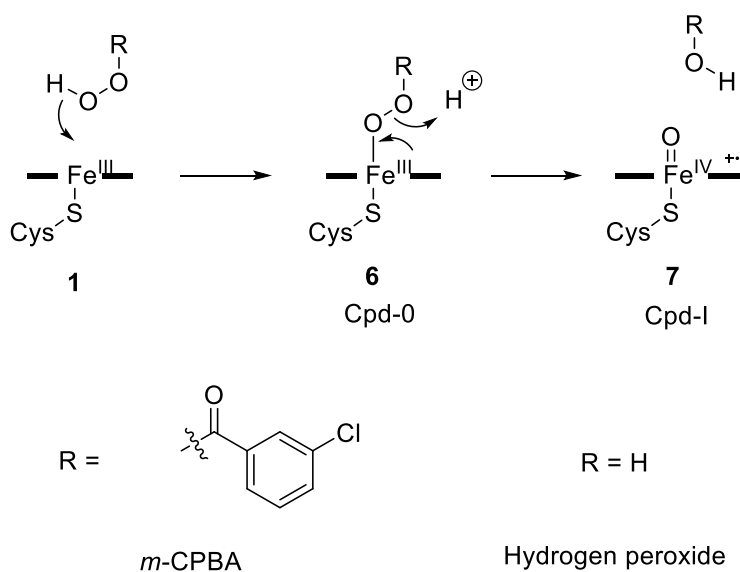


Figure 1.6 The possible mechanism of formation of Compound-0 (when $\text{R}=\text{H}$) and compound-1 by cleavage of O–O bond using peroxy acid or peroxide.

1.1.5. Oxidation of (+)-D-camphor by cytochrome P450_{cam}: regio- and stereoselectivity

Cytochrome P450_{cam} (CYP101A1) was isolated from a gram-negative soil bacterium *Pseudomonas putida* induced by D-camphor rich growth media (Hedegaard &

Gunsalus, 1965; Katagiri et al., 1968; Tyson et al., 1972). Cytochrome P450_{cam} catalyzes the hydroxylation of camphor initiating the degradation cascade of the molecule, which is used as a carbon and energy source by *P. putida* (Katagiri et al., 1968). Since the first X-ray crystallographic structure of P450 was solved by Poulos and coworkers, P450_{cam} has been studied intensively as a model P450 to explore and understand the mechanism of catalysis by P450s (Poulos et al., 1982, 1985). Cytochrome P450-BM3 (CYP102A1) which resembles microsomal P450s, was the second P450 for which the X-ray crystallographic structure was obtained in 1993 (Ravichandran et al., 1993). Recently, 3D structures of camphor-bound and free cytochrome P450_{cam} have also been resolved using NMR spectroscopy (Asciutto et al., 2011, 2012; Hiruma et al., 2013).

Cytochrome P450_{cam} structure

The overall structural fold and topology is the same across all cytochromes P450, though there is less than 20% sequence identity among the genes of P450 superfamily (Hasemann et al., 1995). There are 12 helical segments, which are designated A–L and account for almost 40% of the sequence (414 amino acid residues in P450_{cam}). The prosthetic heme is sandwiched between helix I on distal end and helix L on proximal side, and the heme-iron is bound to conserved cysteine residue (Cys357) on N-terminal end of helix L (Figure 1.7 and Figure 1.8). In other heme-containing proteins such as cytochrome c, hemoglobin, and myoglobin the sixth axial ligand to heme-iron is a conserved histidine on the C-terminal side of the proximal helix. (Poulos et al., 1985).

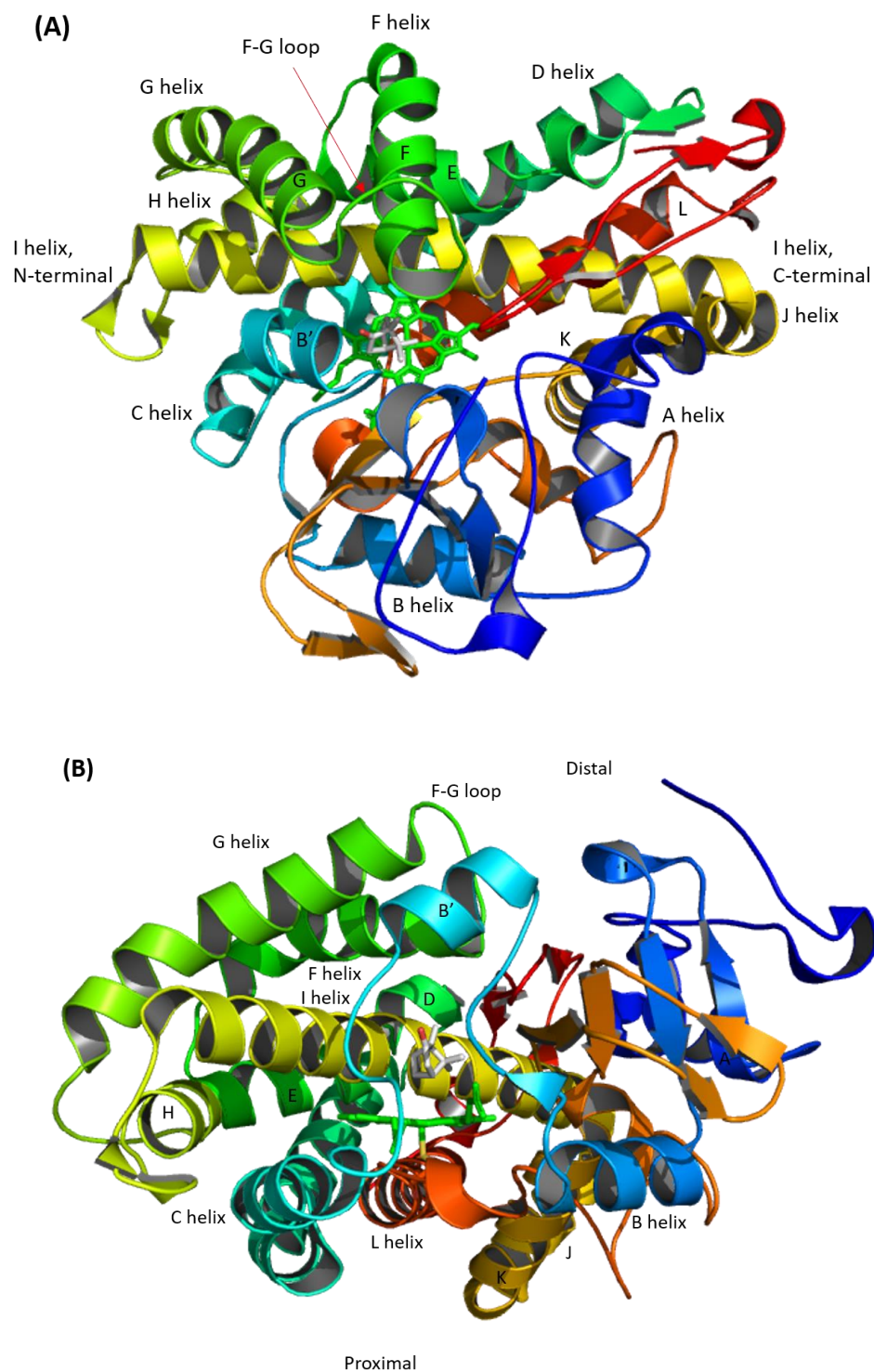


Figure 1.7 Structure of camphor-bound CYP101A1 (PDB entry 3L63, (Lee et al., 2010)). Secondary structures are labeled as described by Pochapsky (Pochapsky & Pochapsky, 2019). Heme is shown as sticks (green) and substrate *d*-camphor in grey. (A) Top view (distal), (B) side view of P450_{cam}.

TTETIQSNANLAPLPPHVPEHLVDFDFMYNPSNLSA	Helix A GVQEAWAVLQESNV	50
PDLVWTRCNGGHWIAT	Helix B RGQLIREAYEDYRHFSSSECPFIP	100
TSMDP	Helix C PEQRQFRALANQVVG	150
	Helix C' MPVVDKLENRIQELACSLIESLRPQ	
	Helix D GQC	
	Helix E NF	
TEDYAEFPPIRIFMLLAGL	Helix F PEEDIPHLKYLTDQMT	200
	Helix G RPDGSMTFEAKEAL	
YDYLIPIEQRRQK	Helix H PGTDAISIVAN	250
	Helix I GQVNGRPIT	
	TSDEAKRMCGLLLVGGL	
DTVVNFLSFSMEFLAKS	Helix J PEHRQELIER	300
	Helix K PERIPAACEELLRRFSLVADGRI	
LTSDYEFHGVQLKKGDKILL	Helix K' PQMLSGLD	350
	ERENACPMHVDFSRQKVSHTTF	
GHGSHL	Helix L *CLGQHLLARREIIVTLKEWLTRI	400
	PDFSIAPGAQIQHKSGIVSGVQ	
ALPLVWDPATTKAV		414

Figure 1.8 Amino acid sequence of cytochrome P450_{cam} with different helices (A – L) shown in different colors (Pochapsky et al., 2003). C357 shown in blue at the N-terminus of Helix L.

Cytochrome P450_{cam} (CYP101A1) is 46.7 kDa protein, which catalyzes the oxidation of D-camphor regio- and stereoselectively to give 5-exo-hydroxycamphor and 5-keto-camphor (in a 2nd round of oxidation), requires two additional proteins putidaredoxin (PdX) and putidaredoxin reductase (PdR) (Figure 1.4). P450_{cam} is remarkable in using reducing equivalents from NADH with 99% coupling efficiency during catalytic cycle, and with a turnover rate > 2000 min⁻¹ (Figure 1.3) (Pochapsky & Pochapsky, 2019). The cysteine residue (C357 in P450_{cam}) serving as a thiolate ligand to heme-iron is conserved in all P450s with signature amino acid sequence FxxGx(H/R)xCxG (Figure 1.7 and Figure 1.8) (Denisov et al., 2005; Raucy & Allen, 2001). The cysteine thiolate plays important role

in heterolytic O–O cleavage of the ferric (Fe^{III})-peroxide (**Cpd-0, 6**) to form iron-oxo species (**Cpd-I, 7**) during the catalytic cycle of P450, due to the electron-releasing nature of the thiolate ligand, it stabilizes the iron-oxo species (Cpd-I, **7**) (Dawson et al., 1976; Murugan & Mazumdar, 2005; Ogliaro et al., 2002; Sono et al., 1982). Mutation of axial ligand cysteine to selenocysteine subtly modifies the structural and electronic properties of the enzyme resulting in decrease in the catalytic activity by 2 fold (Table 1.5, entry **7**, C357U) (Aldag et al., 2009; Vandemeulebroucke et al., 2015). Mutating the cysteine residue results in low activity of P450_{cam} (C357H) or completely inactive P450_{cam} protein (C357M) (Table 1.5, entry **6**) (Murugan & Mazumdar, 2005; Yoshioka et al., 2001).

Another set of conserved amino acid residues common in P450s delivers protons for heterolytic cleavage of O–O bond during catalytic cycle. The distal oxygen in the peroxo-species (**5**) needs to be protonated in order to give the hydroperoxo species, compound-0 (**6**) and further to give compound-I (**7**, Figure 1.3). Asp251 and Thr252 deliver the protons during the catalytic cycle of P450_{cam} through a network of water molecules held in place by H-bonding (Gerber & Sligar, 1992; Hishik et al., 2000; Nagano & Poulos, 2005; Schlichting et al., 2000; Vidakovic et al., 1998; Wang et al., 2008). In Helix I of P450_{cam}, the side chain OH of Thr252 makes a H-bond with the peptide oxygen of Gly248 in the resting state. However, upon reduction and oxygen bonding to the heme-iron, Asp251 moves and the Thr252-G248 H-bond breaks, resulting in Thr252 positioning to donate an H-bond to the distal oxygen. This results in a widening of the kink in helix I, which enables two new water molecules to move in and interact with the distal oxygen to deliver the proton (Poulos, 2005). Mutations in Asp251 or Thr252 result in lower catalytic activity of P450_{cam} (Table 1.5, entry **5**) (Gerber & Sligar, 1992; Nagano & Poulos, 2005; Vidakovic et al., 1998; Wang et al., 2008).

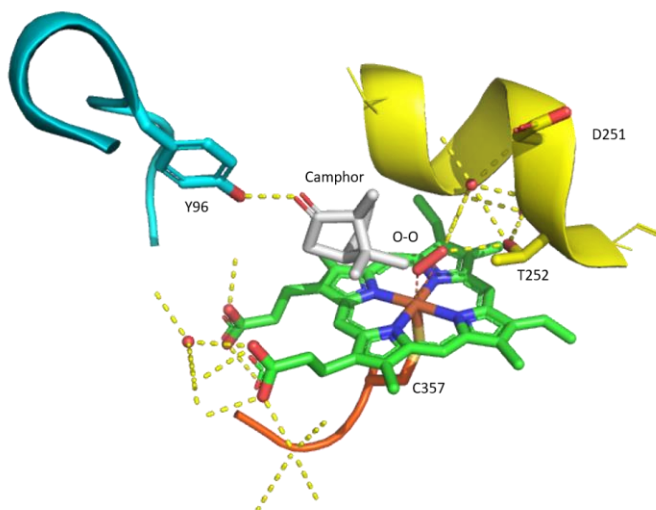


Figure 1.9 H-bonding by D251 and T251 (in helix-I, backbone ribbon is shown in yellow color) through a water network and Heme–Fe–O₂ complex in P450_{cam} (proposed H-bonds are shown as yellow dotted lines). Camphor is shown in grey color, heme in green color and Y96 in cyan color (PDB 2A1M, (Nagano & Poulos, 2005)).

There are two forms of P450_{cam}: substrate-free (open) and substrate-bound (closed). The F-G loop acts as a gate for the camphor entry channel. Upon camphor binding to P450_{cam}, large movement in helices F and G and in the F-G loop are observed, resulting in F-G loop sliding over helix I and closure of the substrate entry channel (Figure 1.10) (Lee et al., 2010, 2011). Ser190 and Thr192 residues, which are present in the F-G loop, are suggested to recognize and direct the substrate (camphor) into the binding pocket (Table 1.5, entry 2) (Behera & Mazumdar, 2008).

Stability of the heme prosthetic group is key in P450 catalytic activity. Mutation of Thr101, which lies in B¹–C loop and makes H-bonding contact to the propionate group of the heme, results in destabilization of heme (Table 1.5, entry 1) (Manna & Mazumdar, 2006).

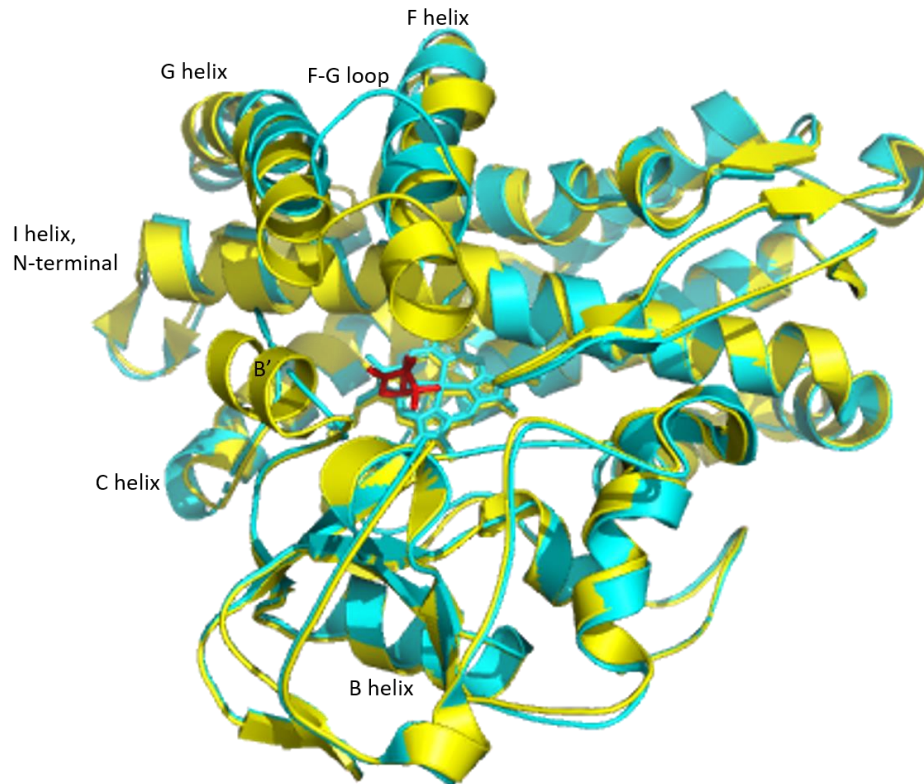


Figure 1.10 Superimposed structures of the open (PDB entry 3L62 cyan color) and the closed (PDB entry 3L63, yellow color) forms of P450_{cam}, camphor in color red (Lee et al., 2010).

Putidaredoxin (PdX), which is a 2Fe-2S containing protein, binds to the proximal end of P450_{cam} and induces changes in B', C, F and G helices. PdX plays a role as an effector for turnover by P450_{cam}, by shuttling the two electrons required for P450_{cam} activity. While the first reduction of Fe^{III}-S to Fe^{II}-S can be achieved by a suitable reductant, the second reduction requires presence of an effector (PdX) to form a PdX-P450-(O₂-Fe^{III}-S) complex (4) and to give peroxo species (5). In the absence of PdX-P450 complex, uncoupling can occur giving superoxide (O₂⁻) and Fe^{III}-S (path a, Figure 1.3) (Glascok et al., 2005; Lipscomb et al., 1976; Pochapsky et al., 2003). PdX binds to P450_{cam} making the interactions between PdX-Asp38 and P450_{cam}-Arg112, and PdX-Trp106 to Arg109 and Asn116 of P450_{cam}. This PdX binding results in movement (2-3 Å) in helix C towards PdX, coupled with movements of helices F and G (Tripathi et al., 2013). Mutating Arg112 (R112C/K/M/Y) results in decrease in catalytic activity or completely diminished activity of P450_{cam} (Table 1.5, entry 2) (Koga et al., 1993; Unno et al., 1996).

Table 1.5 Amino acid residues and their effect on P450_{cam} catalytic activity

#	Residue / Mutants	Impact on structure or activity	References
1	T101V (T101 OH H-bonds with the propionate chain of heme)	Decreased stability of the tertiary structure of the heme cavity in the substrate-bound mutant P450 _{cam}	(Manna & Mazumdar, 2006)
2	R112C/ K/ M/ Y (R109 and R112 are involved in the PdX binding site)	R112 interacts with PdX and is involved in electron transfer. Mutation resulted in decreased activity.	(Koga et al., 1993; Unno et al., 1996)
3	S190D T192E (S190 and T192 are located in the F/G loop)	T192E at F/G loop directs the substrate access channel of the enzyme. Though it is away from the active site, camphor is recognized at the surface and directed to active site.	(Behera & Mazumdar, 2008)
4	G248E/ D (G248 residue is close to 5-methyl group of heme)	Both show lower catalytic activity than WT. Only G248E shows partial covalent binding to heme in the presence of camphor. G248E – mutant protein digestions gave 5-hydroxyheme.	(Limburg et al., 2005)
5	D251N T252A/ I (D251, T252, K178 and R186 anchor a network of water molecules that helps to deliver protons for O-O cleavage in the catalytic cycle)	D251N showed lower activity than wild type by 2 orders. T252I gave active site enlarged oxygen binding pocket – with no Hydrophilic OH-Thr252 resulting in decrease in catalytic activity than WT.	(Gerber & Sligar, 1992; Hishik et al., 2000; Kim et al., 2008; Nagano & Poulos, 2005; Vidakovic et al., 1998; Wang et al., 2015; Wang et al., 2008)
6	C357H/ M (axial ligand of heme-Fe, Thiolate ligand play key role in formation of compound I from compound 0)	C357M – Change of redox potential of heme Fe from -173mV to +260mV. Inactive P450 protein and no spectroscopic signature of substrate binding or formation of reduced carbon monoxide complex were found.	(Murugan & Mazumdar, 2005; Yoshioka et al., 2001)
7	C357U	Catalytic activity decreases by 2 fold.	(Aldag et al., 2009)
8	L358P (next to C357 thiolate ligand)	Mimics PdX-bound P450 _{cam} . L358P mutant promotes the electron-release effect of the axial C357 thiolate ligand.	(Karunakaran et al., 2011; Nagano et al., 2004; Tosha et al., 2004; Yoshioka et al., 2000)
9	L358A/ P K178G L358A-K178G L358A-K178G-D182N	All mutants lost activity, and they showed no change from low spin to high spin upon substrate binding. P450 locked in low spin – no electron transfer to the triple mutant.	(Batabyal et al., 2013)

(+)-D-Camphor oxidation by cytochrome P450_{cam}

Regio- and stereoselective oxidation of (+)-D-camphor (**10**) is catalyzed by cytochrome P450_{cam}. This hydroxylation is the first step towards degradation of camphor which is used as carbon and energy source by *P. putida* (Katagiri et al., 1968). The product of a single hydroxylation, 5-exo-hydroxycamphor (**11**), can be further oxidized by P450_{cam} to give 5-ketocamphor (**12**, Figure 1.11).

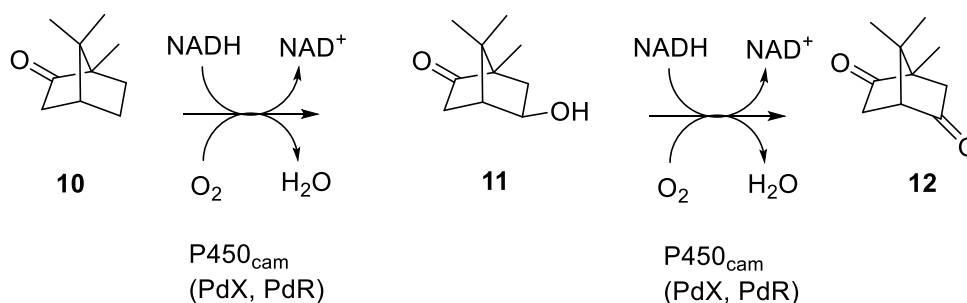


Figure 1.11 Oxidation of camphor by P450_{cam}: formation of 5-exo-hydroxycamphor (11) and 5-ketocamphor (12).

The amino acid residues in the binding pocket of P450_{cam} play key roles in substrate orientation to give stereo- and regioselectivity. Tyrosine-96 (Y96), which lies on the C-terminus of helix B', is a major contributor towards regioselective oxidation of camphor. Tyr96 makes an H-bond with the carbonyl group of camphor (Figure 1.12) (Atkins & Sligar, 1988). Other hydrophobic residues in the binding pocket of P450_{cam} include F87 (B-B' loop), L244, V247 and G248 (helix I), V295 (K-K' loop), and V396 (after helix L, in the C-terminus of P450_{cam}). These residues show weak hydrophobic interactions with camphor (Figure 1.13) (Bell et al., 2003).

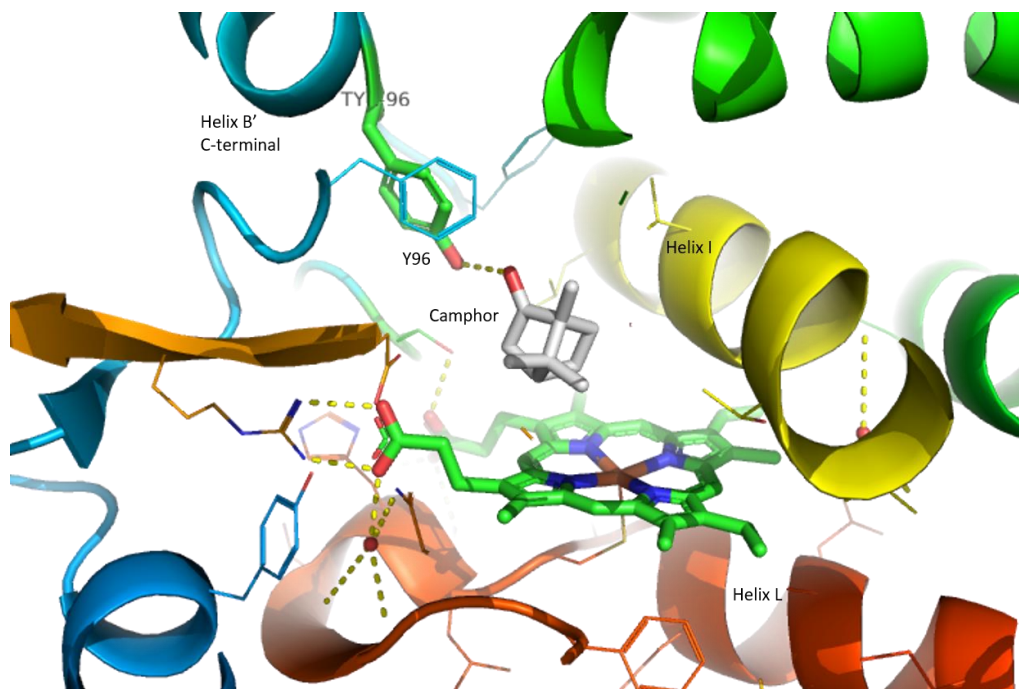


Figure 1.12 The hydrogen bonding between camphor (grey in color) and Tyrosine-96 (Y96, shown in green color) present in Helix B' (proposed H-bonds are shown as yellow dotted lines). (PDB 3L63, (Lee et al., 2010)).

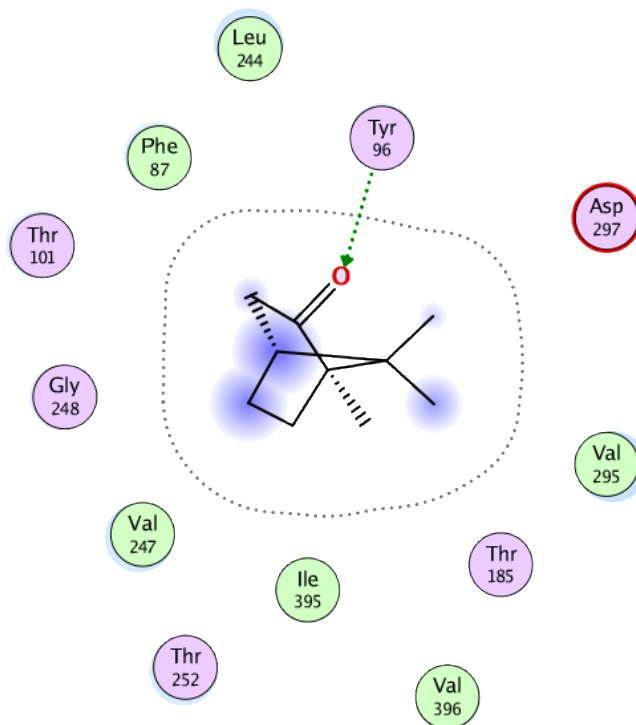


Figure 1.13 Amino acid residues around camphor in the binding pocket of P450_{cam}. Y96 makes an H-bond with the carbonyl group of camphor (PDB 3L63, visualized using Molecular Operating Environment-MOE). Residues shown in purple are polar while residues in green are nonpolar. Residues and ligand atoms with light blue clouds are exposed to the solvent environment.

1.1.6. Engineered P450_{cam} and range of substrates

Xenobiotic metabolizing hepatic P450s usually accept a vast range of substrates but are difficult to express in a recombinant host because of their membrane anchor. On the other hand, bacterial P450s usually have a narrow range of substrates and are easy to express in a recombinant host. Therefore, altering the topology of the active sites of bacterial P450s by mutation, such that they accept non-native substrates, is an obvious target for P450 engineering (Fasan, 2012; Wong et al., 1997). Due to early availability of structural information of P450_{cam} (CYP101A1) and P450-BM3 (CYP102A1), and their high solubilities and expression in recombinant hosts, these bacterial P450s are most commonly studied for this purpose (Bernhardt, 2006). Rational designing (site-directed mutagenesis) and directed evolution (selection of desired mutants from a library of

randomly mutated genes), have both been used to create or select variants with modified properties (Chowdhury & Maranas, 2020; Fasan, 2012; French et al., 2002; Jones et al., 2000; Wackett, 1998).

P450_{cam} mutations and substrate selectivity

Cytochrome P450_{cam} catalyzes the oxidation of its native substrate (+)-D-camphor regio- and stereoselectively at the 5-exo position to give 5-exo-hydroxycamphor (**11**, Figure 1.11) (Gelb, Heimbrook, et al., 1982; Li et al., 1995). P450_{cam} has been engineered to accept a broad range of non-native substrates such as terpenes, alkanes, styrene and aromatic compounds (summarized in Table 1.6, Table 1.7 and Table 1.8). Amino acid residues which were suggested to be important residues in P450_{cam} from early crystal structures have been mutated to study their role in P450_{cam} catalysis (summarized in Table 1.5).

Depending upon the position of amino acid residues in the binding pocket of P450_{cam}, Sligar and coworkers have divided them into three tiers. Residues in Tier 1 (Thr101, Leu244, Gly248, Val295, and Asp297) are located just above the heme. Tier 2 residues (Phe87, Tyr96, Val247, Ile395, and Val396) make a ring above tier 1, while Tier 3 residues (Met184 and Thr185) cover the top of the active site (Figure 1.14) (Bell et al., 2003; Loida & Sligar, 1993). Mutations of residues in the binding pocket have enabled the study of their effects on substrate selectivity and/ or P450_{cam} activity (Table 1.6, Table 1.7, and Table 1.8).

Tyrosine-96 of P450_{cam}, whose phenolic OH makes a H-bond to camphor and directs oxidation towards position-5 of camphor, is one of the most common residues mutated in order to accommodate different substrates. New substrates include alkanes, terpenes or aromatic compounds. Other residues located in the binding pocket of P450_{cam} are also targeted to change substrate selectivity and/ or P450_{cam} activity (Figure 1.14). Tyrosine-96 is replaced by a non-H bonding residue (G, A, V, L, or F) to catalyze *p*-hydroxylation of diphenylmethane, 1,1-diphenylethylene, of styrene to styrene oxide, as well as naphthalene, pyrene and benzocycloarene oxidation (Table 1.6) (Bell et al., 1997; England et al., 1998; Mayhew et al., 2002; Nickerson et al., 1997).

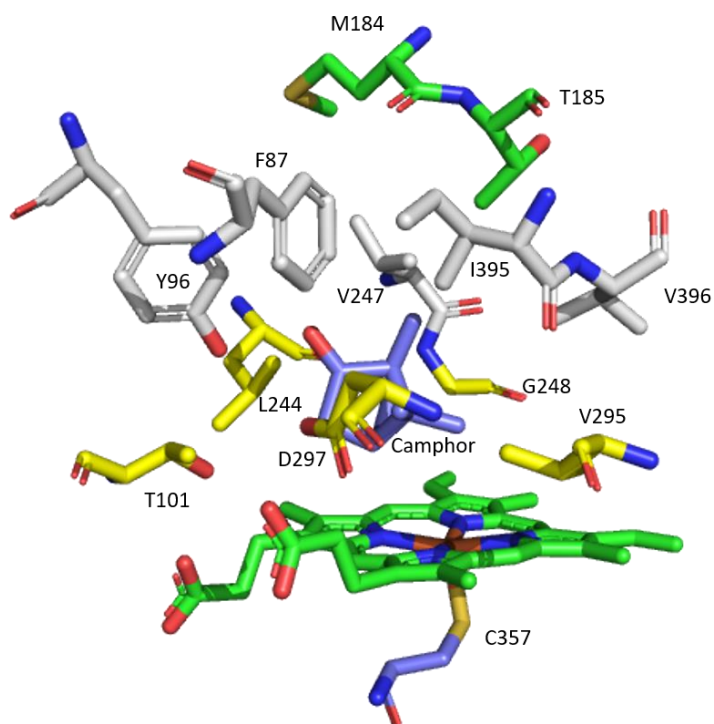


Figure 1.14 “Side-on” view of the cytochrome P450_{cam} active site. Residues in Tier 1, shown in yellow, are positioned near the heme (T101, L244, G248, V295, and D297). Tier 2, shaded light gray, form the upper region of the binding pocket (F87, Y96, V247, I395, and V396), and Tier 3, shown in green, form the top region of the binding pocket (M184, and T185) (Bell et al., 2003; Loida & Sligar, 1993). Camphor is shown in light blue and heme is shown in green. (PDB 3L63).

Oxidation reactions of benzylic carbons and of polycyclic aromatic compounds have been reported using P450_{cam} mutants (Table 1.6) (Eichler et al., 2016; Harford-Cross et al., 2000; Loida & Sligar, 1993; Sibbesen et al., 1998). Oxidation of other substrates which have been reported to be catalyzed by P450_{cam} mutants include monoterpenes (α -pinene and limonene) (Bell et al., 2003; Bell et al., 2001), sesquiterpene (Valencene) (Sowden et al., 2005) and alkanes (propane, and butane) (Bell et al., 2003) (Table 1.7). Aromatic oxidation of polychlorinated benzene to give respective chlorinated phenol, and reductive dehalogenation of pentachloroethane have also been reported to be optimized using P450_{cam} mutants (Table 1.8) (Jones et al., 2000; Manchester & Ornstein, 1995).

Table 1.6 Selected P450_{cam} mutants with modified aromatic compounds as substrates

#	Mutants	Substrates and reactions	References
1	T101M T101I T185V T185L T185F V247A V247M V295I T101M/T185F/V247M	Ethyl benzene oxidation to 1-phenylethanol (benzylic oxidation)	(Loida & Sligar, 1993)
2	Y96G Y96A Y96V Y96L Y96F	<i>Para</i> -hydroxylation of diphenylmethane and 1,1-diphenylethylene. Benzylcyclohexane to diastereoselective 4- <i>trans</i> -bezylcyclohexanol.	(Bell et al., 1997)
3	Y96A Y96F	Styrene oxidation to styrene oxide	(Nickerson et al., 1997)
4	Y96G Y96A Y96V Y96F	Naphthalene and Pyrene oxidation	(England et al., 1998)
5	T185F T185L	Oxidation of alkylbenzenes (benzylic oxidation)	(Sibbesen et al., 1998)
6	Y96A Y96F F87A/Y96F F87L/Y96F	Polycyclic aromatic oxidation	(Harford-Cross et al., 2000)
7	Y96F	Benzocycloarene oxidation	(Mayhew et al., 2002)
8	Y96F M184V/T185F L244F/V247L L244D/V247L	Ethyl benzene oxidation to 1-phenylethanol (benzylic oxidation)	(Eichler et al., 2016)

Table 1.7 Selected P450_{cam} mutants with modified alkanes and terpenes as substrates

#	Mutants	Substrates and reactions	References
1	T185F	Norcamphor oxidation	(Paulsen et al., 1993)
2	Y96F/V247L Y96A/V247A	3-methylpentane and hexane oxidation	(Stevenson et al., 1998)
3	Y96F F87W/Y96F Y96F/V247L F87W/Y96F/V247L	Terpene oxidation ((+)- α -pinene, and (S)-limonene)	(Bell et al., 2001)
4	F87W Y96W T185F L244A	2-ethylhexanol oxidation to 2-ethylhexanoic acid	(French et al., 2001, 2002)
5	Y96F F87W/Y96F Y96F/V247L F87W/Y96F/V247L F87W/Y96F/T101L Y96F/T101L/V247L F87W/Y96F/T101L/V247L F87W/Y96F/T101M/V247L F87W/Y96F/V247L/V295I F87W/Y96F/V247L/V396L F87W/Y96F/T101L/V247L/D297M F87W/Y96F/T101L/L244M/V247L	Butane and propane oxidation to 2-butanol and 2-propanol (increasing hydrophobicity)	(Bell et al., 2003)
6	Y96F F87A/Y96F F87L/Y96F Y96F/V247L F87W/Y96F/V247L F87W/Y96F/L244A/V247L F87W/Y96F/L244A Y96F/L244A/V247L	(+)- α -pinene oxidation	(Bell et al., 2003)
7	T252A	Olefin epoxidation	(Jin et al., 2003)
8	F87A/Y96F F87L/Y96F F87A/Y96F/V247L F87A/Y96F/L244A F87V/Y96F/L244A F87A/Y96F/L244A/V247L	Sesquiterpene ((+)-Valencene) oxidation	(Sowden et al., 2005)
9	Y96A F87A/Y96F V247A Y96F/V247A	Protected cyclohexanol and protected 2-cyclohexenol – oxidation to 4-trans-hydroxylation (less active V247A mutant)	(Bell et al., 2014)

Table 1.8 Selected P450_{cam} mutants with modified chlorinated compounds as substrates

#	Mutants	Substrates and reactions	References
1	F87W	Pentachloroethane (reductive dehalogenation faster than WT)	(Manchester & Ornstein, 1995)
2	Y96F F87W/Y96F F87W/Y96F/F98W F87W/Y96F/V247L	Hydroxylation of polychlorinated benzene to give polychlorinated phenol	(Jones et al., 2000)

1.1.7. Method of enzyme mutations – Random or Targeted Approach

To mutate a desired enzyme, the DNA sequence of that gene needs to be altered. The common approaches to produce DNA mutations are site-directed mutagenesis and random mutagenesis.

Site-directed mutagenesis

Site-directed mutagenesis, also called “rational mutagenesis” is commonly used to introduce mutations at definite sites of a particular DNA fragment. This is done via the polymerase chain reaction (PCR), followed by digestion of parent DNA template by restriction enzymes and transformation of mutated gene into expression host cells (Ahmad et al., 2018; Arkin, 2001; Ling & Robinson, 1997). Site-directed mutagenesis can be single site-directed mutagenesis or multiple site-directed mutagenesis depending upon the number of mutational sites (Liang et al., 2012).

Random mutagenesis

Random mutagenesis of a gene can be achieved by three methods: (1) Multi-template PCR (Kalle et al., 2014), (2) error-prone PCR (McCullum et al., 2010), and (3) Sequence Saturated Mutagenesis (SeSaM) (Ruff et al., 2014; Wong et al., 2004, 2005). Random mutagenesis produces a large number of mutations in a gene, thereby creating a library. This library of mutant genes can be amplified using PCR, and mutant genes are transformed into expression host. To achieve the directed evolution, which mimics the natural evolution, the library of mutant genes (or expressed proteins) is screened for desired function or activity (Behrendorff et al., 2015; Packer & Liu, 2015).

Sequence Saturated Mutagenesis (SeSaM) is a method of random mutagenesis comprised of four steps. (1) Random insertion of a phosphorothioate nucleotide into the targeted gene using PCR followed by cleavage of the phosphorothioate bond, which create a pool of DNA fragments with random lengths. (2) Using terminal deoxynucleotidyl transferase (TdT), DNA fragments are elongated with universal bases at the 3'-OH termini of the fragments. (3) Modified DNA fragments from step (2) are elongated using PCR to their full-length gene. (4) Universal bases (added in step 2) are replaced by standard nucleotides followed by PCR to amplify and create a library of randomly generated DNA fragments that is ready to clone into an expression vector (Wong et al., 2004, 2005).

We used P450_{cam} mutants generated by SeSaM by a former PhD student, Brinda Prasad, and wild-type P450_{cam} to study the dehalogenations of chlorinated persistent organic pollutant 'endosulfan' (Prasad, 2013). I also used site-directed mutagenesis to introduce mutations found in SeSaM generated mutants into a wild-type version of P450_{cam} with a purification tag.

1.2. Endosulfan: a polychlorinated persistent organic pollutant

Many organic chlorinated compounds were introduced as insecticides in the 1950s, and these include bicyclic compounds such as endosulfan (ES, **13**), heptachlor, lindane, chlordane, aldrin, dieldrin and methoxychlor (Figure 1.15). Endosulfan, a hexachlorinated compound, was developed and introduced by *Farbwerke Hoechst AG* in 1954 under the trademark THIODAN[®] (Maier-Bode, 1968).

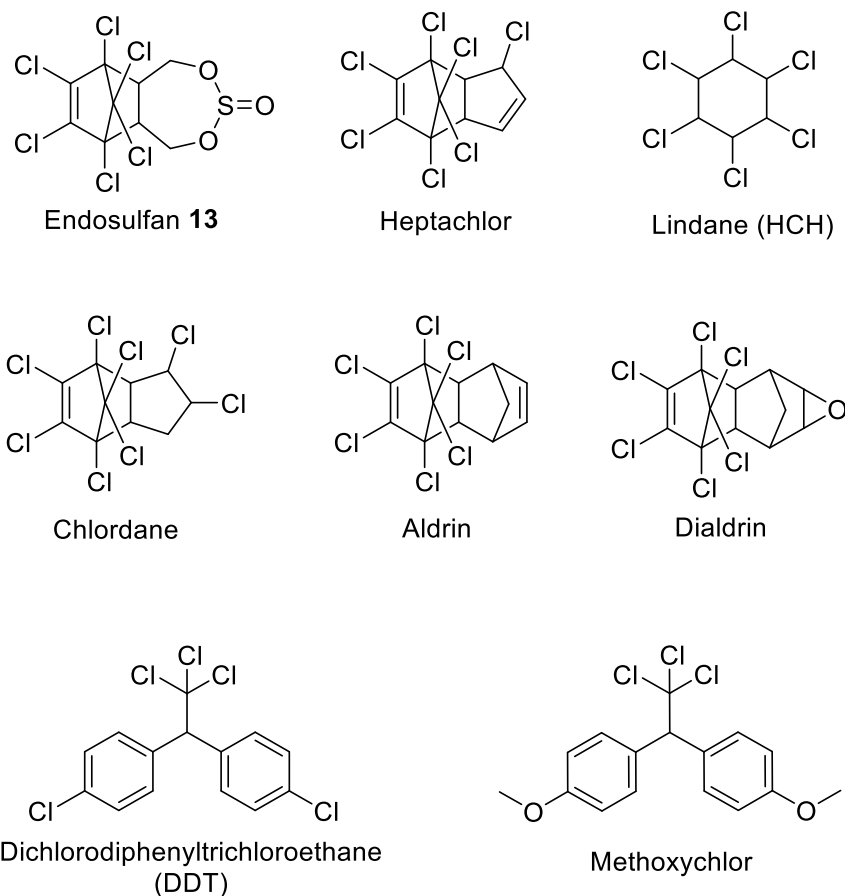


Figure 1.15 Endosulfan and other selected chlorinated compounds.

1.2.1. Endosulfan and its use

Endosulfan (ES) exists as two diastereomers: α -endosulfan and β -endosulfan (Figure 1.16) (Schmidt et al., 1997, 2001). Technical grade ES is a mixture of these two isomers, ranging from 2:1 to 7:3 (α : β). Endosulfan is effective against a broad range of insects and mites. Therefore, it had been used widely on a variety of crops, including cotton, cereals, potatoes, spinach, cauliflower, coffee, tea, apple, pear, raspberry and strawberry (Campbell et al., 1991; Grout & Richards, 1992; Hough-Goldstein & Keil, 1991; Weiss et al., 1991). The United States of America, Mexico, China, India, Brazil, and Australia were among the major users of ES from the 1950s until 2011.

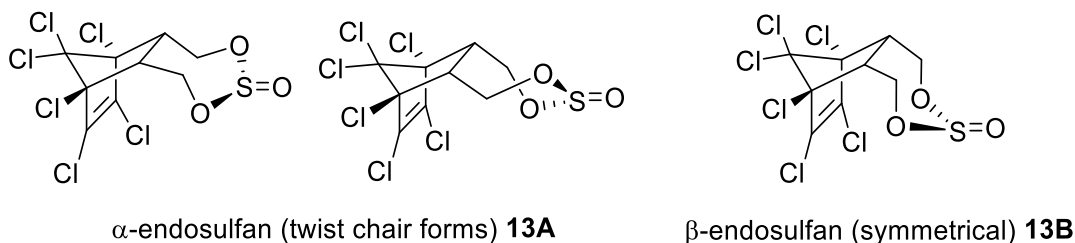


Figure 1.16 Structures of the endosulfan (ES) diastereoisomers, known as α – endosulfan and β – endosulfan.

1.2.2. Endosulfan toxicity

Endosulfan is accumulating in marine environments and is toxic to fish, algae and other marine life (Teklu et al., 2016; Wessel et al., 2007; Zhou et al., 2016). ES shows human neurotoxicity (Enhui et al., 2016) and affects estrogen and androgen receptors in females (Scippo et al., 2004; Vijayan et al., 2007), as well as delays male reproductive development (Saiyed et al., 2003). Adverse effects related to ES and its metabolites in human fetuses and newborn babies have been reported (Cappiello et al., 2014; Cerrillo et al., 2005). Human death due to acute toxicity after deliberate ingestion of ES has also been reported (Blanco-Coronado et al., 2008; Dawson et al., 2010). ES is effective against a wide range of insects, but due to this lack of specificity, it is also harmful to beneficial insects such as honey bees (Stanley et al., 2015).

1.2.3. Endosulfan: a persistent organic pollutant (POP)

Endosulfan has a long half-life in soil (α -ES 35 – 37 days and β -ES 104 – 265 days) and is, therefore, persistent in the environment (Jimenez-Torres et al., 2016). ES has been accumulating in the food chain and has been persistent in the environment (Kelly et al., 2007; Kelly & Gobas, 2003; Muir et al., 2003) due to its hydrophobicity ($\log K_{ow\alpha}$ 4.74 and $\log K_{ow\beta}$ 4.78) (Shen et al., 2005; Shen & Wania, 2005). Also, through passive transport in the atmosphere ES has been found in remote regions, as far south as Antarctica and as far north as the Arctic ocean (Kelly et al., 2007; Kelly & Gobas, 2003; Luek et al., 2017; Muir et al., 2003; Pozo et al., 2004, 2006; Weber et al., 2006). Therefore, ES is classified as a ‘Persistent Organic Pollutant (POP) according to the Stockholm Convention (<http://chm.pops.int/>). In 2011, 80 countries including most European

countries, Australia and Brazil, agreed to ban ES usage (*COP5 - Geneva, 3 May 2011 - United Nations Targets Widely-Used Pesticide Endosulfan for Phase Out*, n.d.; Hogue, 2011; Stockholm Convention, 2011). In the US, ES usage was phased out completely in 2016 (*Endosulfan Phase-out | Pesticides | US EPA*, 2010). In Canada, ES sale was banned by the end of 2015 and its usage was by the end of 2016 (Health Canada, 2011).

1.2.4. Degradation of endosulfan in nature and known metabolites

Because endosulfan is persistent in the environment, its degradation pathways in nature have been studied. ES has a reactive sulfite ester moiety that can be oxidized to sulfate (Figure 1.17). Hydrolysis of ES sulfate in alkaline conditions (for example seawater) results in ES diol (**14**) formation (Kullman & Matsumura, 1996). In soil and aquatic environments, ES sulfate and ES diol are two major metabolites found along with ES (Harman-Fetcho et al., 2005; Lehotay et al., 1998; WAN et al., 2006) (Figure 1.17). Other metabolites formed by biodegradation of ES are: ES lactone (**15**), ES ether (**16**), ES hydroxyether (hemiacetal, **17**), ES monoaldehyde (**18**) and dialdehyde (**19**), among others (Figure 1.17) (Hussain, Arshad, Saleem, & Khalid, 2007; Hussain, Arshad, Saleem, & Zahir, 2007; Kataoka et al., 2010, 2011; Kwon et al., 2002; Sutherland et al., 2000; Sutherland, Horne, Harcourt, et al., 2002; Sutherland, Horne, Russell, et al., 2002; Sutherland, Weir, et al., 2002; Walse et al., 2003).

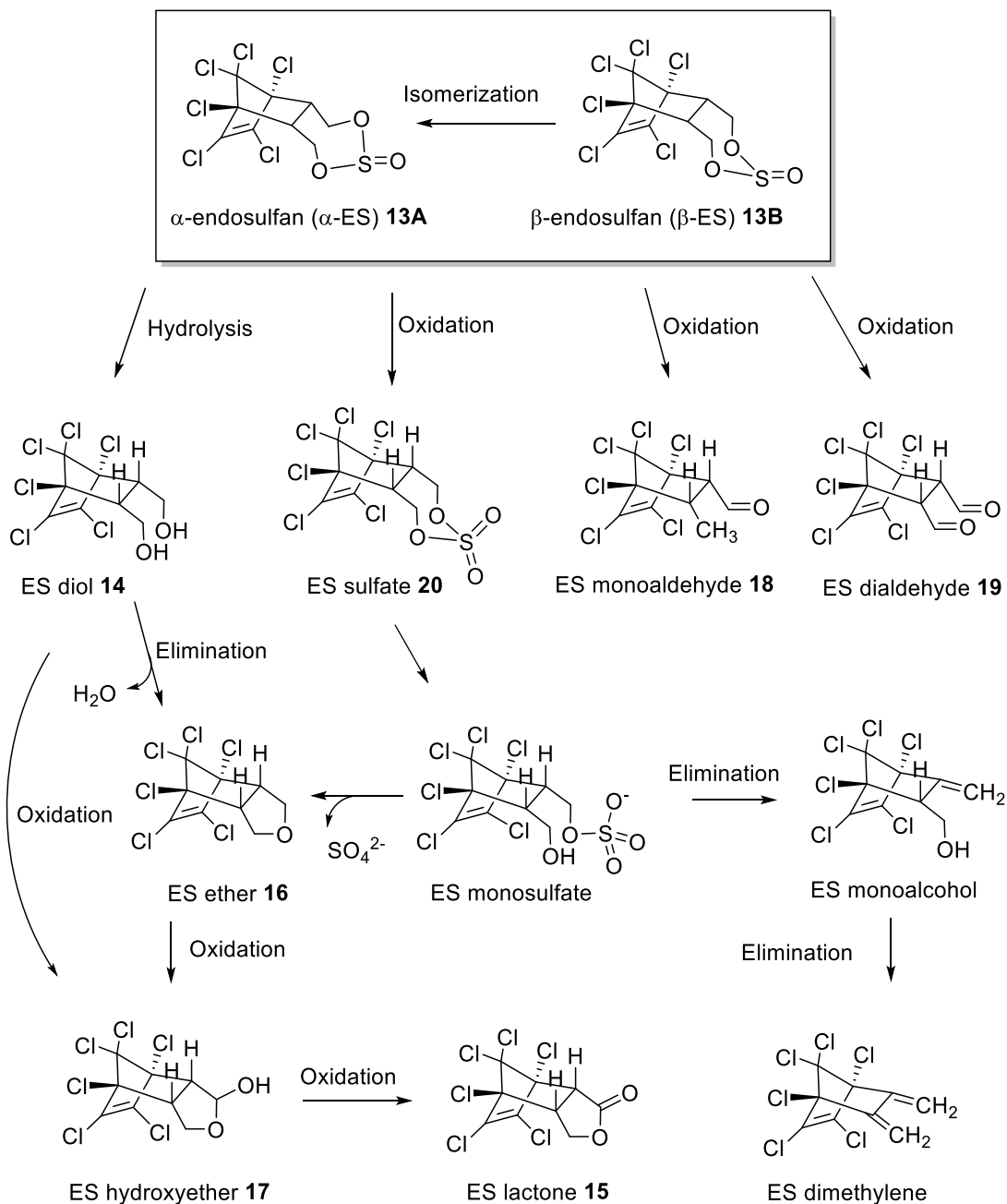


Figure 1.17 Known endosulfan metabolites found in the environment. (Note that they all have the hexachloronorbornene moiety intact).

However, known endosulfan biodegradation only targets the oxidation and/or elimination from the non-chlorinated part of the molecule, such that all known ES metabolites still have six chlorine atoms attached to the bicyclic core (Figure 1.17). These chlorinated metabolites are hydrophobic and can accumulate in the environment, like

endosulfan does. Therefore, dechlorination of endosulfan and/or its metabolites is highly desirable, but still not known in natural biodegradation systems.

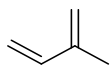
In previous work done in our group, a library of P450_{cam} mutants by Sequence Saturation Mutagenesis (SeSaM) was generated by a former PhD student Brinda Prasad (Kammoonah et al., 2018). The library was placed in an expression host and selected on minimal media containing technical endosulfan as a sole carbon source. Seven mutants of P450_{cam} were selected. These P450_{cam} mutants can convert ES (**13**) and ES diol (**14**), into dechlorinated products (substituted *o*-quinones and/ or catechols). Due to difficulty in isolating/detecting these product(s), we coupled them in the assay to 4-aminoantipyrine (4-AAP, **26**), to give a highly colored polar adduct. 4-AAP is known to produce a colored product when it couples with quinones (Lülsdorf et al., 2015; Vojinović et al., 2004). WT P450_{cam} and mutants were used to study the dehalogenations of chlorinated endosulfan diol (**14**).

1.3. β -Phellandrene: a monoterpene

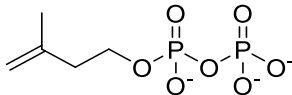
1.3.1. Terpenes and type of terpenes

Terpenes are the most chemically and structurally diverse family of natural products with more than 80,000 members. Terpenes, along with their oxidation products such as epoxides, alcohols, aldehydes and ketones, constitute one of the largest class of organic compounds found in all biological kingdoms, mainly in plants (Christianson, 2017; Dickschat, 2019). Terpenes play many roles in plant defence (Baldwin et al., 2006; Neilson et al., 2013; Phillips & Croteau, 1999), insect chemical communication (Bentz et al., 2015; Keeling, 2016; Schmidt, 1999) and, due to their distinct odor profiles, are useful in the flavouring and perfume industries (Berger, 2007).

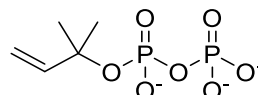
Terpenes have the general formula (C₅H₈)_n and are biosynthesized from isoprene units in the form of isopentenyl pyrophosphate (IPP) and dimethylallyl pyrophosphates (DMAPs) (Figure 1.18). Coupling of these isoprene unites in 'head-to-head' and head-to-tail' fashion followed by a series of carbonium ion rearrangement produces structurally diverse and a wide variety of acyclic and cyclic terpenes (Dickschat, 2015; Koskinen, 2012; Sowden et al., 2005).



Isoprene



Isopentenyl pyrophosphate (IPP)

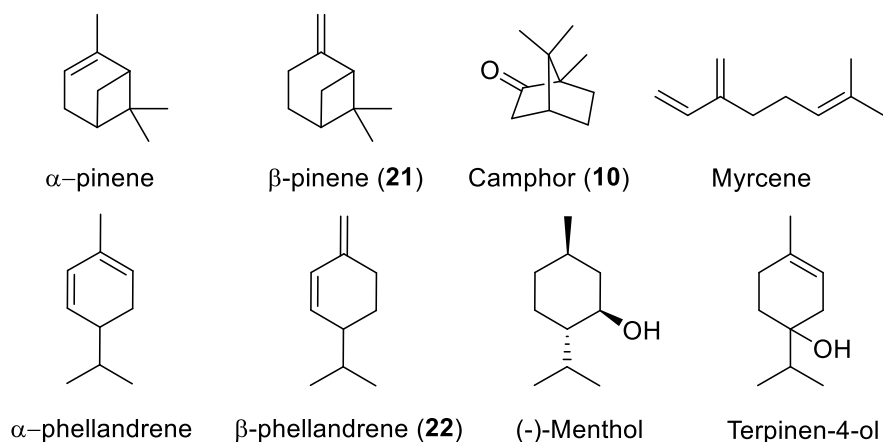


Dimethylallyl pyrophosphates (DMAP)

Figure 1.18 Building blocks of terpenes: isoprene, isopentenyl and dimethylallyl pyrophosphate.

Monoterpenes (C₁₀) are formed by combination of two isoprene units ($n = 2$). Examples of monoterpenes are α -pinene, β -pinene (**21**), camphor (**10**), α -phellandrene, β -phellandrene (**22**), myrcene, menthol, terpinen-4-ol and others. Monoterpenes are more volatile than sesquiterpenes (C₁₅) which are formed from three isoprene units ($n = 3$). Combination of four isoprene units produces diterpenes. Sesterterpenes (C₂₅), triterpenes (C₃₀) and tetraterpenes (C₄₀) are formed from five, six and eight isoprene units, respectively (Figure 1.19). Larger terpenoids are precursor for hormones and other biologically important compounds (Davis & Croteau, 2000; Koskinen, 2012).

(A) Monoterpenes



(B) Other terpenes

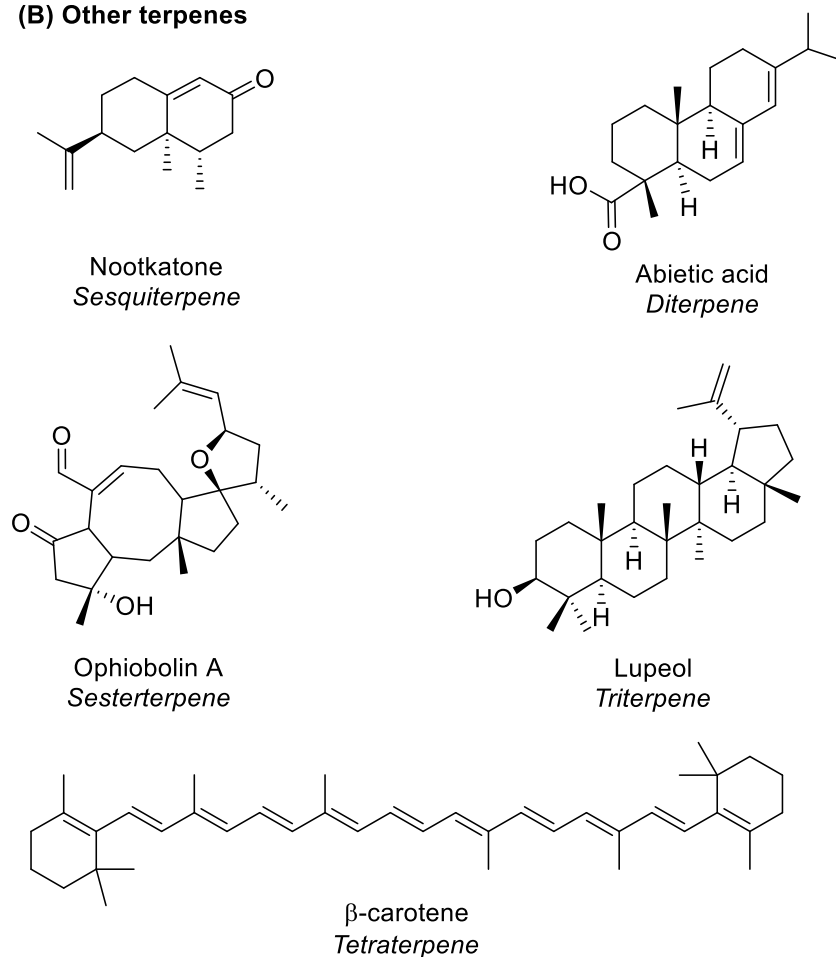


Figure 1.19 Examples of terpenes: (A) monoterpenes, (B) other terpenes: sesquiterpene, diterpene, sesterterpene, triterpene and tetraterpenes.

1.3.2. β -Phellandrene and trees under attack by bark beetles

Monoterpenes constitute a major class of organic compounds derived from plants, and they are found in all parts, such as flowers, fruits, roots and leaves of many plant species. These terpenes are abundantly present in many essential oils and oleoresins (Phillips & Croteau, 1999). Oleoresin is comprised variety of terpenoid compounds mobilized to wounded site of a tree. Although monoterpenes are biosynthesized from the same building blocks by different monoterpene synthases, their structures and functions vary based on their organism's function and environmental needs (Davis & Croteau, 2000; Dickschat, 2011; Keeling & Bohlmann, 2006; Lafever & Croteau, 1993). Their most important role is associated with plant defense mechanisms, manifested as chemical signaling in plant-plant or plant-insect interactions (Allmann & Baldwin, 2010; Baldwin et al., 2006; Keeling & Bohlmann, 2006).

β -Phellandrene (Figure 1.20, **22a** and **22b**) is a monoterpene abundantly present in water-fennel oil and Canada balsam oil (Berry et al., 1937; Macbeth et al., 1938). However, its concentration varies in oleoresins of different species of pine trees and plant essential oils (Council of Europe, 2008; Knudsen et al., 2006).

β -Phellandrene concentration released by lodgepole pine (*Pinus contorta*) and whitebark pine (*P. albicaulis*) trees, is found to increase many fold (2.9 fold in lodgepole pine, 3.7 fold in whitebark pine) when trees are under attack by mountain pine beetle (MPB, *Dendroctonus ponderosae*) (Bentz et al., 2015). Mountain pine beetle is native to the western U.S.A and Canada and attacks a variety of pine trees including lodgepole pine, whitebark pine, western white pine, and others. Since 1990s, it has destroyed 50% of commercial lodgepole pine trees in British Columbia (14 million ha between mid 1990s to 2008). (Meddens et al., 2012; Parks Canada Agency, 2017; Safranyik et al., 2010). On the other hand, pine engravers (*Ips pini* and *Ips latidens*) are attracted towards (-)- β -phellandrene, which acts as a kairomone (a chemical substance released by a member of one species, that serve as a chemical signal to another member of different species) (Bentz et al., 2015; Miller et al., 1991; Miller & Borden, 1990a, 1990b; Miller & Borden, 2000).

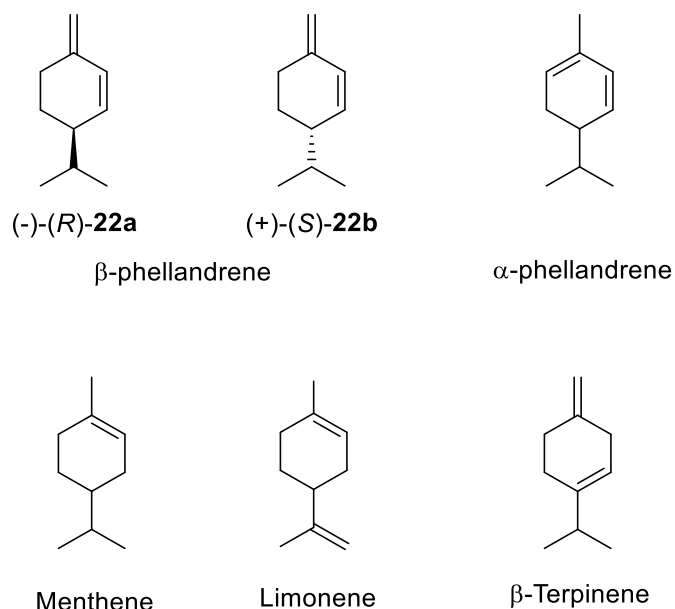


Figure 1.20 β-phellandrene enantiomers, and other monoterpenes.

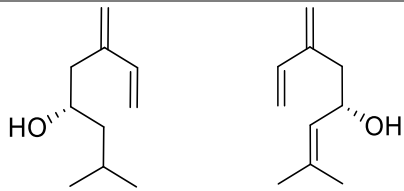
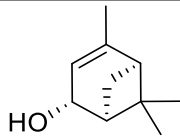
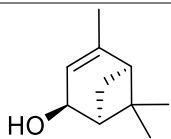
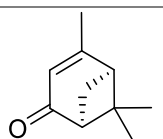
1.3.3. Oxidized monoterpenes

Plants use oxidized monoterpenes to repel, inhibit or reduce the success of invading herbivores and pathogens (Allmann & Baldwin, 2010; Baldwin et al., 2006; Keeling & Bohlmann, 2006). Herbivorous insects such as pine bark beetles use terpenoids produced by pine trees to choose the host and identify the weakened trees. To overcome the pine tree defensive mechanism, these predators can detoxify some terpenoids or use these metabolized terpenoids as pheromones to attract mates or signal others for a mass attack on pine trees. Cytochromes P450 are involved in detoxification or pheromone synthesis from monoterpenes (Aw et al., 2010; Byers, 1983; Chiu, Keeling, & Bohlmann, 2019; Macías-Sámano et al., 1998; Sandstrom et al., 2006; Seybold et al., 1995).

Examples of oxidized monoterpenes which are important for pine bark beetles or pine engraver for their chemical signaling during pine tree attack, include ipsenol, ipsdienol, verbenol and verbenone. Oxidized non-terpene compounds, such as frontalin and *exo*-brevicomin, also play a role in attack staging as aggregation signals in *Dendroctonus* sp. (Table 1.9) (Barkawi et al., 2003; Keeling, 2016; Progar et al., 2014; Song et al., 2014). Ipsenol and ipsdienol are oxidized products of myrcene produced by *Ips* sp. (catalyzed by P450s) (Sandstrom et al., 2008). Ipsenol is a pheromone component

in *Ips*, and ipsdienol is a pheromone component in *Ips* and *Dendroctonus*, both signals to aggregate with other members of their species to overcome tree defenses with high numbers of attacking insects (Table 1.9). *Cis*-verbenol (an attractant pheromone in *Ips*), *trans*-verbenol (produced by *Dendroctonus* sp.), and verbenone (an anti-aggregation pheromone, and kairomone in different species), are oxidized products of α -pinene produced by mountain pine beetle (CYP6DE1) (Chiu, Keeling, & Bohlmann, 2019).

Table 1.9 Examples of oxidized monoterpenes and non-terpene compounds, and their significance

Entry	Monoterpenes	Role	Reference
1	 <p>(4S)-(-)-Ipsenol (4S)-(+)-Ipsdienol</p>	Aggregation pheromones released by male members of <i>Ips</i> sp. (Pine engraver, <i>Ips pini</i>)	(Byers, 1982; D. Miller et al., 1991; Sandstrom et al., 2008; Seybold et al., 1995)
2	 <p><i>trans</i>-Verbenol</p>	Aggregation pheromone in bark beetles (<i>Dendroctonus</i> sp.)	(Byers, 1983; Chiu, Keeling, & Bohlmann, 2019; Pitman et al., 1968)
3	 <p><i>cis</i>-Verbenol</p>	Attractant pheromone component in <i>Ips</i> sp.	(Renwick et al., 1976; Wood et al., 1967)
4	 <p>Verbenone</p>	Released by different species. Anti-aggregation signals with frontalin in bark beetles	(Bedard et al., 1980; Byers & Wood, 1980; Lindren & Miller, 2002)

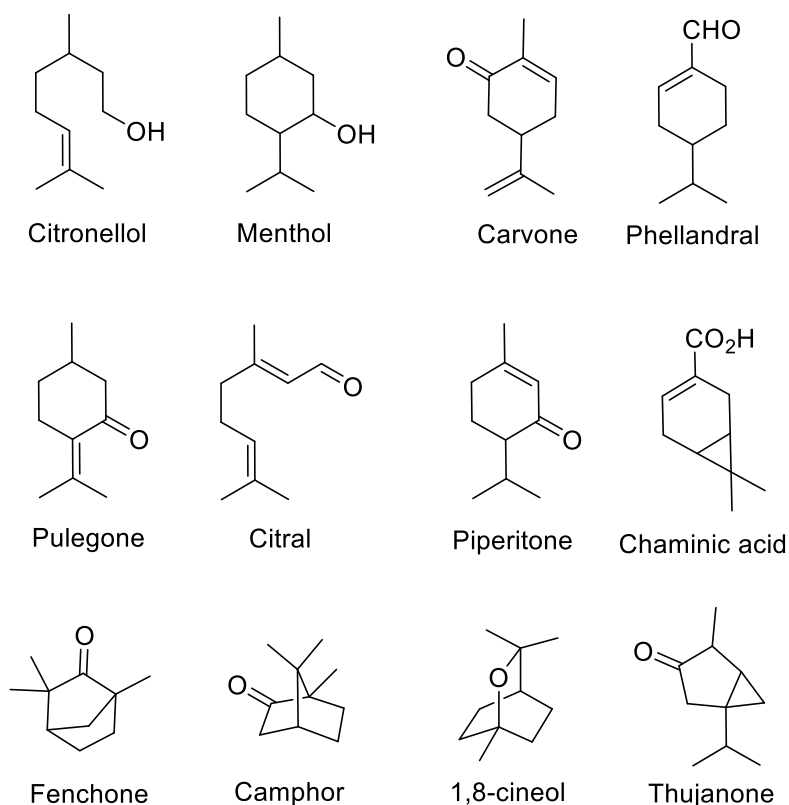


Figure 1.21 Examples of monoterpenes used in flavors, fragrances or medicines.

We have synthesized β -phellandrene (**22**) to study oxidation of β -phellandrene catalyzed by wild-type and mutant P450_{cam} to find new oxidized product(s).

1.4. Objectives of my thesis

My thesis revolves around two objectives: (1) the biodegradation and dehalogenations of the chlorinated compound endosulfan (**13**), and (2) efficient synthesis of β -phellandrene and its oxidation, catalyzed by cytochrome P450_{cam} wild-type and mutants.

In my first objective, the commonly found major metabolite of endosulfan, endosulfan diol (**14**) was used. The selected P450_{cam} mutants can convert ES (**13**) and ES diol (**14**), into dechlorinated products (substituted *o*-quinones and/ or catechols). Due to difficulty in isolating/detecting these product(s), quinones/ catechol metabolites in the assay were coupled to 4-aminoantipyrine (4-AAP, **26**), to give a highly colored polar

adduct. 4-AAP is known to produce a colored product when it couples with quinones (Lülsdorf et al., 2015; Vojinović et al., 2004). Kinetic studies with this coupled assay showed that the mutants, which had originally been selected on endosulfan (**13**), were significantly more effective at dechlorinating this and related compounds, such as the diol (**14**), than the wild-type. Based on these studies, we propose a mechanism by which the six chlorine atoms could be lost, after oxidation of the double bond.

In my second objective, racemic β -phellandrene was synthesized in three steps, starting with β -pinene. Using racemic mixture of β -phellandrene its oxidation, catalyzed by wild-type or *ES7 P450_{cam}*, was studied using an *in vitro* assay.

1.5. Thesis layout

This thesis is divided into five chapters. In this first chapter cytochromes P450, their catalysis and structures, endosulfan and β -phellandrene are introduced, and my objectives are described. In the second chapter, material and methods used in both projects, degradation of endosulfan and oxidation of β -phellandrene catalyzed by P450_{cam} mutants are described. The third chapter contains the results and discussion of the endosulfan degradation project. The fourth chapter contains the results and discussion of the β -phellandrene synthesis and oxidation by P450s. The fifth chapter describes conclusions from this work and suggestions for future experiments that should be done to further identify and characterize the oxidized product of β -phellandrene catalyzed by P450s.

Chapter 2. Materials and methods

Chemicals were of analytical grade and purchased from Sigma-Aldrich Canada (Oakville, Ontario). *m*-chloroperbenzoic acid (*m*-CPBA), endosulfan (a 2:1 mixture of α and β isomers commonly used in the field) and 1,4,5,6,7,7-hexachloro-5-norbornene-2,3-dicarboxylic anhydride (chlorendic anhydride), 4-aminoantipyrine (4-AAP), (-)- β -pinene, aluminum chloride (AlCl_3), methyltriphenylphosphonium bromide Sodium bis(trimethylsilyl)amide and Peroxidase from Horseradish (Type VI, HRP) were purchased from Sigma-Aldrich (Oakville, ON, Canada). *m*-CPBA was purified by reported methods (Armarego, 2003). Solvent evaporations were done on a Buchi Rotavapor (R-200), connected to a liquid nitrogen trap and a laboratory vacuum (Piab[®] LVH40VK) system. Centrifugations were carried out with a Beckmann Avanti J-26 XPI centrifuge (Mississauga, ON, Canada), equipped with JLA 8.1000 and JA 25.50 rotors. NMR spectra were obtained using Bruker AVANCE II 400 MHz and/or 600 MHz instruments. Chloride ion release was measured using an Orion[™] Chloride Electrode (9417BN) by Thermo Scientific (Ottawa, ON, Canada). Gas Chromatography-mass spectrometry (GC-MS) was performed on a Varian Saturn CP3800 GC, fitted with a 30 m SPB5 column (0.2 μm film thickness, 0.25mm internal diameter, Supelco, USA) and interfaced with a Saturn 2000 ion trap mass spectrometer. The GC oven was programmed as follows; 50 °C for 30 s; 7 °C/min to 150 °C, held for 1 min; then 15 °C/min to 250 °C, held 8 min. The ion trap mass detector was used in electron impact (EI, 70 eV) mode and full scanned over range m/z 50-550. Liquid chromatography-mass spectrum (LC-MS) was performed on an Agilent 6210 TOF LC-MS with a Halo[®] C18 column (2.7 μm , 2.1 x 30 mm, Advance Material Technologies, USA). Gradient was used: solvent A (10 % ACN, 5 mM NH_4OAc), and solvent B (90 % ACN, 5 mM NH_4OAc) on a gradient of 0 % \rightarrow 100 % solvent B over 5 min (flow rate of 0.6 mL/min). Acidified silica (silica Gel 60, 23-400 mesh) was prepared by adding into H_3PO_4 (1 ml per 100g of Silica) solution in methanol followed by decanting methanol and evaporation residual methanol using Rotavapor inside a fume hood.

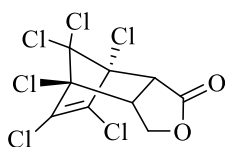
Site-directed mutagenesis of WT P450_{cam} was performed using the QuickChange Lightning site-directed mutagenesis kit (Agilent, Santa Clara, California, US). Primers for mutations were obtained from Integrated DNA Technologies, Inc. (Coralville Iowa, US) and sequencing was done by Eurofins Genomics (Louisville, KY, US).

Docking simulations were performed using Molecular Operating Environment (MOE 2019.01, Chemical Computing Group, Montreal, QC Canada) and images were prepared using PyMOL (The PyMOL Molecular Graphic System, Version 2.0 Schrodinger, LLC.).

2.1. Endosulfan diol biodegradation

2.1.1. Synthesis of substrates and standards

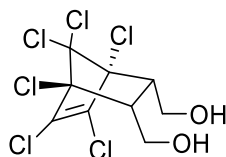
Preparation of endosulfan lactone (ES lactone, 15)



ES lactone **15**

1,4,5,6,7,7-hexachloro-5-norbornene-2,3-dicarboxylic anhydride (chlorendic anhydride, 95 mg, 0.25 mmol) was dissolved in 2 mL of THF (anhydrous), and the solution was added slowly into a suspension of NaBH₄ (20 mg, 0.5 mmol) in 1 mL of THF (anhydrous) at 4 °C and stirred for 20 minutes. Stirring was continued at room temperature for 15 hours. The reaction was quenched with 2 mL HCl (2 M). The product was salted out of the reaction mixture with NaCl (3 g). The organic product was extracted with ethyl ether (5 × 10 mL), and the extract was dried over Na₂SO₄. Solvent was evaporated and crude product was purified on a column of acidified silica, using solvent gradients (ethyl acetate 0 – 100 % with chloroform). The white solid endosulfan lactone **15** was obtained in 90 % yield (81 mg). ¹H NMR (CDCl₃, 400 MHz) δ 3.77 (d, *J* = 9.2 Hz, 1H), 3.85 (td, *J* = 8.9 Hz, 3.2 Hz, 1H), 4.24 (dd, *J* = 10.9 Hz, 3.2 Hz, 1H), 4.44 (dd, *J* = 11.0 Hz, 8.7 Hz, 1H). ¹³C NMR (CDCl₃, 100 MHz) δ 48.24, 52.0, 65.51, 79.77, 80.53, 103.71, 130.36, 132.24, 169.64. GC-MS (EI) *m/z* calculated for C₉H₄Cl₆O₂ [*M*+1]: 356.8.; found: 356.7.

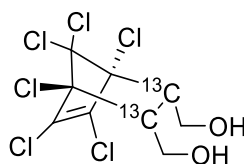
Synthesis of endosulfan diol (ES diol, **14**)



ES diol **14**

A solution of endosulfan lactone **15** (81 mg) in 2 mL of THF (anhydrous) was added slowly into a suspension of LiAlH_4 (20 mg, 0.5 mmol) in 1 mL of THF (anhydrous) at 4 °C and stirred. After 30 minutes, the temperature was increased, and stirring was continued at 40 °C for 6 hours. The reaction was quenched with ice (3 g) and acidified with 1 mL HCl (2 M). The crude organic product was salted out with NaCl (3 g). The organic product was extracted with ethyl ether (5 × 10 ml), and the extract was dried with Na_2SO_4 . The solvent was evaporated, and crude product was purified on a column of silica gel, using solvent gradients (ethyl acetate 0 – 100 % with chloroform). White solid endosulfan diol **14**, (45 mg, 0.125 mmol, yield 50%), MP 205-207 °C, IR spectrum, 3233 cm^{-1} (broad, OH stretch), $^1\text{H NMR}$ (CDCl_3 , 400 MHz) δ 3.03 (broad, s, 2H), 3.29 (m, 2H), 3.71 (m, 2H), 4.05 (d, $J = 11.6\text{ Hz}$, 2H). $^{13}\text{C NMR}$ (CD_3OD , 100 MHz) δ 51.45, 57.76, 80.59, 102.67, 130.70. GC-MS (EI) m/z calculated for $\text{C}_9\text{H}_8\text{Cl}_6\text{O}_2$ [M-17]: 342.9.; found: 342.9.

Synthesis of ^{13}C labeled ES diol



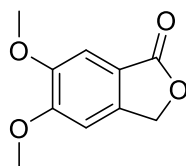
^{13}C -ES diol

Hexachlorocyclopentadiene (17 mg, 62 μmol) and maleic acid (2,3 – ^{13}C) (5 mg, 42 μmol) were added to a glass ampoule. The solvent free reaction mixture in the sealed glass ampoule was heated at 120 °C for 40 hours. During heating the reaction ampoule was contained in a secondary vented glass container for safety. On cooling the reaction mixture to room temperature, the crude product was recrystallized using hot water (~ 75 °C) to give a white solid ^{13}C -chlorendic acid (10 mg, 25 μmol , yield 60%). $^1\text{H NMR}$ (CDCl_3 , 400 MHz) δ 4.07 (s, 2H). $^{13}\text{C NMR}$ (CDCl_3 , 100 MHz) δ 54.52 (^{13}C labeled).

To synthesize ^{13}C -chlorendic acid anhydride, ^{13}C -chlorendic acid (10 mg, 25 μmol) CDCl_3 (1 ml) and acetyl chloride (150 μl , 2 mmol) were added in flame dried – reaction vial attached to water condenser. The reaction mixture was refluxed at 65 – 70 $^\circ\text{C}$ for 2 hours. Crude ^{13}C -chlorendic acid anhydride was obtained along with acetic acid and acetic anhydride by-products. ^1H NMR (CDCl_3 , 400 MHz) δ 4.17 (s, 2H). ^{13}C NMR (CDCl_3 , 100 MHz) δ 53.36 (^{13}C labeled). Crude ^{13}C -chlorendic acid anhydride was used further for ^{13}C -ES diol synthesis without further purification.

LiAlH_4 (775 mg, 20 mmol) was added to reaction vial having crude ^{13}C -chlorendic acid anhydride in CDCl_3 under N_2 gas atmosphere and stirring was continued overnight at room temperature. To quench the reaction, Fieser's workup (*Fieser and Fieser's Reagents for Organic Synthesis, Volume 1 | Wiley, n.d.*) was used. In summary, diethyl ether (20 ml) was added to dilute the reaction mixture, followed by H_2O (770 μl). The mixture was stirred on ice for 5 minutes. NaOH (15% solution, 770 μl) was added followed by H_2O (2.31 ml) and stirring was continued for 15 minutes at room temperature. Solid Na_2SO_4 was added to dry the mixture and the organic solution was filtered. Organic solvent was evaporated to give ^{13}C -ES diol (3 mg, 8 μmol). ^1H NMR (CDCl_3 , 400 MHz) 3.29 (m, 2H), 3.71-3.77 (m, 2H), 4.05 (dd, 2H). ^{13}C NMR (CD_3OD , 100 MHz) δ 51.61 (^{13}C labeled).

Synthesis of 5,6-dimethoxy-2-benzofuran-1(3H)-one (23)

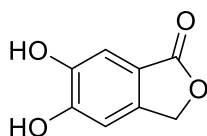


23

Paraformaldehyde (5 g) was added into aqueous hydrogen chloride (37%, 100 ml) and additional hydrogen chloride gas was bubbled through the solution while stirring at room temperature. After 1 hour of stirring, to this solution was added 3,4-dimethoxy benzoic acid (0.6 g), and the reaction mixture was refluxed for 6 hours. Hydrogen chloride gas was continuously bubbled during this time. Then, reaction mixture was cooled and stirred at room temperature for 3 days. Organic product was extracted with ethyl acetate (3 \times 100 ml). The organic phase was neutralized with NaOH (0.1M, 3 \times 20 ml) and the extract was dried with Na_2SO_4 . The solvent was evaporated, and crude product was purified on a column of silica gel, using solvent gradients (ethyl acetate 0 – 100 % with

chloroform). Solid 5,6-dimethoxy-2-benzofuran-1(3H)-one (**23**) was obtained (138 mg). ^1H NMR (CDCl_3 , 400 MHz) δ 3.96 (s, 3H), 4.00 (s, 3H), 5.25 (s, 2H), 6.93 (s, 1H), 7.33 (s, 1H). ^{13}C NMR (100 MHz, CDCl_3) δ 56.23, 56.38, 69.15, 103.53, 106.01, 117.52, 141.10, 150.40, 154.86, 171.39.

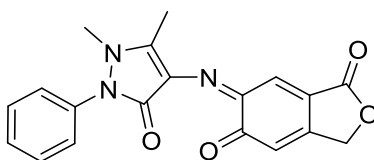
Synthesis of 5,6-dihydroxy-2-benzofuran-1(3H)-one (**24**)



24

To solution of 5,6-dimethoxy-2-benzofuran-1(3H)-one (**23**) (96 mg) in dry CH_2Cl_2 (2 mL), BBr_3 solution (1 M in CH_2Cl_2 , 1.3 ml) was added dropwise under N_2 atmosphere at $-78\text{ }^\circ\text{C}$. After 5 minutes, the temperature was increased slowly, and stirring was continued at room temperature for 7 hours. Then, reaction mixture was cooled again to $-78\text{ }^\circ\text{C}$ and quenched with CH_3OH (25 mL). Once the mixture had warmed to room temperature, water (10 mL) was added, the organic product was extracted with ethyl acetate ($3 \times 30\text{ mL}$), and the extract was dried with Na_2SO_4 . The solvent was evaporated to obtain 5,6-dihydroxy-2-benzofuran-1(3H)-one **24** (78 mg, yield 98 %). ^1H (400 MHz, $\text{DMSO}-d_6$) δ 5.17 (s, 2H), 6.93 (s, 1H), 7.07 (s, 1H), 9.68 (s, 1H), 10.21 (s, 1H). ^{13}C NMR (100 MHz, $\text{DMSO}-d_6$) δ 69.34, 108.66, 109.92, 115.87, 140.81, 147.17, 152.80, 171.33.

Preparation of the 4-aminoantipyrine (4-AAP) adduct of compound (**25**)



25

5,6-Dihydroxy-2-benzofuran-1(3H)-one (**24**) with varying concentrations of (10 μM to 300 μM) was added to potassium phosphate buffer (50 mM phosphate, 200 mM KCl, pH 7.4, 1 mL) with horseradish peroxidase (HRP, 1 unit/ml), H_2O_2 (30 % solution, 0.4 μl per ml) and 4-aminoantipyrine (4-AAP **26**, 2 mM). The reaction mixtures were monitored by UV-Visible spectroscopy and absorbance at 506 nm was recorded. To choose optimum wavelength of coupled product, catechol and phenol were used and coupled with 4-AAP (**26**) under same conditions in control experiments. Later, for steady-state kinetic assay of

ES diol (**14**) and other substrates, the assay was calibrated using 5,6-dihydroxy-2-benzofuran-1(3H)-one – 4-AAP adduct (**25**) at known concentrations, ranging (10 μ M to 300 μ M). Sample of coupled product (**25**) was analyzed by LC-MS.

2.1.2. Molecular biology methods

Transformation of P450_{cam} mutants into an E. coli strain that co-expresses putidaredoxin (PdX) and putidaredoxin reductase (PdR)

To ensure that the P450 has co-expressed redox partners, the plasmids (pALXtreme-1a) of P450_{cam} mutants (*ES1 – ES7*) previously selected on endosulfan (Kammoonah et al., 2018) and WT P450_{cam} (in pET-22b(+)) were transformed into a strain of *E. Coli* BL21(DE3) which contained a previously constructed bicistronic recombinant expression vector (pET-30 Xa/LIC) of putidaredoxin reductase (PdR, CamA) and putidaredoxin (PdX, CamB) using heat shock method (Kammoonah et al., 2018). To isolate the plasmid for this transformation, cultures of each P450_{cam} ES mutant in *E. coli* (BL21(DE3)) were grown individually in Luria Bertani (LB) media (5 mL) containing kanamycin (50 mg/L), and the plasmid was isolated using a Qiagen (QIAprep® Spin miniprep) kit following the instructions. Final DNA solutions were in water (dd).

For transformation, *E. coli* (BL21(DE3)) competent cells (100 μ L) with PdX and PdR were mixed with 10 μ L of P450_{cam} mutant or WT P450_{cam} plasmid (1 ng/ μ L). The sample was incubated on ice (4 °C) for 45 minutes. Then the sample was heat-shocked using a water bath set at 42 °C for 30 seconds. Next, the sample was placed on ice for 2 minutes. SOC medium (1 mL) was added to the tube and the sample was incubated at 37 °C, 250 rpm for 3 hours. Aliquots with different volumes, ranging from 100 μ L to 200 μ L, were plated on LB agar plates containing 50 mg/L of kanamycin and incubated overnight at 37 °C. Individual colonies were picked, grown in 2 mL LB medium (with kanamycin 50 mg/L), and stored as glycerol stocks.

Expression of P450_{cam} mutants and WT in E. coli with PdR and PdX and production of lysates

Each *E. coli* BL21(DE3) strain containing the WT or the mutated cytochrome P450_{cam} plasmid, putidaredoxin (PdX) and putidaredoxin reductase (PdR) was grown in Luria Bertani (LB) medium (50 mL) with kanamycin 50 mg/L, overnight at 37 °C, 250 rpm.

The overnight grown culture was inoculated into fresh LB media (1 L, kanamycin 50 mg/L) and incubated at 37 °C, 250 rpm until an optical density (OD at 600 nm) of ~0.8–0.9 was reached. Cells were harvested by centrifugation at 6000 rpm (4355 × g) at 4 °C for 30 minutes. Collected cell pellets were resuspended in fresh LB medium (1 L, kanamycin 50 mg/L) and incubated for 30 minutes at 37 °C (250 rpm). IPTG (1 mM) and trace additives (FeCl₂ (0.1 μM), 5-aminolevulinic acid (1 mM), Vitamin B1 (10 μM), Na₂S·9H₂O (0.1 μM) and Riboflavin (1 μM)) were added. Incubation was continued for 4–5 hours at 27 °C, with shaking at 250 rpm. After induction was complete, the cells were harvested at 7000 rpm (8983 × g) for 30 minutes and stored in a minimum amount of lysis buffer (20 mM phosphate buffer, pH 7.4 with 100 mM KCl) overnight. Stored cell pellets were resuspended in lysis buffer (50 mL), and disodium EDTA (0.1 mM) was added. The suspension was stirred for 15 min at 4 °C and the pH was adjusted to 7.4 using 0.1 M KOH. Protease inhibitor cocktail: Phenylmethylsulfonyl fluoride (PMSF, 100 μL of 40 mg/mL in EtOH), 100 μL of a mixture of 1 mg of 4-(2-aminoethyl) benzenesulfonyl fluoride hydrochloride (AEBSF), 0.2 mg leupeptin, 0.2 mg aprotinin, and 100 mg lysozyme were added and stirring continued at 4 °C for 40 min. Sonication was carried out in a Branson Ultrasonic sonicator at 50% duty cycle for 10 min. MgSO₄ (10 mM) was added, and the pH was readjusted to 7.4 using 0.1 M KOH. RNase (100 μL of 10 mg/mL solution) and DNase (100 μL of 1 mg/mL solution) were added, and the cell suspension was stirred for at 4 °C for 30 min, followed by sonication for 5 min. The lysate was homogenized with a Potter-Elvehjem tissue homogenizer, and then centrifuged at 7000 rpm (8983 × g), 4 °C, for 30 min. The crude protein in the supernatant was then analyzed for total protein and P450 concentration before using in steady-state kinetic assays.

Site-directed mutations of WT P450_{cam} for His₆ – tagged P450_{cam} mutant protein expression

Neither the WT nor the mutants we used in the previous section had a cleavable purification tag. Therefore, to facilitate expression and purification of the P450 mutants, we performed site-directed mutagenesis on the WT P450_{cam} plasmid (pET-30 Xa/LIC), using 'QuickChange Lightning Multi Site-directed mutagenesis Kit (Agilent)' according to instructions. In summary, ds DNA WT P450_{cam} plasmid template (isolated using Qiagen's QIAprep® Spin miniprep) was used. Using 'QuickChange Lightning Multi Site-directed mutagenesis Kit' components: 10 × QuickChange lightning multi reaction buffer (2.5 μL), Quick Solution (0.6 μL), ds DNA WT P450_{cam} (100 ng), mutagenic primers (100 ng each

primer, see primers list Appendix A1), dNTP mix (1 μ L), QuickChange Lightning Multi enzyme blend (1 μ L) and dd H₂O (to make total 25 μ L). The PCR program was: 1 cycle of denaturation at 95 °C for 3 min, followed by 30 cycles of 95 °C (1.5 min), 55 °C (1 min) and 65 °C (12 min). Final extension was at 65 °C for 5 min. The resulting amplified product was treated with Dpn I restriction enzyme to digest the parent DNA strand (37 °C for 5 min).

Dpn I treated DNA (1.5 μ L) was transformed into XL 10-Gold ultracompetent cells (pre-chilled, 45 μ L) on ice (30 min) followed by heat-pulse at 42 °C (40 seconds). After incubating on ice (2 min), 0.5 mL of NYZ⁺ broth added and incubated at 37 °C (1 hour). This culture (50 μ L) was plated on LB – agar plates (kanamycin 30 mg/L) and incubated overnight at 37 °C. A single colony was transferred to SOC media (kanamycin 30 mg/L) and incubated at 37 °C and 200 rpm overnight. The overnight grown culture was used to isolate DNA using Qiagen (QIAprep[®] Spin miniprep) kit following the instructions. DNA was sequenced (Eurofins Genomics, Louisville, KY) to verify the mutations (see Appendix A14 to Appendix A20). The isolated plasmid was then transferred to *E. coli* BL21(DE3) competent cells (Novagen, EMD Millipore Sigma, Etobicoke, Ontario, Canada) using heat-shock method as described earlier.

WT P450_{cam} and P450_{cam} mutants (His₆ tagged) protein expression and purification

Each *E. coli* BL21(DE3) strain containing the mutated cytochrome WT P450_{cam} plasmid, and P450_{cam} mutant (*ES2*, *ES5*, *ES6* and *ES7*) were expressed as described. Induced cultures were harvested, and cells were lysed as described above. The crude lysate was dialyzed against phosphate buffer (50 mM phosphate buffer, pH 7.4 with 200 mM KCl) overnight using 3.5 KDa (MWCO) dialysis tubing (cat # D304, Biodesign Dialysis tubing[®], NY). Dialysate was purified using Nickel affinity column (Ni⁺²) loaded with His-Bind resin[®] (Novagen) and eluted with increasing Imidazole concentrations (3 – 25 mM) in phosphate buffer (50 mM phosphate buffer, pH 7.4 with 200 mM KCl). Fractions with P450_{cam} (analyzed by UV-Vis and SDS Page) were pooled and dialyzed against phosphate buffer (4 L, 20 mM Tris buffer, pH 7.4 with 50 mM KCl and 1 mM CaCl₂) to remove imidazole before His₆ tag cleavage. His-tag was cleaved using Factor Xa enzyme (Novagen) by adding 10 μ L of a 150 units/mL of enzyme per 2 mg of purified protein and incubating at room temperature for 36 – 48 hours. Factor Xa enzyme was removed by Xarrest[™] Agarose (Novagen) and His₆ tag fragment was removed by Nickel affinity

column (Ni^{2+}) loaded with His-Bind resin[®]. Purified P450_{cam} protein was analyzed by SDS Page (see Appendix A4) and UV-Visible spectroscopy (see below) before kinetic studies.

2.1.3. Assays and spectroscopy of P450 enzymes

Analysis of protein samples for P450 concentration

Concentration of P450 in each crude lysate of P450_{cam} mutants and WT P450_{cam} was measured by UV analysis (at 280 nm total protein, 418 nm for mutants P450_{cam} and WT P450_{cam}) as described previously (Kammoonah et al., 2018). The affinity tag purified and Factor Xa cleaved P450 mutants and WT were also analyzed by CO difference spectroscopy. The UV (400-500nm) spectra of oxidized P450_{cam} mutants and WT P450_{cam} were recorded in phosphate buffer (50 mM phosphate buffer, pH 7.4 with 200 mM KCl). CO gas was bubbled for 2 minutes (1 bubble per second) followed by addition of sodium dithionite ($\text{Na}_2\text{S}_2\text{O}_4$, few grains) to reduce the P450 heme iron. UV spectra were recorded again (400-500 nm) to see the Fe-CO peak at 450 nm (see Appendix A5).

Steady-state kinetic assays for endosulfan diol (ES diol 14) with the crude lysates of P450_{cam} mutant(s) using 4-aminoantipyrine (4-AAP) coupled assay with horseradish peroxidase (HRP) and H₂O₂

Steady-state kinetic assays were performed in 1 mL potassium phosphate buffer (50 mM phosphate, 200 mM KCl, pH 7.4) with varying concentrations of endosulfan diol (50 μM to 500 μM), 5 μM of crude protein P450_{cam} mutant, NADH (800 μM), horseradish peroxidase (HRP, 1 unit/ml), H_2O_2 (30 % solution, 0.4 μl per ml) and 4-aminoantipyrine (4-AAP **26**, 2 mM). The reaction mixtures were monitored by UV-Visible spectroscopy for 3 and/or 20 minutes at 506 nm. Three controls were run: 1) in the absence of the substrate, 2) without HRP, or 3) without P450_{cam}. The kinetic assay was performed by first adding the phosphate buffer, 4-AAP, H_2O_2 , NADH, HRP and P450_{cam} mutant protein, then adding the substrate (α -ES/ ES diol) and recording the absorbance at 506 nm. The assay was calibrated using 5,6-dihydroxy-2-benzofuran-1(3H)-one – 4-AAP adduct **25** at known concentrations, ranging from 10 μM to 300 μM , prepared under the same conditions as the enzymatic assay.

To obtain initial rates, the amount of product was divided by 15 s, the time it took to insert the cuvette in the holder and start the monitoring of the reaction. The reason for doing this was that there was a rapid burst of activity, followed by a flattened progress

curve (e.g. see Figure 3.2). In many cases, by the time absorbance at 506 nm was detected, the progress curve was already flattening. Thus, the kinetic data presented here correspond to a 15 s endpoint and not the true initial rate.

For assays with purified P450_{cam} mutants (K314E, *ES6* and *ES7*) and WT P450_{cam} (1 μM of the purified enzyme, and redox partners PdX and PdR 3 μM) were used. Otherwise, the assay was the same as for the crude lysates.

Using *m*-CPBA as a shunting agent, assay was repeated with purified *ES7* P450_{cam} without using redox partners (PdX and PdR). *ES7* mutant (1 μM of the purified enzyme), *m*-CPBA (1 mM) and ES diol (5 μM to 100 μM) were used. Otherwise, the assay was the same as the crude lysate.

Titration of endosulfan diol (ES diol, 14) and (+)-camphor (10) with the purified P450_{cam} mutant(s) and dissociation constant (K_d)

Purified P450_{cam} mutant proteins (3 μM) were prepared in phosphate buffer (50 mM phosphate buffer, pH 7.4 with 200 mM KCl). ES diol **14** (2.5 μM – 250 μM) and (+)-camphor (1 μM – 50 μM) were added in aliquots using a Hamilton syringe, and UV-Visible spectra were recorded (350-500 nm, see Figure 3.5).

The total change in absorbance (ΔA) at 417 nm (substrate free) and 390 nm (with substrate) was plotted the concentration of substrate added, and this was used to calculate dissociation constant (*K_d*) using a single site binding model in GraphPad Prism® (GraphPad Software Inc. CA).

$$\Delta A = (\Delta A_{390}) + (\Delta A_{417})$$

Chloride release from endosulfan diol with a NADH regeneration system and chloride release detection by chloride electrode

The assay was performed in 5 mL potassium phosphate buffer (100 mM phosphate, pH 7.4) with endosulfan diol **14** (300 μM or 500 μM), purified WT-P450_{cam} or *ES7* mutant (1 μM), purified redox partners PdX (5 μM), and PdR (1 μM), NADH (500 μM), and alcohol dehydrogenase (350 units).

Chloride (Cl⁻) ion concentrations were measured using a chloride ion selective electrode (chloride ISE) before and after adding ES diol **14**. Samples (1 ml) were taken

before and after adding ES diol, and 4-AAP coupled assay with HRP and H₂O₂ were performed as described above. To measure interference with chloride readings, control experiments were performed using known sodium chloride solution and addition of 1) NADH, or 2) NAD⁺ (see Appendix A7).

Chloride release from endosulfan diol with *m*-CPBA as a shunt and chloride release detection by a chloride selective electrode

The assay was performed in 5 mL potassium phosphate buffer (100 mM phosphate, pH 7.4) with ES diol **14** (300 μM or 500 μM), purified WT-P450_{cam} or *ES7* mutant (5 μM), *m*-CPBA (1 mM). Chloride (Cl⁻) ion concentrations were measured using a chloride ion selective electrode (chloride ISE) before and after adding ES diol **14**. Samples (1 ml) were taken before and after adding ES diol **14**, and 4-AAP coupled assay with HRP and H₂O₂ were performed as described above. To measure interference with chloride reading control experiments were performed using known sodium chloride solution and addition of 1) *m*-CPBA, and 2) chlorobenzoic acid (see Appendix A9).

At the end of the assay, the organic products were extracted with ethyl acetate (3 × 100 ml) and dried with Na₂SO₄. The solvent was evaporated, and crude extract was analyzed by ¹H NMR and LC-MS.

Extraction and identification of products; assays with ¹³C labeled substrate (¹³C-ES diol)

The assay was performed in 4 mL potassium phosphate buffer (100 mM phosphate, pH 7.4) with ¹³C-ES diol (300 μM), purified *ES7* mutant (5 μM), *m*-CPBA (1 mM). Chloride (Cl⁻) ion concentrations were measured using a chloride ion selective electrode (chloride ISE) before and after adding ¹³C-ES diol **14**. Samples (0.5 ml) were taken before and after adding ¹³C-ES diol, and 4-AAP coupled assay with HRP and H₂O₂ were performed as described above. A control experiment with non-labelled ES diol was also performed under same conditions.

At the end of the assay, the organic products were extracted with ethyl acetate (3 × 100 ml) and dried with Na₂SO₄. The solvent was evaporated, and crude extract was analyzed by ¹³C NMR.

2.1.4. *In silico* docking studies

Docking simulations were performed using Molecular Operating Environment (MOE, Chemical Computing Group, Montreal, QC Canada). The amino acids and 3D structure information of P450_{cam} (CYP101A1) were obtained from Protein Data Bank. P450_{cam} with PDB code 2L8M (Reduced and CO-bond in the presence of camphor) was used for docking studies (Asciutto et al., 2011). The protein PDB file was imported to MOE, and residue was mutated to generate the P450_{cam} mutants (*ES1-ES7*, *IND1*, and *K314E*). For WT and mutants P450_{cam} protein preparation for docking, protocol was followed as described by Kammoonah et al. (Kammoonah et al., 2018). In summary, camphor and carbon monoxide molecules are removed from the PDB structure. Each residue of the protein was protonated at pH 7.4, temperature 298 K, and 0.25 M salts, and the charges were assigned according to default settings using the “Compute | Protonate 3D” algorithm (Labute, 2009) followed by energy minimization of the structure using the “Amber10:EHT” forcefield. Prior to docking, potential docking sites were identified on the protein by applying the “site finder” algorithm (Volkamer et al., 2010) to the selected atoms of the P450 polypeptide and the heme group. The algorithm returns binding sites on the protein, ranked according to size. For these simulations, the highest-ranked site (Site 1) was selected by selection of placeholders known as “dummies” in the program. Ligands (shown in Figure 2.1) were constructed in MOE using “builder” and a database of ligands was generated as an “.mdb” file.

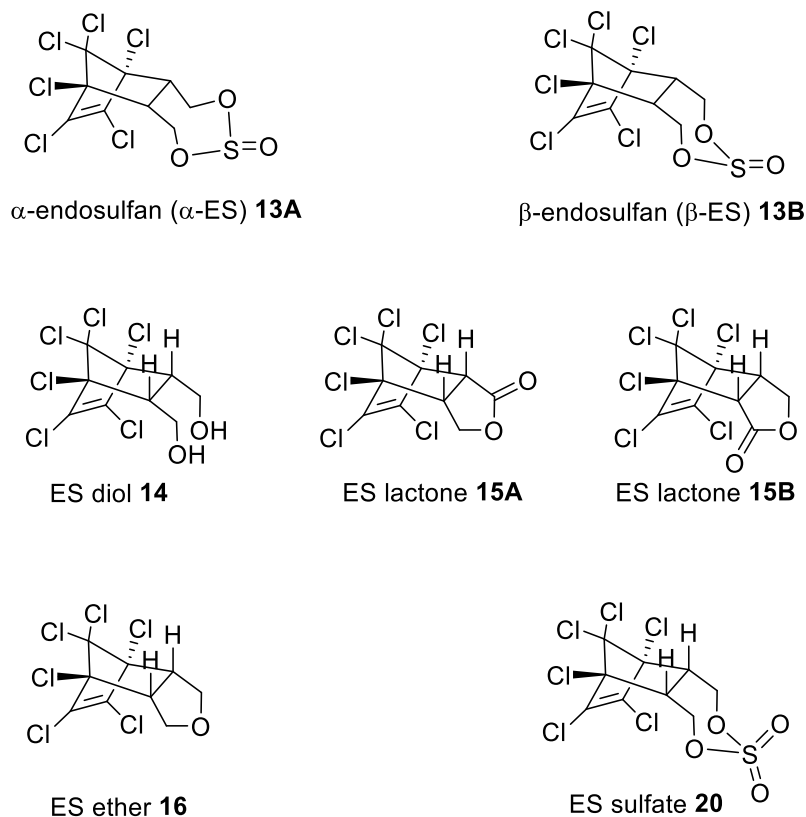


Figure 2.1 List of endosulfan and metabolites used as ligands for *in silico* docking studies.

Ligands were docked using all atoms of the polypeptide and the heme prosthetic group as the “receptor”. Triangle matcher was the algorithm used for placement of the ligands in the selected site. Ligands poses were scored by London dG, and refined for an induced fit. Final scoring of poses utilized the GBVI/WSA dG (Generalized Born Volume Integral/ Weighted surface area) algorithm (Corbeil et al., 2012; Labute, 2008; Wojciechowski & Lesyng, 2004); a maximum of 30 poses were retained. The distribution of poses was estimated based on each structure’s conformational energy. Conformational energy (E_{conf}) was obtained from the database with the docking results and was in kcal/mol. Distance between heme-iron to C1, C2 (C=C bond), C3 and C4 (Figure 2.2) of each ligand was recorded to take the average. The pose with minimum distance between heme-iron to C1 and C2 is selected to compare it with the kinetic data obtained above.

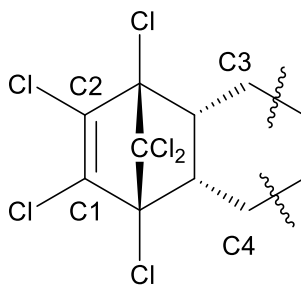
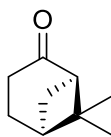


Figure 2.2 Carbon number assigned to endosulfan ligands used to calculate the distance to the heme-iron in MOE docking studies.

2.2. β -phellandrene oxidation

2.2.1. Synthesis of racemic β -phellandrene (22)

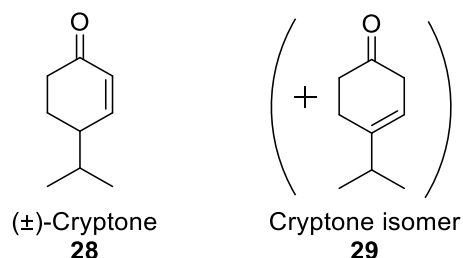
Synthesis of (+)-nopinone (27) from (-)- β -pinene (21)



27

(-)- β -Pinene **21** (1.02 g, 7.54 mmol) was added to a solvent mixture of water (15 ml), CCl_4 (10 ml) and MeCN (10 ml). NaIO_4 (6.7 g, 31.3 mmol) and $\text{RuCl}_3 \cdot n\text{H}_2\text{O}$ (catalyst, 51 mg) were added into reaction mixture. The reaction mixture was stirred for 2 hours at room temperature. After 2 hours of stirring, 20 ml of water was added, and the organic product was extracted using dichloromethane (3×100 ml). The organic layer was filtered through celite and charcoal mixture and was dried over Na_2SO_4 . The organic solvent was removed by distillation at 40-50 °C, giving an oily crude product as the residue. The crude product was purified using column chromatography (EtOAc: Hexanes 1:9), giving (+)-nopinone **27** (0.86 g, 6.20 mmol, 84%). $[\alpha]_{\text{D}}^{20} +27.43$ ($c = 1.29$ in CHCl_3). ^1H NMR (CDCl_3 , 400 MHz) δ 0.87 (s, 3H), 1.35 (s, 3H), 1.60 (d, $J = 10.1$ Hz, 1H), 1.90 – 2.01 (m, 1H), 2.07 (dddd, $J = 13.3$ Hz, 11.1 Hz, 3.9 Hz, 2.1 Hz, 1H), 2.21 – 2.30 (m, 1H), 2.36 (ddd, $J = 19.1$ Hz, 9.1 Hz, 2.1 Hz, 1H), 2.48 – 2.67 (m, 3H). ^{13}C NMR (CDCl_3 , 100 MHz) δ 21.42, 22.13, 25.28, 25.91, 32.80, 40.42, 41.21, 58.00, 214.96. NMR spectra were consistent with the reported (Kawashima et al., 2014).

Synthesis of racemic cryptone (**28**) from (+)-nopinone (**27**)

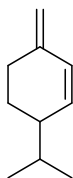


(+)-nopinone (**27**) (2.6 g, 19.5 mmol) was added in CH₂Cl₂ (75 ml) and stirred on ice. Powdered AlCl₃ (3.9 g, 29 mmol) was added into the reaction flask and the mixture was stirred for 90 minutes on ice (4 °C) under N₂. The reaction mixture was poured on ice (20 g), and 2M HCl was added to dissolve AlCl₃. The organic product was extracted with CH₂Cl₂ (3 × 100 ml). The organic layer was dried over MgSO₄, and solvent was removed at 4 °C on ice under vacuum (using a rotary evaporator). Crude product was purified, and isomers were separated using silica column. Elution with hexanes/ ethyl acetate 9:1 gave racemic (±)-cryptone **28** as a light brown oily product (2.1 g, 15.1 mmol, 77%). [α]_D²⁰ -2.26 (c = 0.15 in CHCl₃). ¹H NMR (CDCl₃, 400 MHz) δ 0.98 (d, *J* = 5.9 Hz, 3H), 1.00 (d, *J* = 5.9 Hz, 3H), 1.74 – 1.90 (m, 2H), 2.03 (dtd, *J* = 13.7 Hz, 4.6 Hz, 1.6 Hz, 1H), 2.28 – 2.42 (m, 2H), 2.54 (dtd, *J* = 16.7, 4.3, 1.0 Hz, 1H), 6.04 (ddd, *J* = 10.3 Hz, 2.7 Hz, 1.0 Hz, 1H), 6.92 (ddd, *J* = 10.3 Hz, 2.4 Hz, 1.6 Hz, 1H). ¹³C NMR (CDCl₃, 100 MHz) δ 19.48, 19.64, 25.27, 31.52, 37.42, 42.53, 129.70, 154.32, 200.11. NMR spectra were consistent with the reported (Mori, 2006).

Cryptone isomer **29** (0.26g, 1.9 mmol, 10%): ¹H NMR (CDCl₃, 400 MHz) δ 1.06 (d, *J* = 6.9 Hz, 6H), 2.33 (hept, *J* = 7.2 Hz, 6.7 Hz, 1H), 2.39 – 2.46 (m, 2H), 2.49 (dd, *J* = 7.3 Hz, 5.3 Hz, 2H), 2.87 (dd, *J* = 3.7 Hz, 1.7 Hz, 2H), 5.47 (td, *J* = 3.7 Hz, 1.2 Hz, 1H). ¹³C NMR (CDCl₃, 100 MHz) δ 21.13, 26.34, 34.74, 38.88, 39.64, 115.45, 144.61, 211.46.

The reaction of the ring opening of nopinone (**27**) to give cryptone (**28**) and the ketone (**29**), was monitored by taking 0.5 ml of reaction sample at different time intervals and analyzed by GC after mini work-up as above.

Synthesis of β -phellandrene (22) from cryptone (28)



22

Sodium bis(trimethylsilyl)amide (NaHMDS, 4.5 g, 24.6 mmol) was added slowly into a flask containing methyl triphenylphosphonium bromide ($\text{Ph}_3\text{PCH}_3\text{Br}$, 8.8 g, 24.6 mmol) under N_2 . The reaction mixture was stirred for 6 hours on ice, followed by dropwise addition of (\pm)-cryptone (2.6 g, 19.4 mmol) under N_2 . Stirring was continued overnight at room temperature. After 18 hours of stirring, the reaction was quenched using a mixture of water and pentane (1:1, 100 ml). The organic product was extracted with pentane (3 \times 100 ml). The organic layer was dried over Na_2SO_4 , and organic solvent was evaporated at 4 $^\circ\text{C}$ on ice in a rotary evaporator. The crude product was purified using column chromatography (100% pentane) to give scalemic β -phellandrene (1.8 g, 13.6 mmol, 70%). $[\alpha]_D^{20}$ -1.33 (c = 1.0 in CHCl_3). ^1H NMR (CDCl_3 , 400 MHz) δ 0.92 (d, J = 6.8 Hz, 3H), 0.94 (d, J = 6.8 Hz, 3H), 1.42 (tdd, J = 12.7 Hz, 10.0 Hz, 3.9 Hz, 1H), 1.66 (dq, J = 13.6 Hz, 6.8 Hz, 1H), 1.76 – 1.82 (m, 1H), 2.05 – 2.12 (m, 1H), 2.26 – 2.36 (m, 1H), 2.47 (dt, J = 14.8 Hz, 4.3 Hz, 1H), 4.76 (s, 1H), 4.78 (s, 1H), 5.78 (d, J = 10.0 Hz, 1H), 6.17 (dd, J = 10.0 Hz, 2.6 Hz, 1H). ^{13}C NMR (CDCl_3 , 100 MHz) δ 19.50, 19.70, 25.72, 30.19, 31.92, 42.07, 109.91, 129.49, 134.24, 143.74. NMR spectra were consistent with the reported ones (Bergstrom et al., 2006).

2.2.2. Enzymatic Assays

WT P450_{cam} and ES7 mutant (His₆ tagged) protein expression and purification

Each *E. coli* BL21(DE3) strain containing WT P450_{cam} plasmid and ES7 P450_{cam} mutant, were expressed as described. Induced cultures were harvested, and cells were lysed as described above. The crude lysate was dialyzed against phosphate buffer (50 mM phosphate buffer, pH 7.4 with 200 mM KCl) overnight using 3.5 KDa (MWCO) dialysis tubing (cat #D304, Biodesign Dialysis tubing[®], NY). Dialysate was purified using Nickel affinity column (Ni^{+2}) loaded with His-Bind resin[®] (Novagen) and eluted with increasing Imidazole concentrations (3 – 25 mM) in phosphate buffer (50 mM phosphate buffer, pH

7.4 with 200 mM KCl). Fractions with P450_{cam} (analyzed by UV-Vis and SDS Page) were pooled and dialyzed against phosphate buffer (4 L, 20 mM Tris buffer, pH 7.4 with 50 mM KCl and 1 mM CaCl₂) to remove imidazole before His₆ tag cleavage. His-tag was cleaved using Factor Xa enzyme (Novagen) by adding 10 µL of enzyme per 2 mg of protein and incubating at room temperature for 36 – 48 hours. Factor Xa enzyme was removed by Xarrest™ Agarose (Novagen) and His₆ tag fragment was removed by Nickel affinity column (Ni²⁺) loaded with His-Bind resin®. Purified P450_{cam} protein was analyzed by SDS Page (see Appendix A4) and UV-Visible spectroscopy (see below) before kinetic studies.

Titration of β-phellandrene with the purified WT P450_{cam} or ES7 mutant, and dissociation constant (K_d)

Purified WT P450_{cam} and ES7 proteins (1.5 µM) were prepared in phosphate buffer (50 mM phosphate buffer, pH 7.4 with 200 mM KCl). β-phellandrene (1 µM – 37 µM) was added in aliquots using a Hamilton syringe, and UV-Visible spectra were recorded (350-500 nm, see Figure 4.2).

The total change in absorbance (ΔA) at 417 nm (substrate free) and 390 nm (with substrate) was plotted against the concentration of substrate added, and this was used to calculate the dissociation constant (K_d) using a single-site binding model in GraphPad Prism® (GraphPad Software Inc. CA).

$$\Delta A = (\Delta A_{390}) + (\Delta A_{417})$$

In-vitro assays of β-phellandrene oxidation using WT or ES7 P450_{cam} with m-CPBA as a shunt

In vitro enzymatic assays were performed in 1 mL potassium phosphate buffer (50 mM phosphate, 100 mM KCl, pH 7.4) that contained P450_{cam} or ES7 (5 µM), *m*-CPBA (1 mM), and substrate β-phellandrene (1 mM) in three replicates. Three control experiments were run: (1) No substrate (P450_{cam} and *m*-CPBA), (2) No enzyme (*m*-CPBA with substrate), (3) camphor as substrate (positive control, with enzyme and *m*-CPBA). The reaction mixtures were incubated for 20 minutes at room temperature (~22 °C) and extracted with chloroform (10 µM indanone as internal standard) (2 × 500 µl). The organic extracts were dried over Na₂SO₄ and analyzed by GC-MS.

2.2.3. *In silico* docking studies

For WT P450_{cam} and ES7 mutant, *in silico* docking was done using protocol described above (section 2.1.4) using β -phellandrene as ligand. Ligands (β -phellandrene, (-)-**22a** and (+)-**22b**) were constructed in MOE using “builder”, as described above.

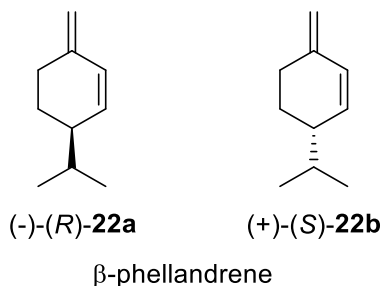


Figure 2.3 Enantiomers of β -phellandrene used as ligands in MOE docking studies.

Distance between heme-iron to C4, C5 and C6 (Figure 2.4) of each ligand was recorded. The poses with minimum distance between heme-iron to C4, C5 and C6 are selected to find potential regioselectivity by P450_{cam} for β -phellandrene oxidation.

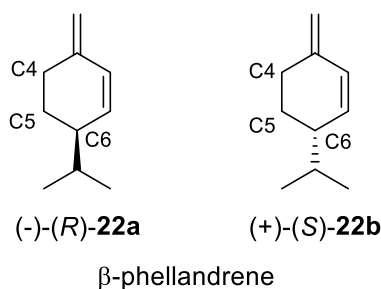


Figure 2.4 Carbon number assigned to ligands (β -phellandrene) used to calculate the distance to the heme-iron in MOE docking studies.

Chapter 3. Endosulfan diol degradation by P450_{cam} mutants

3.1. Results

3.1.1. Mutants obtained

The mutants obtained by sequence saturation mutagenesis (SeSaM) are listed in Table 3.1. In this ES-selected set of mutants, two mutations occurred twice: K314E and D297N. Furthermore, residue A296 was found to have mutated twice, but to different residues: A296V (in ES2) and A296P (in ES5). The selected variants had more than one mutation, except ES5 and ES6 (G120S). Interestingly, mutation of K314 was also noticed in the set of mutants selected on 3-chloroindole we labelled *IND* (Kammoonah et al., 2018), and residue V247 was mutated to F in two cases (ES7 and *IND1*).

Table 3.1 Mutations of P450_{cam} discovered previously by selection of a SeSaM library on minimal media containing endosulfan (13) and *m*-CPBA

Mutant name	Mutations
ES1	T56A/N116H/D297N
ES2	F292S/A296V/K314E/P321T
ES3	Q108R/R290Q/I318N
ES4	S221R/I281N
ES5	A296P
ES6	G120S
ES7	V247F/D297N/K314E

3.1.2. Coupled assay optimization

The selected P450_{cam} mutants can convert ES (13) and ES diol (14), into dechlorinated products (substituted *o*-quinones and/ or catechols). These metabolites were coupled with 4-AAP to give highly colored adduct (Figure 3.1). The dye 4-AAP is known to produce a colored product when it couples with quinones (Lülsdorf et al., 2015; Vojinović et al., 2004).

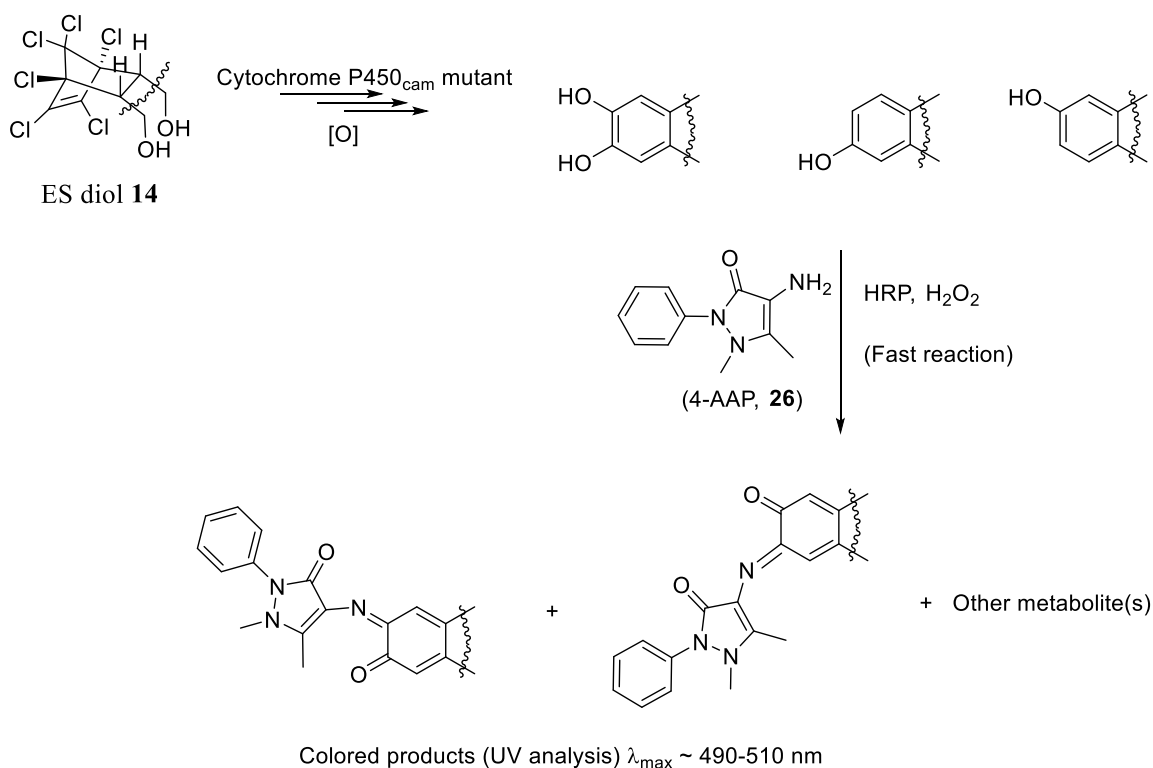


Figure 3.1 Degradation of ES diol (**14**) by P450_{cam} mutants and detection of the metabolites in a coupled assay with 4-aminoantipyrine (**4-AAP**, **26**), a system used to detect quinones.

The steady state kinetic assay was optimized with crude *ES7* lysate, to obtain the conditions described in the methods. α -ES (**13**) and ES diol (**14**) were compared at two concentrations, 100 μM and 200 μM and in both cases ES diol was the substrate that gave more product with absorbance at 506 nm (Figure 3.2, A and B). To ensure that the product at 506 nm was not due to random activity, three controls were run alongside a dose response with ES diol (**14**) and *ES7* (Figure 3.2, D): 1) omitting the substrate but keeping the oxidative enzymes P450 and HRP, 2) omitting the P450 but using 500 μM of ES diol (**14**) and HRP and 3) omitting the HRP but using P450 and 500 μM of ES diol (**14**). This assay reveals an important result: the formation of the colored 4-AAP adduct requires active P450 and the ES diol (**14**) substrate, but it does not require HRP. When this 4-AAP assay is used in phenol analysis (Lülsdorf et al., 2015; Wong et al., 2005; Zeng et al., 2015), HRP is added to cause *in situ* formation of *ortho* or *para* quinones which then react with the 4-AAP (**26**) to give the adduct (Figure 3.1 and Figure 3.2). The observation that colored product formed in the absence of HRP (Figure 3.2, D) suggests that the action of

the P450 gives rise to a quinone. We will return to this point later. We decided to keep HRP in the assay mixture to ensure that the quinone formed by action of the P450 on ES diol is not reduced by other reagents in the mixture such as the NADH.

As seen in Figure 3.2 C and D, the rate of formation of the colored product depended on the substrate concentration.

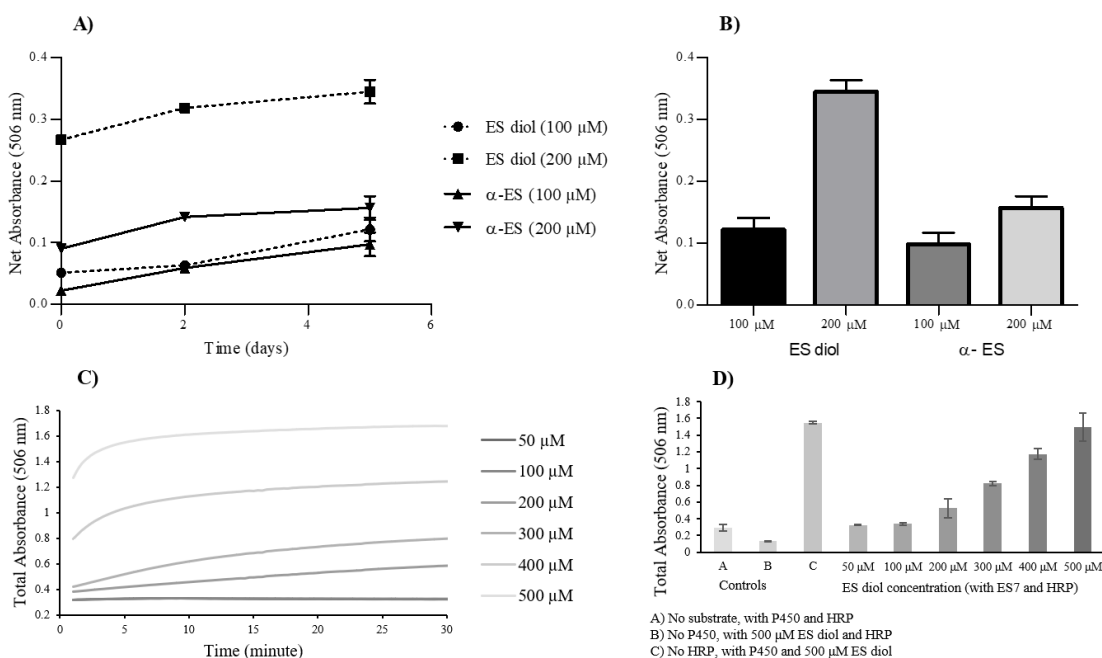


Figure 3.2 *ES7* and ES diol (14) assay optimization (A) net absorbance at 506 nm using α -ES (13) and ES diol (14) during 5 days assay, (B) net absorbance at 506 nm using α -ES (13) and ES diol (14) after 5 days assay, (C) total absorbance at different concentrations of ES diol (14) using *ES7* in the coupled assay, (D) total absorbance with *ES7* and using different concentrations of ES diol (14).

3.1.3. Initial screen with crude lysates

The steady state kinetic assays were performed using crude lysate of WT-P450_{cam} and mutants (*ES1-ES7* and *IND1*), with ES diol (14) as a substrate. The metabolites were coupled with 4-AAP *in-situ* (as described above) and monitored at 506 nm (Table 3.2, Figure 3.3). The *IND1* mutant, selected previously for dechlorination of 3-chloroindole from

the SeSaM library, was also included in this study for comparison with ES mutants, because it had the highest 3-chloroindole dechlorination activity (Kammoonah et al., 2018). The rate of 4-AAP adduct formation was highest for the mutant *ES2* in terms of turnover number (k_{cat}) and catalytic efficiency (k_{cat}/K_M) followed by *ES7*. *ES6*, with a single mutation, was the least active of the ES mutants. WT-P450_{cam} was significantly less active than the mutants (Table 3.2 and Figure 3.3). Interestingly, *IND1* was among the more active mutants (Table 3.2), even though it had not arisen by selection on ES (**13**). All these mutants followed sigmoidal kinetics, which required the use of an allosteric model (as opposed to the classic Michaelis Menten model) for analysis (Figure 3.3).

Table 3.2 Kinetic data of ES diol (14) with WT-P450_{cam} and mutants (using crude lysate)

Mutants	k_{cat} ($\mu\text{M/s} \cdot \mu\text{M P450}$)	K_M (μM)	k_{cat}/K_M ($1/\text{s} \cdot \mu\text{M}$)
WT ^a	$\sim 0.8 \pm 0.0$	1024.6	$0.8 \pm 0.0 \times 10^{-3}$
<i>IND1</i> ^b	4.4 ± 0.5	363.3	$12.0 \pm 1.5 \times 10^{-3}$
<i>ES1</i>	3.8 ± 1.1	393.2	$9.6 \pm 2.8 \times 10^{-3}$
<i>ES2</i>	6.2 ± 2.3	372.8	$16.6 \pm 6.1 \times 10^{-3}$
<i>ES3</i>	3.2 ± 0.2	443.8	$7.2 \pm 0.4 \times 10^{-3}$
<i>ES4</i>	3.0 ± 0.6	318.6	$9.3 \pm 1.8 \times 10^{-3}$
<i>ES5</i>	3.9 ± 1.1	371.3	$10.4 \pm 2.9 \times 10^{-3}$
<i>ES6</i>	2.7 ± 0.5	387.8	$7.0 \pm 1.3 \times 10^{-3}$
<i>ES7</i>	4.3 ± 1.2	332.3	$12.8 \pm 3.7 \times 10^{-3}$

^a WT data from Lineweaver-Burk equation

^b *IND1*- E156G/V247F/V253G/F256S

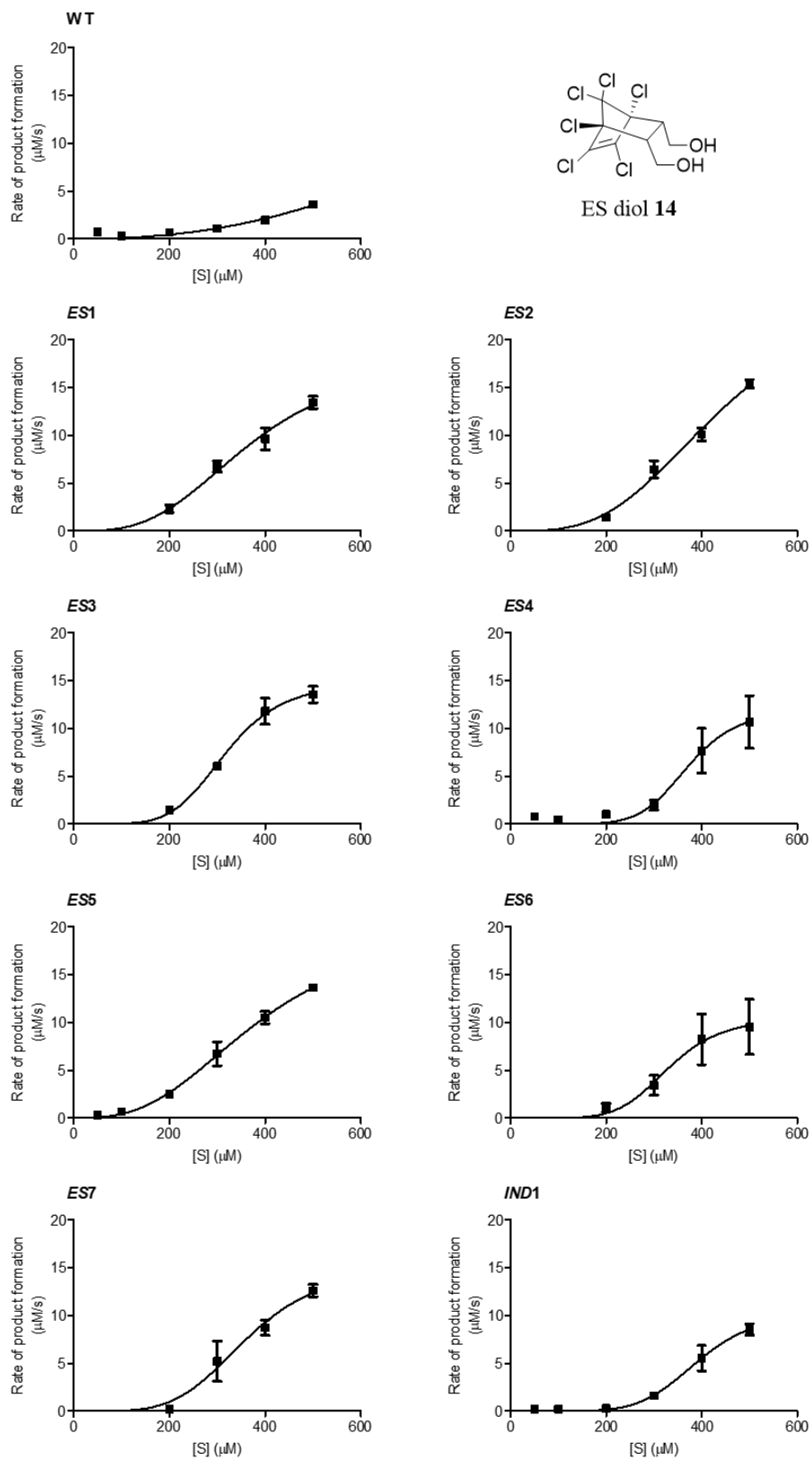


Figure 3.3 Allosteric sigmoidal kinetics of ES diol (14) with WT-P450_{cam} and mutants (using crude lysate).

Mutants *ES2* and *ES7* were selected for further studies because of their comparatively high activity; mutants *ES5* and *ES6* were also chosen because of their single mutation. These P450s were prepared by site-directed mutagenesis from the wild-type construct with a cleavable His₆-tag for easy purification.

3.1.4. His₆-tagged P450s: stability and kinetics

ES6 and *ES7* were successfully cloned, expressed, purified, and the His₆-tag was removed successfully from the P450 using Factor Xa. However, mutant *ES2* which was the most active one (Table 3.2), did not express well, and what little could be isolated from cultures could not be purified without loss of the heme. Mutant *ES5*, which also had a mutation of A296 (like *ES2*) expressed well, but cleavage of the His₆-tag by Factor Xa enzyme resulted in secondary cleavage and undesired fragments (see Appendix A6), as well as heme loss. Thus, mutants *ES2* and *ES5* could not be produced by this method.

Due to the instability of mutant *ES2*, two variants of *ES2* were generated: F292S/A296V and K314E. For these, F292S/A296V again did not express and lost the heme, whereas K314E did express (see below). Thus, we conclude that mutation of A296 is detrimental to the stability of P450_{cam}.

Comparing mutations in *ES2* and *ES7*, both share the K314E mutation. In order to study the effect of this single mutation, a variant with the K314E mutation was generated (see above). Expression and purification of this variant were successful.

Steady state kinetic assays were performed using purified WT-P450_{cam} and mutants *ES6*, *ES7* and K314E, with ES diol (**14**) as a substrate. Increased catalytic activity (turnover number as well as catalytic efficiency) was noticed in the purified *ES6* and *ES7* mutants compared to the crude lysates used previously (Table 3.2 and Table 3.3). The catalytic activity of *ES7* was highest, followed by *ES6* and K314E, and all these variants were significantly more active than the WT-P450_{cam} (Table 3.3).

Table 3.3 Kinetic data of ES diol (14) with purified WT-P450_{cam} and mutants

Mutant	Mutations	k_{cat} ($\mu\text{M}/\text{s} \cdot \mu\text{M P450}$)	K_M (μM)	k_{cat}/K_M ($1/\text{s} \cdot \mu\text{M}$)
WT ^a		$\sim 0.15 \pm 0.04$	385	$0.4 \pm 0.1 \times 10^{-3}$
ES2	F292S/A296V/K314E/P321T	n.d	n.d	n.d
ES5	A296P	n.d	n.d	n.d
K314E	K314E	3.8 ± 0.3	370	$10.1 \pm 0.7 \times 10^{-3}$
ES6	G120S	5.7 ± 0.3	368	$15.5 \pm 0.9 \times 10^{-3}$
ES7	V247F/D297N/K314E	12.6 ± 4.7	394	$31.9 \pm 12.0 \times 10^{-3}$
ES7 ^b	V247F/D297N/K314E	1.7 ± 0.2	28 ± 9	$60.7 \pm 0.7 \times 10^{-3}$
F292S/296V	F292S/ A296V	n.d	n.d	n.d

^a WT data from Lineweaver-Burk equation.

^b ES7 mutant – using *m*-CPBA as a shunt.

n.d = Not determined because the mutant enzyme was unstable and could not be purified.

3.1.5. Steady-state kinetic assay using redox partners vs. using only *m*-CPBA (shunt)

Using ES7, one of the most active P450_{cam} mutants, with redox partners (PdX, and PdR) and NADH as electron source, allosteric sigmoidal kinetics were observed in ES diol (14) degradation studies. In contrast, mutant ES7 showed Michaelis-Menten kinetics when *m*-CPBA was used as a shunt in ES diol degradation (Figure 3.4). Overall, the k_{cat} with *m*-CPBA was lower ($1.7 \pm 0.2 \mu\text{M}/\text{s} \cdot \mu\text{M P450}$) than with the redox partners ($12.6 \pm 4.7 \mu\text{M}/\text{s} \cdot \mu\text{M P450}$), but the K_M with *m*-CPBA was also lower than with the redox partners (Table 3.3).

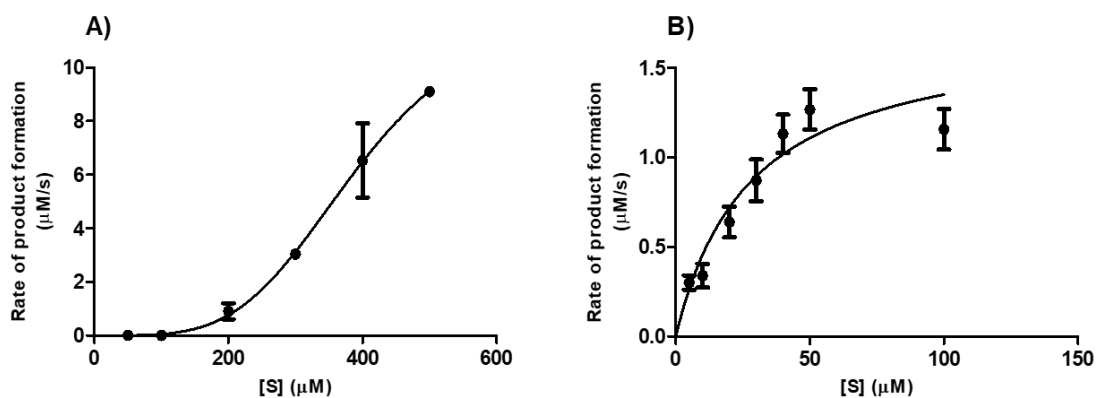


Figure 3.4 Steady state kinetic assays of ES7 using ES diol (14). (A) using redox partners (PdX and PdR) and NADH, and (B) using *m*-CPBA as a shunt.

3.1.6. Ligand binding and dissociation constant (K_d) using selected purified mutants and WT-P450_{cam}

Dissociation constants (K_d) were measured using the change in spin shift of the P450, often seen upon substrate binding. WT-P450_{cam} shows a characteristic peak (λ_{max} 418 nm – low spin Fe-III) without camphor (**10**, natural substrate) and on addition of camphor this peak is blue shifted (λ_{max} 392 nm – high spin Fe-III) due to the change in spin state of iron (Fe) in the heme molecule (Figure 3.5). On titrating mutants and WT-P450_{cam} with ES diol (**14**), the spin change of Fe in heme was observed (Figure 3.5). This change in spin state as the substrate is titrated into the enzyme is used to calculate K_d values for ES diol (Table 3.4). Using camphor as substrate, K_d for WT-P450_{cam} was found 1.7 ± 0.04 μ M (1.6 ± 0.3 μ M by (Atkins & Sligar, 1988)). K314E mutant binds camphor more strongly than WT with K_d value 1.0 ± 0.04 μ M. However, ES6 and ES7 showed higher K_d values for both camphor and ES diol than WT-P450_{cam} (Table 3.4). Similar patterns of K_d values with respect to WT-P450_{cam} and mutants were observed using ES diol (**14**) as substrate (Table 3.4). However, overall K_d values of ES diol are higher than those for camphor.

Table 3.4 Dissociation constant measured using Camphor (**10**) and ES diol (**14**) with purified WT P450_{cam} and mutants

Mutants	Mutations	(d)-Camphor (10) K_d (μ M)	ES diol (14) K_d (μ M)
WT	-	1.7 ± 0.04	41.6 ± 5.5
K314E	K314E	1.0 ± 0.04	31.3 ± 3.7
ES6	G120S	2.4 ± 0.05	108.9 ± 27.4
ES7	V247F/D297N/K314E	10.4 ± 0.43	143.2 ± 17.4

^a Values are the mean \pm Standard deviation (S.D.) of 3 replicates.

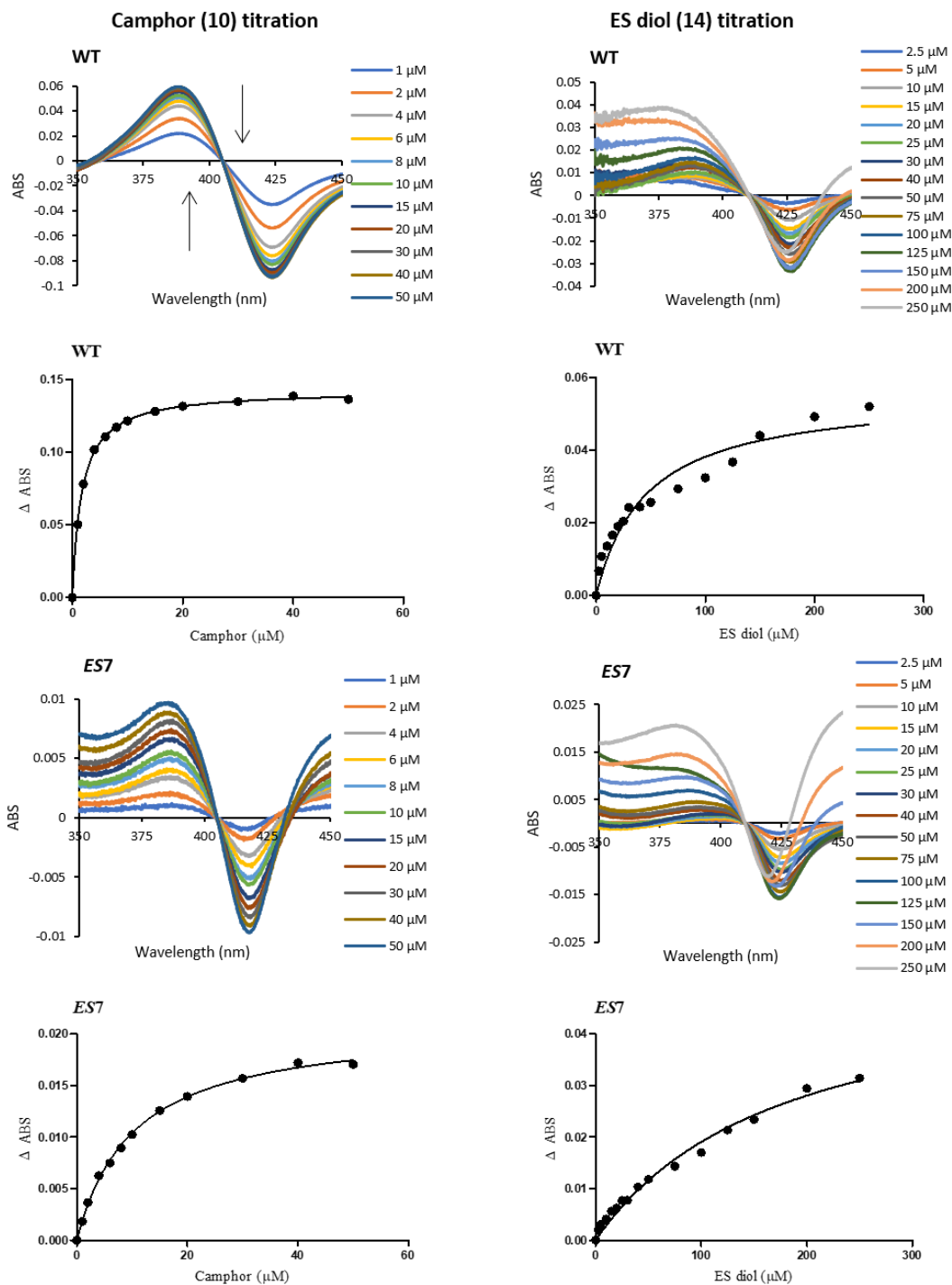


Figure 3.5 Titrations of wild-type (WT) P450cam (top) and mutant *ES7* (bottom) with camphor (10) (left set of graphs) or ES diol (14) (right set of graphs). The spectra (top set of graphs for each enzyme) show the blue shift in the Soret band as substrate is titrated into the enzyme preparation. The isotherms (lower set of graphs for each enzyme) depict the change in the Soret band (the increase in absorption at the blue-shifted wavelength relative to the decrease in absorption of the original Soret band).

3.1.7. Chloride release with purified WT-P450_{cam} and ES7 mutants

Using the *ES7* mutant, chloride ions released were detected instantly on adding ES diol (**14**) (300 and 500 μM) to the reaction mixture. However, NADH was found to enhance chloride electrode readings, giving overestimates, whereas NAD^+ was found to suppress chloride readings, giving slight underestimates (see Appendix A7). Alcohol dehydrogenase was used to regenerate NADH *in situ*, to maintain a constant level of NADH, but a slower rate of NADH production by alcohol dehydrogenase (1 nmol/minute) than NADH being used by *ES7*-P450_{cam} mutant resulted in lower chloride ion readings than expected (see Appendix A8). For this reason, chloride release experiments were repeated without the redox partner system or NADH, by using only the purified P450 enzyme and *m*-CPBA as a shunt. Overall, chloride release was detected with the *ES7* mutant, while with WT-P450_{cam} (ES diol 500 μM) chloride ion release was not detected (Figure 3.6). Colorimetric analysis of product formation from chloride release assays revealed that, on average, 5.2 ± 0.7 and 5.7 ± 0.2 chloride ions were released per colored product formed by the *ES7* mutant using non-labeled ES diol (**14**) and ^{13}C -ES diol respectively (Table 3.5).

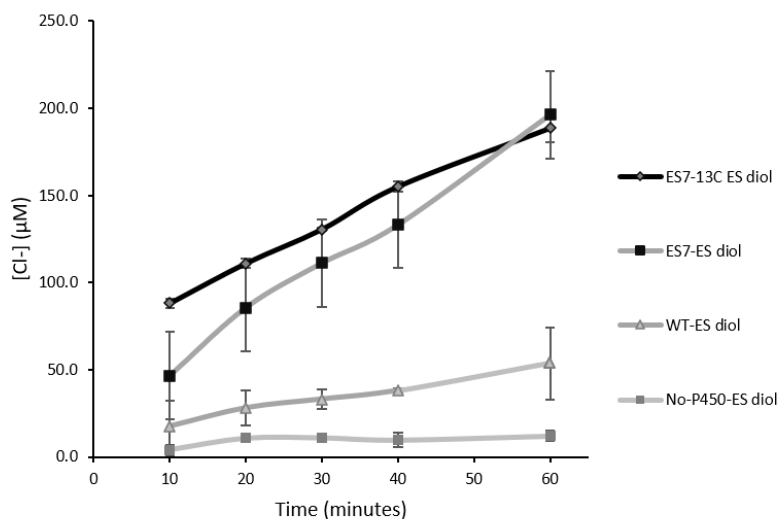


Figure 3.6 Chloride release using ES diol (**14**) and *m*-CPBA, with WT-P450_{cam} (ES diol **14**, 300 μM), *ES7* (^{13}C -ES diol **14**, 300 μM), *ES7* (ES diol **14**, 300 μM) and No P450_{cam} control.

Table 3.5 Ratio of chloride released to quinone (4-AAP coupled) formed in assay with *m*-CPBA as shunt

Conditions	Chloride [Cl ⁻] ions detected (μM) ^a	4-AAP coupled-product (μM) ^a	Ratio (Cl ⁻ per 4-AAP) ^a
ES7-P450 _{cam} , ES diol (14), and <i>m</i> -CPBA	196 ± 32	38 ± 5	5.2 ± 0.7
ES7-P450 _{cam} , ¹³ C-ES diol, and <i>m</i> -CPBA	188 ± 8	35 ± 6	5.7 ± 0.2
WT-P450 _{cam} , ES diol (14), and <i>m</i> -CPBA	53 ± 20	23 ± 6	2.3 ± 0.6
ES diol (14) and <i>m</i> -CPBA only (control)	12 ± 3	0	0

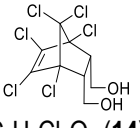
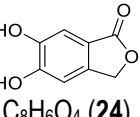
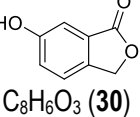
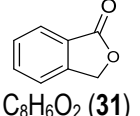
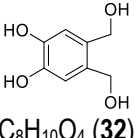
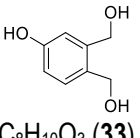
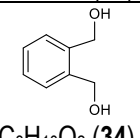
^a Values are the mean ± Standard deviation (S.D.) of 3 replicates.

3.1.8. Isolation of products using purified WT-P450_{cam} and ES7 mutant

Products extracted from chloride release assay (using NADH system) were analyzed by LC-MS. Mono- and dihydroxy benzene derived metabolites were detected (Table 3.6). Major metabolites which are detected are dihydroxy phthalide (**24**) which matches with the synthetic standard sample, and 3,4-bis(hydroxymethyl) phenol (**33**) (Table 3.6). The product 4,5-bis(hydroxymethyl)benzene-1,2-diol (**32**) was also detected, but in lesser quantity than **33**.

Products from the set of 4-AAP coupled assays performed with crude lysate were also analyzed using LC-MS. The material detected from the assays matches with the standard product (**25**) (Appendix A10).

Table 3.6 Metabolites detected from ES7 using ES diol (14)

Substrate/ metabolites	Exact mass		Expected mass	ES7- No substrate	ES7- ES diol (14) (500 μ M)	ES7- ES diol (14) (300 μ M)
 <chem>C9H8Cl6O2</chem> (14)	355.831 (Molar Mass =360.8)	m/z	377.896 (M+NH ₄) ⁺	N.D	377.896 (M+NH ₄) ⁺	377.896 (M+NH ₄) ⁺
		Abundance		N.D	8580	1043
 <chem>C8H6O4</chem> (24)	166.027	m/z	167.045 (M+H) ⁺	N.D	149.023 (M+H- H ₂ O) ⁺	149.023 (M+H- H ₂ O) ⁺
		Abundance		N.D	3275	530
 <chem>C8H6O3</chem> (30)	150.032	m/z		N.D	N.D	N.D
		Abundance		N.D	N.D	N.D
 <chem>C8H6O2</chem> (31)	134.037	m/z		N.D	N.D	N.D
		Abundance		N.D	N.D	N.D
 <chem>C8H10O4</chem> (32)	170.058	m/z		N.D	188.101 (M+NH ₄) ⁺	N.D
		Abundance		N.D	165	N.D
 <chem>C8H10O3</chem> (33)	154.063	m/z		N.D	155.069 (M+H) ⁺	177.061 (M+Na) ⁺
		Abundance		N.D	1265	6330
 <chem>C8H10O2</chem> (34)	138.068	m/z		N.D	139.074 (M+H) ⁺	N.D
		Abundance		N.D	192	N.D

N.D = Not detected

3.1.9. Results from product isolation and ¹³C NMR study

Products extracted from the chloride release assay of ¹³C-ES diol, with ES7 and *m*-CPBA as shunt, were analyzed by ¹³C NMR. A new ¹³C-NMR peak was observed at 109.99 ppm in the isolate from ¹³C-ES diol assay. In the control experiment using non-labelled ES diol (**14**) this peak was not observed (Figure 3.7 and see Appendix A11).

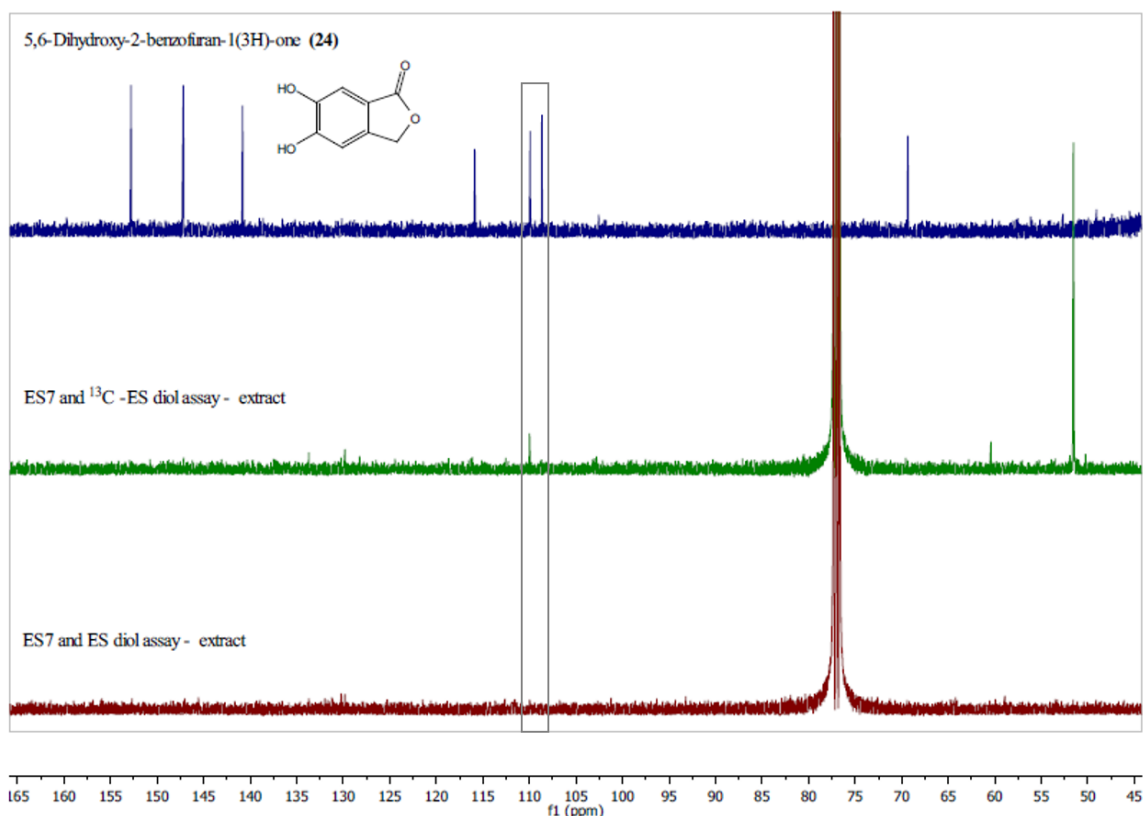


Figure 3.7 ^{13}C NMR spectra. Blue: spectrum of dihydroxy phthalide (5,6-dihydroxy-2-benzofuran-1(3H)-one, **24**). Comparison of extracts from assays with ^{13}C -ES diol (green) and ES diol (**14**) (brown) with *ES7* (using *m*-CPBA).

3.1.10. *In-silico* docking studies

To gain insight into how endosulfan and its analogues fit into active sites of the selected mutants and WT-P450_{cam}, *in silico* docking calculations were performed. The average distances of heme-Fe to C1, C2, C3 and C4 are summarized in Figure 3.9. It was noticed that these chlorinated substrates are positioned in the active sites in such a way that either the C1 and C2 are closer to heme-Fe or C3 and C4 (example of ES diol (**14**) in Figure 3.8). Thus, the average distances of these carbons to heme-Fe, is not significantly different to each other (mutants vs WT-P450_{cam}, Figure 3.9). However, the poses of ES diol (**14**) in mutants and WT-P450_{cam} are selected based on with shortest distance between heme-Fe to C1 (D_1) and C2 (D_2) and minimum difference between Fe-C1 and Fe-C2 distances (minimum difference D_1 - D_2) (Figure 3.10).

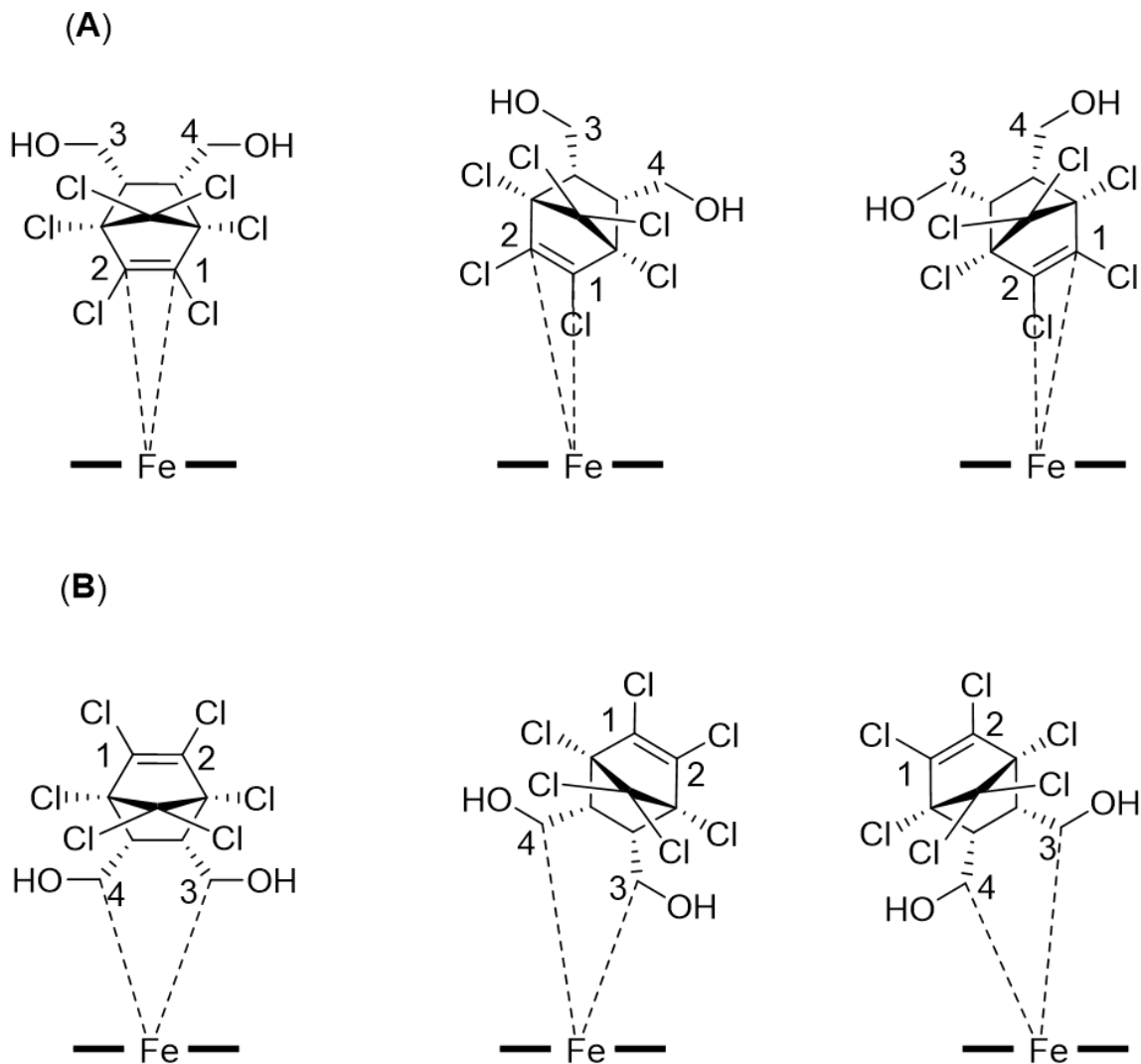


Figure 3.8 Schematic representation of orientation of ES diol (14) found in *in silico* docking studies using MOE. (A) C1 and C2 are closer to heme-Fe, (B) C3 and C4 are closer to heme-Fe (The heme-Fe is represented as “-Fe-”).

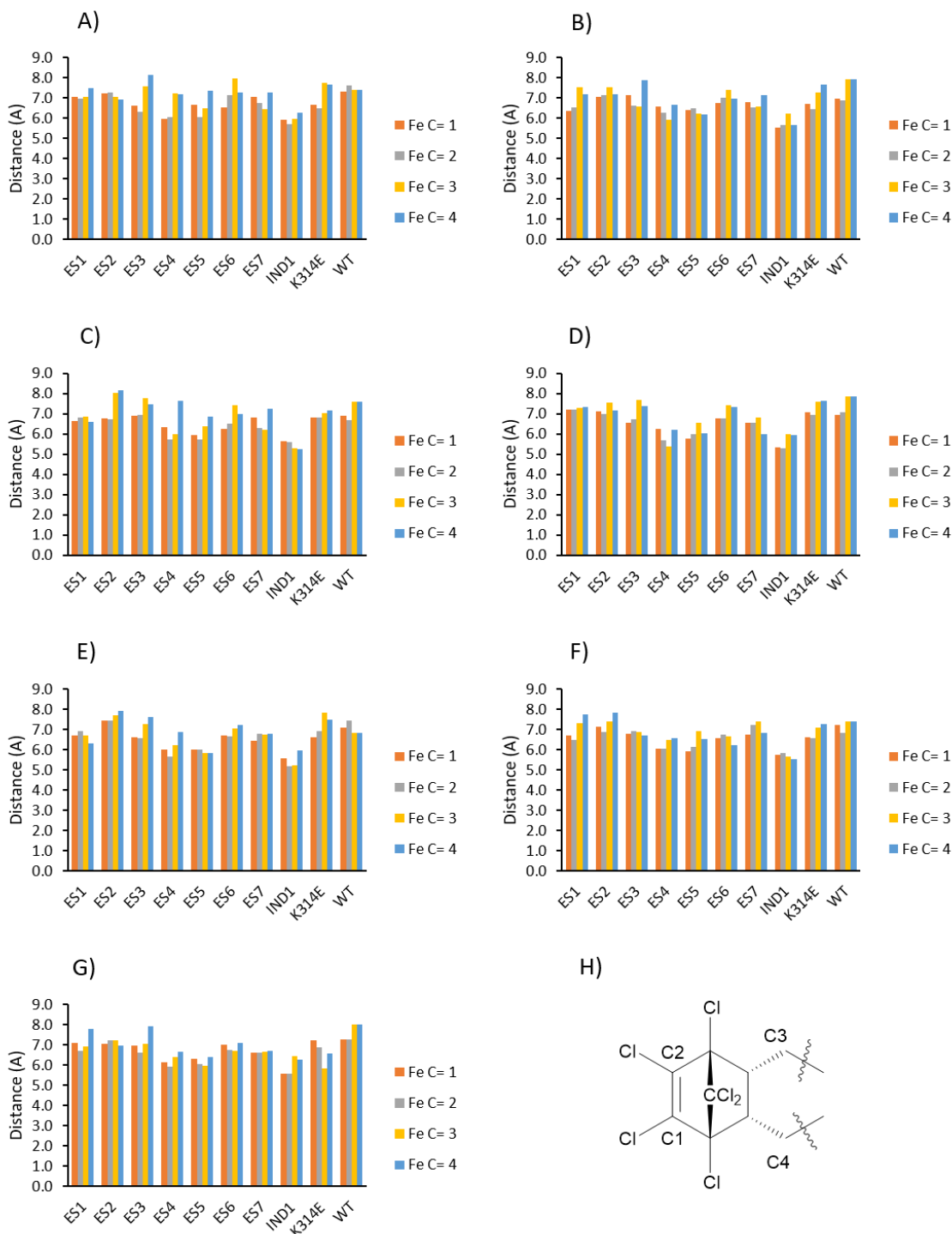


Figure 3.9 Average distances of C1, C2, C3 and C4 from heme-Fe in WT-P450_{cam}, K314E, ES1-7 and IND1 mutants. (A) α -ES (13A), (B) β -ES (13B), (C) ES diol (14), (D) ES lactone (15A), (E) ES lactone (15B), (F) ES ether (16), (G) ES sulfate (20), and (H) carbon numbers assigned to endosulfan bicyclic core for the purpose of this discussion.

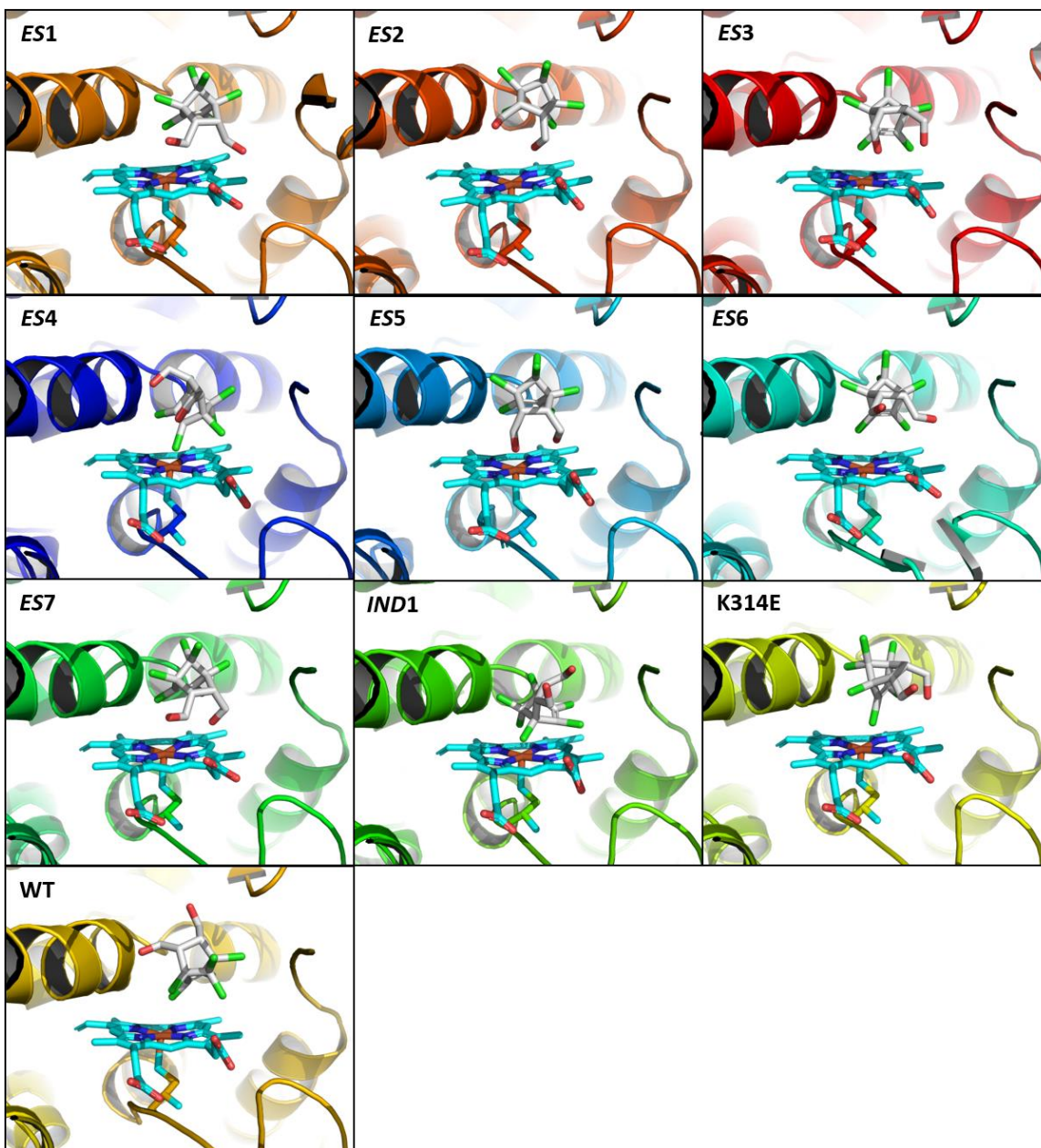


Figure 3.10 Selected poses of ES diol (14) positioned above the heme in the active sites of WT-P450_{cam} and mutants (selected based on Equation 3.1).

To understand the epoxidation of ES substrates catalyzed by P450s, the distance is represented by a “x” value calculated from the selected pose. The “x” value is calculated using average distance between Fe-C1/C2 (the minimum distance, D_1 and D_2), the difference between Fe-C1 (D_1) and Fe-C2 (D_2) distances (Equation 3.1).

$$x = (\text{Average of } D_1 \text{ and } D_2) \times (\text{Difference between } D_1 \text{ and } D_2) \quad \text{Equation 3.1}$$

The calculated “x”-value from ES diol (**14**) selected poses, was compared with the kinetic data obtained in *in vitro* assays using crude lysate of WT-P450_{cam} and mutants. WT-P450_{cam} shows higher “x”-value which has lower catalytic activity than ES2 and other mutants (Figure 3.11).

The best poses were also selected for other substrates and “x”-values were calculated to compare WT-P450_{cam} and mutants. WT-P450_{cam} has higher “x”-value for α -ES (**13A**) and ES diol (**14**) compared to the selected P450_{cam} mutants (*ES1 – ES7*). This relates to the selection of mutants capable of degradation of ES (**13**) during the screening of the randomly generated SeSaM mutant library (Figure 3.12).

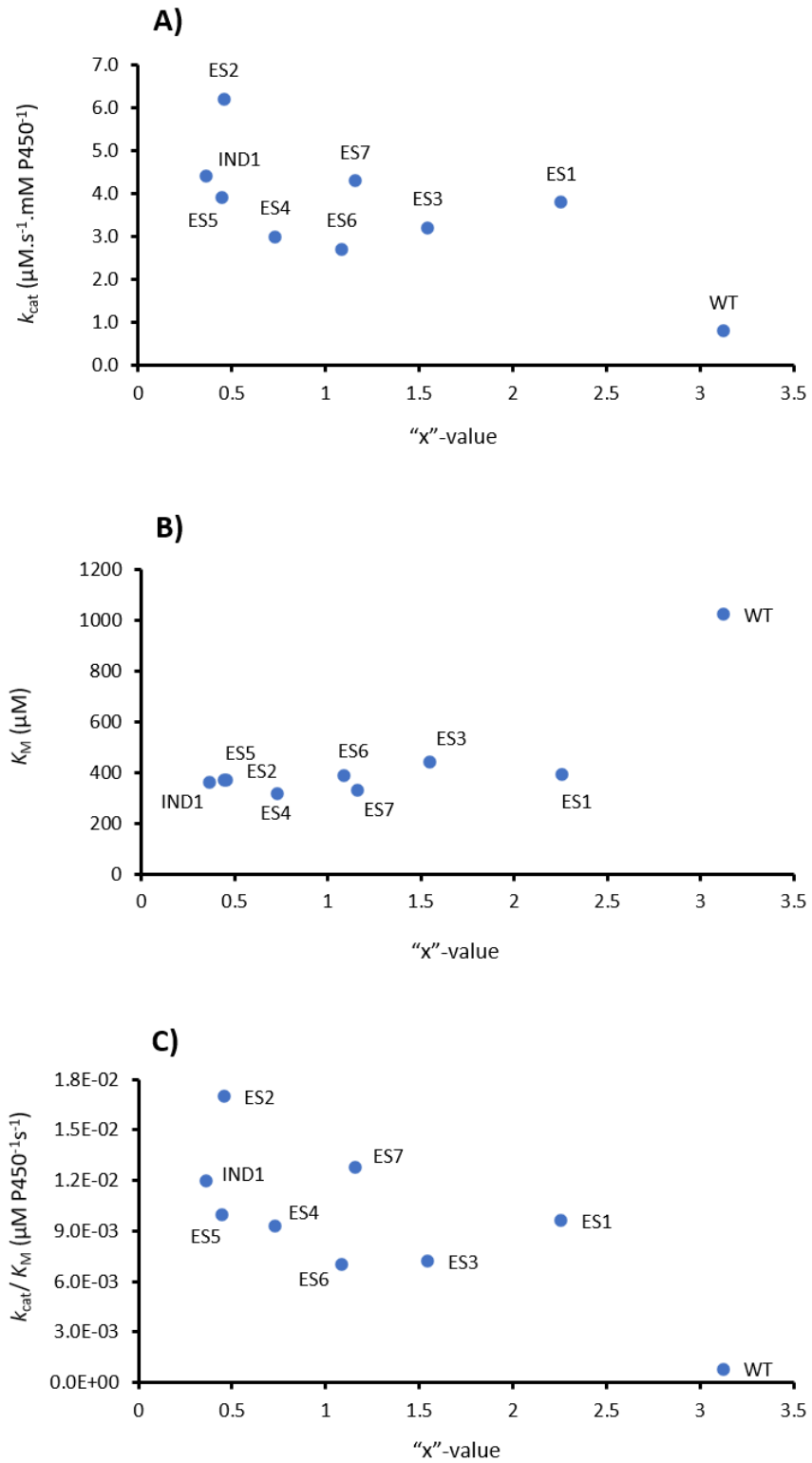


Figure 3.11 Comparison of the calculated "x"-value with kinetic data of WT-P450_{cam} and mutants (crude lysate). (A) k_{cat} vs. "x"-value, (B) K_M vs. "x"-value, (C) k_{cat}/K_M vs. "x"-value.

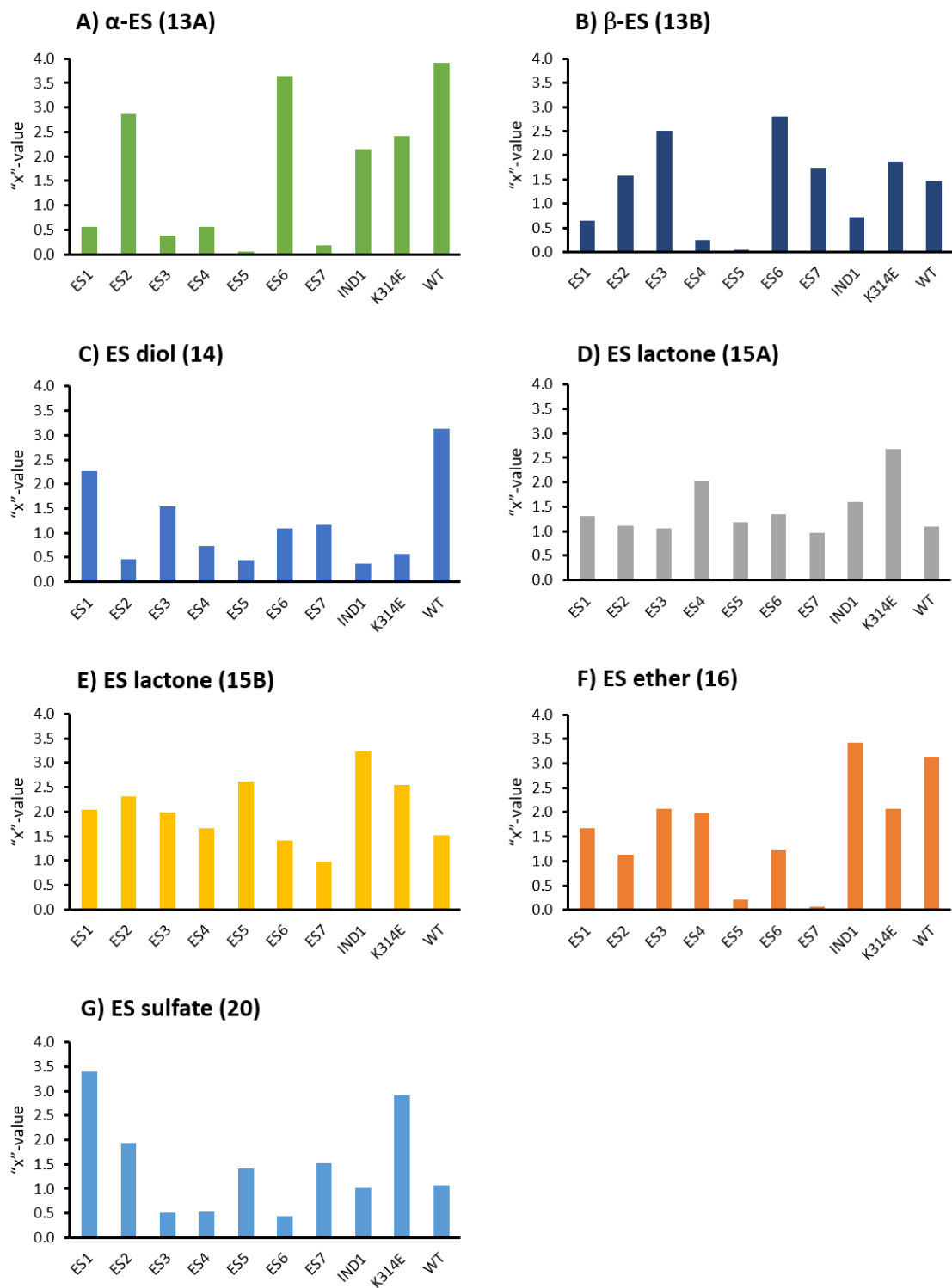


Figure 3.12 Different substrates and calculated "x"-values from the selected poses in WT-P450_{cam} and mutants in MOE docking (see Figure 2.1 for list of substrates).

ES1 mutant and ES diol (14)

ES1 mutant (T56A/N116H/D297N) was more active than WT-P450_{cam}, however, it was less active than *ES2* and *ES7* mutants in degradation of ES diol (Table 3.2). T56A and N116H, which are located on the loop between helices A and B, and helix C respectively, are not present in the active site directly. However, D297N mutation, which is located on the loop between helices K and K' near the active site of P450, makes a network of H-bonding to the hydroxyl of ES diol (**14**) and propionate chain of heme (Figure 3.13, Appendix A12).

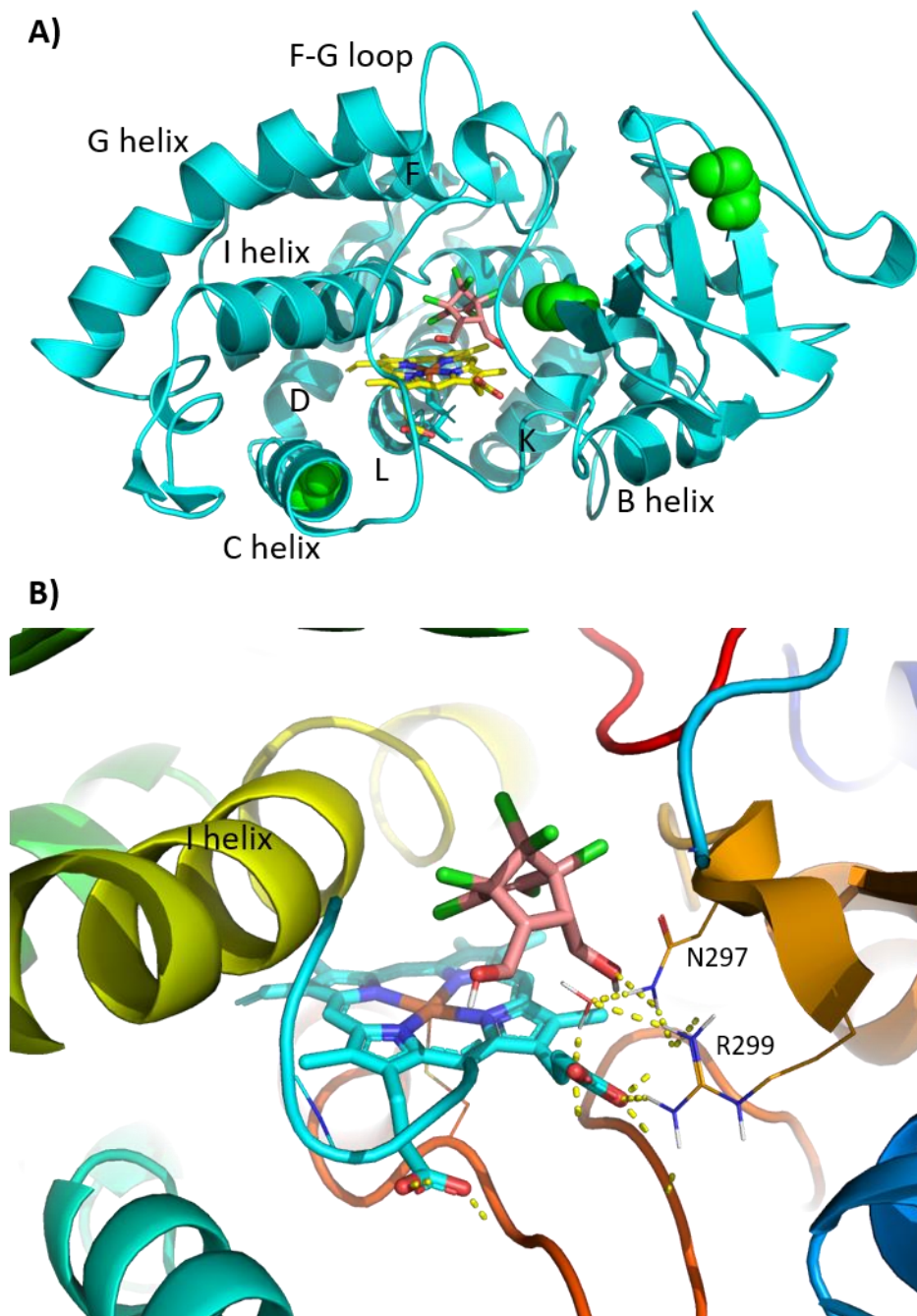


Figure 3.13 The *in silico* molecular docking results of ES1 (T56A/N116H/D297N) and ES diol (14). (A) P450 is shown in cyan color, heme in yellow color, mutations are shown in green colored spheres, and ES diol in pink color. (B) Orientation of ES diol (14) in active site (proposed H-bonds are shown as yellow dotted lines).

ES2 mutant and ES diol (14)

Steady-state kinetic results showed that *ES2* (F292S/A296V/K314E/P321T) was the most active mutant with highest rate (k_{cat}) of degradation of ES diol (**14**) among the mutants (Table 3.2). F292S and A296V mutations are located directly at the active site close to heme in C-terminus of helix K and on the loop between helices K – K', respectively. In contrast, the K314E and P321T mutations are present away from active site, on the loop between helices K and K', and N-terminus of helix K', respectively. Thr101 makes a H-bond to the hydroxyl of ES diol (**14**) bound in the active site of P450 (Figure 3.14, Appendix A12). However, the Asp297 residue does not make any H-bond directly to the propionate chain of heme as noticed in other mutants and WT, thus, affecting the stability of the heme in P450 (Figure 3.14). This decrease in stability of the heme was noticed when *ES2* and F292S/A296V mutants were cloned with a His₆-tag and lost heme during purification (as described above), indicating that the F292S/A296V mutations possibly affect the H-bonding network of Asp297. The F292S mutation resulted in a change from a hydrophobic residue (Phe) to a polar neutral residue (Ser), which can play an additional role in altering the H-bonding network in the overall protein structure. Also, the K314E mutation resulted in a negatively charged residue (Glu) from positively charged residue (Lys). Based on the increased activity towards ES diol (**14**) by a single K314E mutant, it is reasonable to propose that the residue plays a role in increasing in catalytic activity of *ES2* towards ES diol, relative to the wild-type (WT).

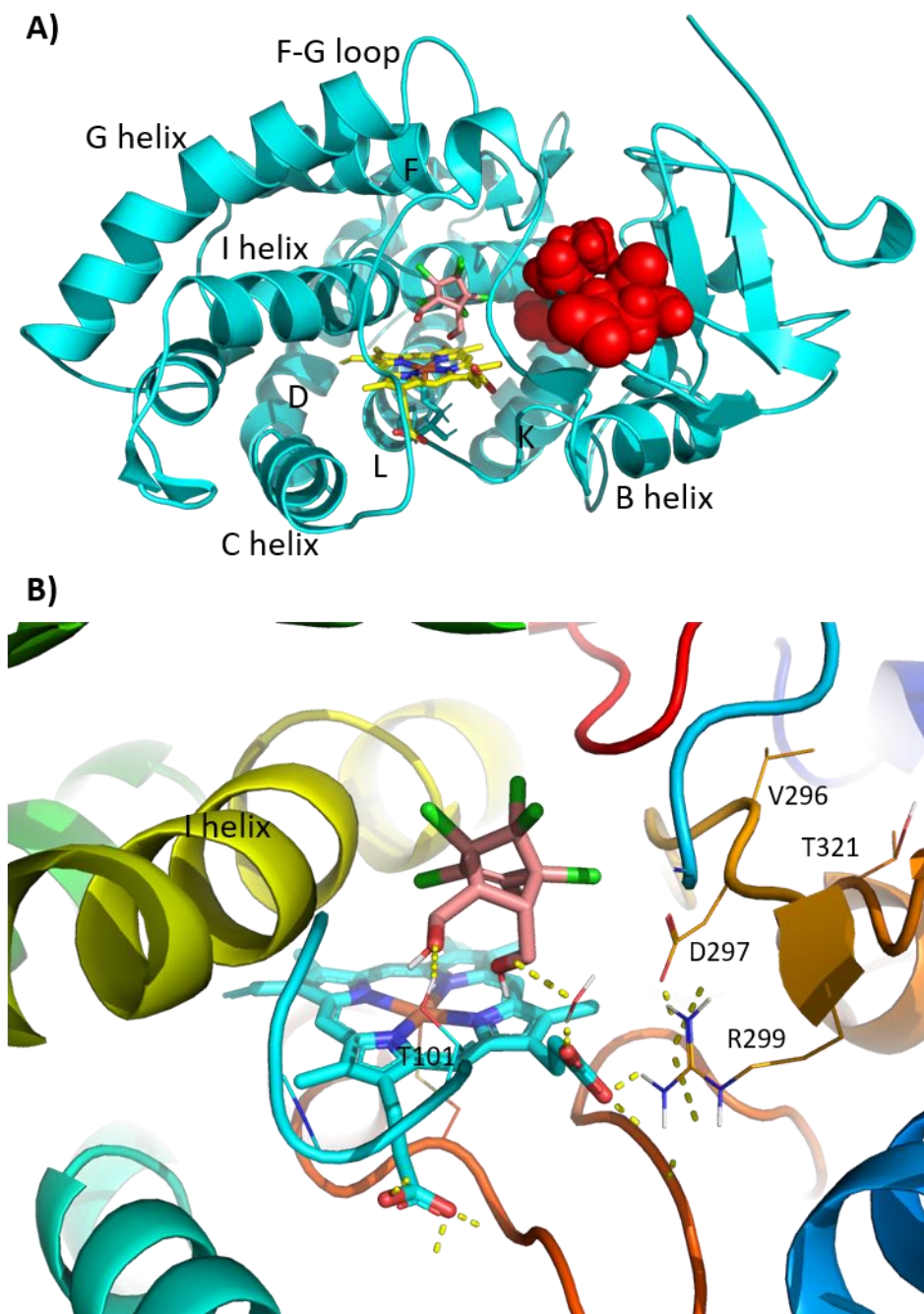


Figure 3.14 The *in silico* molecular docking results of *ES2* (F292S/A296V/K314E/P321T) and *ES diol* (14). (A) P450 is shown in cyan color, heme in yellow color, mutations are shown in red colored spheres, and *ES diol* in pink color. (B) Orientation of *ES diol* (14) in active site (proposed H-bonds are shown as yellow dotted lines).

ES3 mutant and ES diol (14)

The *ES3* (Q108R/R290Q/I318N) mutant was less active than the *ES2* mutant towards degradation of ES diol (**14**) (Table 3.2). The Q108R mutation which is located in helix C at the proximal end of heme, is close to Arg109 and Arg112 residues, both of which play a role in PdX binding and electron transfer (Koga et al., 1993). The R290Q and I318N mutations are located on helix K and on the loop between helices K and K', respectively. ES diol (**14**) bound in the active site is stabilized through a network of H-bonding with the Asp297 and Arg299 residues (Figure 3.15, Appendix A12).

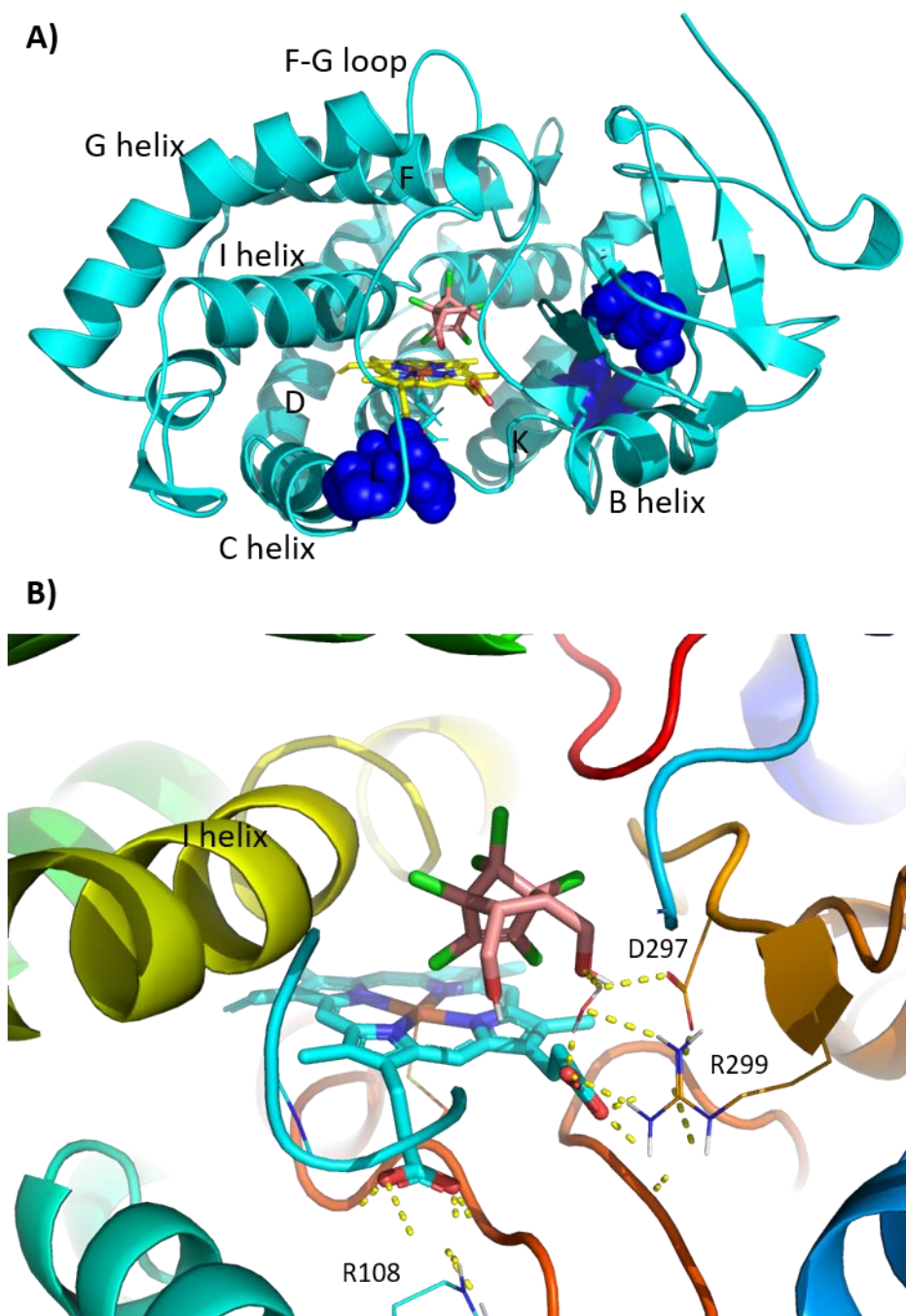


Figure 3.15 The *in silico* molecular docking results of *ES3* (Q108R/R290Q/I318N) and *ES diol* (14). (A) P450 is shown in cyan color, heme in yellow color, mutations are shown in blue colored spheres, and *ES diol* in pink color. (B) Orientation of *ES diol* (14) in active site (proposed H-bonds are shown as yellow dotted lines).

ES4 mutant and ES diol (14)

The *ES4* (S221R/I281N) mutant showed a lower catalytic activity than the *ES2* mutant towards degradation of ES diol (**14**) (Table 3.2). The two mutations S221I and I281N, are both away from active site and are present in helix H and helix K, respectively. ES diol (**14**) bound in the active site is stabilized by hydrophobic interactions with surrounding residues in the active site, without making any H-bond contacts (Figure 3.16, Appendix A12). Serine, a polar residue, is replaced by the non-polar residue isoleucine, which may have effects on helices F and G. These helices play a role in guiding substrate entrance to the active site. In contrast, the other mutation resulted in a replacement of a non-polar Ile to a polar residue Asn in helix K. However, the possible effect of I281N mutation, which is on proximal end of P450_{cam} close to helix I, may have effects on helix I. Helix I has conserved cysteine (Cys357) on N-terminus, bound to heme-Fe.

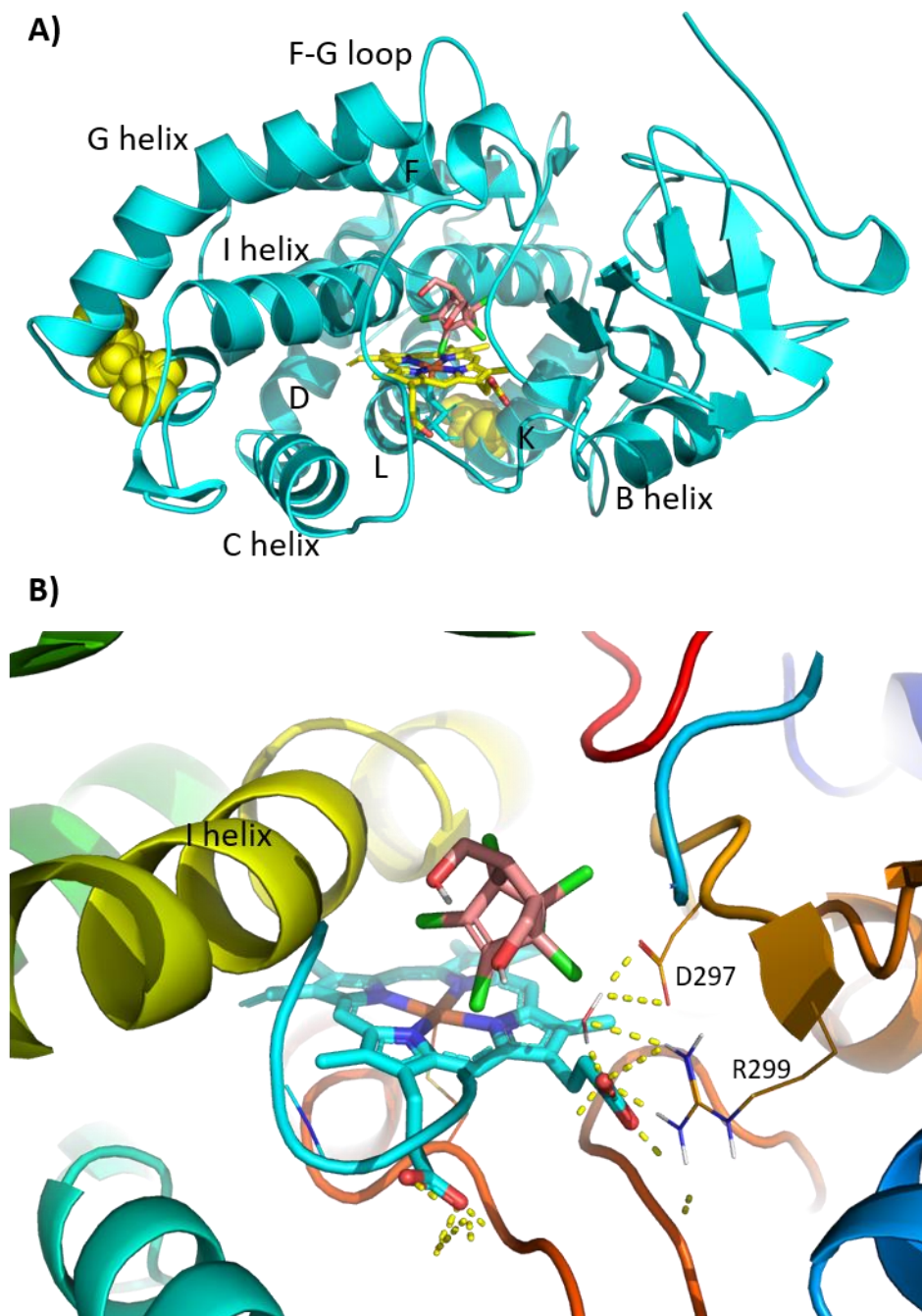


Figure 3.16 The *in silico* molecular docking results of *ES4* (S221R/I281N) and *ES diol* (14). (A) P450 is shown in cyan color, heme in yellow color, mutations are shown in yellow colored spheres, and *ES diol* in pink color. (B) Orientation of *ES diol* (14) in active site (proposed H-bonds are shown as yellow dotted lines).

ES5 mutant and ES diol (14)

The *ES5* (A296P) has single mutation which is located directly in the active site, at the loop between helices K and K'. The A296P mutation is also close to the loop (I395 and V396), which is present at the top of the active site along with F-G loop, may have effects on substrate entry. Like in the *ES4* mutant, ES diol (**14**) bound in active site of *ES5* is stabilized by hydrophobic interactions with surrounding residues in the active site, without making any H-bond (Figure 3.17, Appendix A12). Ala296 residue was also found mutated in *ES2* mutant but into valine (Table 3.1). *ES5* was found to be active more than WT-P450_{cam} towards ES diol (**14**) degradation even though it only has a single mutation (Table 3.2).

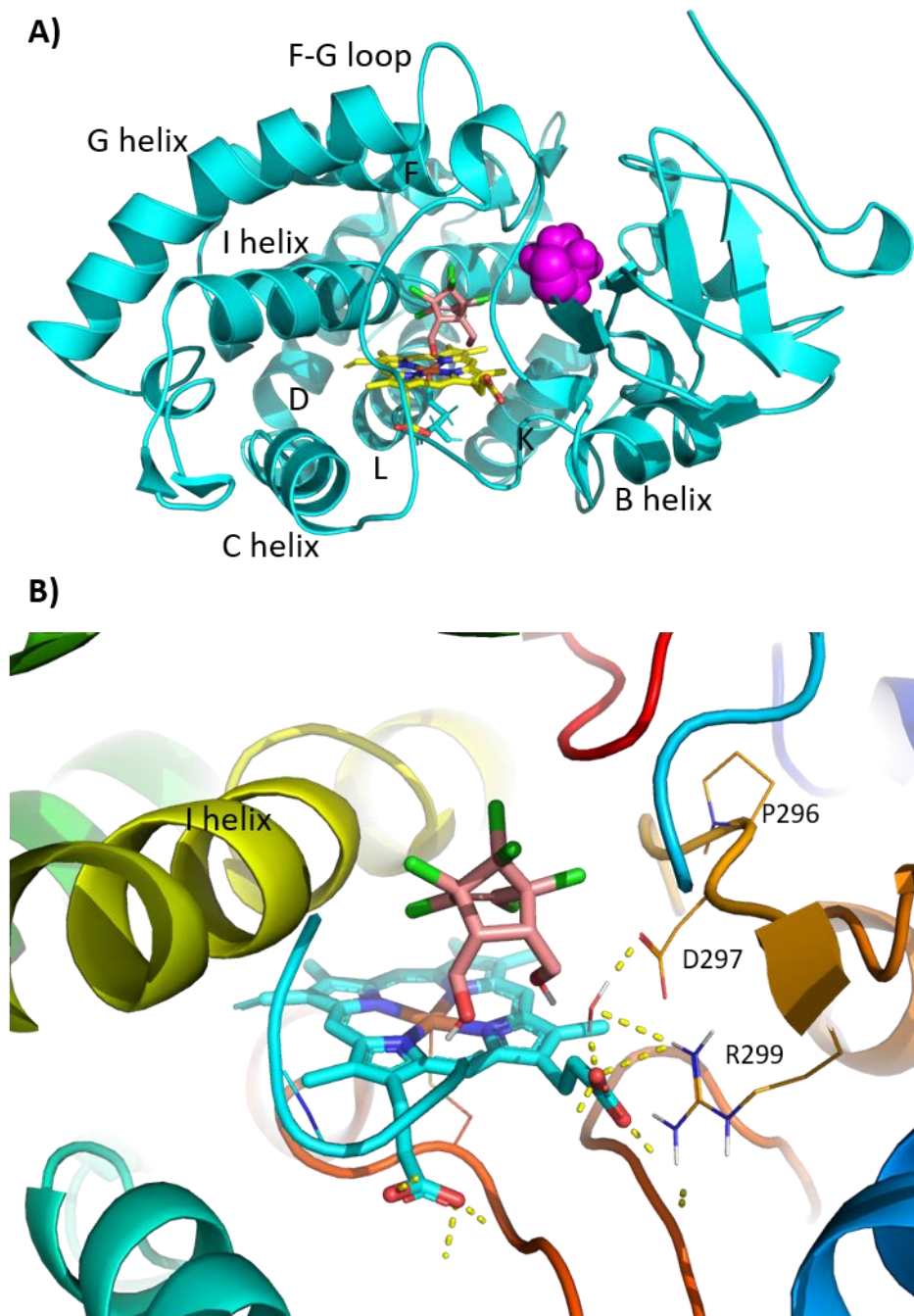


Figure 3.17 The *in silico* molecular docking results of *ES5* (A296P) and *ES diol* (14). (A) P450 is shown in cyan color, heme in yellow color, mutation is shown in magenta colored spheres, and *ES diol* in pink color. (B) Orientation of *ES diol* (14) in active site (proposed H-bonds are shown as yellow dotted lines).

ES6 mutant and ES diol (14)

The *ES6* (G120S) is another selected mutant with a single mutation, which showed significant activity towards ES diol (**14**) degradation. The G120S mutation is present at the C-terminus of helix C, on the proximal end of P450_{cam}, where a neutral residue (Gly) has been replaced with a polar residue (Ser). Like in *ES2*, Thr101 makes a H-bond to the hydroxyl of ES diol (**14**) bound in active site of *ES6* (Figure 3.18, Appendix A12).

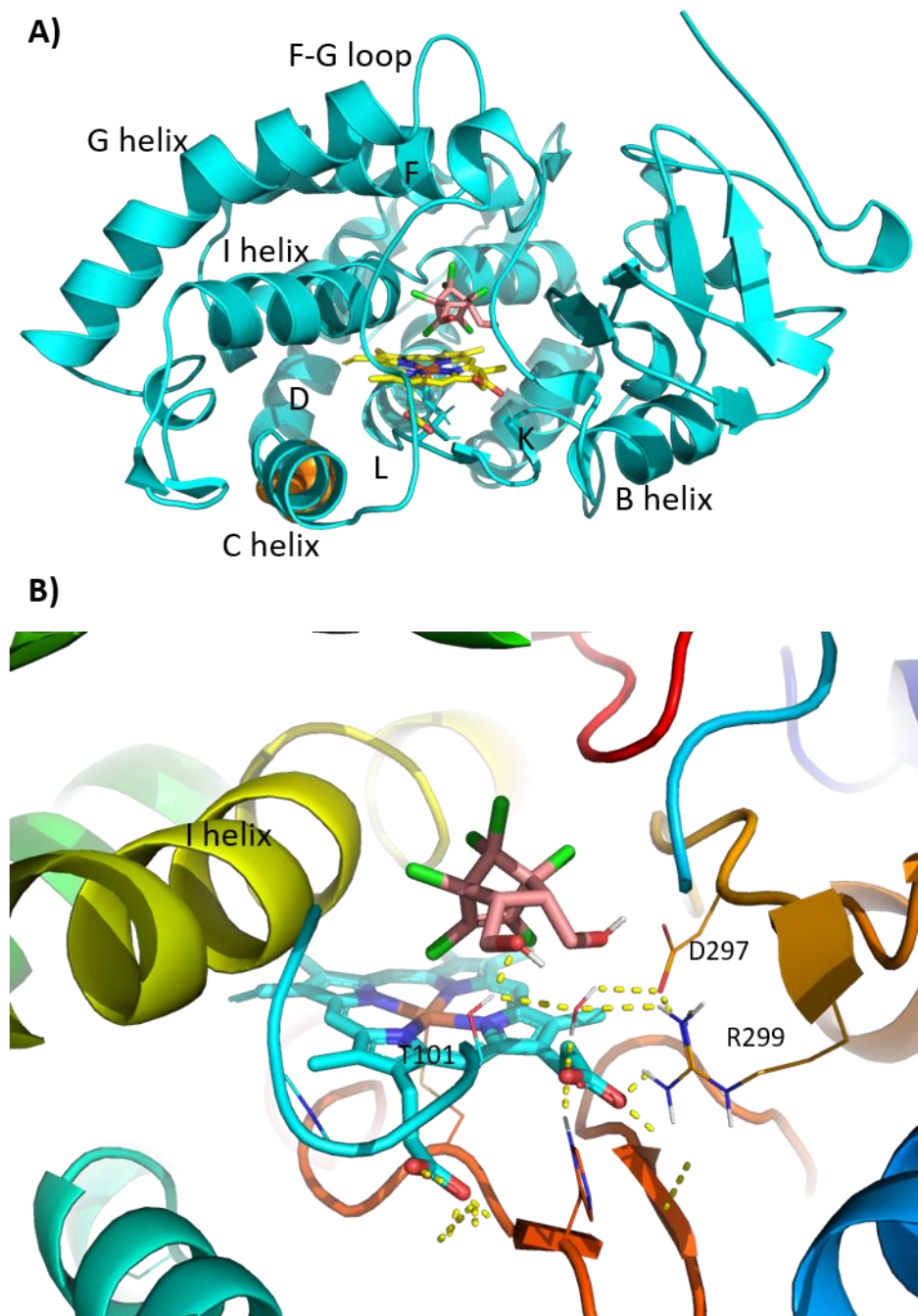


Figure 3.18 The *in silico* molecular docking results of *ES6* (G120S) and *ES diol* (14). (A) P450 is shown in cyan color, heme in yellow color, mutation is shown in magenta colored spheres, and *ES diol* in pink color. (B) Orientation of *ES diol* (14) in active site (proposed H-bonds are shown as yellow dotted lines).

ES7 mutant and ES diol (14)

The *ES7* (V247F/D297N/K314E) mutant has three mutated residues, and the mutations D297N and K314E mutations were also found in the other two mutants *ES1* and *ES2*, respectively. V247F and D297N are located in the active site close to the heme, in helix I and in the loop between helices K and K', respectively. K314E is located away from active site in the loop between helices K and K'. Residues Thr101 and Asn297 could play a key role in orientation of ES diol (**14**) bound in the active site through a network of H-bonding (Figure 3.19, Appendix A13). *ES7* was most active mutant after *ES2* towards ES diol (**14**) degradation (Table 3.2 and Table 3.3) and, unlike *ES2*, it was stable during purification as the his₆ tagged form. The mutation V247F, which also occurred in *IND1* (see below), which was also more active than WT, shows possible interactions of phenyl ring with C1 C2 pi bond of ES diol (**14**). Thus, V247F may play a key role in the orientation of the substrate ES diol (**14**) in the active site. Therefore, it is reasonable to conclude that the mutation V247F contributed to the improvement in activity towards ES diol (**14**) in this case.

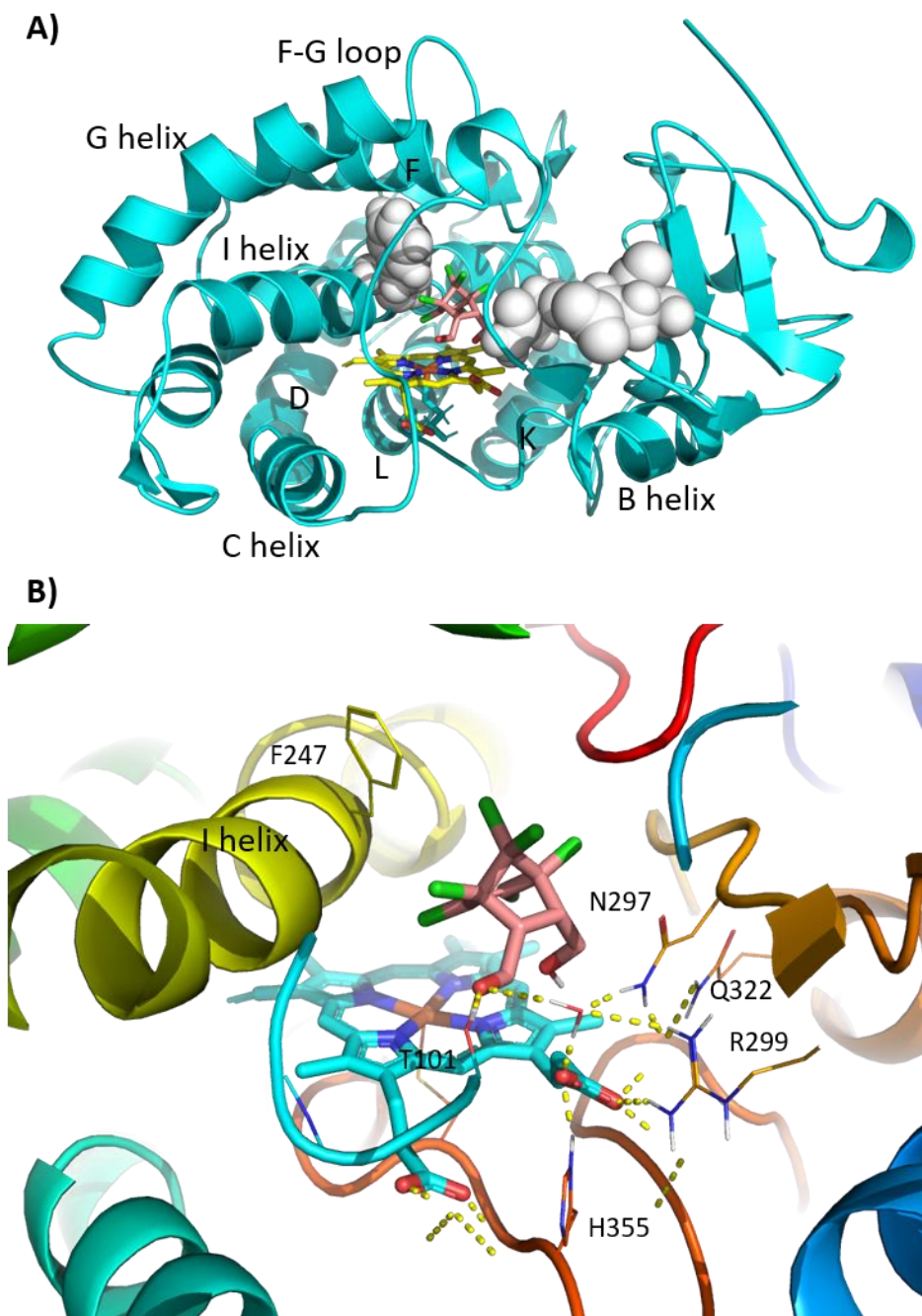


Figure 3.19 The *in silico* molecular docking results of *ES7* (V247F/D297N/K314E) and *ES diol* (14). (A) P450 is shown in cyan color, heme in yellow color, mutations are shown in white colored spheres, and *ES diol* in pink color. (B) Orientation of *ES diol* (14) in active site (proposed H-bonds are shown as yellow dotted lines).

IND1 mutant and ES diol (14)

The *IND1* (E156G/V247F/V253G/F256S) mutant, which was selected on 3-chloroindole from the SeSaM library previously (Kammoonah et al., 2018), was also found to be active toward biodegradation of ES diol (**14**) (Table 3.2). Residue 156 (mutated E156G) is located at the N-terminus of helix E, away from the active site, whereas other three mutations are present on helix I within the active site. Mutation V247F, which is also found in the *ES7* variant, indicates that this mutated residue may play important role in the improvement of activity towards degradation of ES diol (**14**). However, the orientation of residue 247F in *IND1* is different than in *ES7*. This different orientation of phenyl ring of residue 247F in *IND1* and *ES7*, indicates that the orientation of the phenyl ring also plays a role in improvement in activity towards degradation of ES diol (**14**) in both mutants. In this model of *IND1* with ES diol (**14**) bound, residues Thr101 and Asp297 play a key role in the orientation of the substrate bound in the active site through a network of H-bonding interactions (Figure 3.20, Appendix A13).

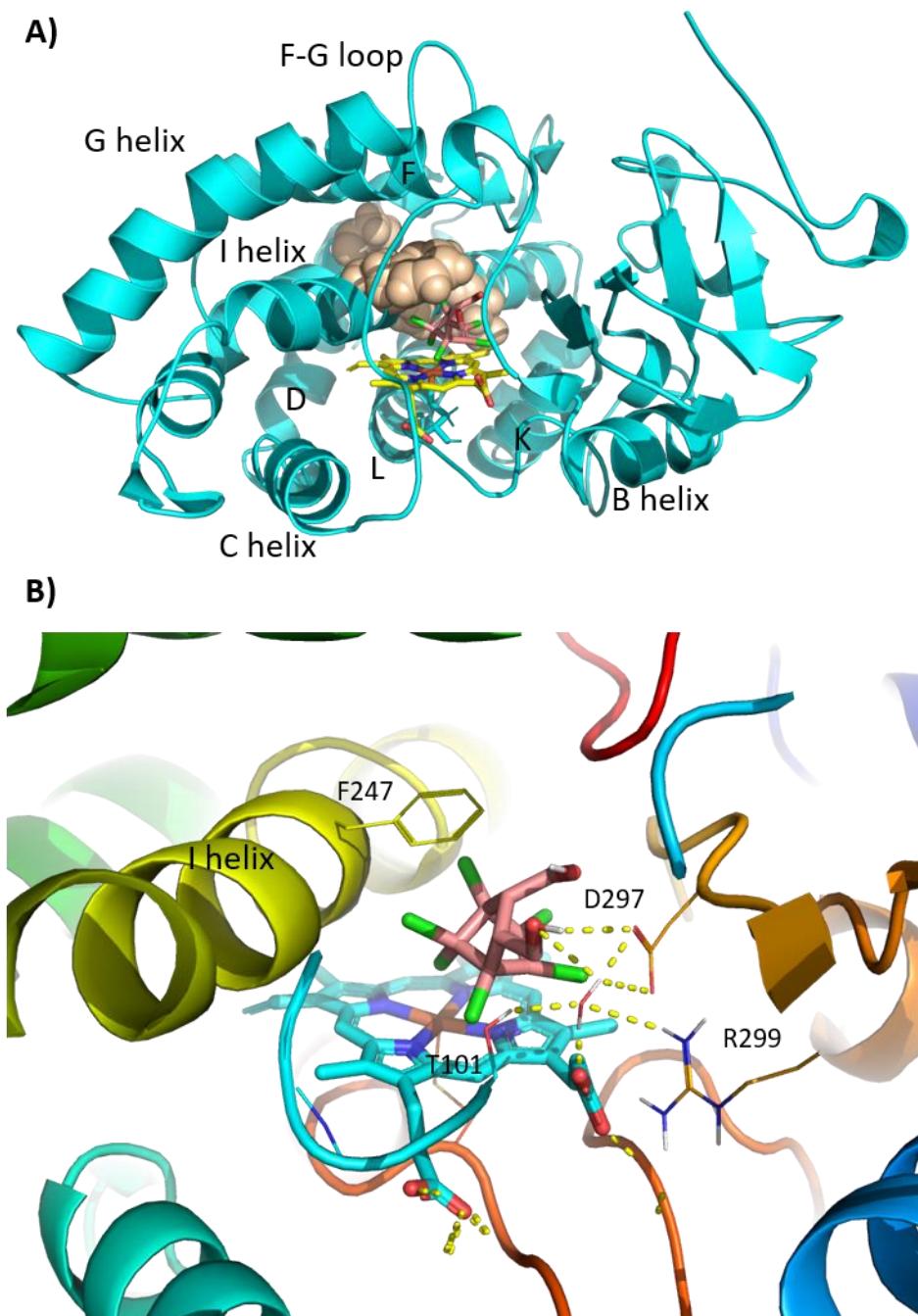


Figure 3.20 The *in silico* molecular docking results of *IND1* (E156G/V247F/V253G/F256S) and ES diol (14). (A) P450 is shown in cyan color, heme in yellow color, mutations are shown in wheat colored spheres, and ES diol in pink color. (B) Orientation of ES diol (14) in active site (proposed H-bonds are shown as yellow dotted lines).

K314E mutant and ES diol (14)

The mutation K314E was found in two most active mutants (*ES2* and *ES7*), and the single mutant K314E was found to be more active towards ES diol degradation than WT-P450_{cam} (Table 3.3). Even though K314E is located away from the active site in the loop between helices K and K', the model of variant K314E with ES diol (**14**) bound in the active site, shows that the substrate is stabilized through a network of H-bonding interactions between Asp297 and Arg299 residues (Figure 3.21, Appendix A13).

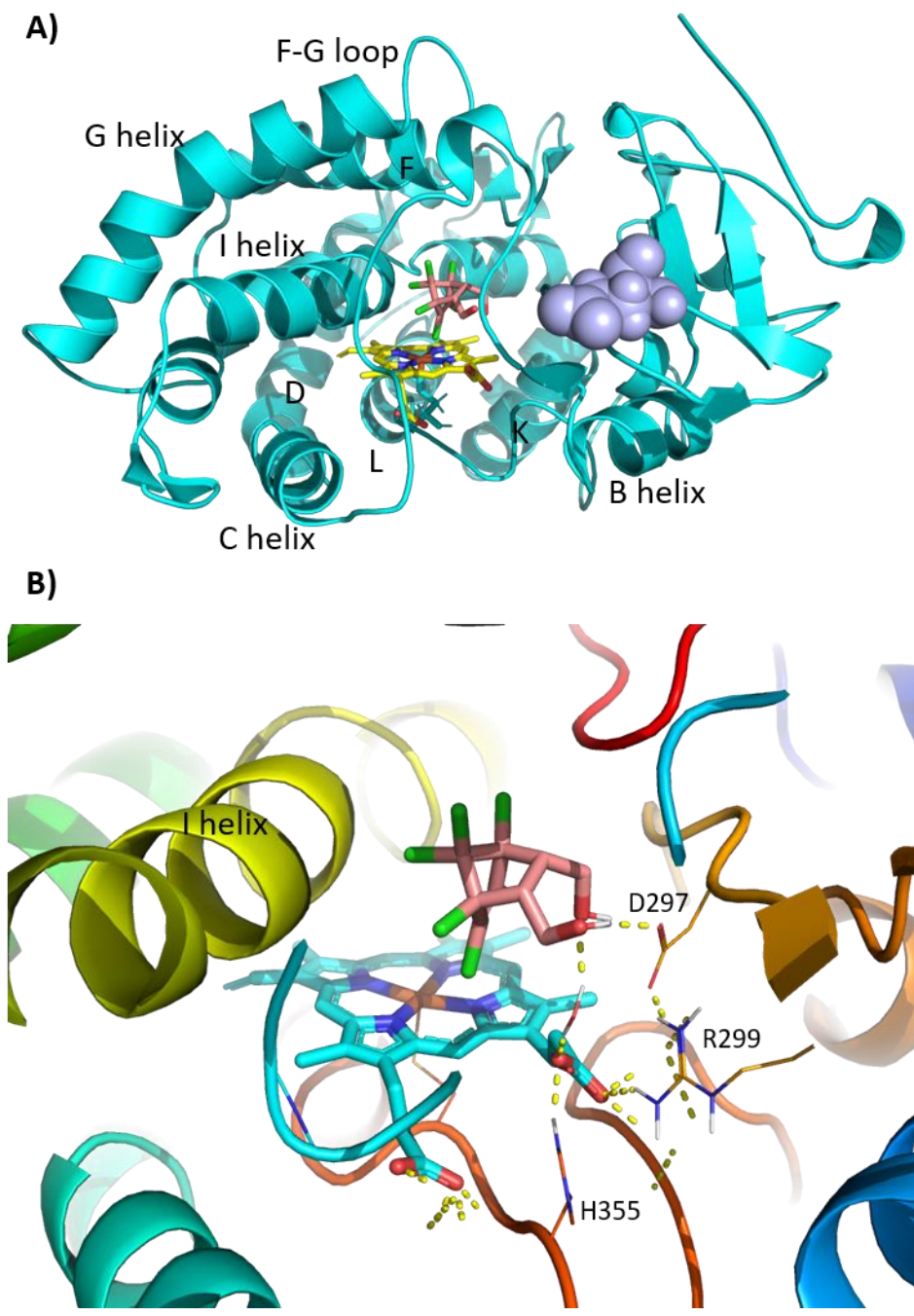


Figure 3.21 The *in silico* molecular docking results of K314E and ES diol (14). (A) P450 is shown in cyan color, heme in yellow color, mutation is shown in light blue colored spheres, and ES diol in pink color. (B) Orientation of ES diol (14) in active site (proposed H-bonds are shown as yellow dotted lines).

WT-P450_{cam} and ES diol (14)

WT-P450_{cam} showed very low activity towards ES diol (**14**) degradation compared to the mutants (Table 3.2 and Table 3.3). Most of the poses in the docking simulation studies show ES diol (**14**) was not positioned very well for epoxidation, with its C=C bond above the heme, compared to the active P450_{cam} mutants (Figure 3.22). ES diol (**14**) bound in the active site of WT is stabilized by hydrophobic interactions with surrounding residues in the active site without making H-bonding contacts. The key difference between WT and mutants is in the orientation of ES diol (**14**) within the active site. In the WT, both hydroxyl groups of ES diol (**14**) are oriented towards the distal end of the protein (towards the loop between helices F and G Figure 3.22, Appendix A13). This positions the double bond between C1 and C2 of the substrate too far away from the heme-Fe to be effectively epoxidized (see proposed mechanism below section 3.2.1). As can be seen in Figure 3.11, a high “x” score, which is reflective of a large distance between C1, C2 and the heme-Fe, correlates with lower activity as reflected in k_{cat} .

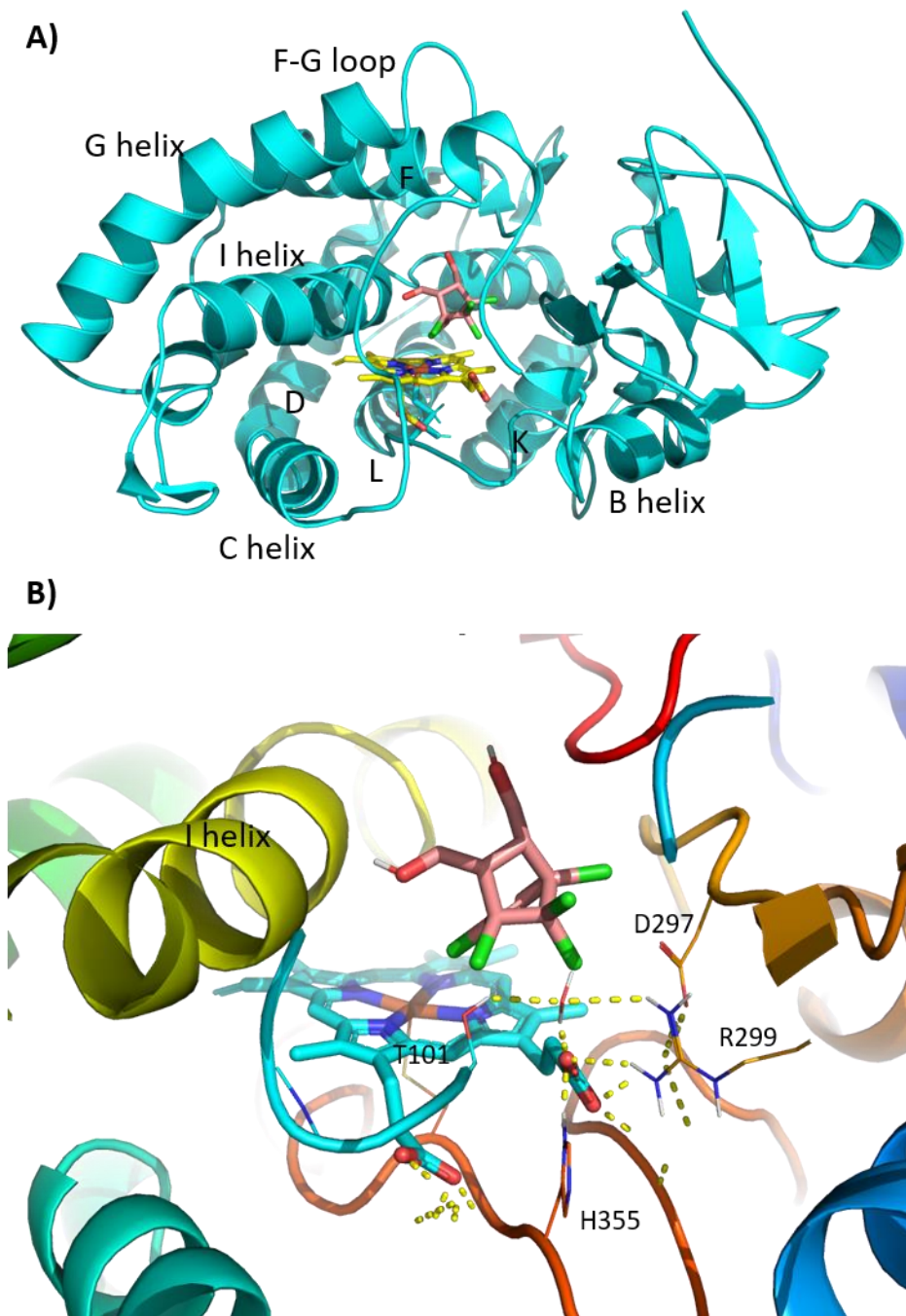


Figure 3.22 The *in silico* molecular docking results of WT-P450_{cam} and ES diol (14). (A) P450 is shown in cyan color, heme is in yellow color, and ES diol in pink color. (B) Orientation of ES diol (14) in active site (proposed H-bonds are shown as yellow dotted lines).

3.2. Discussion

3.2.1. Proposed mechanism of dehalogenation

Previously reported dehalogenation studies of chlorinated organic compounds by WT-P450_{cam} were limited to small organochloride compounds including halomethanes, tri, tetra, penta, and hexa-chloroethane, tetrachloroethene, and dichloropropane. These studies were done under low oxygen conditions resulting in reductive dehalogenation of those substrates (Lefever & Wackett, 1994; Li & Wackett, 1993; Logan et al., 1993; Wackett, 1995; Wackett et al., 1994). In this study, dehalogenation of endosulfan diol was investigated using P450_{cam} mutants, under oxidizing conditions. We detected aromatic products **24**, **32**, **33** and **34**. We demonstrated that they come from ES diol (**14**) and that their formation is coupled with the loss of ~ 6 Cl⁻ ions on average. Based on these observations, we propose a mechanism for the dehalogenation of endosulfan diol by these mutants (Figure 3.23).

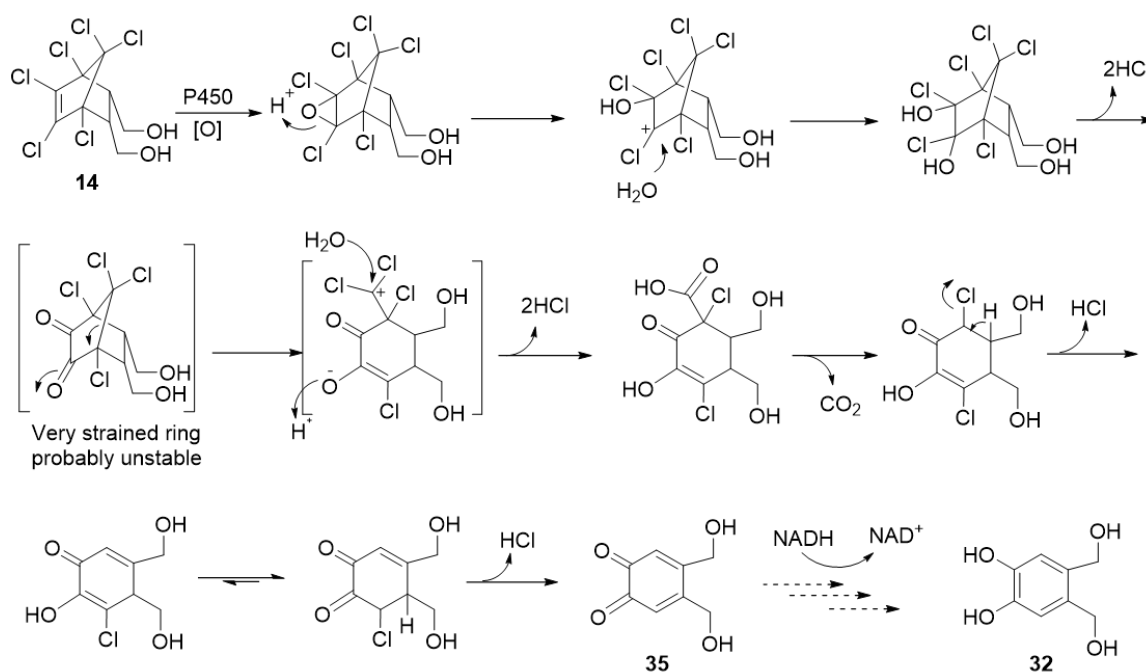


Figure 3.23 Proposed mechanism of degradation of ES diol (**14**) by P450_{cam} mutants, such as *ES7*. The proposed route accounts for the loss of 6 Cl⁻ ions from the ES diol core structure and of the bridge as CO₂.

The proposed mechanism of dehalogenation is initiated by oxidation of the sterically hindered and electron poor double bond of ES diol (**14**) by the active P450_{cam} mutants. This oxidative dehalogenation of ES diol was observed under two conditions: 1) using the redox partners of P450_{cam} PdR and PdX and the natural electron donor NADH and O₂ from the air, or 2) using an artificial shunting agent, *m*-CPBA, with the P450_{cam} mutants. Both of these conditions are oxidizing, whereas previously observed dehalogenation of polychlorinated ethane congeners by P450_{cam} was proposed to involve two-electron reduction of the substrate under low oxygen conditions (Li & Wackett, 1993).

Oxidation of the double bond of ES diol (**14**) initiates a dehalogenation cascade comprised of multiple chloride elimination steps, which results in the formation of a quinone product (**35**) (Figure 3.23). Consistent with formation of an *ortho*-quinone we observed a colored product in the 4-AAP coupled assay in the absence of HRP (Figure 3.2, D). However, HRP was added to convert any phenolic metabolites back to quinones, in order to quantify them together in the 4-AAP coupled assay. Phenolic products **32**, **33** and **34** form by reduction of the very reactive *ortho*-quinone with NADH, which is present in excess in the reaction mixture. Interestingly, in a preliminary study, in which we transformed *ES7* into *P. putida* (ATCC17453) and incubated that with ES (**13**), *o*-phthalaldehyde was isolated from the culture mixture after a few days of incubation (Prasad, 2013). Formation of lactone (**24**) involves reduction of *ortho*-quinone (**35**), preceded (at the ES diol level) or followed by oxidation of one CH₂OH groups to the carboxylate level and spontaneous lactonization.

Consistent with dehalogenation, the release of chloride ions was detected and quantified using a chloride ion electrode, and we have found close to 6 chloride ions released per quinone product formed, as would be expected for the proposed mechanism (Figure 3.6). This is a new biodegradation of the ES, in which the chlorine atoms attached to the bicyclic core of the compounds are removed. Previously reported biodegradation of endosulfan by fungal strains (*Phanerochaete chrysosporiu*, (Kullman & Matsumura, 1996), *Aspergillus terreus* and *Cladosporium oxysporum* (Mukherjee & Mittal, 2005), *Mortierella* sp. (Kataoka et al., 2010), *Chaetosartorya stromatoides* and *Aspergillus terricola* (Hussain, Arshad, Saleem, & Zahir, 2007)) or bacterial strains (*Pseudomonas spinosa*, *Pseudomonas aeruginosa*, and *Burkholderia cepacian*, (Hussain, Arshad, Saleem, & Khalid, 2007), *Mycobacterium* sp. (Sutherland, Horne, Harcourt, et al., 2002),

Pandoraea sp. (Siddique et al., 2003), *Klebsiella pneumoniae* (Kwon et al., 2002)) etc. resulted in chlorinated endosulfan metabolites such as ES diol (Figure 1.17).

3.2.2. Effects of mutation in ES variants of P450_{cam}

In our study wild type P450_{cam} did not show significant dehalogenation activity, whereas the mutants previously selected on minimal media with endosulfan and *m*-CPBA (Kammoonah et al., 2018) were significantly more active in dechlorination of ES diol than the wild-type. Camphor, the natural substrate of cytochrome P450_{cam}, is oxidized regio- and stereoselectively to 5-exohydroxycamphor (Prasad et al., 2011). Endosulfan and related compounds are larger than camphor, though their bicyclic core resembles it. In order to accommodate substrates with different size and/or shape than camphor, several amino acid residues in the catalytic site of P450_{cam} have been mutated rationally (Figure 1.14). Tyr96 hydrogen bonds with the carbonyl group of camphor, and Phe87 makes hydrophobic interactions with camphor. Both residues play a key role in regioselective and stereoselective oxidation of camphor at the 5-position (Bell et al., 2003). Therefore, Tyr96 and Phe87 are the most commonly mutated amino acid residues in P450_{cam} mutants (Table 1.6, Table 1.7 and Table 1.8). For example, the following alterations of P450_{cam} substrate selectivity have been reported: naphthalene oxidation by Y96G/A/V/F mutants (England et al., 1998) and polycyclic aromatic oxidation by F87L/A-Y96F mutants (Harford-Cross et al., 2000), epoxidation of styrene to styrene oxide by Y96A and Y96F mutants (9 fold and 25 fold higher than WT P450_{cam} respectively) (Nickerson et al., 1997), benzocycloarene oxidation by Y96F mutant (Mayhew et al., 2002), 2-ethylhexanol to 2-ethylhexanoic acid (F87W, Y96W, T185F, and L244A mutants) (French et al., 2001, 2002), hydroxylation of polychlorinated benzene to give polychlorinated phenol (F87W-Y96F-F98W and F87W-Y96F-V247L mutants) (Jones et al., 2000). Only the F87W mutant of P450_{cam} was found active towards reductive dehalogenation of pentachloroethane (Manchester & Ornstein, 1995).

Leu244, Val247 and Val295, which make hydrophobic contacts with camphor bound in the active site (Poulos et al., 1985), have also been mutated to study the oxidation of different hydrophobic substrates (Table 1.6, Table 1.7 and Table 1.8). In our case, Val247 and Asp297, which were mutated in *ES7* (V247F/D297N/K314E), are the only residues in the mutants we isolated from our random mutagenesis and selection that were previously altered rationally in P450_{cam} mutants (Table 1.6, Table 1.7 and Table 1.8).

Val247 was previously mutated along with Phe87, Tyr96 and other amino acids to study terpene oxidation (V247L) (Bell et al., 2003; Bell et al., 2001; Sowden et al., 2005), propane and butane oxidation (V247L) (Bell et al., 2003), hexane oxidation (V247A/L) (Stevenson et al., 1998), and benzylic oxidation of ethyl benzene (V247L/M/A) (Eichler et al., 2016; Loida & Sligar, 1993). However, residue Asp297 was mutated previously only to study propane and butane oxidation (D297M) (Bell et al., 2003) (Table 1.6, Table 1.7 and Table 1.8). The other residues we found in our set of mutants (T56, Q108, N116, G120, S221, I281, R290, F292, A296, K314, I318 and P321) have never been reported to have been altered.

Certain residues in P450_{cam} which play key roles in catalytic activity and stability of P450_{cam} are summarized in Table 1.5. Any mutation in these residues has resulted in either a decrease or complete loss of catalytic activity of P450_{cam}. For example, Cys357, which is the axial ligand of heme-Fe, is crucial for the P450_{cam} catalytic cycle. C357H/M mutation resulted in complete loss of P450_{cam} activity (Murugan & Mazumdar, 2005; Yoshioka et al., 2001). Even mutation of Leu358, which is next to Cys357, has a detrimental effect on the thiolate axial ligand to Fe from the side chain of Cys357, which resulted in loss of P450_{cam} catalytic activity (Batabyal et al., 2013; Karunakaran et al., 2011; Tosha et al., 2004; Yoshioka et al., 2000). Residues Asp251 and Thr252, along with Lys178 and Arg186, which are involved in a network of H-bonding, play a crucial role in proton delivery to the distal oxygen of the peroxo (**5**) and hydroperoxo (**6**) complexes during the catalytic cycle (Figure 1.3). They deliver protons through a water network (Schlichting et al., 2000; Vidakovic et al., 1998), ensuring that Compound 0 (Figure 1.3, **6**) is protonated distally to eliminate water, resulting in the Fe^{IV}-oxo-porphyrin cation radical species known as Compound-I (Cpd-I, Figure 1.3, **7**) (Gerber & Sligar, 1992; Hishik et al., 2000; Kim et al., 2008; Nagano & Poulos, 2005; Vidakovic et al., 1998; Wang et al., 2015). In our selected mutants, these residues which are important for proton delivery or electron transfer during catalytic cycle of P450, were found not to be mutated.

Residue Thr101 makes a H-bond with the propionate chain of heme and is important for heme retention in the enzyme (Manna & Mazumdar, 2006). However, certain residues which are neither present directly in the active site of P450_{cam} nor play role in P450_{cam} structure stability, can play a role in substrate availability or selection. For example, Ser190, which is present on the surface of the enzyme in the loop between helices F and G, can recognize and direct camphor towards the binding site (Behera &

Mazumdar, 2008). While the rational mutation studies, summarized in Tables Table 1.5, Table 1.6 and Table 1.7, address important residues in P450_{cam}, we have noticed that some of the mutations we observed (G120S, K314E) are not directly present in the substrate binding site, and their effect in improving endosulfan (**13**) biodegradation is somewhat unexpected (Figure 3.24).

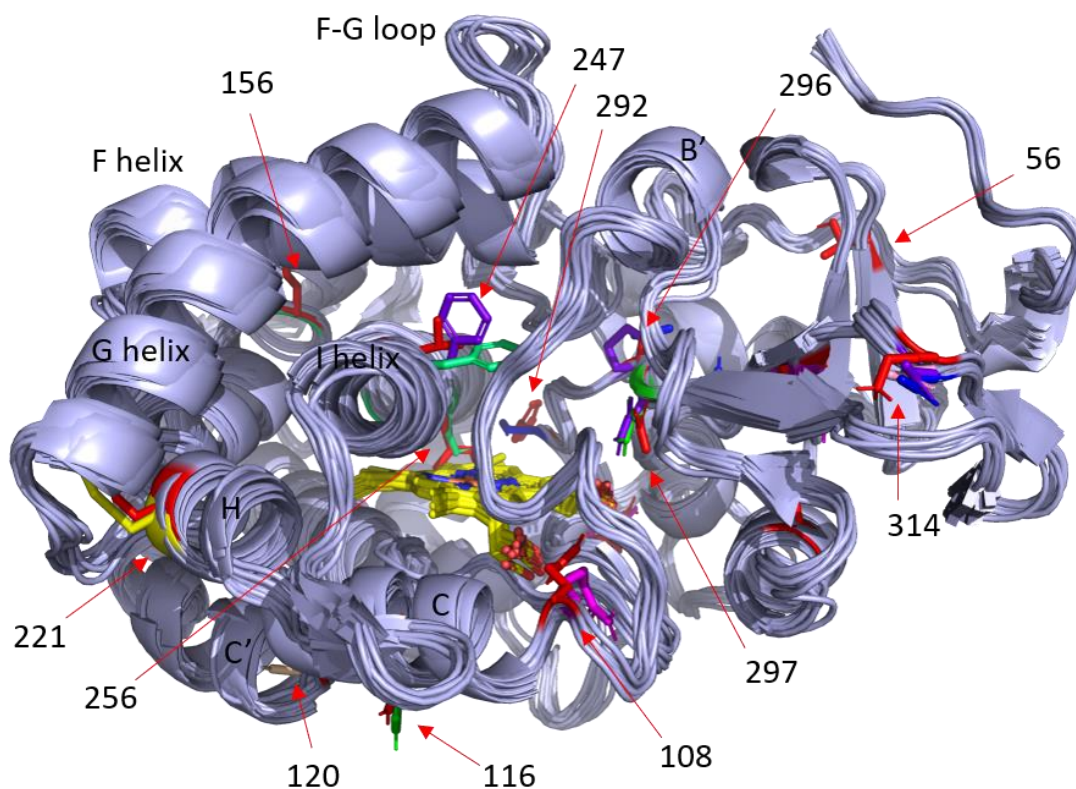


Figure 3.24 Superimposed structures of WT-P450_{cam} and mutants (ES diol is not shown). P450 is shown in light blue color, heme in yellow color, and mutated residues are identified with the residue number. Residues are colored: ES1 in green, ES2 in blue, ES3 in magenta, ES4 in yellow, ES5 in orange, ES6 in wheat, ES7 in purple blue, IND1 in light green, K314E in pink and WT in red.

Putidaredoxin (PdX) binds to the proximal end of P450_{cam}, and Arg112 along with Arg109 are important residues for electron transfer from PdX to P450_{cam} (Koga et al., 1993). Apart from shuttling electrons from putidaredoxin reductase to P450_{cam}, PdX also

plays an effector role during catalysis of P450_{cam} (Batabyal et al., 2016; Lipscomb et al., 1976; Tosha et al., 2003; Tripathi et al., 2013; Tyson et al., 1972). Upon substrate binding to the active site of P450_{cam}, the first electron transfer to high-spin (HS) heme-Fe^{III} (substrate bound, **2**) yielding heme-Fe^{II} (substrate bound, **3**), can be achieved using a suitable reductant (Figure 1.3). However, P450_{cam} requires PdX specifically for the second electron transfer, needed to make ferric peroxo complex (**5**) from ferric superoxo species (**4**) (Figure 1.3) (Lipscomb et al., 1976; Pochapsky et al., 2001). The binding of PdX to P450_{cam}, induces displacement in helix C, which is then transmitted to helix B' and other helices (B, E, F, G, and I) on the distal end of the P450_{cam} (Myers et al., 2013; Pochapsky et al., 2003; Pochapsky & Pochapsky, 2019; Tripathi et al., 2013). Displacements in helices F and G, are the main features of the open (substrate free)/ close (substrate bound) transition (Figure 1.10), while helix B' is present near the active site of P450_{cam} (Lee et al., 2010). Different spectroscopic data show that PdX favors the open-conformation of P450_{cam} (or shifts the closed state to the open state) (Hiruma et al., 2013; Pochapsky et al., 2003; Tripathi et al., 2013; Unno et al., 1997). It is suggested that the reduced PdX transfers the electrons to a substrate-bound closed conformation of P450_{cam} giving ferric-hydroperoxo complex (**6**, Figure 1.3) bound to oxidized PdX. The oxidized PdX is supposed to convert this into the open-conformation (Myers et al., 2013; Ortiz de Montellano, 2015). In our selected P450_{cam} mutants, some of the mutations are located in these helices which have shown some displacement upon PdX binding in these and other studies. For example, Q108R (*ES3*), N116H (*ES1*), and G120S (*ES6*) mutations are located in helix C directly at the binding site of PdX (Figure 3.24). These mutations may play a similar effector role to some extent as PdX or enhance it in the presence of PdX. Mutation S221R in helix H, can induce displacement in the F/G helices to affect the dynamics between the open and closed conformations of P450_{cam}.

As PdX favors the open conformation of P450_{cam}, camphor is being used in large excess to saturate the P450_{cam} for the catalytic activity (Glascock et al., 2005). However, in our studies of ES diol (**14**) degradation using P450_{cam} mutants with PdX and PdR to source the electron from NADH, we observed allosteric sigmoidal kinetics (Figure 3.3). This sigmoidal kinetics indicates that due to the higher dissociation constant (K_d) of ES diol (**14**) compared to camphor (Table 3.4), we need higher concentration of ES diol (**14**) to fully saturate the P450s in the closed conformation to notice the catalytic activity using PdX and PdR. In the presence redox partners (PdX and PdR), one may observe sigmoidal

kinetics because there is a rate-limiting step between substrate binding and the formation of Cpd I (Figure 1.3, 7) which probably requires a closed conformation of P450s. Cpd I is needed to epoxidize that electron-poor double bond of ES diol (**14**), as we have proposed (Figure 3.23). On the other hand, using *m*-CPBA as shunt, it allows the enzyme to access Cpd I directly (Figure 1.3). Thus, using *m*-CPBA as a shunt with *ES7*, we observed Michaelis-Menten kinetics using lower concentrations of ES diol (**14**) (Figure 3.4).

3.3. Conclusion

We have succeeded in the biodegradation of polychlorinated persistent-organic-pollutant endosulfan (**13**) and its most common metabolite endosulfan diol (**14**), using selected P450_{cam} mutants (*ES1-ES7*, *IND1*, *K314E*). We also have proposed a mechanism of dehalogenation where six HCl molecules are released per molecule of ES diol, which were confirmed by using an ion selective chloride electrode. Further, non-chlorinated metabolites of ES diol were detected by LC-MS and ¹³C-labelled product was detected by NMR. These results are consistent with the proposed mechanism of dehalogenation. The metabolites were coupled with 4-aminoantipyrine (4-AAP) to give the colored product which was detected by UV to quantify and measure the rate of degradation, and to compare the activity of the selected P450_{cam} mutants. WT-P450_{cam} showed very little activity ($k_{\text{cat}} = 0.8 \mu\text{M}/\text{s} \cdot \mu\text{M P450}$) compared to the mutants. Among the mutants, *ES2* (F292S/A296V/K314E/P321T) and *ES7* (V247F/D297N/K314E) were the most active mutants with high turnover number ($k_{\text{cat}} = 6.2 \pm 2.3 \mu\text{M}/\text{s} \cdot \mu\text{M P450}$, and $4.3 \pm 1.2 \mu\text{M}/\text{s} \cdot \mu\text{M P450}$, respectively), and high catalytic efficiency ($k_{\text{cat}}/K_{\text{M}} = 16.6 \pm 6.1 \times 10^{-3} 1/\text{s} \cdot \mu\text{M}$, and $12.8 \pm 3.7 \times 10^{-3} 1/\text{s} \cdot \mu\text{M}$, respectively). However, *ES2* is unstable when cloned with a His₆-tag for purification. Catalytic activity of *ES7* ($k_{\text{cat}} = 12.6 \pm 4.7 \mu\text{M}/\text{s} \cdot \mu\text{M P450}$) was increased when purified proteins were used. *ES5* (A296P) and *ES6* (G120S), each with a single mutation, were also found to be more active than WT-P450_{cam}, but less active than *ES7* and *ES2*. The steady-state kinetic data suggest that the multiple substitutions may play a role in improving P450_{cam} activity. However, some mutations which may not be present directly at the active site of P450 but at a position important for overall protein dynamics, may contribute to change the substrate selectivity and the activity.

In molecular docking studies, the orientation of the ES diol in selected poses also support the proposed mechanism of dehalogenation, which is initiated with the oxidation of the C=C bond on the bulky chlorinated endosulfan diol molecule.

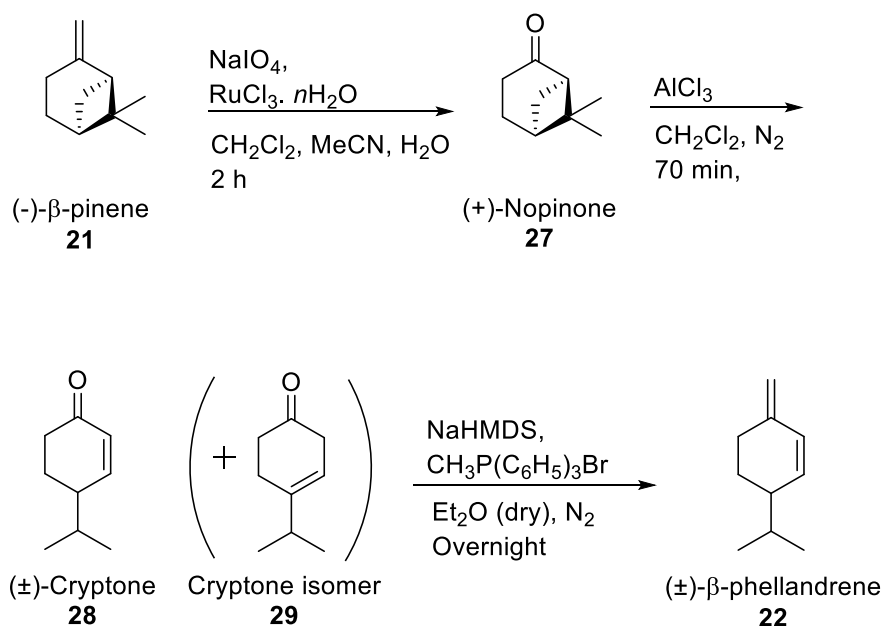
P450_{cam} variants that are efficient in the degradation and dehalogenation of endosulfan and ES diol could be used in the dehalogenation of other organochlorine substrates such as dechlorane plus and heptachlor which have similar polychlorinated moiety.

Chapter 4. Oxidation of β -phellandrene by WT-P450_{cam} and ES7 mutant

4.1. Results

4.1.1. Synthesis of β -phellandrene

Synthesis of β -phellandrene (**22**) commenced with a commercially available monoterpene, (-)- β -pinene (**21**, Scheme 4.1).



Scheme 4.1 Synthesis of β -phellandrene from β -pinene.

Oxidation of β -pinene to synthesize (+)-nopinone (27)

Oxidation of (-)- β -pinene (**21**) to (+)-nopinone (**27**) using KMnO_4 as oxidizing agent under different conditions resulted in up to 46% yield of (+)-Nopinone (**27**) in 24 hours of reaction (Table 4.1). However, using a catalytic amount of RuCl_3 with NaIO_4 (Kawashima et al., 2014) has not only increased the yield significantly, but also requires less time to complete the reaction (2 hours, 84% yield) (Table 4.1, entry 4).

Table 4.1 Synthesis of (+)-Nopinone (27) using different oxidizing agents/conditions

Entry	Oxidizing agent	Solvent mixture	Reaction time at RT	Yield
1	KMnO ₄ , alumina *	CH ₂ Cl ₂ , <i>t</i> -BuOH	24 hours	39%
2	KMnO ₄ , acidic alumina *	CH ₂ Cl ₂ , <i>t</i> -BuOH	24 hours	46%
3	NaIO ₄ , KMnO ₄ (cat) *	H ₂ O, <i>t</i> -BuOH	24 hours	30%
4	NaIO ₄ , RuCl ₃ .nH ₂ O (cat)	CH ₃ CN, H ₂ O, CCl ₄	2 hours	84%

* See reaction procedure in Appendix B.

Ring opening of (+)-nopinone using AlCl₃ to give (±)-cryptone (28)

Ring opening of (+)-nopinone (**27**) using AlCl₃ according to previous known method (Mori, 2006) yielded (±)-Cryptone (**28**) (77% yield), along with the β,γ-unsaturated ketone (**29**, 10% isolated yield). The β, γ-unsaturated ketone isomer (**29**) was separated, using silica gel column chromatography. Ketone **29** is the synthetic precursor of β-terpinene, another important monoterpene. The racemization of cryptone and the formation of by-product ketone **29** is a consequence of the formation of a carbocation during the ring opening of (+)-nopinone to cryptone catalyzed by the Lewis acid (AlCl₃) (Figure 4.1). The cryptone isomer (**29**) was observed during the ring opening reaction along with cryptone (**28**) over the time (Table 4.2).

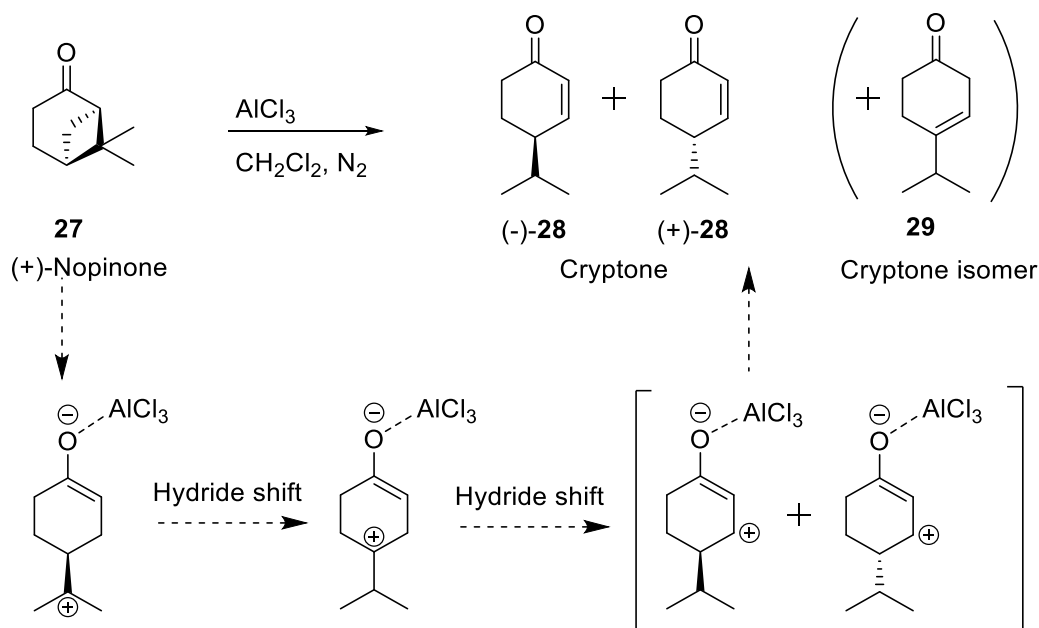


Figure 4.1 Ring opening of (+)-nopinone (**27**) to cryptone (**28**) catalyzed by Lewis acid (AlCl₃).

Table 4.2 Ring opening of nopinone (27) and product ratio over time

#	Reaction Time	Ratio (%)		
		(+)-nopinone (27)	(±)-cryptone (28)	Cryptone isomer (29)
1	5 minutes	97	2	1
2	30 minutes	81	16	3
3	1 hour	65	32	3
4	2 hours	13	77	10
5	3 hours	2	92	6

Wittig reaction of (±)-cryptone (28) to give (±)-β-phellandrene (22)

Wittig reaction of (±)-cryptone (**28**) with methyl triphenylphosphonium bromide gave (±)-β-phellandrene (**22**, 70% yield), according to the literature (Bergstrom et al., 2006). Optical rotation of the final product shows that it is racemic (±)-β-phellandrene (see section 2.1.1). Our scheme of (±)-β-phellandrene synthesis starting with (-)-β-pinene in 3 steps is the most efficient synthesis (46 % yield in 3 steps). Racemic β-phellandrene was used further for enzymatic assays.

4.1.2. Enzymatic assays***Ligand binding and dissociation constant (K_d) using purified WT-P450_{cam} and the ES7 mutant***

The dissociation constant (K_d) of (±) β-phellandrene was measured using the change in the spin state equilibrium of the P450 heme, often seen upon substrate binding, as mentioned in section 3.1.6. In the absence of natural substrate camphor (**10**), WT-P450_{cam} shows a characteristic peak (λ_{max} 418 nm – low spin Fe-III), which is blue shifted (λ_{max} 392 nm – high spin Fe-III) upon addition of camphor due to the change in the spin state of iron (Fe) in the heme molecule. On titrating the ES7 mutant and WT-P450_{cam} with β-phellandrene (**22**), the spin change of Fe in heme was observed (Figure 4.2).

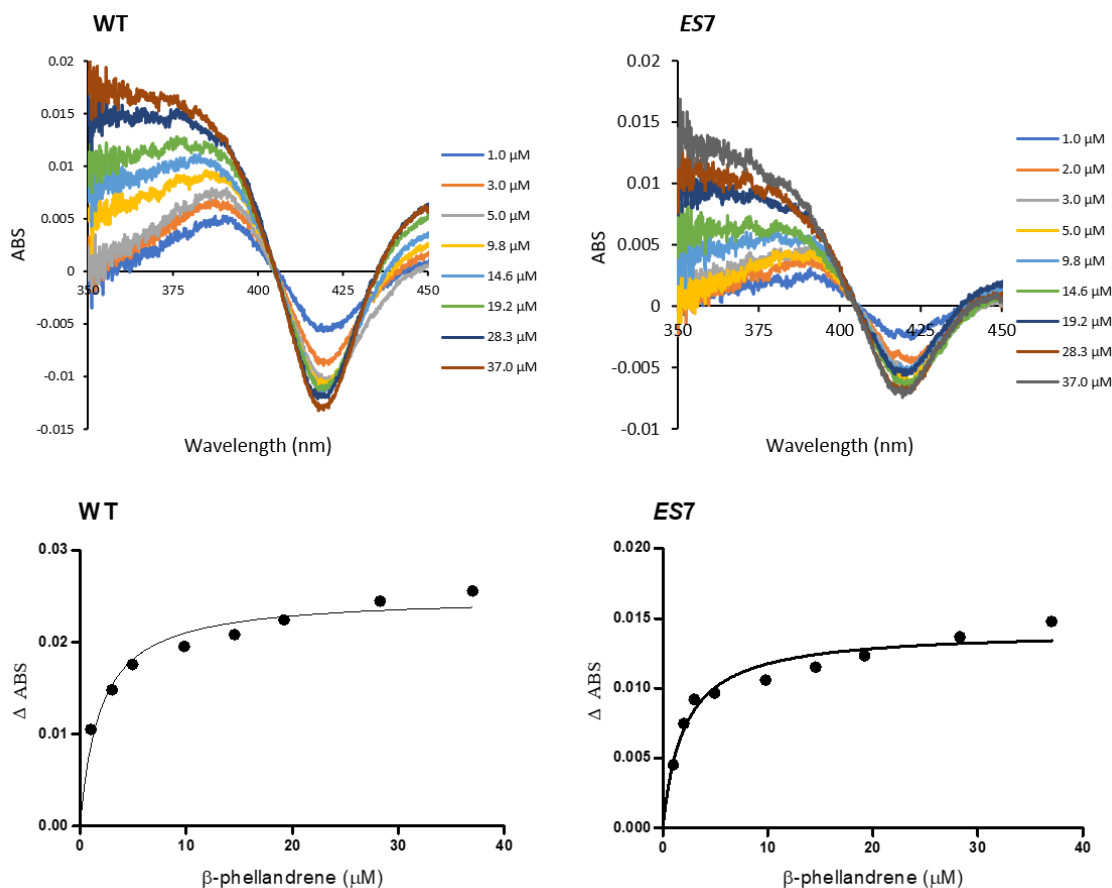


Figure 4.2 Titrations of wild-type (WT) (left set of graphs) P450cam and mutant *ES7* (right set of graphs) with β -phellandrene (**22**). The spectra (top set of graphs for each enzyme) show the blue shift in the Soret band as substrate is titrated into the enzyme preparation. The isotherms (lower set of graphs for each enzyme) depict the change in the Soret band (the increase in absorption at the blue-shifted wavelength relative to the decrease in absorption of the original Soret band).

The change in spin state as the substrate is titrated into the enzyme is used to calculate K_d values for β -phellandrene (**22**) (Table 4.3), which were: $1.9 \pm 0.38 \mu\text{M}$ and $2.0 \pm 0.04 \mu\text{M}$ for WT and *ES7* mutant respectively, which is very close to the K_d of camphor-WT P450_{cam} (Table 4.3).

Table 4.3 Dissociation constant measured using β -phellandrene (**22**) with purified WT P450_{cam} and ES7 mutant

P450 _{cam}	Mutations	(<i>d</i>)-Camphor (10) K_d (μ M) *	β -phellandrene (22) K_d (μ M)
WT	-	1.7 \pm 0.04	1.9 \pm 0.38
ES7	V247F/D297N/K314E	10.4 \pm 0.43	2.0 \pm 0.34

* Values are calculated above in section 3.1.6.

***In-vitro* assay of β -phellandrene oxidation using WT P450_{cam} with *m*-CPBA as a shunt**

To determine whether β -phellandrene (**22**) is a potential substrate for P450_{cam} and to find possible oxidation product(s), experiments were performed using purified WT-P450_{cam} and *m*-CPBA (as shunt) in an *in vitro* assay. Organic extracts from these *in vitro* assays were analyzed using GC-MS.

When experiments were performed *in vitro* using WT-P450_{cam}, *m*-CPBA (shunt) and β -phellandrene (substrate), a new peak (retention time 9.3 minutes in GC) with mass 152 m/z (M^+) was exclusively detected in the extracts from the treatments after 20 minutes of incubation at room temperature. This peak was absent in the controls: (1) no P450_{cam}, and (2) no substrate (β -phellandrene). Absence of this peak (152 m/z) in the control without WT-P450_{cam} indicates that a new product must have resulted from oxidation of β -phellandrene catalyzed by WT-P450_{cam}. The new peak's mass spectrum, which shows an increase of the mass by 16 units (M^+ 152 m/z) from that of β -phellandrene (M^+ 136 m/z), also supports the new product as resulting from oxidation of β -phellandrene (Figure 4.3).

The peak area of the 152 m/z peak (9.3 minutes), along with that of other peaks which are noticeably different or representing oxidized product (with 16 mass units increase), in treatments vs. controls are summarized in Figure 4.4. These peaks with retention time of 10.5 min, 10.6 min, 10.8 min and 11.0 min, which may represent the epoxidized products of β -phellandrene, were also present in the control – no P450_{cam}, indicating the epoxidized products by *m*-CPBA oxidation of β -phellandrene (**22**) (Figure 4.3 and Figure 4.4). There are four possible diastereomers resulting from epoxidation of racemic β -phellandrene (**22**) which has two C=C bonds (Figure 4.3). The epoxidized products, resulting from reaction of β -phellandrene with *m*-CPBA, are distinct from the potential hydroxylation product at 9.3 min (see mass spectra in Appendix B1).

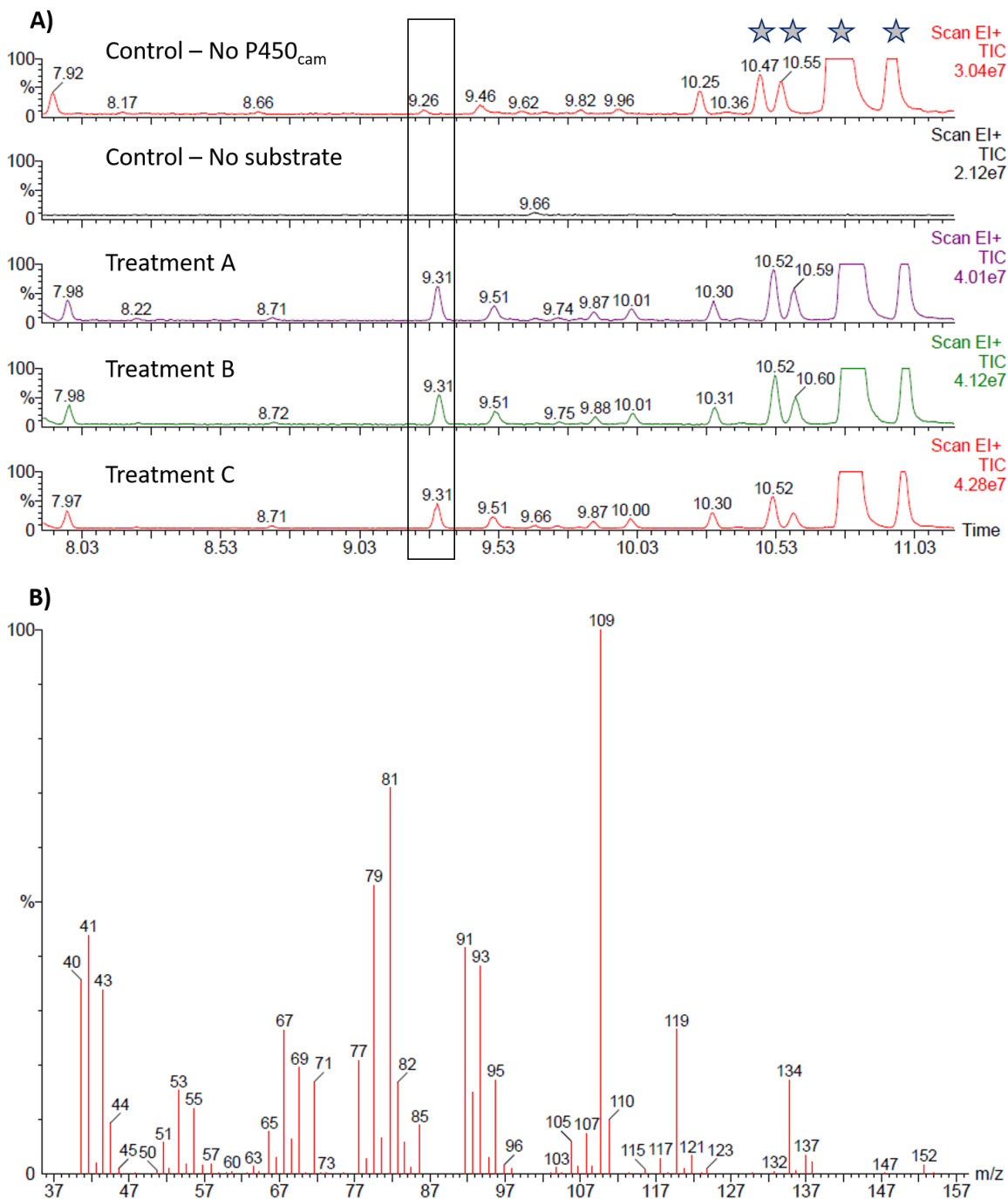


Figure 4.3 GC-MS analysis of extracts from the *in-vitro* assay using WT-P450_{cam}, *m*-CPBA and β -phellandrene. (A) Gas chromatograms: Control – no P450_{cam} using *m*-CPBA and β -phellandrene only, control – no substrate using WT-P450_{cam} and *m*-CPBA only, and treatment experiments using WT-P450_{cam}, *m*-CPBA and β -phellandrene. Peaks belonging to epoxidized products with retention times 10.5, 10.5, 10.8 and 11.0 min are represented by a 'star'. (B) Mass spectrum of the new peak at 9.3 minutes from treatment-A using WT-P450_{cam}.

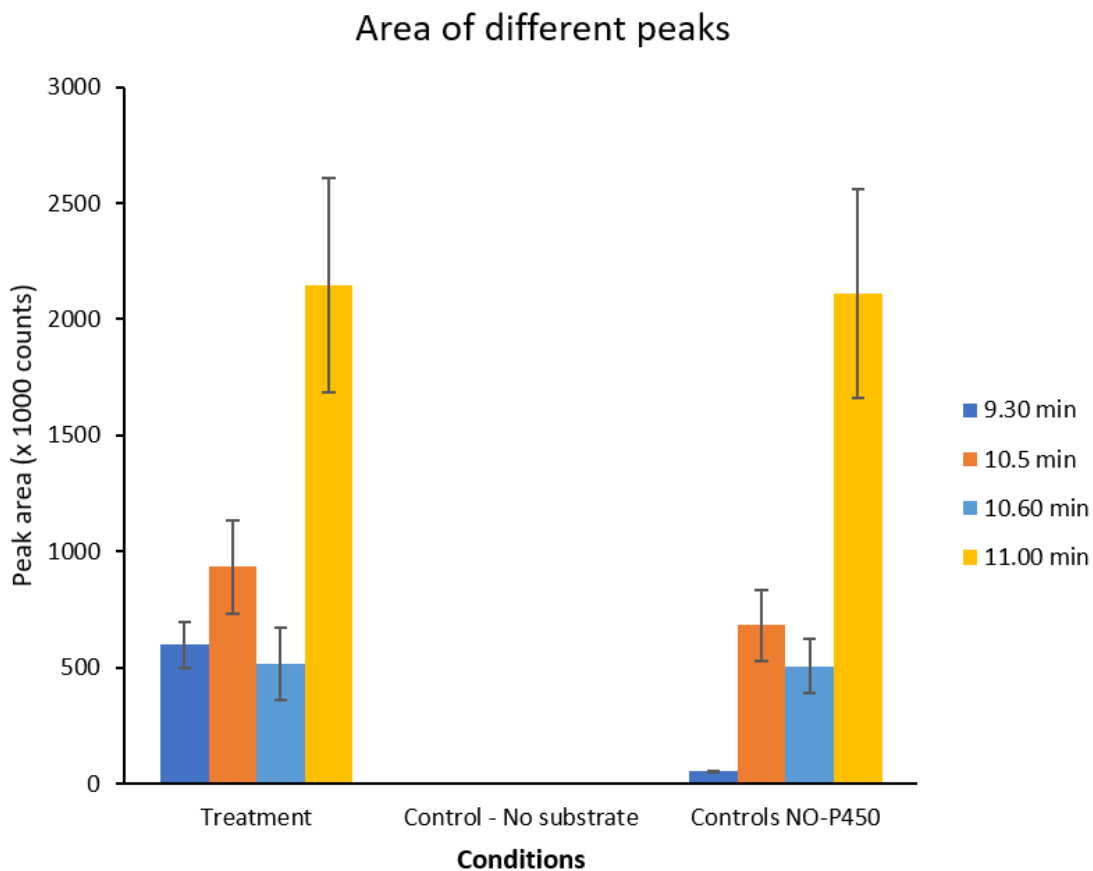


Figure 4.4 Area of the peaks at different retention time from *in-vitro* assay of β -phellandrene oxidation using WT-P450_{cam} and *m*-CPBA.

Note: The peak at 10.8 minutes from GC-MS, is omitted in this graph due to large peak area count

***In-vitro* assay of β -phellandrene oxidation using ES7 P450_{cam} mutant with *m*-CPBA as a shunt**

In vitro assays of β -phellandrene (**22**) oxidation were repeated using ES7 P450_{cam} and *m*-CPBA (shunt). Organic extracts from these experiments were analyzed using GC-MS. The peak (152 m/z) with retention time 9.30 minutes was also detected in treatments using ES7 P450_{cam} mutant and *m*-CPBA (shunt), similar to that of WT-P450_{cam} experiments. While the peak was not detected in the controls: no substrate (β -phellandrene **22**), and no P450_{cam} (Figure 4.5 and Figure 4.6). Epoxidized products were also noticed in these experiments (Figure 4.5 and Appendix B2).

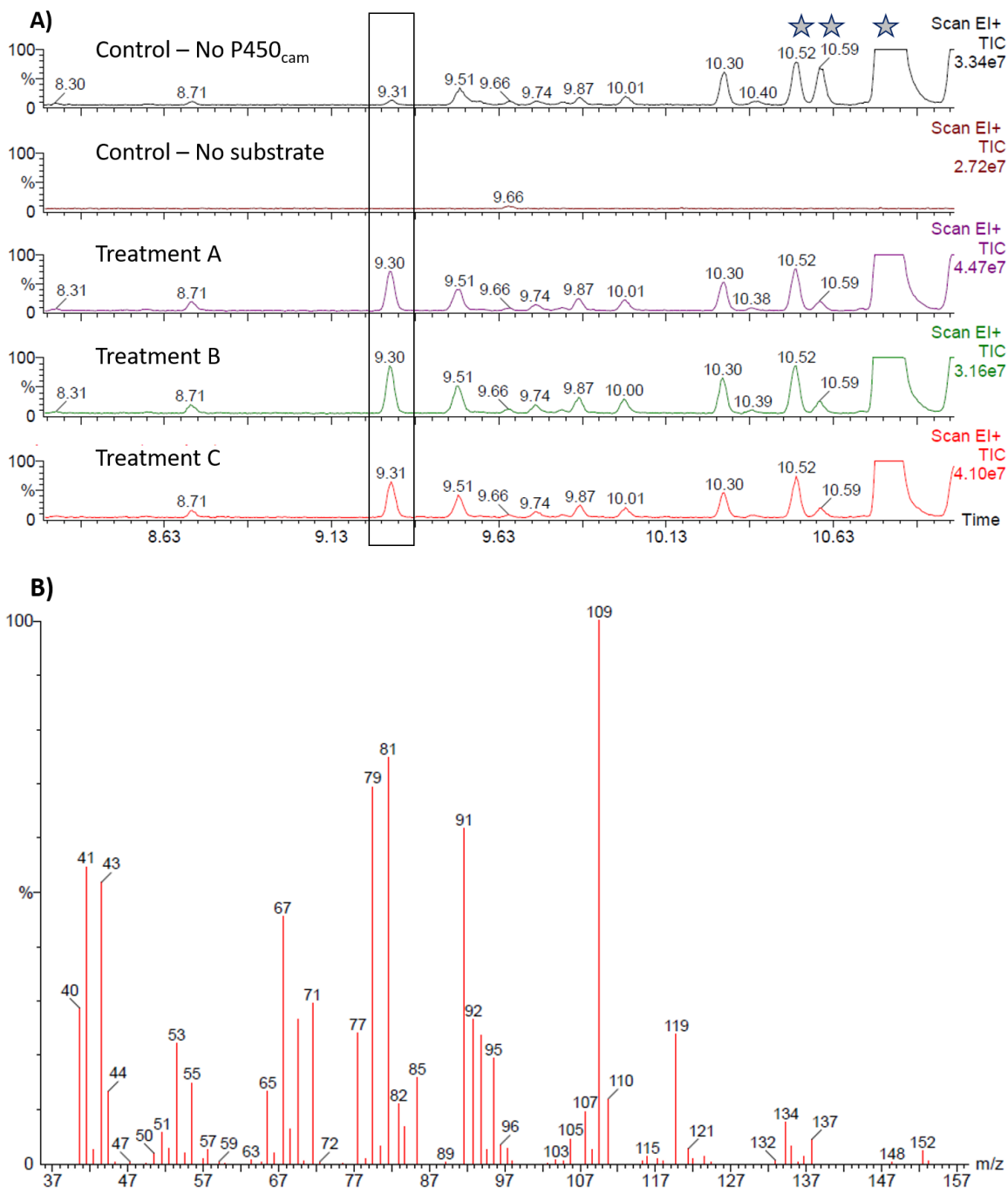


Figure 4.5 GC-MS analysis of extracts from the *in-vitro* assay using ES7-P450_{cam}, *m*-CPBA and β -phellandrene. (A) Gas chromatograms: Control – no P450_{cam} using *m*-CPBA and β -phellandrene only, control – no substrate using ES7-P450_{cam} and *m*-CPBA only, and treatment experiments using ES7-P450_{cam}, *m*-CPBA and β -phellandrene. Peaks belonging to epoxidized products with retention time 10.5, 10.5, 10.8 and 11.0 min are represented by a 'star'. (B) Mass spectrum of new peak at 9.3 minutes from treatment-A using ES7-P450_{cam}.

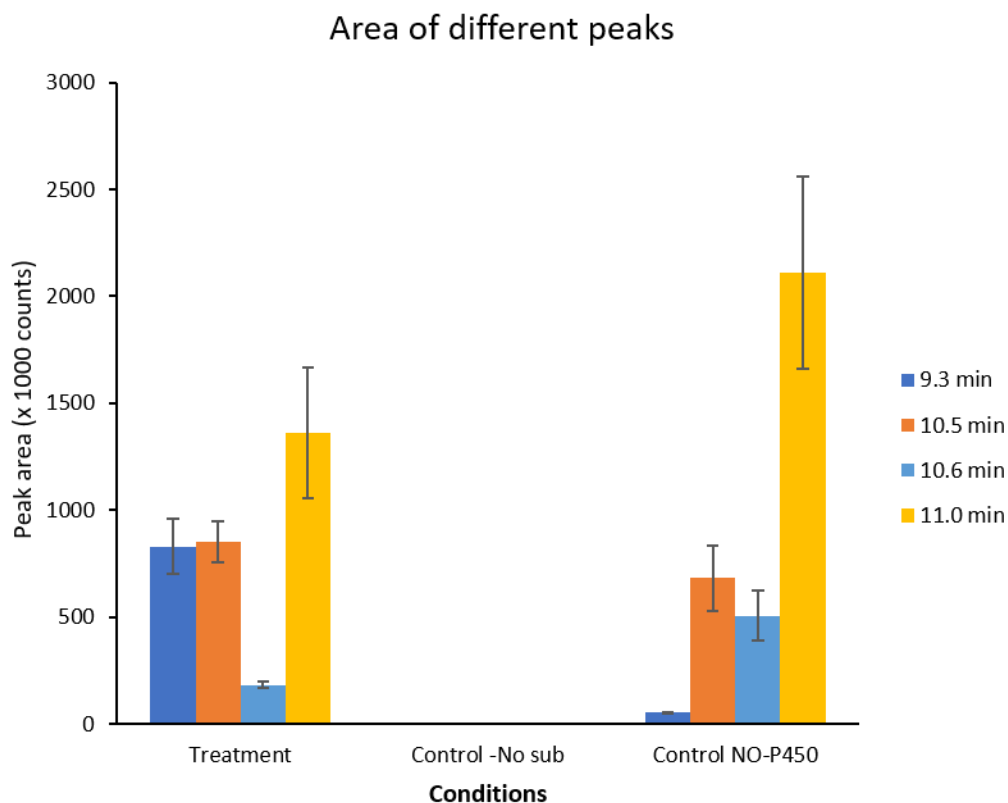


Figure 4.6 Area of the peaks at different retention time from *in-vitro* assay of β -phellandrene oxidation using *ES7*-P450_{cam} and *m*-CPBA.

Note: The peak at 10.8 minutes from GC-MS, is omitted in this graph due to large peak area count.

In order to compare the catalytic activity of *ES7* and WT-P450_{cam} towards oxidation of β -phellandrene (**22**), peak areas of the peak (retention time 9.3 minutes) were calculated. The *ES7* mutant has shown catalytic activity towards β -phellandrene (**22**) oxidation at similar rate to WT-P450_{cam} (Figure 4.7).

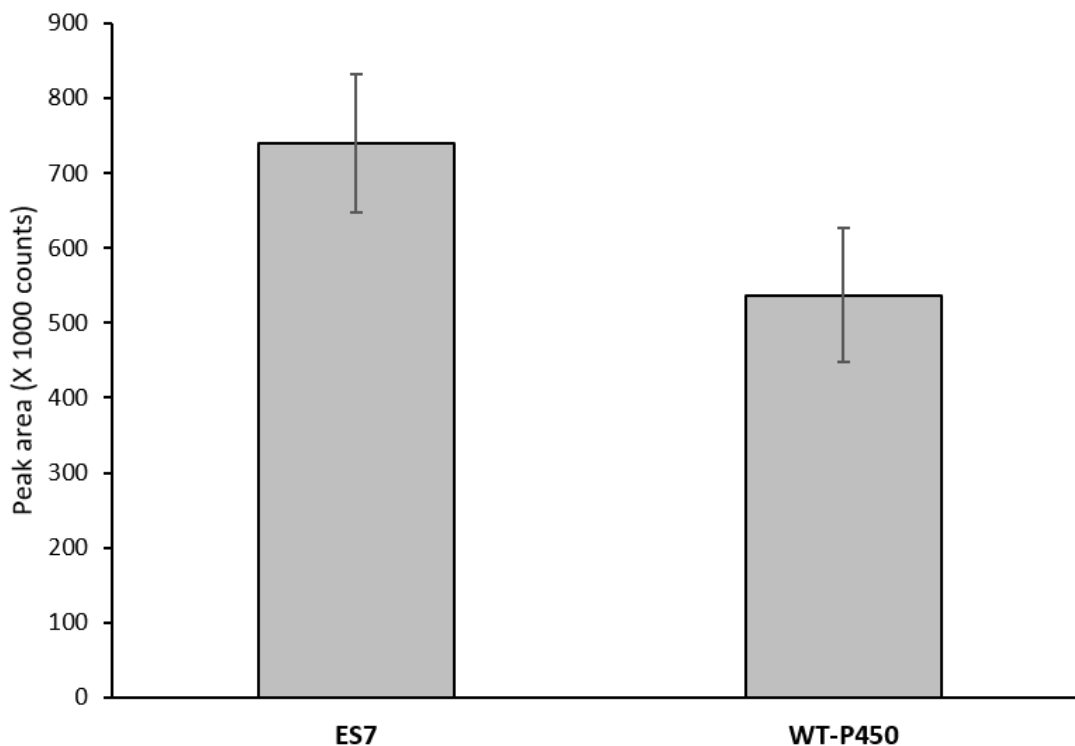


Figure 4.7 Comparing the catalytic activity: peak areas of the peak (152 m/z, with retention time at 9.3 minutes) from the *in-vitro* assay of β -phellandrene oxidation using WT-P450_{cam} and ES7 mutants.

Fragmentation pattern in mass spectrum and expected oxidation products of β -phellandrene

P450s are known to insert oxygen into C=C or C–H bonds resulting in epoxidation or hydroxylation, respectively. Oxidation of β -phellandrene catalyzed by P450_{cam} may result in epoxidized or hydroxylated products (Figure 4.8). Using *m*-CPBA as a shunt in these experiments of β -phellandrene (**22**) oxidation, the new product (152 m/z, at 9.3 minutes) is most likely hydroxylated, as epoxidized products (**36** and **37**) will also be present in control (No P450_{cam}) experiments (Figure 4.3 and Figure 4.5). To predict the possible hydroxylated product of β -phellandrene (**22**), the fragmentation pattern in mass the spectrum is a useful tool.

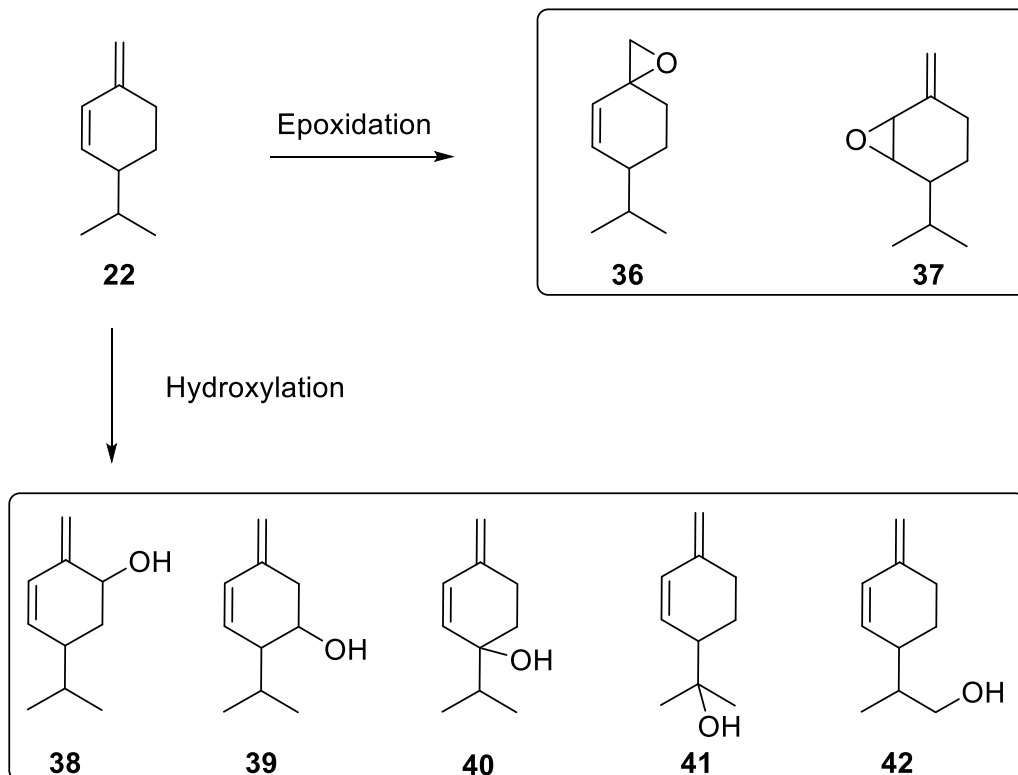


Figure 4.8 Possible oxidized products of β -phellandrene catalyzed by P450_{cam}.

The mass spectrum of β -phellandrene (22) shows the fragmentation peaks 136, 121, 93 m/z, which represent M^+ ($C_{10}H_{16}^+$), $M^+ - 15$ ($C_9H_{13}^+$), $M^+ - 43$ ($C_7H_9^+$), respectively. The base peak 93 m/z which results from fragmentation of the isopropyl group is more common due to the stability of the resulting fragments (Figure 4.9).

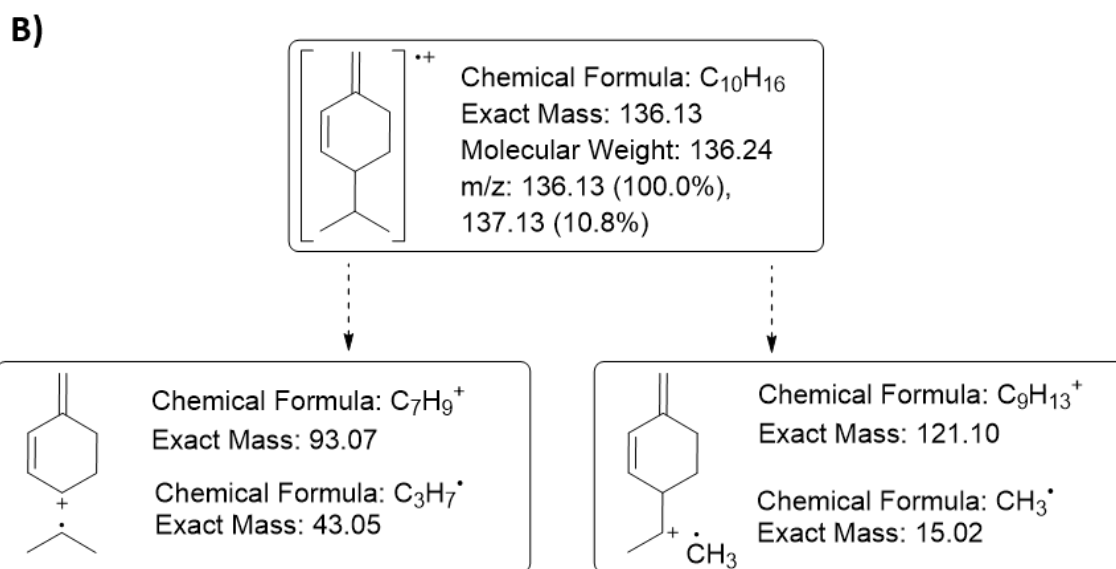
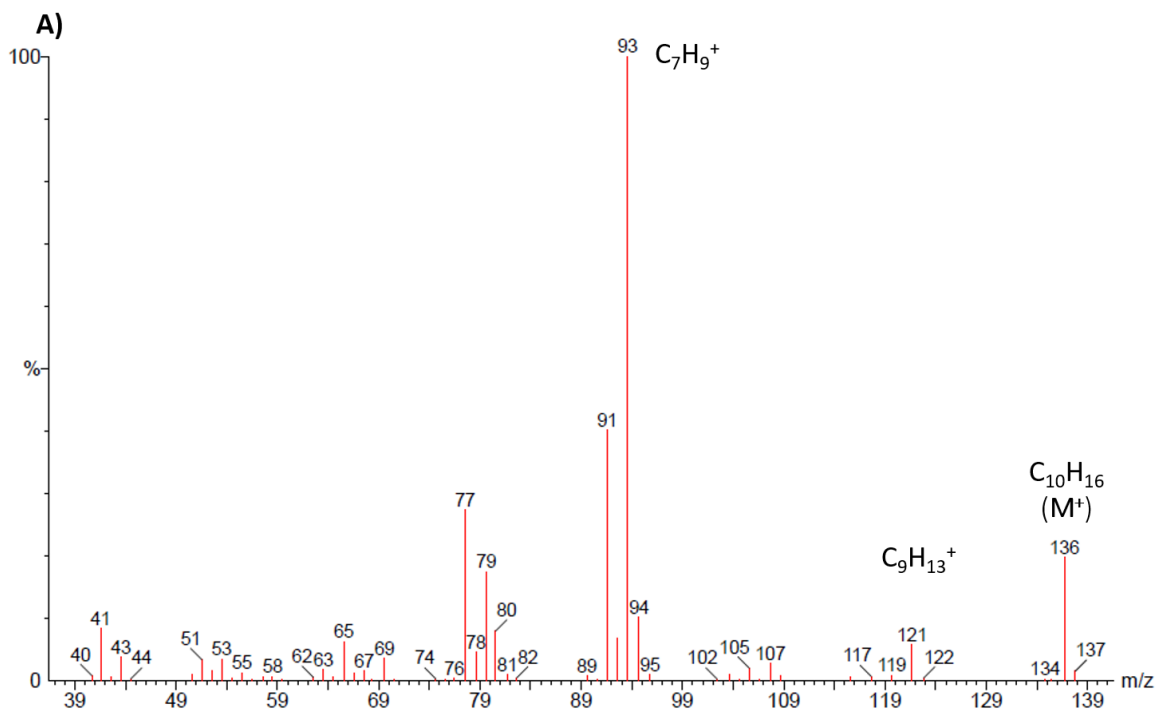


Figure 4.9 Analysis of mass spectrum of β -phellandrene (22): (A) mass spectrum (electron impact (EI) ionization), (B) possible fragmentations of β -phellandrene (22) from EI.

The mass spectrum of the new peak (retention time 9.3 minutes) from the *in vitro* assay of β -phellandrene oxidation by WT-P450_{cam} and *ES7*, shows a base peak 109 m/z. Upon comparing the base peak of 109 m/z to the base peak (93 m/z) of β -phellandrene

mass spectra, the additional 16 amu mass of the fragment (109 m/z) supports the idea of oxidation of the ring ($C_7H_9O^+$ from **38**, **39** or **40**) and not of the isopropyl chain (Figure 4.10). The expected oxidized products of β -phellandrene, **41** and **42**, will have same base peak ion (93 m/z) as β -phellandrene upon loss of the hydroxylated isopropyl group. In the new product, the m/z 93 ion is much less prominent than m/z 109, so it is unlikely that the product has structures **41** or **42**. In contrast, structures **38**, **39** and **40** should all have a prominent m/z 109 fragment ion (Figure 4.11, Figure 4.12 and Figure 4.13).

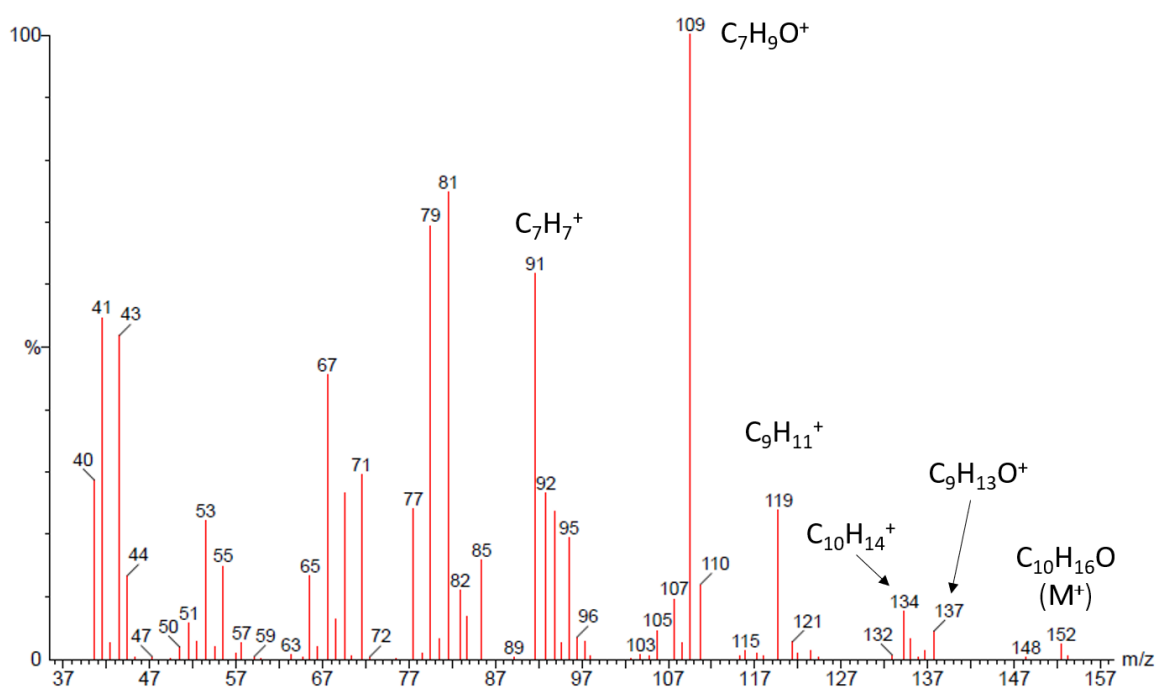


Figure 4.10 Mass spectrum of the peak (retention time 9.3 minutes) of oxidized β -phellandrene product and fragmented ion peaks.

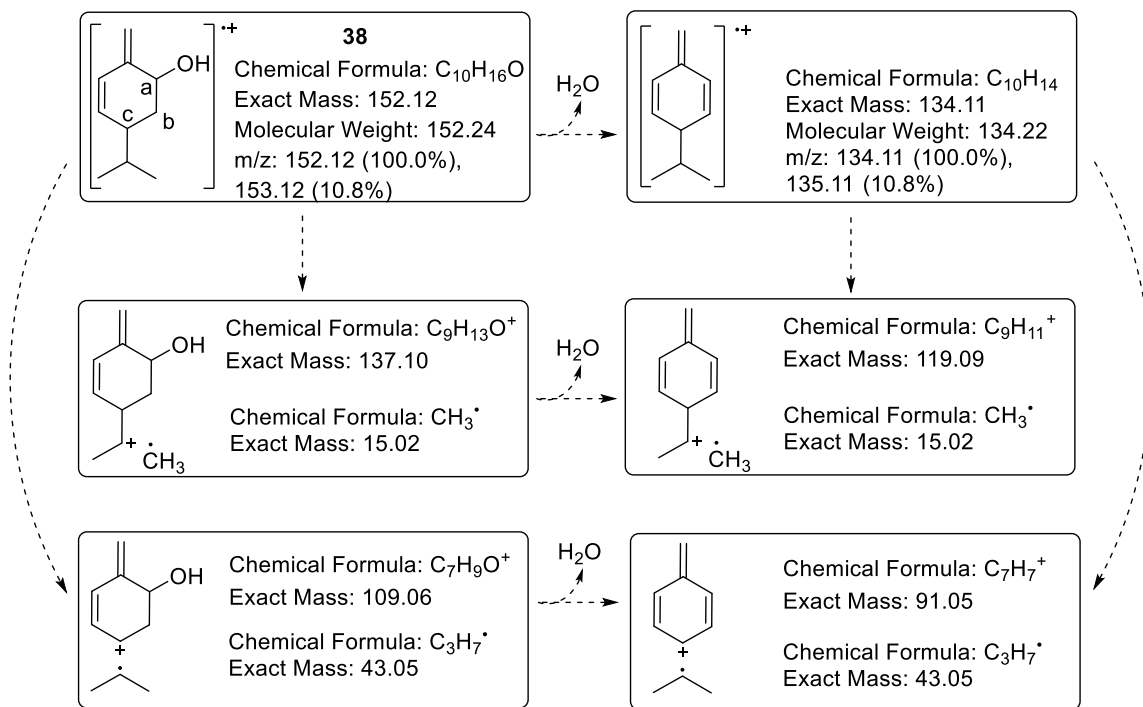


Figure 4.11 Expected fragmentation of β -phellandrene oxidized product 38 in mass spectrum (EI).

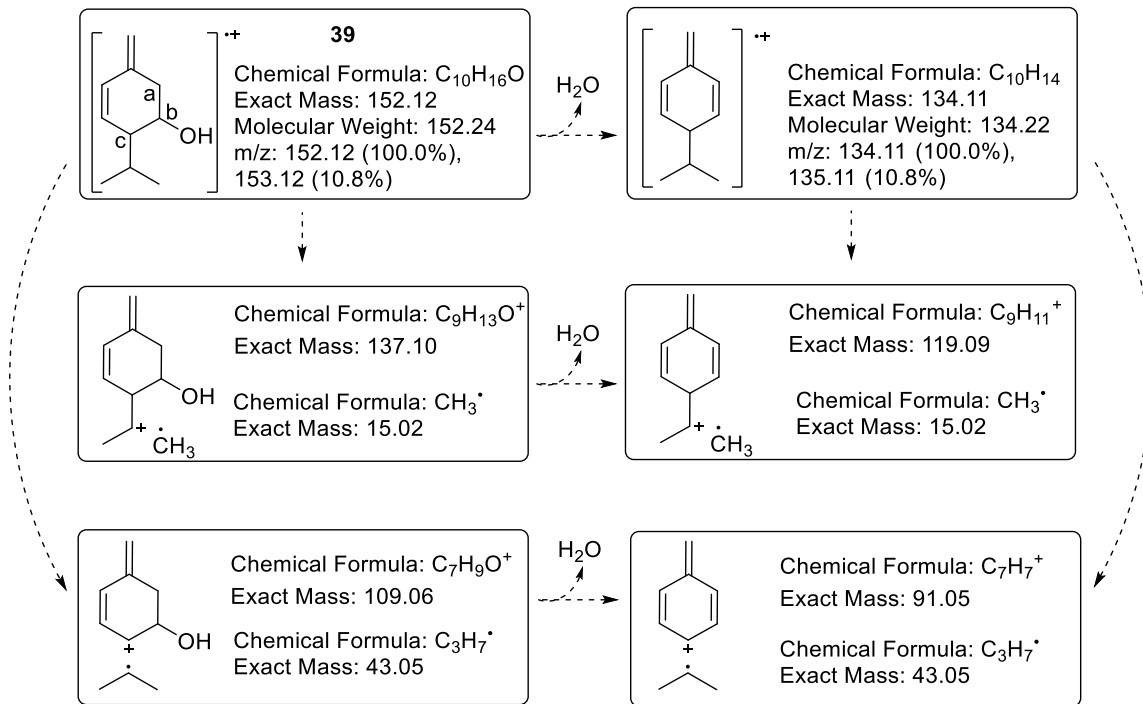


Figure 4.12 Expected fragmentation of β -phellandrene oxidized product 39 in mass spectrum (EI).

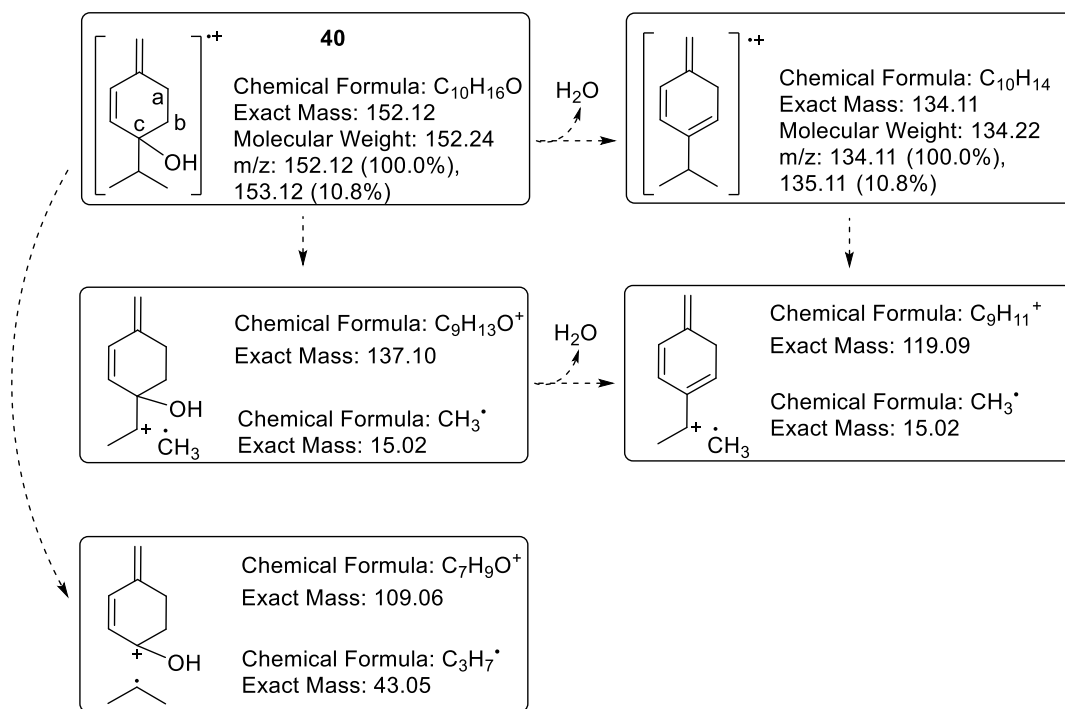


Figure 4.13 Expected fragmentation of β -phellandrene oxidized product **40** in mass spectrum (EI).

Ion peaks found in mass spectrum which are 152, 137, 134, 119, 109, and 91 m/z, represent C₁₀H₁₆O (M⁺), C₉H₁₃O⁺ (M⁺ - 15), C₉H₁₄⁺ (M⁺ - 18), C₉H₁₁⁺ (M⁺ - 33), C₇H₉O⁺ (M⁺ - 43), and C₇H₇⁺ (M⁺ - 51), respectively. Base peak 109 m/z resulted from fragmentation of iso-propyl group resulting in a carbocation at allylic position. These ions indicate the presence of an oxidized product **38**, **39** or **40** (Figure 4.10), which has resulted from hydroxylation at a secondary or tertiary carbon of β -phellandrene, catalyzed by P450_{cam}.

4.1.3. *In-silico* docking studies using MOE

To find the potential regioselectivity of hydroxylation of β -phellandrene catalyzed by WT-P450_{cam} and *ES7* mutants, *in silico* docking simulations were performed using both enantiomers of β -phellandrene ((-)-*R*-**22a** and (+)-*S*-**22b**). The *in vitro* assays using WT-P450_{cam} and *ES7* mutants, show a new hydroxylated product of β -phellandrene, when using *m*-CPBA as shunt. Therefore, the carbon atoms of β -phellandrene which are potential sites for hydroxylation, are considered here only (C4, C5, and C6, Figure 2.4). The distances of heme-Fe to C4, C5 and C6 were measured. The shortest distance

between heme-Fe to C4, C5 or C6, was found to be between heme-Fe to C4, when β -phellandrene ((-)-**22a** and (+)-**22b**) was docked in both *ES7* and WT-P450_{cam} (Appendix B3 and Appendix B4). The poses of β -phellandrene ((-)-**22a** and (+)-**22b**) docked in the *ES7* mutant and WT-P450_{cam} are selected, based on the shortest distance between heme-Fe to either C4, C5 or C6 (Figure 4.14).

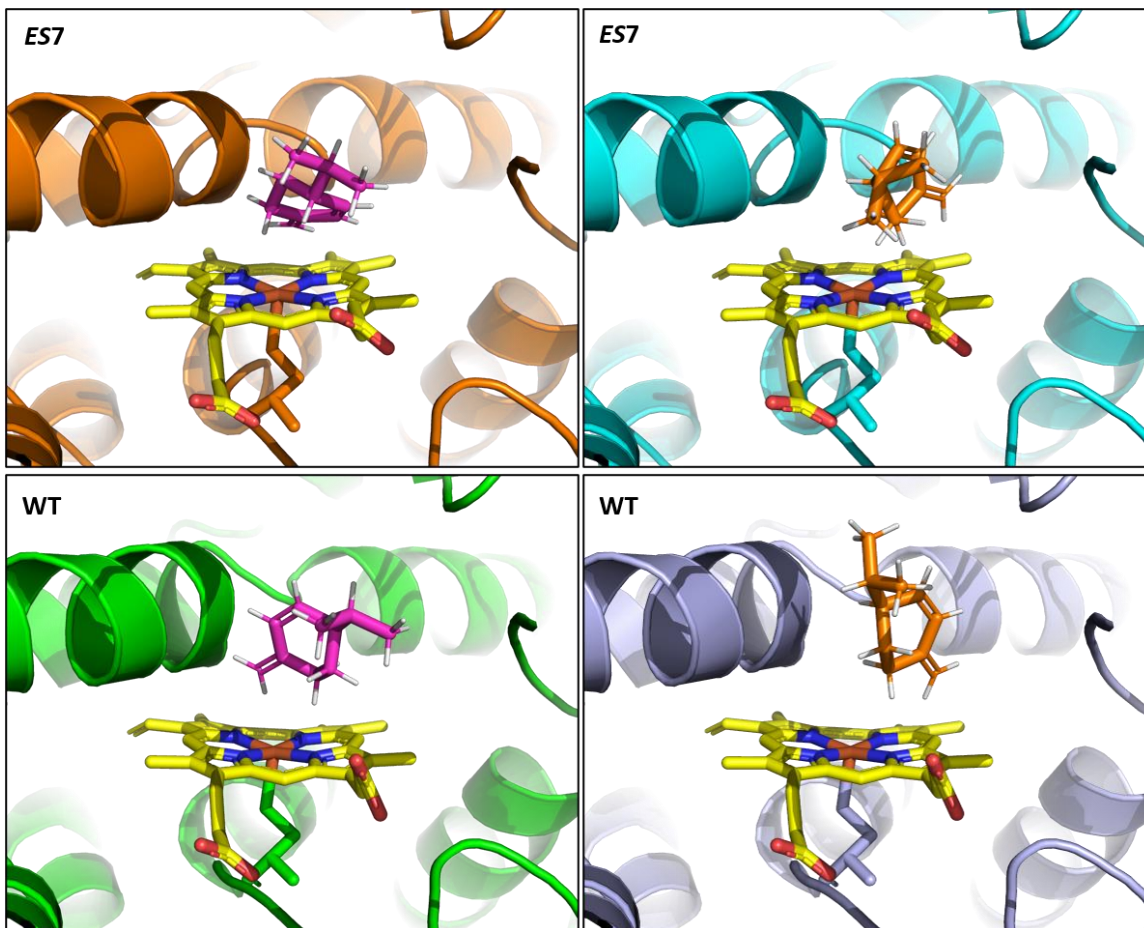


Figure 4.14 Selected poses of (-)-*R*- β -phellandrene (**22a**, left side, shown in magenta) and (+)-*S*- β -phellandrene (**22b**, right side, shown in orange) positioned above the heme (shown in yellow color) in the active sites of the *ES7* mutant and WT-P450_{cam}.

Comparing the distances from heme-Fe to carbon atoms (C4, C5 and C6) in β -phellandrene, C4 was found to be closer than C5 and C6. However, in the case of WT-P450_{cam}, the distances from heme-Fe to C4 and C5 (4.60 Å and 5.91 Å, respectively) in (-

-R-22 enantiomer are shorter than C4 and C5 (5.44 Å and 6.89 Å, respectively) in (+)-*S-22* enantiomer. In contrast, in the *ES7* mutant, distances from heme-Fe to C4 and C5 (4.36 Å and 5.81 Å, respectively) in (-)-*R-22* enantiomer are the same (4.68 Å and 5.80 Å, respectively) in the (+)-*S-22* enantiomer (Figure 4.15). This shows WT-P450_{cam} may have some preference to (-)-*R-22* enantiomer over (+)-*S-22* enantiomer for hydroxylation and, more importantly, that C4 would be the position of hydroxylation. This idea is more favoured, as C4 is allylic (which makes it easier than C5 to hydroxylate) and much less hindered than C6.

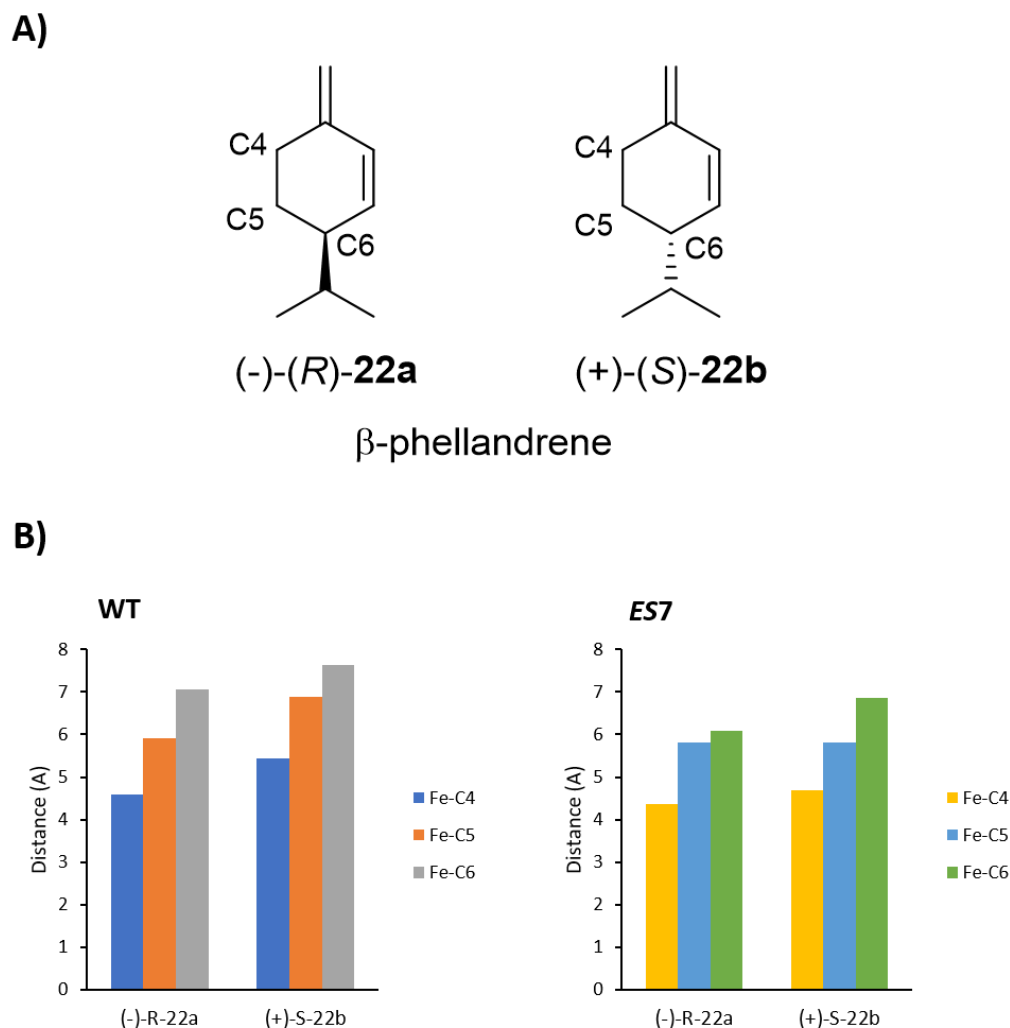


Figure 4.15 *In-silico* docking studies, (A) carbon numbers assigned to β -phellandrene (22), and (B) minimum distances of C4, C5 and C6 from heme-Fe in WT-P450_{cam} (left), and in the *ES7* mutant (right) in selected poses.

In β -phellandrene, C4 and C5 are prochiral carbons which will result in new chiral centres upon hydroxylation catalyzed by P450_{cam} (Figure 4.16). P450_{cam} may oxidize either of the prochiral carbon to give a new chiral center with stereoselectivity. Comparing both enantiomers of β -phellandrene (**22a**, **22b**) docked in the *ES7* mutant, H_R of C4 from both enantiomers β -phellandrene ((-)-*R*-**22a** and (+)-*S*-**22b**), has the same orientation above the heme-Fe. This supports the stereoselective hydroxylation of both enantiomers of β -phellandrene (**22**) giving *R*-hydroxylated products (on C4) (Figure 4.17). Thus, *ES7* may give a mixture of diastereomers of the hydroxylated product from the racemic mixture of β -phellandrene (**22**) if the stereoselective hydroxylation of both enantiomers is at the same rate by *ES7*.

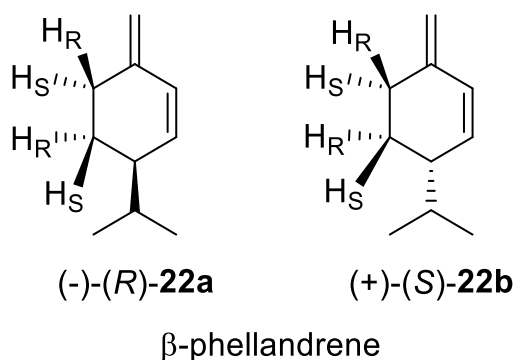


Figure 4.16 Enantiomers of β -phellandrene (**22**) with prochiral CH₂ groups shown.

In WT-P450_{cam}, comparing both enantiomers of β -phellandrene (**22a**, **22b**) docked in that enzyme, H_S of C4 from (-)-*R*- β -phellandrene (**22a**) is oriented above the heme-Fe, while H_R of C4 from (+)-*S*- β -phellandrene (**22b**) is oriented above the heme-Fe (Figure 4.18). Thus, WT may give the *S*-hydroxylated (on C4) product from (-)-*R*- β -phellandrene (**22a**) and *R*-hydroxylated (on C4) product from (+)-*S*- β -phellandrene (**22b**). Thus, the hydroxylated products of racemic β -phellandrene (**22**) are expected to be enantiomeric mixtures of the *trans* *p*-mentha-1(7),5-dien-2-ol if both enantiomers of β -phellandrene (**22**) are oxidized by WT-P450_{cam} at the same rate and with the same stereoselectivity as shown in the docking studies.

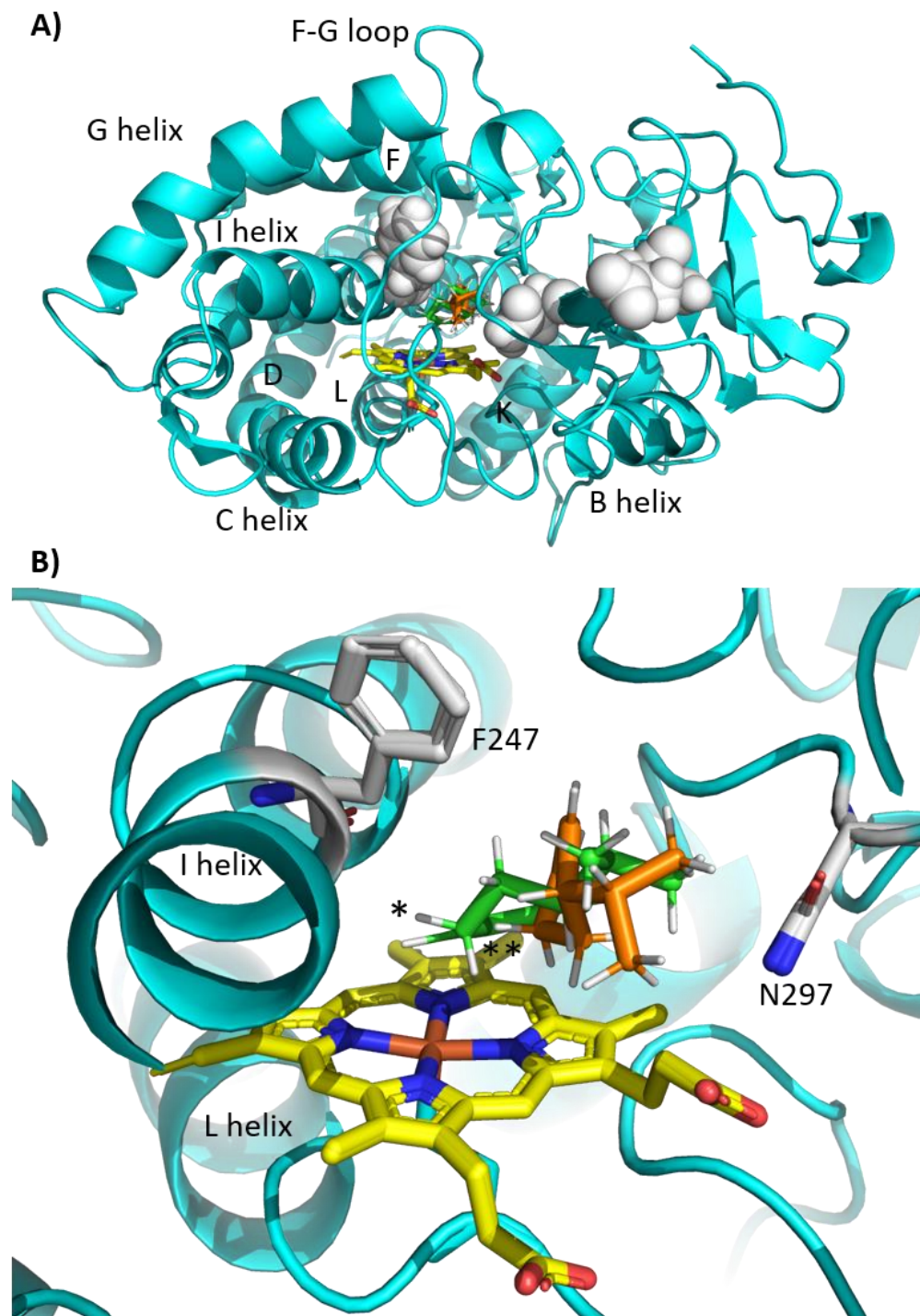


Figure 4.17 The *in silico* molecular docking results of ES7 (V247F/D297N/K314E) and superimposed poses of (-)-*R*- β -phellandrene (22a, shown in green) and (+)-*S*- β -phellandrene (22b, shown in orange): (A) P450 is shown in cyan, heme in yellow, mutations are shown in white colored spheres, (B) Orientation of (-)-*R*- β -phellandrene (22a, shown in green, H_R on prochiral C4 indicated by (*)) and (+)-*S*- β -phellandrene (22b, shown in orange, H_R on prochiral C4 indicated by (**)) in the active site.

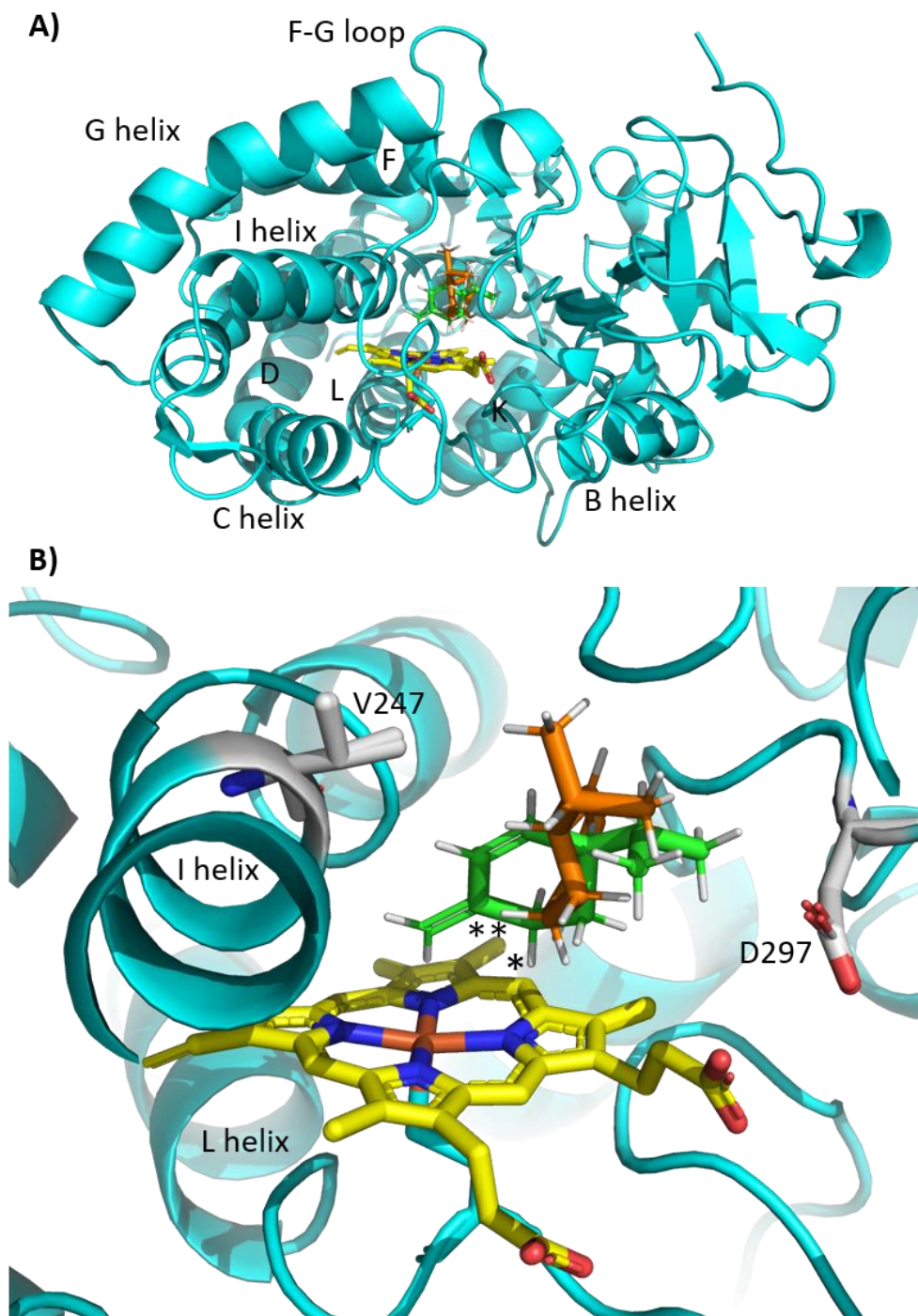


Figure 4.18 The *in silico* molecular docking results of WT-P450_{cam} and superimposed poses of (-)-*R*- β -phellandrene (22a, shown in green) and (+)-*S*- β -phellandrene (22b, shown in orange): (A) P450 is shown in cyan, heme in yellow, (B) Orientation of (-)-*R*- β -phellandrene (22a, shown in green, H_R on prochiral C4 indicated by (*)) and (+)-*S*- β -phellandrene (22b, shown in orange, H_R on prochiral C4 indicated by (**)) in the active-site (residues shown in white sticks were found to be mutated in ES7 mutant).

4.2. Discussion

4.2.1. Short synthesis racemic β -phellandrene

Racemic β -phellandrene (**22**) was synthesized in 3 steps with 46 % overall yield starting with β -pinene (**21**). The intermediate compounds, (+)-nopinone (**27**) and (\pm)-cryptone (**28**, and the isomer **29**) have their own significance and importance. (+)-Nopinone (**27**), which is synthesized by oxidation of β -pinene (**21**), is an important compound used to synthesize other organic compounds and to generate chiral ligand PINDY, MINDY *etc.* of metal catalysts (Chang et al., 2006; Hida et al., 2009; Krzemiński & Wojtczak, 2005; Malkov et al., 2003; Sauer et al., 2009). Synthesis of (+)-nopinone (**27**) using oxidation of (-)- β -pinene (**21**) has been reported using ozonolysis (Hall, 1963; J. L. Zhang et al., 2013), KMnO_4 (Sauer et al., 2009; Szuppa et al., 2010), NaIO_4 (Kawashima et al., 2014) or OsO_4 (Coxon et al., 1968) as oxidizing agents. Using NaIO_4 as oxidizing agent has improved yield of nopinone synthesis with short reaction time compared to using KMnO_4 as oxidizing agent.

(\pm)-Cryptone (**28**) is also an important α,β -unsaturated ketone, which has been used to synthesize other organic compounds. Examples of such compounds are xenitorins (B and C), nootkatone, eudesmane, katsumadain C, torreyol, cedrelanol, labiatin A and australin A, and others (Chen et al., 2010; Chen & Baran, 2009b; Clark et al., 2011; Daub et al., 2017; Queiroga et al., 1996; P. Zhang et al., 2012). Enantioselective synthesis of (-)-cryptone and (+)-cryptone is challenging. Synthesis of racemic cryptone (**28**) via Birch-reduction of *p*-isopropylphenol was first reported in 1955 (Soffer & Jevnik, 1955a) (Table 4.4).

Table 4.4 Syntheses of cryptone (28) reported previously

Starting material	Conditions / reaction type	Enantioselectivity (yield)	Reference
<i>p</i> -isopropylphenol	Birch-reduction	None (34% in 4 steps)	(Soffer & Jevnik, 1955b)
4-isopropyl-cyclohexanone	a) LDA, TMSCl, b) Pd(OAc) ₂ , benzoquinone,	None (92% in 2 steps)	(Findley et al., 2008)
Methyl vinyl ketone, and 3-Methylbutanal	Stork's enamine	None (54% in 3 steps)	(Mori, 2006)
(S)-Perillyl alcohol	(Multiple steps)	ee 91.5–93% (28% in 6 steps)	(Mori, 2006)
(+)-Nopinone	(Multiple steps)	ee 86 % (42% in 5 steps)	(Kato et al., 1992)
Methyl vinyl ketone, and 3-Methylbutanal	Robinson annulation (pyrrolidine chiral base catalyst)	ee 89% (63% in 3 steps)	(Chen & Baran, 2009a)

Synthesis of β -phellandrene (**22**) from 1-*p*-menthene or limonene, both of which yielded mixtures of α -phellandrene and β -phellandrene (**22**) along with other monoterpenes without any selectivity, has also been reported (Buinova et al., 1982; Valterová et al., 1992). However, Wittig reaction of racemic cryptone (**28**) with methyl triphenylphosphonium bromide to synthesize racemic β -phellandrene (**22**), which had been reported previously (Bergström et al., 2006; Kang et al., 2013), is used here (70 % yield).

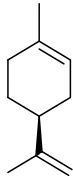
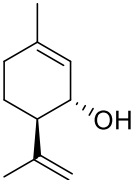
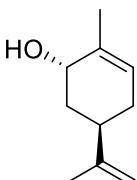
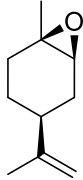
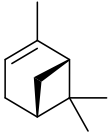
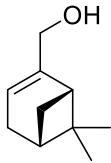
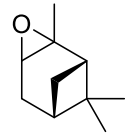
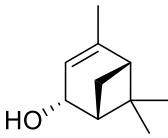
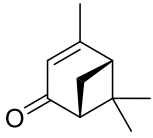
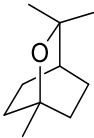
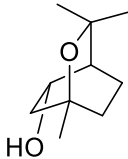
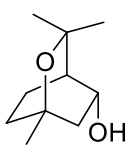
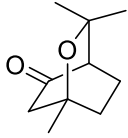
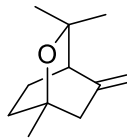
4.2.2. Oxidation of β -phellandrene (**22**) by WT-P450_{cam} and ES7 mutant using *m*-CPBA as a shunt

β -Phellandrene has same binding affinity to ES7 (V247F/D297N/K314E) and WT-P450_{cam} (K_d $2.0 \pm 0.34 \mu\text{M}$ and $1.9 \pm 0.34 \mu\text{M}$, respectively), whereas the natural substrate of WT-P450_{cam}, (*d*)-camphor (**10**) has dissociation constant (K_d) $1.7 \pm 0.34 \mu\text{M}$ and $10.4 \pm 0.43 \mu\text{M}$ for WT-P450_{cam} and ES7, respectively. Oxidation of β -phellandrene (**22**) catalyzed by WT-P450_{cam} and ES7 using *in vitro* assays with *m*-CPBA as shunt, was observed. The oxidized product is proposed to be hydroxylated β -phellandrene. WT-P450_{cam}, which regio- and stereoselectively oxidizes its natural substrate D-camphor to 5-exo-hydroxycamphor, has been reported to catalyze hydroxylation and epoxidation of monoterpenes (Table 4.5). Limonene, which has structure resembling to β -phellandrene structure, upon oxidation catalyzed by P450_{cam}, results in hydroxylation at allylic carbon to

give *trans*-carveol and *trans*-isopiperitenol, and an epoxide (Table 4.5, entry 1). Bicyclic hydrophobic monoterpene, α -pinene is oxidized to myrtenol and *cis*-verbenol, verbenone (oxidation at allylic carbon) along with epoxide (Table 4.5, entry 2), catalyzed by P450_{cam}. Using different mutants of P450_{cam}, improvement in regioselectivity as well as catalytic activity towards α -pinene oxidation was also reported (Bell et al., 2003; Bell et al., 2001). Importance of verbenone and *cis*-verbenol in chemical signaling in bark beetles, has been discussed above (section 1.3.3).

Oxidation 1,8-cineol was also reported to give mixture of 5-*endo*-hydroxylated and 5-*exo*-hydroxylated products at sterically hindered secondary carbons regioselectively, catalyzed by WT-P450_{cam}. Upon a second round of oxidation, it gave a mixture of (1*S*)-5-ketocineol (major) and (1*R*)-5-ketocineol (minor) (Stok et al., 2016). Examples of oxidation of these monoterpenes catalyzed by WT-P450_{cam} show that P450_{cam} can catalyze hydroxylation as well as epoxidation of monoterpenes, which we have also observed in oxidation of β -phellandrene catalyzed by WT-P450_{cam} and *ES7* mutant.

Table 4.5 Example of monoterpene oxidation catalyzed by WT-P450_{cam}

Entry	Substrate	Oxidized products	References
1	 (S)-limonene	 <i>trans</i> -isopiperitenol  <i>trans</i> -carveol  <i>cis</i> -limonene epoxide	(Bell et al., 2001)
2	 (+)- α -pinene	 (+)-myrtenol  α -pinene epoxide  (+)- <i>cis</i> -verbenol  verbenone	(Bell et al., 2003; S. G. Bell et al., 2001)
3	 1,8-cineol	 5- <i>endo</i> -hydroxycineol  5- <i>exo</i> -hydroxycineol  (1 <i>R</i>)-5-ketocineol  (1 <i>S</i>)-5-ketocineol	(Stok et al., 2016)

The role and importance of different residues in WT-P450_{cam} has been discussed above (section 3.2.2). Docking simulations show that both enantiomers of β -phellandrene (**22**) can fit in the active site of both the WT-P450_{cam} and the *ES7* mutant. The hydrophobic residues around the active site of P450_{cam} stabilize both enantiomers without a major discrimination between the enantiomers of β -phellandrene (**22**) (Figure 4.14). However, residue Val247 which is located in helix I and is mutated (V247F) in *ES7*, may play a role in stereoselective hydroxylation of β -phellandrene (**22**) by having a bulky aromatic ring (in *ES7*) compared to the smaller alkyl group (in WT). This was supported when both enantiomers of β -phellandrene ((-)-*R*-**22a**, and (+)-*S*-**22b**) were docked and H_R from prochiral carbon C4 in both enantiomers, have the same orientation above heme-Fe (Figure 4.17). In WT-P450_{cam}, H_R from prochiral carbon (C4) in both enantiomers have opposite orientations above heme-Fe when both enantiomers of β -phellandrene ((-)-*R*-**22a**, and (+)-*S*-**22b**) were docked in WT-P450_{cam} (Figure 4.18). WT-P450_{cam} shows regio- and stereoselectivity towards oxidation of (+)-D-camphor, its natural substrate. The enantiomer (-)-L-camphor which binds to WT-P450_{cam} with slightly loose than (+)-D-camphor (K_d 2.6 \pm 0.3 and 1.6 \pm 0.3 μ M at 277 K, respectively, (Kadkhodayan et al., 1995)) has more flexible orientation in the active site of P450_{cam} (Das et al., 2000; Schlichting et al., 1997). However, both enantiomers of camphor give 5-*exo*-hydroxycamphor upon oxidation by WT-P450_{cam} (Kadkhodayan et al., 1995). Oxidation of terpenes shown in Table 4.5, show WT-P450_{cam} is also stereoselective towards limonene and α -pinene oxidation (Bell et al., 2003; Bell et al., 2001). In the oxidation of 1,8-cineol, WT-P450_{cam} shows regioselectivity as well as some stereoselectivity giving 5-*exo*-hydroxycineol (minor) and 5-*endo*-hydroxycineol (major) (Table 4.5, entry 3) (Stok et al., 2016).

4.3. Conclusion

In conclusion, we have synthesized racemic β -phellandrene (**22**) in three steps (44 % overall yield) starting with (-)- β -pinene (**21**), a commercially available monoterpene. The intermediate compounds, (+)-nopinone (**27**) and (\pm)-cryptone (**28**) which were synthesized, have their own importance in synthesis of many organic compounds and in commercial use. Oxidation of (-)- β -pinene (**21**) to (+)-nopinone (**27**) was optimized and ring opening of (+)-nopinone (**27**) to give (\pm)-cryptone (**28**) using Lewis acid (AlCl₃), was achieved. Thus, the synthetic route of β -phellandrene (**22**) is very useful, not only to get β -phellandrene (**22**), but also to obtain (+)-nopinone (**27**) and (\pm)-cryptone (**28**).

The racemic β -phellandrene (**22**) was tested and found to be a potential substrate for the mutant we named *ES7* (V247F/D297N/K314E) and WT-P450_{cam}. Using the racemic mixture of β -phellandrene (**22**) in the *in vitro* assays with WT-P450_{cam} and *ES7* mutant, and *m*-CPBA as shunt, a new oxidized product (M^+ 152 *m/z*) of β -phellandrene (**22**, M^+ 136 *m/z*) was identified in GC-MS, which was absent in control experiments. This oxidized product is proposed to be hydroxylated product of β -phellandrene (**22**), catalyzed by both WT-P450_{cam} and *ES7* mutant with the same rate of oxidation.

Molecular docking studies show that a prochiral carbon C4 (an allylic and secondary carbon) of both enantiomers of β -phellandrene (**22**) is closer to heme-Fe than C5 (prochiral carbon) and C6 (an allylic and tertiary carbon), in WT-P450_{cam} as well as in *ES7* mutant. In WT-P450_{cam}, these distances between heme-Fe to C4 of (-)-*R*- β -phellandrene (**22a**) and (+)-*S*- β -phellandrene (**22b**) are 4.60 Å and 5.44 Å, respectively. Whereas in *ES7*, the distances between heme-Fe to C4 prochiral carbon of (-)-*R*- β -phellandrene (**22a**) and (+)-*S*- β -phellandrene (**22b**) are 4.36 Å and 4.68 Å, respectively. This indicates that WT may have preference for one of the enantiomers of β -phellandrene (**22**) over the other to a small extent, while *ES7* may have the same preference for both enantiomers of β -phellandrene (**22**).

Chapter 5. Future work

5.1. Endosulfan and related substrates

In this work, we have used *ES1-ES7* mutants which were selected against endosulfan (mixture of α -ES **13A** and β -ES **13B**) to study the biodegradation and dehalogenation of endosulfan (ES). However, most of the work was done in this study using ES diol (**14**) which is a major metabolite of ES (**13**) and is commonly found in nature. We have confirmed the dehalogenation of ES diol by monitoring and quantifying the chloride releases using chloride ion selective electrode, and using ^{13}C -labelled ES diol, which also supports the proposed mechanism of degradation of ES diol. We have compared the mutants to find out the most active one towards ES diol dehalogenation. We also have compared the mutants to accept the ES diol (**14**) using *in-silico* docking studies, as well as compared the mutants which can accommodate other chlorinated metabolites of ES. However, in future, we can use these chlorinated metabolites (ES lactone (**15**), ES ether (**16**), ES sulfate (**20**) and others) by ES mutants using *in vitro* and *in vivo* assays, to compare the dehalogenation of these chlorinated metabolites of endosulfan catalyzed by ES mutants.

X-ray crystallography or NMR techniques have been in use to determine the 3D structure of P450_{cam} (WT and mutants) with different substrates. Similarly, such techniques can be used to determine the P450_{cam} structure when ES diol (**14**) is bound to the active site of the most active mutant P450_{cam} (*ES7*). The mutants P450_{cam} appear to partition between oxidizing the electron poor C=C bond (mostly) and oxidizing one of the two CH_2OH groups to give lactone. Such a structure of mutant P450_{cam} with ES diol (**14**) would be helpful to understand how the substrate is positioned in the active site and it would be a starting point for additional docking studies to understand why the enzyme oxidizes the electron poor double bond over the more easily oxidized CH_2OH group.

The sigmoidal kinetics arises because of a change in the way redoxin interacts with P450. In future, titrating the enzyme with PdX, and keeping P450_{cam} and PdR concentration constant will be helpful to find the concentration of PdX at the level saturating the enzyme wherein the kinetics stop being sigmoidal and resemble the *m*-CPBA kinetics. This will be helpful in future also to find the required number of copies of

redox partners (PdX and PdR) with *ES7* mutant P450_{cam} when it would be transformed into a suitable bacterium, to biodegrade these chlorinated compounds.

This set of mutants (*ES1-ES7*) that were selected on endosulfan (**13**), are potentially useful to study the biodegradation of other polychlorinated organic pollutants which were used either as pesticide/ insecticides such as heptachlor (**43**, (Reed & Koshlukova, 2014)), chlordane (**44**, (Blaylock, 2005; Koshlukova & Reed, 2014)), aldrin (**45**, (Honeycutt & Shirley, 2014)), or a chlorinated flame retardant dechlorane plus (**46**, (Sverko et al., 2011)). All these compounds have similar chlorinated norbornane ring system (Figure 5.1).

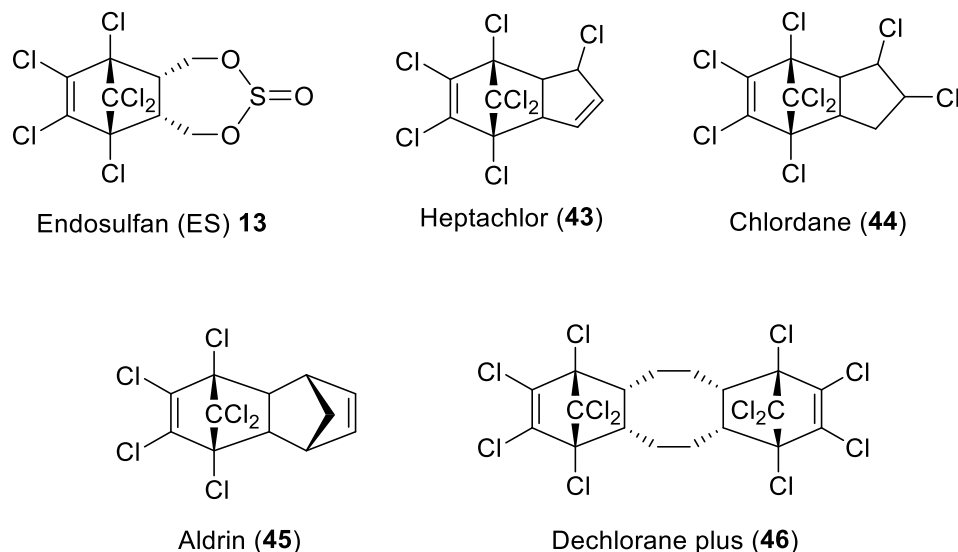


Figure 5.1 Endosulfan (ES, **13**) and other related polychlorinated organic compounds.

5.2. Oxidation of β -phellandrene by P450_{cam}

Synthesis of racemic β -phellandrene (**22**) was achieved in 3 steps starting from β -pinene (**21**). Using *in vitro* assays with WT-P450_{cam} and *ES7* mutant, a new oxidized product of β -phellandrene (**22**) was found, which was oxidized by P450_{cam}. The oxidized product is proposed to be hydroxylated product (**38**, **39** or **40**) of β -phellandrene (**22**), and hydroxylation has occurred on one of the carbons in the ring of β -phellandrene (**22**) (Figure

4.8). However, to characterize the oxidized product and identify the structure, reactions need to be done at large scale (50 or 100 ml) to isolate the oxidized product and characterize it by ^1H NMR and ^{13}C NMR. This will also help us further to find if WT-P450_{cam} and *ES7* have any stereoselectivity in oxidizing β -phellandrene (**22**).

Further, the set of ES mutants, which show different activity towards ES diol (**14**) biodegradation, will also be used to oxidize β -phellandrene (**22**) and to find if these P450_{cam} mutants have different activity or regio- and stereoselectivity towards β -phellandrene (**22**) oxidation.

In future, these oxidized products of β -phellandrene (**22**), will be used to find if these compounds show any effect as attractant or repellent of pine bark beetles or pine engravers, which are major pest of pine trees in North America. Having standards of oxidized β -phellandrene products should facilitate our understanding of β -phellandrene as a stress signal in many plants and how the oxidized products might contribute to this signalling process.

References

- Agudo, R., Roiban, G.-D., Lonsdale, R., Ilie, A., & Reetz, M. T. (2015). Biocatalytic Route to Chiral Acyloins: P450-Catalyzed Regio- and Enantioselective α -Hydroxylation of Ketones. *The Journal of Organic Chemistry*, *80*(2), 950–956. <https://doi.org/10.1021/jo502397s>
- Ahmad, A. A., Salleh, H. M., & Noorbachta, I. A. (2018). Site-Directed Mutagenesis on Plasmid Using Polymerase Chain Reaction. In A. Amid, S. Sulaiman, D. N. Jimat, & N. F. M. Azmin (Eds.), *Multifaceted Protocol in Biotechnology* (pp. 1–11). Springer. https://doi.org/10.1007/978-981-13-2257-0_1
- Ahmad, S., Kirkland, K. E., & Blomquist, G. J. (1987). Evidence for a sex pheromone metabolizing cytochrome P-450 mono-oxygenase in the housefly. *Archives of Insect Biochemistry and Physiology*, *6*(2), 121–140. <https://doi.org/10.1002/arch.940060206>
- Aldag, C., Gromov, I. A., García-Rubio, I., Koenig, K. von, Schlichting, I., Jaun, B., & Hilvert, D. (2009). Probing the role of the proximal heme ligand in cytochrome P450cam by recombinant incorporation of selenocysteine. *Proceedings of the National Academy of Sciences*, *106*(14), 5481–5486. <https://doi.org/10.1073/pnas.0810503106>
- Allmann, S., & Baldwin, I. T. (2010). Insects Betray Themselves in Nature to Predators by Rapid Isomerization of Green Leaf Volatiles. *Science*, *329*(5995), 1075–1078. <https://doi.org/10.1126/science.1191634>
- Altarsha, M., Benighaus, T., Kumar, D., & Thiel, W. (2010). Coupling and uncoupling mechanisms in the methoxythreonine mutant of cytochrome P450cam: A quantum mechanical/molecular mechanical study. *JBIC Journal of Biological Inorganic Chemistry*, *15*(3), 361–372. <https://doi.org/10.1007/s00775-009-0608-3>
- Andersen, J. F., Utermohlen, J. G., & Feyereisen, R. (1994). Expression of Housefly CYP6A1 and NADPH-Cytochrome P450 Reductase in Escherichia coli and Reconstitution of an Insecticide-Metabolizing P450 System. *Biochemistry*, *33*(8), 2171–2177. <https://doi.org/10.1021/bi00174a025>
- Arkin, M. (2001). In vitro Mutagenesis. In S. Brenner & J. H. Miller (Eds.), *Encyclopedia of Genetics* (pp. 1010–1014). Academic Press. <https://doi.org/10.1006/rwgn.2001.0714>
- Armarego, W. L. F. (2003). *Purification of laboratory chemicals* (5th ed.). Butterworth-Heinemann.
- Asciutto, E. K., Dang, M., Pochapsky, S. S., Madura, J. D., & Pochapsky, T. C. (2011). Experimentally Restrained Molecular Dynamics Simulations for Characterizing the Open States of Cytochrome P450cam. *Biochemistry*, *50*(10), 1664–1671. <https://doi.org/10.1021/bi101820d>

- Asciutto, E. K., Young, M. J., Madura, J., Pochapsky, S. S., & Pochapsky, T. C. (2012). Solution Structural Ensembles of Substrate-Free Cytochrome P450cam. *Biochemistry*, *51*(16), 3383–3393. <https://doi.org/10.1021/bi300007r>
- Atkins, W. M., & Sligar, S. G. (1988). The roles of active site hydrogen bonding in cytochrome P-450cam as revealed by site-directed mutagenesis. *Journal of Biological Chemistry*, *263*(35), 18842–18849.
- Aw, T., Schlauch, K., Keeling, C. I., Young, S., Bearfield, J. C., Blomquist, G. J., & Tittiger, C. (2010). Functional genomics of mountain pine beetle (*Dendroctonus ponderosae*) midguts and fat bodies. *BMC Genomics*, *11*(1), 215. <https://doi.org/10.1186/1471-2164-11-215>
- Axelrod, J. (1955). The Enzymatic Demethylation of Ephedrine. *Journal of Pharmacology and Experimental Therapeutics*, *114*(4), 430–438.
- Baciacchi, E., Lanzalunga, O., & Pirozzi, B. (1997). Oxidations of benzyl and phenethyl phenyl sulfides. Implications for the mechanism of the microsomal and biomimetic oxidation of sulfides. *Tetrahedron*, *53*(36), 12287–12298. [https://doi.org/10.1016/S0040-4020\(97\)00560-7](https://doi.org/10.1016/S0040-4020(97)00560-7)
- Baldwin, I., Halitschke, R., Paschold, A., Dahl, C., & Preston, C. (2006). Volatile Signaling in Plant-Plant Interactions: “Talking Trees” in the Genomics Era. *Science*, *311*(5762), 812–815. <https://doi.org/10.1126/science.1118446>
- Barkawi, L. S., Francke, W., Blomquist, G. J., & Seybold, S. J. (2003). Frontalin: De novo biosynthesis of an aggregation pheromone component by *Dendroctonus* spp. bark beetles (Coleoptera: Scolytidae). *Insect Biochemistry and Molecular Biology*, *33*(8), 773–788. [https://doi.org/10.1016/S0965-1748\(03\)00069-9](https://doi.org/10.1016/S0965-1748(03)00069-9)
- Batabyal, D., Lewis-Ballester, A., Yeh, S.-R., & Poulos, T. L. (2016). A Comparative Analysis of the Effector Role of Redox Partner Binding in Bacterial P450s. *Biochemistry*, *55*(47), 6517–6523. <https://doi.org/10.1021/acs.biochem.6b00913>
- Batabyal, D., Li, H., & Poulos, T. L. (2013). Synergistic Effects of Mutations in Cytochrome P450cam Designed To Mimic CYP101D1. *Biochemistry*, *52*(32), 5396–5402. <https://doi.org/10.1021/bi400676d>
- Bedard, W. D., Tilden, P. E., Lindahl, K. Q., Wood, D. L., & Rauch, P. A. (1980). Effects of verbenone and trans-verbenol on the response of *Dendroctonus brevicornis* to natural and synthetic attractant in the field. *Journal of Chemical Ecology*, *6*(6), 997–1013. <https://doi.org/10.1007/BF00994657>
- Behera, R. K., & Mazumdar, S. (2008). Roles of two surface residues near the access channel in the substrate recognition by cytochrome P450cam. *Biophysical Chemistry*, *135*(1), 1–6. <https://doi.org/10.1016/j.bpc.2008.02.016>

- Behrendorff, J. B. Y. H., Huang, W., & Gillam, E. M. J. (2015). Directed evolution of cytochrome P450 enzymes for biocatalysis: Exploiting the catalytic versatility of enzymes with relaxed substrate specificity. *Biochemical Journal*, *467*(1), 1–15. <https://doi.org/10.1042/BJ20141493>
- Beilen, J. B. van, Holtackers, R., Lüscher, D., Bauer, U., Witholt, B., & Duetz, W. A. (2005). Biocatalytic Production of Perillyl Alcohol from Limonene by Using a Novel Mycobacterium sp. Cytochrome P450 Alkane Hydroxylase Expressed in *Pseudomonas putida*. *Applied and Environmental Microbiology*, *71*(4), 1737–1744. <https://doi.org/10.1128/AEM.71.4.1737-1744.2005>
- Bell, S., Chen, X., Sowden, R. J., Xu, F., Williams, J. N., Wong, L.-L., & Rao, Z. (2003). Molecular Recognition in (+)- α -Pinene Oxidation by Cytochrome P450cam. *Journal of the American Chemical Society*, *125*(3), 705–714. <https://doi.org/10.1021/ja028460a>
- Bell, S. G., Orton, E., Boyd, H., Stevenson, J.-A., Riddle, A., Campbell, S., & Wong, L.-L. (2003). Engineering cytochrome P450cam into an alkane hydroxylase. *Dalton Transactions*, *11*, 2133–2140. <https://doi.org/10.1039/B300869J>
- Bell, S. G., Rouch, D. A., & Wong, L.-L. (1997). Selective aliphatic and aromatic carbon-hydrogen bond activation catalysed by mutants of cytochrome p450cam. *Journal of Molecular Catalysis B: Enzymatic*, *3*(6), 293–302. [https://doi.org/10.1016/S1381-1177\(97\)00009-X](https://doi.org/10.1016/S1381-1177(97)00009-X)
- Bell, S. G., Sowden, R. J., & Wong, L.-L. (2001). Engineering the haem monooxygenase cytochrome P450cam for monoterpene oxidation. *Chemical Communications*, *7*, 635–636. <https://doi.org/10.1039/B100290M>
- Bell, S. G., Spence, J. T. J., Liu, S., George, J. H., & Wong, L.-L. (2014). Selective aliphatic carbon–hydrogen bond activation of protected alcohol substrates by cytochrome P450 enzymes. *Organic & Biomolecular Chemistry*, *12*(15), 2479–2488. <https://doi.org/10.1039/C3OB42417K>
- Bell, S. G., Xu, F., Forward, I., Bartlam, M., Rao, Z., & Wong, L.-L. (2008). Crystal Structure of CYP199A2, a Para-Substituted Benzoic Acid Oxidizing Cytochrome P450 from *Rhodospseudomonas palustris*. *Journal of Molecular Biology*, *383*(3), 561–574. <https://doi.org/10.1016/j.jmb.2008.08.033>
- Bentz, B., Boone, C., & Raffa, K. (2015). Tree response and mountain pine beetle attack preference, reproduction and emergence timing in mixed whitebark and lodgepole pine stands. *Agricultural and Forest Entomology*, *17*(4), 421–432. <https://doi.org/10.1111/afe.12124>
- Benveniste, I., Salaün, J.-P., Simon, A., Reichhart, D., & Durst, F. (1982). Cytochrome P-450-Dependent ω -Hydroxylation of Lauric Acid by Microsomes from Pea Seedlings. *Plant Physiology*, *70*(1), 122–126. <https://doi.org/10.1104/pp.70.1.122>

- Berger, R. G. (Ed.). (2007). *Flavours and Fragrances: Chemistry, Bioprocessing and Sustainability*. Springer-Verlag. <https://doi.org/10.1007/978-3-540-49339-6>
- Bergstrom, M. A., Luthman, K., Nilsson, J. L. G., & Karlberg, A. (2006). Conjugated Dienes as Prohaptens in Contact Allergy: In Vivo and in Vitro Studies of Structure-Activity Relationships, Sensitizing Capacity, and Metabolic Activation. *Chemical Research in Toxicology*, 19(6), 760–769. <https://doi.org/10.1021/tx060006n>
- Bergström, M. A., Luthman, K., Nilsson, J. L. G., & Karlberg, A.-T. (2006). Conjugated Dienes as Prohaptens in Contact Allergy: In Vivo and in Vitro Studies of Structure-Activity Relationships, Sensitizing Capacity, and Metabolic Activation. *Chemical Research in Toxicology*, 19(6), 760–769. <https://doi.org/10.1021/tx060006n>
- Bernhardt, R. (2006). Cytochromes P450 as versatile biocatalysts. *Journal of Biotechnology*, 124(1), 128–145. <https://doi.org/10.1016/j.jbiotec.2006.01.026>
- Berry, P. A., Macbeth, A. K., & Swanson, T. B. (1937). 299. D-Phellandral and d-4-isopropyl- Δ^2 -cyclohexen-1-one. *J. Chem. Soc.*, 1448, 1448–1450. <https://doi.org/10.1039/JR9370001448>
- Black, S. D., & Coon, M. J. (1982). Structural features of liver microsomal NADPH-cytochrome P-450 reductase. Hydrophobic domain, hydrophilic domain, and connecting region. *Journal of Biological Chemistry*, 257(10), 5929–5938.
- Blanco-Coronado, J. L., Repetto, M., Ginestal, R. J., Vicente, J. R., Yelamos, F., & Lardelli, A. (2008). Acute Intoxication by Endosulfan. *Journal of Toxicology: Clinical Toxicology*. <https://doi.org/10.3109/15563659209017943>
- Blanksby, S. J., & Ellison, G. B. (2003). Bond Dissociation Energies of Organic Molecules. *Accounts of Chemical Research*, 36(4), 255–263. <https://doi.org/10.1021/ar020230d>
- Blaylock, B. L. (2005). Chlordane. In P. Wexler (Ed.), *Encyclopedia of Toxicology (Second Edition)* (pp. 540–542). Elsevier. <https://doi.org/10.1016/B0-12-369400-0/00211-8>
- Born, S. L., Caudill, D., Fliter, K. L., & Purdon, M. P. (2002). Identification of the Cytochromes P450 That Catalyze Coumarin 3,4-Epoxidation and 3-Hydroxylation. *Drug Metabolism and Disposition*, 30(5), 483–487. <https://doi.org/10.1124/dmd.30.5.483>
- Bradshaw, W. H., Conrad, H. E., Corey, E. J., Gunsalus, I. C., & Lednicer, D. (1959). MICROBIOLOGICAL DEGRADATION OF (+)-CAMPHOR. *Journal of the American Chemical Society*, 81(20), 5507–5507. <https://doi.org/10.1021/ja01529a060>

- Brodie, B. B., Axelrod, J., Cooper, J. R., Gaudette, L., La Du, B. N., Mitoma, C., & Udenfriend, S. (1955). Detoxication of Drugs and Other Foreign Compounds by Liver Microsomes. *Science*, *121*(3147), 603–604. <https://doi.org/10.1126/science.121.3147.603>
- Buinova, É. F., Urbanovich, T. R., Udarov, B. G., & Izotova, L. V. (1982). Transformations of p-menthadienes under the action of potassium tert-butanolate in dimethyl sulfoxide. *Chemistry of Natural Compounds*, *18*(5), 555–559. <https://doi.org/10.1007/BF00575037>
- Byers, J. A. (1983). Bark beetle conversion of a plant compound to a sex-specific inhibitor of pheromone attraction. *Science (New York, N. Y.)*, *220*(4597), 624–626. <https://doi.org/10.1126/science.220.4597.624>
- Byers, J. A., & Wood, D. L. (1980). Interspecific inhibition of the response of the bark beetles, *Dendroctonus brevicomis* and *Ips paraconfusus*, to their pheromones in the field. *Journal of Chemical Ecology*, *6*(1), 149–164. <https://doi.org/10.1007/BF00987534>
- Byers, John A. (1982). Male-specific conversion of the host plant compound, myrcene, to the pheromone, (+)-ipsdienol, in the bark beetle, *Dendroctonus brevicomis*. *Journal of Chemical Ecology*, *8*(2), 363–371. <https://doi.org/10.1007/BF00987784>
- Campbell, C. D., Walgenbach, J. F., & Kennedy, G. G. (1991). Effect of Parasitoids on Lepidopterous Pests in Insecticide-Treated and Untreated Tomatoes in Western North Carolina. *Journal of Economic Entomology*, *84*(6), 1662–1667. <https://doi.org/10.1093/jee/84.6.1662>
- Cappiello, A., Famigliini, G., Palma, P., Termopoli, V., Lavezzi, A. M., & Maturri, L. (2014). Determination of selected endocrine disrupting compounds in human fetal and newborn tissues by GC-MS. *Analytical and Bioanalytical Chemistry*, *406*(12), 2779–2788. <https://doi.org/10.1007/s00216-014-7692-0>
- Castro, C. E., Wade, R. S., & Belser, N. O. (1985). Biodehalogenation: Reactions of cytochrome P-450 with polyhalomethanes. *Biochemistry*, *24*(1), 204–210. <https://doi.org/10.1021/bi00322a029>
- Cerrillo, I., Granada, A., López-Espinosa, M.-J., Olmos, B., Jiménez, M., Caño, A., Olea, N., & Fátima Olea-Serrano, M. (2005). Endosulfan and its metabolites in fertile women, placenta, cord blood, and human milk. *Environmental Research*, *98*(2), 233–239. <https://doi.org/10.1016/j.envres.2004.08.008>
- Chang, W.-S., Shia, K.-S., Liu, H.-J., & Wei Ly, T. (2006). The first total synthesis of xenitorins B and C: assignment of absolute configuration. *Organic & Biomolecular Chemistry*, *4*(20), 3751–3751. <https://doi.org/10.1039/b610427d>

- Chang, Y.-T., & Loew, G. (2000). Homology Modeling, Molecular Dynamics Simulations, and Analysis of CYP119, a P450 Enzyme from Extreme Acidothermophilic Archaeon *Sulfolobus solfataricus*. *Biochemistry*, 39(10), 2484–2498. <https://doi.org/10.1021/bi991966u>
- Chen, K., & Baran, P. S. (2009a). Total synthesis of eudesmane terpenes by site-selective C–H oxidations. *Nature*, 459. <https://doi.org/10.1038/nature08043>
- Chen, K., & Baran, P. S. (2009b). Total synthesis of eudesmane terpenes by site-selective C–H oxidations. *Nature*, 459(7248), 824–828. <https://doi.org/10.1038/nature08043>
- Chen, K., Ishihara, Y., Galán, M. M., & Baran, P. S. (2010). Total synthesis of eudesmane terpenes: Cyclase phase. *Tetrahedron*, 66(26), 4738–4744. <https://doi.org/10.1016/j.tet.2010.02.088>
- Chiu, C. C., Keeling, C. I., & Bohlmann, J. (2019). The cytochrome P450 CYP6DE1 catalyzes the conversion of α -pinene into the mountain pine beetle aggregation pheromone trans-verbenol. *Scientific Reports*, 9(1), 1477. <https://doi.org/10.1038/s41598-018-38047-8>
- Chiu, C. C., Keeling, C. I., Henderson, H. M., & Bohlmann, J. (2019). Functions of mountain pine beetle cytochromes P450 CYP6DJ1, CYP6BW1 and CYP6BW3 in the oxidation of pine monoterpenes and diterpene resin acids. *PLOS ONE*, 14(5), e0216753. <https://doi.org/10.1371/journal.pone.0216753>
- Chowdhury, G., Calcutt, M. W., & Guengerich, F. P. (2010). Oxidation of N-Nitrosoalkylamines by human cytochrome P450 2A6: Sequential oxidation to aldehydes and carboxylic acids and analysis of reaction steps. *The Journal of Biological Chemistry*, 285(11), 8031–8044. <https://doi.org/10.1074/jbc.M109.088039>
- Chowdhury, R., & Maranas, C. D. (2020). From directed evolution to computational enzyme engineering—A review. *AIChE Journal*, 66(3), e16847. <https://doi.org/10.1002/aic.16847>
- Christianson, D. W. (2017). Structural and Chemical Biology of Terpenoid Cyclases. *Chemical Reviews*, 117(17), 11570–11648. <https://doi.org/10.1021/acs.chemrev.7b00287>
- Clark, J. S., Vignard, D., & Parkin, A. (2011). Synthesis of the tricyclic core of labiatin A and Australin A. *Organic Letters*, 13(15), 3980–3983. <https://doi.org/10.1021/ol201498g>
- Cook, D. J., Finnigan, J. D., Cook, K., Black, G. W., & Charnock, S. J. (2016). Cytochromes P450: History, Classes, Catalytic Mechanism, and Industrial Application. In C. Z. Christov (Ed.), *Advances in Protein Chemistry and Structural Biology* (Vol. 105, pp. 105–126). Academic Press. <https://doi.org/10.1016/bs.apcsb.2016.07.003>

- COP5—Geneva, 3 May 2011—United Nations targets widely-used pesticide endosulfan for phase out. (n.d.). Retrieved March 9, 2020, from <http://chm.pops.int/Implementation/PublicAwareness/PressReleases/COP5Geneva,3May2011Endosulfanphaseout/tabid/2216/Default.aspx>
- Corbeil, C. R., Williams, C. I., & Labute, P. (2012). Variability in docking success rates due to dataset preparation. *Journal of Computer-Aided Molecular Design*, 26(6), 775–786. <https://doi.org/10.1007/s10822-012-9570-1>
- Council of Europe. (2008). *Natural sources of flavourings*. (Volume 3). Strasbourg : Council of Europe Pub.
- Coxon, J. M., Dansted, E., Hartshorn, M. P., & Richards, K. E. (1968). The synthesis of some 2,10-epoxypinanes. *Tetrahedron*, 24(3), 1193–1197. [http://dx.doi.org/10.1016/0040-4020\(68\)88067-6](http://dx.doi.org/10.1016/0040-4020(68)88067-6)
- Cryle, M. J., & Voss, J. J. D. (2006). Is the Ferric Hydroperoxy Species Responsible for Sulfur Oxidation in Cytochrome P450s? *Angew. Chem. Int. Ed.*, 45, 8221–8223. <https://doi.org/10.1002/anie.200603411>
- Daiber, A., Shoun, H., & Ullrich, V. (2005). Nitric oxide reductase (P450nor) from *Fusarium oxysporum*. *Journal of Inorganic Biochemistry*, 99(1), 185–193. <https://doi.org/10.1016/j.jinorgbio.2004.09.018>
- Das, B., Helms, V., Lounnas, V., & Wade, R. C. (2000). Multicopy molecular dynamics simulations suggest how to reconcile crystallographic and product formation data for camphor enantiomers bound to cytochrome P-450cam. *Journal of Inorganic Biochemistry*, 81(3), 121–131. [https://doi.org/10.1016/S0162-0134\(00\)00095-7](https://doi.org/10.1016/S0162-0134(00)00095-7)
- Daub, M. E., Prudhomme, J., Ben Mamoun, C., Le Roch, K. G., & Vanderwal, C. D. (2017). Antimalarial Properties of Simplified Kalihinol Analogues. *ACS Medicinal Chemistry Letters*, 8(3), 355–360. <https://doi.org/10.1021/acsmedchemlett.7b00013>
- Davis, E. M., & Croteau, R. (2000). Cyclization Enzymes in the Biosynthesis of Monoterpenes, Sesquiterpenes, and Diterpenes. In F. J. Leeper & J. C. Vederas (Eds.), *Biosynthesis: Aromatic Polyketides, Isoprenoids, Alkaloids* (pp. 53–95). Springer. https://doi.org/10.1007/3-540-48146-X_2
- Davydov, R., Macdonald, I. D. G., Makris, T. M., Sligar, S. G., & Hoffman, B. M. (1999). EPR and ENDOR of Catalytic Intermediates in Cryoreduced Native and Mutant Oxy-Cytochromes P450cam: Mutation-Induced Changes in the Proton Delivery System. *Journal of the American Chemical Society*, 121(45), 10654–10655. <https://doi.org/10.1021/ja9918829>

- Davydov, R., Makris, T. M., Kofman, V., Werst, D. E., Sligar, S. G., & Hoffman, B. M. (2001). Hydroxylation of Camphor by Reduced Oxy-Cytochrome P450cam: Mechanistic Implications of EPR and ENDOR Studies of Catalytic Intermediates in Native and Mutant Enzymes. *Journal of the American Chemical Society*, *123*(7), 1403–1415. <https://doi.org/10.1021/ja003583l>
- Dawson, A. H., Eddleston, M., Senarathna, L., Mohamed, F., Gawarammana, I., Bowe, S. J., Manuweera, G., & Buckley, N. A. (2010). Acute Human Lethal Toxicity of Agricultural Pesticides: A Prospective Cohort Study. *PLOS Medicine*, *7*(10), e1000357. <https://doi.org/10.1371/journal.pmed.1000357>
- Dawson, J. H., Holm, R. H., Trudell, J. R., Barth, G., Linder, R. E., Bunnenberg, E., Djerassi, C., & Tang, S. C. (1976). Magnetic circular dichroism studies. 43. Oxidized cytochrome P-450. Magnetic circular dichroism evidence for thiolate ligation in the substrate-bound form. Implications for the catalytic mechanism. *Journal of the American Chemical Society*, *98*(12), 3707–3709. <https://doi.org/10.1021/ja00428a054>
- Denisov, I. G., Makris, T. M., Sligar, S. G., & Schlichting, I. (2005). Structure and Chemistry of Cytochrome P450. *Chemical Reviews*, *105*(6), 2253–2278. <https://doi.org/10.1021/cr0307143>
- Di Nardo, G., Fantuzzi, A., Sideri, A., Panicco, P., Sassone, C., Giunta, C., & Gilardi, G. (2007). Wild-type CYP102A1 as a biocatalyst: Turnover of drugs usually metabolised by human liver enzymes. *JBIC Journal of Biological Inorganic Chemistry*, *12*(3), 313–323. <https://doi.org/10.1007/s00775-006-0188-4>
- Dickschat, J. S. (2011). Isoprenoids in three-dimensional space: The stereochemistry of terpene biosynthesis. *Natural Product Reports*, *28*(12), 1917. <https://doi.org/10.1039/c1np00063b>
- Dickschat, J. S. (2015). Bacterial terpene cyclases. *Natural Product Reports*, *33*(1), 87–110. <https://doi.org/10.1039/C5NP00102A>
- Dickschat, J. S. (2019). Bacterial Diterpene Biosynthesis. *Angewandte Chemie International Edition*, *58*(45), 15964–15976. <https://doi.org/10.1002/anie.201905312>
- Duée, E. D., Fanchon, E., Vicat, J., Sieker, L. C., Meyer, J., & Moulis, J.-M. (1994). Refined crystal structure of the [2[4Fe-4S] ferredoxin from *Clostridium acidurici* at 1.84 Å resolution. *Journal of Molecular Biology*, *243*(4), 683–695. [https://doi.org/10.1016/0022-2836\(94\)90041-8](https://doi.org/10.1016/0022-2836(94)90041-8)
- Egawa, T., Shimada, H., & Ishimura, Y. (1994). Evidence for Compound I Formation in the Reaction of Cytochrome-P450cam with m-Chloroperbenzoic Acid. *Biochemical and Biophysical Research Communications*, *201*(3), 1464–1469. <https://doi.org/10.1006/bbrc.1994.1868>

- Eichler, A., Gricman, Ł., Herter, S., Kelly, P. P., Turner, N. J., Pleiss, J., & Flitsch, S. L. (2016). Enantioselective Benzylic Hydroxylation Catalysed by P450 Monooxygenases: Characterisation of a P450cam Mutant Library and Molecular Modelling. *ChemBioChem*, 17(5), 426–432. <https://doi.org/10.1002/cbic.201500536>
- Endosulfan Phase-out | Pesticides | US EPA*. (2010). US Environmental Protection Agency. <https://archive.epa.gov/pesticides/reregistration/web/html/endosulfan-agreement.html#agreement>
- England, P. A., Harford-Cross, C. F., Stevenson, J.-A., Rouch, D. A., & Wong, L.-L. (1998). The oxidation of naphthalene and pyrene by cytochrome P450cam. *FEBS Letters*, 424(3), 271–274. [https://doi.org/10.1016/S0014-5793\(98\)00189-6](https://doi.org/10.1016/S0014-5793(98)00189-6)
- Enhui, Z., Na, C., MengYun, L., Jia, L., Dan, L., Yongsheng, Y., Ying, Z., & DeFu, H. (2016). Isomers and their metabolites of endosulfan induced cytotoxicity and oxidative damage in SH-SY5Y cells. *Environmental Toxicology*, 31(4), 496–504. <https://doi.org/10.1002/tox.22066>
- Fasan, R. (2012). Tuning P450 Enzymes as Oxidation Catalysts. *ACS Catalysis*, 2(4), 647–666. <https://doi.org/10.1021/cs300001x>
- Fieser and Fieser's Reagents for Organic Synthesis, Volume 1 | Wiley*. (n.d.). Wiley.Com. Retrieved May 20, 2020, from <https://www.wiley.com/en-us/Fieser+and+Fieser%27s+Reagents+for+Organic+Synthesis%2C+Volume+1-p-9780471258759>
- Findley, T. J. K., Sucunza, D., Miller, L. C., Davies, D. T., & Procter, D. J. (2008). A flexible, stereoselective approach to the decorated cis-hydrindane skeleton: Synthesis of the proposed structure of faurinone. *Chemistry (Weinheim an Der Bergstrasse, Germany)*, 14(23), 6862–6865. <https://doi.org/10.1002/chem.200800930>
- Fjærvik, E., & Zotchev, S. B. (2005). Biosynthesis of the polyene macrolide antibiotic nystatin in *Streptomyces noursei*. *Applied Microbiology and Biotechnology*, 67(4), 436–443. <https://doi.org/10.1007/s00253-004-1802-4>
- French, K. J., Rock, D. A., Rock, D. A., Manchester, J. I., Goldstein, B. M., & Jones, J. P. (2002). Active Site Mutations of Cytochrome P450cam Alter the Binding, Coupling, and Oxidation of the Foreign Substrates (R)- and (S)-2-Ethylhexanol. *Archives of Biochemistry and Biophysics*, 398(2), 188–197. <https://doi.org/10.1006/abbi.2001.2732>
- French, K. J., Strickler, M. D., Rock, D. A., Rock, D. A., Bennett, G. A., Wahlstrom, J. L., Goldstein, B. M., & Jones, J. P. (2001). Benign Synthesis of 2-Ethylhexanoic Acid by Cytochrome P450cam: Enzymatic, Crystallographic, and Theoretical Studies. *Biochemistry*, 40(32), 9532–9538. <https://doi.org/10.1021/bi010063+>

- Froehlich, J. E., Itoh, A., & Howe, G. A. (2001). Tomato Allene Oxide Synthase and Fatty Acid Hydroperoxide Lyase, Two Cytochrome P450s Involved in Oxylipin Metabolism, Are Targeted to Different Membranes of Chloroplast Envelope. *Plant Physiology*, 125(1), 306–317. <https://doi.org/10.1104/pp.125.1.306>
- Fukuda, E., Kino, H., Matsuzawa, H., & Wakagi, T. (2001). Role of a highly conserved YPITP motif in 2-oxoacid:ferredoxin oxidoreductase. *European Journal of Biochemistry*, 268(21), 5639–5646. <https://doi.org/10.1046/j.1432-1033.2001.02504.x>
- Gelb, M. H., Heimbrook, D. C., Malkonen, P., & Sligar, S. G. (1982). Stereochemistry and deuterium isotope effects in camphor hydroxylation by the cytochrome P450cam monooxygenase system. *Biochemistry*, 21(2), 370–377. <https://doi.org/10.1021/bi00531a026>
- Gelb, M. H., Malkonen, P., & Sligar, S. G. (1982). Cytochrome P450cam catalyzed epoxidation of dehydrocamphor. *Biochemical and Biophysical Research Communications*, 104(3), 853–858. [https://doi.org/10.1016/0006-291X\(82\)91327-4](https://doi.org/10.1016/0006-291X(82)91327-4)
- Gerber, N. C., & Sligar, S. G. (1992). Catalytic mechanism of cytochrome P-450: Evidence for a distal charge relay. *Journal of the American Chemical Society*, 114(22), 8742–8743. <https://doi.org/10.1021/ja00048a081>
- Girhard, M., Klaus, T., Khatri, Y., Bernhardt, R., & Urlacher, V. B. (2010). Characterization of the versatile monooxygenase CYP109B1 from *Bacillus subtilis*. *Applied Microbiology and Biotechnology*, 87(2), 595–607. <https://doi.org/10.1007/s00253-010-2472-z>
- Girvan, H. M., & Munro, A. W. (2016). Applications of microbial cytochrome P450 enzymes in biotechnology and synthetic biology. *Current Opinion in Chemical Biology*, 31, 136–145. <https://doi.org/10.1016/j.cbpa.2016.02.018>
- Glascock, M. C., Ballou, D. P., & Dawson, J. H. (2005). Direct Observation of a Novel Perturbed Oxyferrous Catalytic Intermediate during Reduced Putidaredoxin-initiated Turnover of Cytochrome P-450-CAM PROBING THE EFFECTOR ROLE OF PUTIDAREDOXIN IN CATALYSIS. *Journal of Biological Chemistry*, 280(51), 42134–42141. <https://doi.org/10.1074/jbc.M505426200>
- Green, A. J., Rivers, S. L., Cheesman, M., Reid, G. A., Quaroni, L. G., Macdonald, I. D. G., Chapman, S. K., & Munro, A. W. (2001). Expression, purification and characterization of cytochrome P450 Biol: A novel P450 involved in biotin synthesis in *Bacillus subtilis*. *JBIC Journal of Biological Inorganic Chemistry*, 6(5), 523–533. <https://doi.org/10.1007/s007750100229>
- Grogan, G., Roberts, S., Wan, P., & Willetts, A. (1993). Camphor-grown *Pseudomonas putida*, a multifunctional biocatalyst for undertaking Baeyer-Villiger monooxygenase-dependent biotransformations. *Biotechnology Letters*, 15(9), 913–918. <https://doi.org/10.1007/BF00131756>

- Grout, T. G., & Richards, G. I. (1992). Susceptibility of *Euseius addoensis addoensis* (Acari: Phytoseiidae) to field-weathered residues of insecticides used on citrus. *Experimental & Applied Acarology*, *15*(3), 199–204. <https://doi.org/10.1007/BF01195791>
- Groves, J. T., McClusky, G. A., White, R. E., & Coon, M. J. (1978). Aliphatic hydroxylation by highly purified liver microsomal cytochrome P-450. Evidence for a carbon radical intermediate. *Biochemical and Biophysical Research Communications*, *81*(1), 154–160. [https://doi.org/10.1016/0006-291X\(78\)91643-1](https://doi.org/10.1016/0006-291X(78)91643-1)
- Guan, X., Fisher, M. B., Lang, D. H., Zheng, Y.-M., Koop, D. R., & Rettie, A. E. (1998). Cytochrome P450-dependent desaturation of lauric acid: Isoform selectivity and mechanism of formation of 11-dodecenoic acid. *Chemico-Biological Interactions*, *110*(1), 103–121. [https://doi.org/10.1016/S0009-2797\(97\)00145-2](https://doi.org/10.1016/S0009-2797(97)00145-2)
- Guengerich, F. P., & Böcker, R. H. (1988). Cytochrome P-450-catalyzed dehydrogenation of 1,4-dihydropyridines. *Journal of Biological Chemistry*, *263*(17), 8168–8175.
- Guengerich, F. Peter. (2001). Common and Uncommon Cytochrome P450 Reactions Related to Metabolism and Chemical Toxicity. *Chemical Research in Toxicology*, *14*(6), 611–650. <https://doi.org/10.1021/tx0002583>
- Guengerich, F. Peter. (2015). Human Cytochrome P450 Enzymes. In P. R. Ortiz de Montellano (Ed.), *Cytochrome P450: Structure, Mechanism, and Biochemistry* (pp. 523–785). Springer International Publishing. https://doi.org/10.1007/978-3-319-12108-6_9
- Guengerich, F. Peter, & Kim, D. H. (1991). Enzymic oxidation of ethyl carbamate to vinyl carbamate and its role as an intermediate in the formation of 1,N6-ethenoadenosine. *Chemical Research in Toxicology*, *4*(4), 413–421. <https://doi.org/10.1021/tx00022a003>
- Guengerich, F., Waterman, M. R., & Egli, M. (2016). Recent Structural Insights into Cytochrome P450 Function. *Trends in Pharmacological Sciences*, *37*(8), 625–640. <https://doi.org/10.1016/j.tips.2016.05.006>
- Gustafsson, M. C. U., Roitel, O., Marshall, K. R., Noble, M. A., Chapman, S. K., Pessegueiro, A., Fulco, A. J., Cheesman, M. R., von Wachenfeldt, C., & Munro, A. W. (2004). Expression, Purification, and Characterization of *Bacillus subtilis* Cytochromes P450 CYP102A2 and CYP102A3: Flavocytochrome Homologues of P450 BM3 from *Bacillus megaterium*. *Biochemistry*, *43*(18), 5474–5487. <https://doi.org/10.1021/bi035904m>
- Hagmann, M., & Grisebach, H. (1984). Enzymatic rearrangement of flavanone to isoflavone. *FEBS Letters*, *175*(2), 199–202. [https://doi.org/10.1016/0014-5793\(84\)80736-X](https://doi.org/10.1016/0014-5793(84)80736-X)

- Hall, H. K. (1963). Synthesis and Polymerization of 3-Azabicyclo-[4.3.1]decan-4-one and 7,7-Dimethyl-2-azabicyclo[4.1.1]octan-3-one. *The Journal of Organic Chemistry*, 28(11), 3213–3214. <https://doi.org/10.1021/jo01046a508>
- Haniu, M., Armes, L. G., Yasunobu, K. T., Shastry, B. A., & Gunsalus, I. C. (1982). Amino acid sequence of the *Pseudomonas putida* cytochrome P-450. II. Cyanogen bromide peptides, acid cleavage peptides, and the complete sequence. *Journal of Biological Chemistry*, 257(21), 12664–12671.
- Hannemann, F., Bichet, A., Ewen, K. M., & Bernhardt, R. (2007). Cytochrome P450 systems—Biological variations of electron transport chains. *Biochimica et Biophysica Acta (BBA) - General Subjects*, 1770(3), 330–344. <https://doi.org/10.1016/j.bbagen.2006.07.017>
- Harford-Cross, C. F., Carmichael, A. B., Allan, F. K., England, P. A., Rouch, D. A., & Wong, L.-L. (2000). Protein engineering of cytochrome P450cam (CYP101) for the oxidation of polycyclic aromatic hydrocarbons. *Protein Engineering, Design and Selection*, 13(2), 121–128. <https://doi.org/10.1093/protein/13.2.121>
- Harman-Fetcho, J. A., Hapeman, C. J., McConnell, L. L., Potter, T. L., Rice, C. P., Sadeghi, A. M., Smith, R. D., Bialek, K., Sefton, K. A., Schaffer, B. A., & Curry, R. (2005). Pesticide Occurrence in Selected South Florida Canals and Biscayne Bay during High Agricultural Activity. *Journal of Agricultural and Food Chemistry*, 53(15), 6040–6048. <https://doi.org/10.1021/jf047803g>
- Harris, D. L., & Loew, G. H. (1998). Theoretical Investigation of the Proton Assisted Pathway to Formation of Cytochrome P450 Compound I. *Journal of the American Chemical Society*, 120(35), 8941–8948. <https://doi.org/10.1021/ja981059x>
- Hasemann, C. A., Kurumbail, R. G., Boddupalli, S. S., Peterson, J. A., & Deisenhofer, J. (1995). Structure and function of cytochromes P450: a comparative analysis of three crystal structures. *Structure*, 3(1), 41–62. [https://doi.org/10.1016/S0969-2126\(01\)00134-4](https://doi.org/10.1016/S0969-2126(01)00134-4)
- Haurand, M., & Ullrich, V. (1985). Isolation and characterization of thromboxane synthase from human platelets as a cytochrome P-450 enzyme. *Journal of Biological Chemistry*, 260(28), 15059–15067.
- Hawkes, D. B., Adams, G. W., Burlingame, A. L., Montellano, P. R. O. de, & Voss, J. J. D. (2002). Cytochrome P450cin (CYP176A), Isolation, Expression, and Characterization. *Journal of Biological Chemistry*, 277(31), 27725–27732. <https://doi.org/10.1074/jbc.M203382200>
- Health Canada. (2011, February 4). *Discontinuation of Endosulfan* [Transparency - other]. Health Canada. <https://www.canada.ca/en/health-canada/services/consumer-product-safety/reports-publications/pesticides-pest-management/decisions-updates/reevaluation-note/2011/discontinuation-endosulfan-rev2011-01.html>

- Hecker, M., & Ullrich, V. (1989). On the mechanism of prostacyclin and thromboxane A₂ biosynthesis. *Journal of Biological Chemistry*, 264(1), 141–150.
- Hedegaard, J., & Gunsalus, I. C. (1965). Mixed Function Oxidation IV. AN INDUCED METHYLENE HYDROXYLASE IN CAMPHOR OXIDATION. *Journal of Biological Chemistry*, 240(10), 4038–4043.
- Hida, T., Mitsumori, S., Honma, T., Hiramatsu, Y., Hashizume, H., Okada, T., Kakinuma, M., Oda, K., Hasegawa, A., Masui, T., & Nogusa, H. (2009). Practical Diastereoselective Synthesis and Scale-up Study of (+) -2- ((1 R , 2 R , 3 R , 5 S) -2- Amino-6 , 6-dimethylbicyclo [3. 1. 1] hept-3-yl) ethanol: A Key Intermediate of the Novel Prostaglandin D₂ Receptor Antagonist S-5751
Abstract: *Organic Process Research & Development*, 13(6), 1413–1418.
- Hiruma, Y., Hass, M. A. S., Kikui, Y., Liu, W.-M., Ölmez, B., Skinner, S. P., Blok, A., Kloosterman, A., Koteishi, H., Löhr, F., Schwalbe, H., Nojiri, M., & Ubbink, M. (2013). The Structure of the Cytochrome P450cam–Putidaredoxin Complex Determined by Paramagnetic NMR Spectroscopy and Crystallography. *Journal of Molecular Biology*, 425(22), 4353–4365.
<https://doi.org/10.1016/j.jmb.2013.07.006>
- Hishik, T., Shimada, H., Nagano, S., Egawa, T., Kanamori, Y., Makino, R., Park, S.-Y., Adachi, S., Shiro, Y., & Ishimura, Y. (2000). X-Ray Crystal Structure and Catalytic Properties of Thr252Ile Mutant of Cytochrome P450cam: Roles of Thr252 and Water in the Active Center. *The Journal of Biochemistry*, 128(6), 965–974. <https://doi.org/10.1093/oxfordjournals.jbchem.a022848>
- Hogue, C. (2011). Endosulfan Banned Worldwide. *Chemical & Engineering News*, 89(19), 15. <https://doi.org/10.1021/cen042811152405>
- Honeycutt, M., & Shirley, S. (2014). Aldrin. In P. Wexler (Ed.), *Encyclopedia of Toxicology (Third Edition)* (pp. 126–129). Academic Press.
<https://doi.org/10.1016/B978-0-12-386454-3.00094-4>
- Hough-Goldstein, J., & Keil, C. B. (1991). Prospects for Integrated Control of the Colorado Potato Beetle (Coleoptera: Chrysomelidae) Using *Perillus bioculatus* (Hemiptera: Pentatomidae) and Various Pesticides. *Journal of Economic Entomology*, 84(6), 1645–1651. <https://doi.org/10.1093/jee/84.6.1645>
- Hunter, D. J. B., Roberts, G. A., Ost, T. W. B., White, J. H., Müller, S., Turner, N. J., Flitsch, S. L., & Chapman, S. K. (2005). Analysis of the domain properties of the novel cytochrome P450 RhF. *FEBS Letters*, 579(10), 2215–2220.
<https://doi.org/10.1016/j.febslet.2005.03.016>
- Hussain, S., Arshad, M., Saleem, M., & Khalid, A. (2007). Biodegradation of α - and β -endosulfan by soil bacteria. *Biodegradation*, 18(6), 731–740.
<https://doi.org/10.1007/s10532-007-9102-1>

- Hussain, S., Arshad, M., Saleem, M., & Zahir, Z. A. (2007). Screening of soil fungi for in vitro degradation of endosulfan. *World Journal of Microbiology and Biotechnology*, 23(7), 939–945. <https://doi.org/10.1007/s11274-006-9317-z>
- Ilie, A., Lonsdale, R., Agudo, R., & Reetz, M. T. (2015). A diastereoselective P450-catalyzed epoxidation reaction: Anti versus syn reactivity. *Tetrahedron Letters*, 56(23), 3435–3437. <https://doi.org/10.1016/j.tetlet.2015.03.076>
- Irmisch, S., Clavijo McCormick, A., Günther, J., Schmidt, A., Boeckler, G. A., Gershenzon, J., Unsicker, S. B., & Köllner, T. G. (2014). Herbivore-induced poplar cytochrome P450 enzymes of the CYP71 family convert aldoximes to nitriles which repel a generalist caterpillar. *The Plant Journal*, 80, 1095–1107. <https://doi.org/10.1111/tpj.12711>
- Itoh, A., & Howe, G. A. (2001). Molecular Cloning of a Divinyl Ether Synthase IDENTIFICATION AS A CYP74 CYTOCHROME P-450. *Journal of Biological Chemistry*, 276(5), 3620–3627. <https://doi.org/10.1074/jbc.M008964200>
- Iyanagi, T., & Mason, H. S. (1973). Properties of hepatic reduced nicotinamide adenine dinucleotide phosphate-cytochrome c reductase. *Biochemistry*, 12(12), 2297–2308. <https://doi.org/10.1021/bi00736a018>
- Jackson, C. J., Lamb, D. C., Marczylo, T. H., Warrilow, A. G. S., Manning, N. J., Lowe, D. J., Kelly, D. E., & Kelly, S. L. (2002). A Novel Sterol 14 α -Demethylase/Ferredoxin Fusion Protein (MCCYP51FX) from *Methylococcus capsulatus* Represents a New Class of the Cytochrome P450 Superfamily. *Journal of Biological Chemistry*, 277(49), 46959–46965. <https://doi.org/10.1074/jbc.M203523200>
- Ji, L., Faponle, A. S., Quesne, M. G., Sainna, M. A., Zhang, J., Franke, A., Kumar, D., van Eldik, R., Liu, W., & de Visser, S. P. (2015). Drug Metabolism by Cytochrome P450 Enzymes: What Distinguishes the Pathways Leading to Substrate Hydroxylation Over Desaturation? *Chemistry – A European Journal*, 21(25), 9083–9092. <https://doi.org/10.1002/chem.201500329>
- Jimenez-Torres, C., Ortiz, I., San-Martin, P., & Hernandez-Herrera, R. I. (2016). Biodegradation of malathion, α - and β -endosulfan by bacterial strains isolated from agricultural soil in Veracruz, Mexico. *Journal of Environmental Science and Health, Part B*, 51(12), 853–859. <https://doi.org/10.1080/03601234.2016.1211906>
- Jin, S., Makris, T. M., Bryson, T. A., Sligar, S. G., & Dawson, J. H. (2003). Epoxidation of Olefins by Hydroperoxo-Ferric Cytochrome P450. *Journal of the American Chemical Society*, 125(12), 3406–3407. <https://doi.org/10.1021/ja029272n>
- Jones, J. P., O'Hare, E. J., & Wong, L.-L. (2000). The oxidation of polychlorinated benzenes by genetically engineered cytochrome P450cam: Potential applications in bioremediation. *Chemical Communications*, 3, 247–248. <https://doi.org/10.1039/A909536E>

- Kadkhodayan, S., Coulter, E. D., Maryniak, D. M., Bryson, T. A., & Dawson, J. H. (1995). Uncoupling Oxygen Transfer and Electron Transfer in the Oxygenation of Camphor Analogues by Cytochrome P450-CAM: DIRECT OBSERVATION OF AN INTERMOLECULAR ISOTOPE EFFECT FOR SUBSTRATE C-H ACTIVATION(*). *Journal of Biological Chemistry*, 270(47), 28042–28048. <https://doi.org/10.1074/jbc.270.47.28042>
- Kalle, E., Kubista, M., & Rensing, C. (2014). Multi-template polymerase chain reaction. *Biomolecular Detection and Quantification*, 2, 11–29. <https://doi.org/10.1016/j.bdq.2014.11.002>
- Kammoonah, S., Prasad, B., Balaraman, P., Mundhada, H., Schwaneberg, U., & Plettner, E. (2018). Selecting of a cytochrome P450cam SeSaM library with 3-chloroindole and endosulfan – Identification of mutants that dehalogenate 3-chloroindole. *Biochimica et Biophysica Acta (BBA) - Proteins and Proteomics*, 1866(1), 68–79. <https://doi.org/10.1016/j.bbapap.2017.09.006>
- Kang, J. S., Kim, E., Lee, S. H., & Park, I.-K. (2013). Inhibition of acetylcholinesterases of the pinewood nematode, *Bursaphelenchus xylophilus*, by phytochemicals from plant essential oils. *Pesticide Biochemistry and Physiology*, 105(1), 50–56. <https://doi.org/10.1016/j.pestbp.2012.11.007>
- Karunakaran, V., Denisov, I., Sligar, S. G., & Champion, P. M. (2011). Investigation of the Low Frequency Dynamics of Heme Proteins: Native and Mutant Cytochrome P450cam and Redox Partner Complexes. *The Journal of Physical Chemistry B*, 115(18), 5665–5677. <https://doi.org/10.1021/jp112298y>
- Katagiri, M., Ganguli, B. N., & Gunsalus, I. C. (1968). A Soluble Cytochrome P-450 Functional in Methylene Hydroxylation. *Journal of Biological Chemistry*, 243(12), 3543–3546.
- Kataoka, R., Takagi, K., & Sakakibara, F. (2010). A new endosulfan-degrading fungus, *Mortierella* species, isolated from a soil contaminated with organochlorine pesticides. *Journal of Pesticide Science*, 35(3), 326–332. <https://doi.org/10.1584/jpestics.G10-10>
- Kataoka, R., Takagi, K., & Sakakibara, F. (2011). Biodegradation of endosulfan by *Mortierella* sp. strain W8 in soil: Influence of different substrates on biodegradation. *Chemosphere*, 85(3), 548–552. <https://doi.org/10.1016/j.chemosphere.2011.08.021>
- Kato, M., Watanabe, M., Tooyama, Y., Vogler, B., & Yoshikoshi, A. (1992). Efficient and Convenient Syntheses of (R)-(-)-Cryptone and (S)-(-)-4-Isopropenyl-2-cyclohexen-1-one. *Synthesis*, 1992(11), 1055–1057. <https://doi.org/10.1055/s-1992-26297>

- Kawashima, H., Kaneko, Y., Sakai, M., & Kobayashi, Y. (2014). Synthesis of cyclobakuchiols A, B, and C by using conformation-controlled stereoselective reactions. *Chemistry - A European Journal*, *20*(1), 272–278. <https://doi.org/10.1002/chem.201303538>
- Kayser, H., Wtnkler, T., & Spindler-Barth, M. (1997). 26-Hydroxylation of Ecdysteroids is Catalyzed by a Typical Cytochrome P-450-Dependent Oxidase and Related to Ecdysteroid Resistance in an Insect Cell Line. *European Journal of Biochemistry*, *248*(3), 707–716. <https://doi.org/10.1111/j.1432-1033.1997.00707.x>
- Keeling, C. I. (2016). Chapter Seven—Bark Beetle Research in the Postgenomic Era. In C. Tittiger & G. J. Blomquist (Eds.), *Advances in Insect Physiology* (Vol. 50, pp. 265–293). Academic Press. <https://doi.org/10.1016/bs.aiip.2015.12.004>
- Keeling, Christopher I., & Bohlmann, J. (2006). Genes, enzymes and chemicals of terpenoid diversity in the constitutive and induced defence of conifers against insects and pathogens. *New Phytologist*, *170*(4), 657–675. <https://doi.org/10.1111/j.1469-8137.2006.01716.x>
- Keeling, Christopher I., Henderson, H., Li, M., Dullat, H. K., Ohnishi, T., & Bohlmann, J. (2013). CYP345E2, an antenna-specific cytochrome P450 from the mountain pine beetle, *Dendroctonus ponderosae* Hopkins, catalyses the oxidation of pine host monoterpene volatiles. *Insect Biochemistry and Molecular Biology*, *43*(12), 1142–1151. <https://doi.org/10.1016/j.ibmb.2013.10.001>
- Kelly, B. C., & Gobas, F. A. P. C. (2003). An Arctic Terrestrial Food-Chain Bioaccumulation Model for Persistent Organic Pollutants. *Environmental Science & Technology*, *37*(13), 2966–2974. <https://doi.org/10.1021/es021035x>
- Kelly, B. C., Ikonou, M. G., Blair, J. D., Morin, A. E., & Gobas, F. A. P. C. (2007). Food Web-Specific Biomagnification of Persistent Organic Pollutants. *Science*, *317*(5835), 236–239. <https://doi.org/10.1126/science.1138275>
- Kim, D., Heo, Y.-S., & Ortiz de Montellano, P. R. (2008). Efficient catalytic turnover of cytochrome P450cam is supported by a T252N mutation. *Archives of Biochemistry and Biophysics*, *474*(1), 150–156. <https://doi.org/10.1016/j.abb.2008.02.044>
- Kim, S. H., Yang, T.-C., Perera, R., Jin, S., Bryson, T. A., Sono, M., Davydov, R., Dawson, J. H., & Hoffman, B. M. (2005). Cryoreduction EPR and 13C, 19F ENDOR study of substrate-bound substates and solvent kinetic isotope effects in the catalytic cycle of cytochrome P450cam and its T252A mutant. *Dalton Transactions*, *21*, 3464–3469. <https://doi.org/10.1039/B506764M>
- Kim, T.-W., Hwang, J.-Y., Kim, Y.-S., Joo, S.-H., Chang, S. C., Lee, J. S., Takatsuto, S., & Kim, S.-K. (2005). Arabidopsis CYP85A2, a Cytochrome P450, Mediates the Baeyer-Villiger Oxidation of Castasterone to Brassinolide in Brassinosteroid Biosynthesis. *The Plant Cell*, *17*(8), 2397–2412. <https://doi.org/10.1105/tpc.105.033738>

- Kizawa, H., Tomura, D., Oda, M., Fukamizu, A., Hoshino, T., Gotoh, O., Yasui, T., & Shoun, H. (1991). Nucleotide sequence of the unique nitrate/nitrite-inducible cytochrome P-450 cDNA from *Fusarium oxysporum*. *Journal of Biological Chemistry*, 266(16), 10632–10637.
- Klingenberg, M. (1958). Pigments of rat liver microsomes. *Archives of Biochemistry and Biophysics*, 75(2), 376–386. [https://doi.org/10.1016/0003-9861\(58\)90436-3](https://doi.org/10.1016/0003-9861(58)90436-3)
- Knudsen, J. T., Eriksson, R., & Gershenzon, J. (2006). Diversity and Distribution of Floral Scent. *The Botanical Review*, 72, 1–120.
- Koga, H., Sagara, Y., Yaoi, T., Tsujimura, M., Nakamura, K., Sekimizu, K., Makino, R., Shimada, H., Ishimura, Y., Yura, K., Go, M., Ikeguchi, M., & Horiuchi, T. (1993). Essential role of the Arg112 residue of cytochrome P450cam for electron transfer from reduced putidaredoxin. *FEBS Letters*, 331(1–2), 109–113. [https://doi.org/10.1016/0014-5793\(93\)80307-G](https://doi.org/10.1016/0014-5793(93)80307-G)
- Koo, L. S., Tschirret-Guth, R. A., Straub, W. E., Moënné-Loccoz, P., Loehr, T. M., & Montellano, P. R. O. de. (2000). The Active Site of the Thermophilic CYP119 from *Sulfolobus solfataricus*. *Journal of Biological Chemistry*, 275(19), 14112–14123. <https://doi.org/10.1074/jbc.275.19.14112>
- Koshlukova, S. E., & Reed, N. R. (2014). Chlordane. In P. Wexler (Ed.), *Encyclopedia of Toxicology (Third Edition)* (pp. 841–845). Academic Press. <https://doi.org/10.1016/B978-0-12-386454-3.00111-1>
- Koskinen, A. M. P. (2012). *Asymmetric Synthesis of Natural Products*. John Wiley & Sons, Incorporated. <http://ebookcentral.proquest.com/lib/sfu-ebooks/detail.action?docID=945111>
- Krzemiński, M. P., & Wojtczak, A. (2005). Chiral terpene auxiliaries. Part 1: Highly enantioselective reduction of ketones with borane catalyzed by an oxazaborolidine derived from (-)- β -pinene. *Tetrahedron Letters*, 46(48), 8299–8302. <https://doi.org/10.1016/j.tetlet.2005.09.172>
- Kullman, S. W., & Matsumura, F. (1996). Metabolic pathways utilized by *Phanerochaete chrysosporium* for degradation of the cyclodiene pesticide endosulfan. *Applied and Environmental Microbiology*, 62(2), 593–600.
- Kwon, G.-S., Kim, J.-E., Kim, T.-K., Sohn, H.-Y., Koh, S.-C., Shin, K.-S., & Kim, D.-G. (2002). *Klebsiella pneumoniae* KE-1 degrades endosulfan without formation of the toxic metabolite, endosulfan sulfate. *FEMS Microbiology Letters*, 215(2), 255–259. <https://doi.org/10.1111/j.1574-6968.2002.tb11399.x>
- Labute, P. (2008). The generalized Born/volume integral implicit solvent model: Estimation of the free energy of hydration using London dispersion instead of atomic surface area. *Journal of Computational Chemistry*, 29(10), 1693–1698. <https://doi.org/10.1002/jcc.20933>

- Labute, P. (2009). Protonate3D: Assignment of ionization states and hydrogen coordinates to macromolecular structures. *Proteins: Structure, Function, and Bioinformatics*, 75(1), 187–205. <https://doi.org/10.1002/prot.22234>
- Lafever, R., & Croteau, R. (1993). Hydride Shifts in the Biosynthesis of the p-Menthane Monoterpenes α -Terpinene, γ -Terpinene, and β -Phellandrene. *Archives of BioChemistry and Biophysics*, 301(2), 361–366.
- Lee, S. H., Kwon, Y., Kim, D., & Park, C. B. (2013). Cytochrome P450-Catalyzed O - Dealkylation Coupled With Photochemical NADPH Regeneration. *Biotechnology and Bioengineering*, 110(2), 383–390. <https://doi.org/10.1002/bit.24729>
- Lee, Y. T., Glazer, E. C., Wilson, R. F., Stout, C. D., & Goodin, D. B. (2011). Three Clusters of Conformational States in P450cam Reveal a Multistep Pathway for Closing of the Substrate Access Channel,. *Biochemistry*, 50(5), 693–703. <https://doi.org/10.1021/bi101726d>
- Lee, Y. T., Wilson, R. F., Rupniewski, I., & Goodin, D. B. (2010). P450cam Visits an Open Conformation in the Absence of Substrate,. *Biochemistry*, 49(16), 3412–3419. <https://doi.org/10.1021/bi100183g>
- Lefever, M. R., & Wackett, L. P. (1994). Oxidation of Low Molecular Weight Chloroalkanes by Cytochrome P450CAM. *Biochemical and Biophysical Research Communications*, 201(1), 373–378. <https://doi.org/10.1006/bbrc.1994.1711>
- Lehotay, S. J., Harman-Fetcho, J. A., & McConnell, L. L. (1998). Agricultural pesticide residues in oysters and water from two chesapeake bay tributaries. *Marine Pollution Bulletin*, 37(1), 32–44. [https://doi.org/10.1016/S0025-326X\(98\)00129-5](https://doi.org/10.1016/S0025-326X(98)00129-5)
- Li, H., Narasimhulu, S., Havran, L. M., Winkler, J. D., & Poulos, T. L. (1995). Crystal Structure of Cytochrome P450cam Complexed with Its Catalytic Product, 5-exo-Hydroxycamphor. *Journal of the American Chemical Society*, 117(23), 6297–6299. <https://doi.org/10.1021/ja00128a019>
- Li, S., & Wackett, L. P. (1993). Reductive dehalogenation by cytochrome P450CAM: Substrate binding and catalysis. *Biochemistry*, 32(36), 9355–9361. <https://doi.org/10.1021/bi00087a014>
- Liang, X., Peng, L., Li, K., Peterson, T., & Katzen, F. (2012). A method for multi-site-directed mutagenesis based on homologous recombination. *Analytical Biochemistry*, 427(1), 99–101. <https://doi.org/10.1016/j.ab.2012.05.002>
- Limburg, J., LeBrun, L. A., & Ortiz de Montellano, P. R. (2005). The P450cam G248E Mutant Covalently Binds Its Prosthetic Heme Group. *Biochemistry*, 44(10), 4091–4099. <https://doi.org/10.1021/bi047686i>

- Lin, H.-C., Tsunematsu, Y., Dhingra, S., Xu, W., Fukutomi, M., Chooi, Y.-H., Cane, D. E., Calvo, A. M., Watanabe, K., & Tang, Y. (2014). Generation of Complexity in Fungal Terpene Biosynthesis: Discovery of a Multifunctional Cytochrome P450 in the Fumagillin Pathway. *Journal of the American Chemical Society*, *136*(11), 4426–4436. <https://doi.org/10.1021/ja500881e>
- Lindren, B. S., & Miller, D. R. (2002). Effect of verbenone on five species of bark beetles (Coleoptera: Scolytidae) in Lodgepole pine forests. *Environmental Entomology* *31*(5): 759-765. <https://www.fs.usda.gov/treesearch/pubs/20326>
- Ling, M. M., & Robinson, B. H. (1997). Approaches to DNA Mutagenesis: An Overview. *Analytical Biochemistry*, *254*(2), 157–178. <https://doi.org/10.1006/abio.1997.2428>
- Lipscomb, J. D., Sligar, S. G., Namtvedt, M. J., & Gunsalus, I. C. (1976). Autooxidation and hydroxylation reactions of oxygenated cytochrome P-450cam. *Journal of Biological Chemistry*, *251*(4), 1116–1124.
- Logan, M. S. P., Newman, L. M., Schanke, C. A., & Wacket, L. P. (1993). Cosubstrate effects in reductive dehalogenation by *Pseudomonas putida* G786 expressing cytochrome P-450CAM. *Biodegradation*, *4*(1), 39–50. <https://doi.org/10.1007/BF00701453>
- Loida, P. J., & Sligar, S. G. (1993). Molecular recognition in cytochrome P-450: Mechanism for the control of uncoupling reactions. *Biochemistry*, *32*(43), 11530–11538. <https://doi.org/10.1021/bi00094a009>
- Lonsdale, R., Harvey, J. N., & Mulholland, A. J. (2010). Compound I Reactivity Defines Alkene Oxidation Selectivity in Cytochrome P450cam. *The Journal of Physical Chemistry B*, *114*(2), 1156–1162. <https://doi.org/10.1021/jp910127j>
- Luek, J. L., Dickhut, R. M., Cochran, M. A., Falconer, R. L., & Kylin, H. (2017). Persistent organic pollutants in the Atlantic and southern oceans and oceanic atmosphere. *Science of The Total Environment*, *583*, 64–71. <https://doi.org/10.1016/j.scitotenv.2016.12.189>
- Lülsdorf, N., Vojcic, L., Hellmuth, H., Weber, T. T., Mußmann, N., Martinez, R., & Schwaneberg, U. (2015). A first continuous 4-aminoantipyrine (4-AAP)-based screening system for directed esterase evolution. *Applied Microbiology and Biotechnology*, *99*(12), 5237–5246. <https://doi.org/10.1007/s00253-015-6612-3>
- Macbeth, A. K., Smith, G. E., & West, T. F. (1938). β -Phellandrene. *J. Chem. Soc.*, 119–123. <https://doi.org/10.1039/JR9380000119>
- Macías-Sámano, J. E., Borden, J. H., Gries, R., Pierce, H. D., Gries, G., & King, G. G. S. (1998). Primary Attraction of the Fir Engraver, *Scolytus ventralis*. *Journal of Chemical Ecology*, *24*(6), 1049–1075. <https://doi.org/10.1023/A:1022354503443>

- Maier, T., Förster, H.-H., Asperger, O., & Hahn, U. (2001). Molecular Characterization of the 56-kDa CYP153 from *Acinetobacter* sp. EB104. *Biochemical and Biophysical Research Communications*, 286(3), 652–658. <https://doi.org/10.1006/bbrc.2001.5449>
- Maier-Bode, H. (1968). Properties, effect, residues and analytics of the insecticide endosulfan. In F. A. Gunther (Ed.), *Residue Reviews / Rückstands-Berichte* (Vol. 22, pp. 1–44). Springer US. https://doi.org/10.1007/978-1-4615-8434-6_1
- Malkov, A. V., Pernazza, D., Bell, M., Bella, M., Massa, A., Teplý, F., Meghani, P., & Kozlovskiy, P. (2003). Synthesis of new chiral 2,2'-bipyridine ligands and their application in Copper-catalyzed asymmetric allylic oxidation and cyclopropanation. *Journal of Organic Chemistry*, 68(12), 4727–4742. <https://doi.org/10.1021/jo034179i>
- Manchester, J. I., & Ornstein, R. L. (1995). Enzyme-catalyzed dehalogenation of pentachloroethane: Why F87W-cytochrome P450cam is faster than wild type. *Protein Engineering, Design and Selection*, 8(8), 801–807. <https://doi.org/10.1093/protein/8.8.801>
- Manna, S. K., & Mazumdar, S. (2006). Role of Threonine 101 on the Stability of the Heme Active Site of Cytochrome P450cam: Multiwavelength Circular Dichroism Studies. *Biochemistry*, 45(42), 12715–12722. <https://doi.org/10.1021/bi060848l>
- Mayhew, M. P., Roitberg, A. E., Tewari, Y., Holden, M. J., Vanderah, D. J., & Vilker, V. L. (2002). Benzocycloarene hydroxylation by P450 biocatalysis. *New Journal of Chemistry*, 26(1), 35–42. <https://doi.org/10.1039/B107584P>
- McCullum, E. O., Williams, B. A. R., Zhang, J., & Chaput, J. C. (2010). Random Mutagenesis by Error-Prone PCR. In J. Braman (Ed.), *In Vitro Mutagenesis Protocols: Third Edition* (pp. 103–109). Humana Press. https://doi.org/10.1007/978-1-60761-652-8_7
- McLean, M. A., Maves, S. A., Weiss, K. E., Krepich, S., & Sligar, S. G. (1998). Characterization of a Cytochrome P450 from the Acidothermophilic Archaea *Sulfolobus solfataricus*. *Biochemical and Biophysical Research Communications*, 252(1), 166–172. <https://doi.org/10.1006/bbrc.1998.9584>
- Meddens, A. J. H., Hicke, J. A., & Ferguson, C. A. (2012). Spatiotemporal patterns of observed bark beetle-caused tree mortality in British Columbia and the western United States. *Ecological Applications*, 22(7), 1876–1891. <https://doi.org/10.1890/11-1785.1>
- Meesters, R. J. W., Duisken, M., & Hollender, J. (2009). Cytochrome P450-catalysed arene-epoxidation of the bioactive tea tree oil ingredient p-cymene: Indication for the formation of a reactive allergenic intermediate? *Xenobiotica*, 39(9), 663–671. <https://doi.org/10.1080/00498250902989094>

- Mehareenna, Y. T., Li, H., Hawkes, D. B., Pearson, A. G., De Voss, J., & Poulos, T. L. (2004). Crystal Structure of P450cin in a Complex with Its Substrate, 1,8-Cineole, a Close Structural Homologue to d-Camphor, the Substrate for P450cam,. *Biochemistry*, *43*(29), 9487–9494. <https://doi.org/10.1021/bi049293p>
- Mehareenna, Y. T., Slessor, K. E., Cavaignac, S. M., Poulos, T. L., & Voss, J. J. D. (2008). The Critical Role of Substrate-Protein Hydrogen Bonding in the Control of Regioselective Hydroxylation in P450cin. *Journal of Biological Chemistry*, *283*(16), 10804–10812. <https://doi.org/10.1074/jbc.M709722200>
- Meyer, A. H., Dybala-Defratyka, A., Alaimo, P. J., Geronimo, I., Sanchez, A. D., Cramer, C. J., & Elsner, M. (2014). Cytochrome P450-catalyzed dealkylation of atrazine by *Rhodococcus* sp. Strain NI86/21 involves hydrogen atom transfer rather than single electron transfer. *Dalton Transactions*, *43*(32), 12175–12186. <https://doi.org/10.1039/C4DT00891J>
- Miller, D., & Borden, J. (1990a). /3-PHELLANDRENE: KAIROMONE FOR PINE ENGRAVER, *Ips pini* (COLEOPTERA: SCOLYTIDAE). *Journal of Chemical Ecology*, *16*(8), 2519–2531.
- Miller, D., & Borden, J. (1990b). The use of monoterpenes as kairomones by *Ips latidens* (LeConte)(Coleoptera: Scolytidae). *The Canadian Entomologist*, *122*, 301–307. <https://doi.org/10.4039/Ent122301-3>
- Miller, D., Borden, J., King, G. G. S., & Slessor, K. (1991). Ipsenol—An Aggregation Pheromone for *Ips-Latidens* (Leconte) (Coleoptera, Scolytidae). *Journal of Chemical Ecology*, *17*(8), 1517–1527.
- Miller, D. R., & Borden, J. H. (2000). DOSE-DEPENDENT AND SPECIES-SPECIFIC RESPONSES OF PINE BARK BEETLES (COLEOPTERA : SCOLYTIDAE) TO MONOTERPENES IN ASSOCIATION WITH PHEROMONES. *The Canadian Entomologist*, *132*, 183–195.
- Miura, Y., & Fulco, A. J. (1974). (ω -2) Hydroxylation of Fatty Acids by a Soluble System from *Bacillus megaterium*. *Journal of Biological Chemistry*, *249*(6), 1880–1888.
- Miwa, G. T., Garland, W. A., Hodshon, B. J., Lu, A. Y., & Northrop, D. B. (1980). Kinetic isotope effects in cytochrome P-450-catalyzed oxidation reactions. Intermolecular and intramolecular deuterium isotope effects during the N-demethylation of N,N-dimethylphenthermine. *Journal of Biological Chemistry*, *255*(13), 6049–6054.
- Mizutani, M., & Sato, F. (2011). Unusual P450 reactions in plant secondary metabolism. *Archives of Biochemistry and Biophysics*, *507*(1), 194–203. <https://doi.org/10.1016/j.abb.2010.09.026>
- Mori, K. (2006). Synthesis of (1S,4R)-4-isopropyl-1-methyl-2-cyclohexen-1-ol, the aggregation pheromone of the ambrosia beetle *Platypus quercivorus*, its racemate, (1R,4R)- and (1S,4S)-isomers. *Tetrahedron Asymmetry*, *17*(14), 2133–2142. <https://doi.org/10.1016/j.tetasy.2006.07.030>

- Muir, D., Savinova, T., Savinov, V., Alexeeva, L., Potelov, V., & Svetochev, V. (2003). Bioaccumulation of PCBs and chlorinated pesticides in seals, fishes and invertebrates from the White Sea, Russia. *Science of The Total Environment*, 306(1), 111–131. [https://doi.org/10.1016/S0048-9697\(02\)00488-6](https://doi.org/10.1016/S0048-9697(02)00488-6)
- Mukherjee, I., & Mittal, A. (2005). Bioremediation of Endosulfan Using *Aspergillus terreus* and *Cladosporium oxysporum*. *Bulletin of Environmental Contamination and Toxicology*, 75(5), 1034–1040. <https://doi.org/10.1007/s00128-005-0853-2>
- Murugan, R., & Mazumdar, S. (2005). Structure and Redox Properties of the Haem Centre in the C357M Mutant of Cytochrome P450cam. *ChemBioChem*, 6(7), 1204–1211. <https://doi.org/10.1002/cbic.200400399>
- Mutter, A. C., Tyryshkin, A. M., Campbell, I. J., Poudel, S., Bennett, G. N., Silberg, J. J., Nanda, V., & Falkowski, P. G. (2019). De novo design of symmetric ferredoxins that shuttle electrons in vivo. *Proceedings of the National Academy of Sciences*, 116(29), 14557–14562. <https://doi.org/10.1073/pnas.1905643116>
- Myers, W. K., Lee, Y.-T., Britt, R. D., & Goodin, D. B. (2013). The Conformation of P450cam in Complex with Putidaredoxin Is Dependent on Oxidation State. *Journal of the American Chemical Society*, 135(32), 11732–11735. <https://doi.org/10.1021/ja405751z>
- Nagano, S., & Poulos, T. L. (2005). Crystallographic Study on the Dioxygen Complex of Wild-type and Mutant Cytochrome P450cam IMPLICATIONS FOR THE DIOXYGEN ACTIVATION MECHANISM. *Journal of Biological Chemistry*, 280(36), 31659–31663. <https://doi.org/10.1074/jbc.M505261200>
- Nagano, S., Tosha, T., Ishimori, K., Morishima, I., & Poulos, T. L. (2004). Crystal Structure of the Cytochrome P450cam Mutant That Exhibits the Same Spectral Perturbations Induced by Putidaredoxin Binding. *Journal of Biological Chemistry*, 279(41), 42844–42849. <https://doi.org/10.1074/jbc.M404217200>
- Nakayama, N., Takemae, A., & Shoun, H. (1996). Cytochrome P450foxy, a Catalytically Self-Sufficient Fatty Acid Hydroxylase of the Fungus *Fusarium oxysporum*. *The Journal of Biochemistry*, 119(3), 435–440.
- Narhi, L. O., & Fulco, A. J. (1986). Characterization of a catalytically self-sufficient 119,000-dalton cytochrome P-450 monooxygenase induced by barbiturates in *Bacillus megaterium*. *Journal of Biological Chemistry*, 261(16), 7160–7169.
- Narhi, L. O., & Fulco, A. J. (1987). Identification and characterization of two functional domains in cytochrome P-450BM-3, a catalytically self-sufficient monooxygenase induced by barbiturates in *Bacillus megaterium*. *Journal of Biological Chemistry*, 262(14), 6683–6690.
- Neilson, E. H., Goodger, J. Q. D., Woodrow, I. E., & Møller, B. L. (2013). Plant chemical defense: At what cost? *Trends in Plant Science*, 18(5), 250–258. <https://doi.org/10.1016/j.tplants.2013.01.001>

- Nelson, D. R. (2018). Cytochrome P450 diversity in the tree of life. *Biochimica et Biophysica Acta (BBA) - Proteins and Proteomics*, 1866(1), 141–154. <https://doi.org/10.1016/j.bbapap.2017.05.003>
- Nelson, D. R., Koymans, L., Kamataki, T., Stegeman, J. J., Feyereisen, R., Waxman, D. J., Waterman, M. R., Gotoh, O., Coon, M. J., Estabrook, R. W., Gunsalus, I. C., & Nebert, D. W. (1996). P450 superfamily: Update on new sequences, gene mapping, accession numbers and nomenclature. [Review]. *Pharmacogenetics*, 6(1), 1–42.
- Nickerson, D. P., Harford-Cross, C. F., Fulcher, S. R., & Wong, L.-L. (1997). The catalytic activity of cytochrome P450cam towards styrene oxidation is increased by site-specific mutagenesis. *FEBS Letters*, 405(2), 153–156. [https://doi.org/10.1016/S0014-5793\(97\)00174-9](https://doi.org/10.1016/S0014-5793(97)00174-9)
- Nishida, C. R., & Ortiz de Montellano, P. R. (2005). Thermophilic cytochrome P450 enzymes. *Biochemical and Biophysical Research Communications*, 338(1), 437–445. <https://doi.org/10.1016/j.bbrc.2005.08.093>
- Nomura, T., Kushiro, T., Yokota, T., Kamiya, Y., Bishop, G. J., & Yamaguchi, S. (2005). The Last Reaction Producing Brassinolide Is Catalyzed by Cytochrome P-450s, CYP85A3 in Tomato and CYP85A2 in Arabidopsis. *Journal of Biological Chemistry*, 280(18), 17873–17879. <https://doi.org/10.1074/jbc.M414592200>
- Nordblom, G. D., White, R. E., & Coon, M. J. (1976). Studies on hydroperoxide-dependent substrate hydroxylation by purified liver microsomal cytochrome P-450. *Archives of Biochemistry and Biophysics*, 175(2), 524–533. [https://doi.org/10.1016/0003-9861\(76\)90541-5](https://doi.org/10.1016/0003-9861(76)90541-5)
- Ogliaro, F., de Visser, S. P., & Shaik, S. (2002). The 'push' effect of the thiolate ligand in cytochrome P450: A theoretical gauging. *Journal of Inorganic Biochemistry*, 91(4), 554–567. [https://doi.org/10.1016/S0162-0134\(02\)00437-3](https://doi.org/10.1016/S0162-0134(02)00437-3)
- Ohashi, M., & Omura, T. (1978). Presence of the NADPH-Cytochrome P-450 Reductase System in Liver and Kidney Mitochondria. *The Journal of Biochemistry*, 83(1), 249–260. <https://doi.org/10.1093/oxfordjournals.jbchem.a131898>
- Oku, Y., Ohtaki, A., Kamitori, S., Nakamura, N., Yohda, M., Ohno, H., & Kawarabayasi, Y. (2004). Structure and direct electrochemistry of cytochrome P450 from the thermoacidophilic crenarchaeon, *Sulfolobus tokodaii* strain 7. *Journal of Inorganic Biochemistry*, 98(7), 1194–1199. <https://doi.org/10.1016/j.jinorgbio.2004.05.002>
- Omura, T., Sanders, E., Estabrook, R. W., Cooper, D. Y., & Rosenthal, O. (1966). Isolation from adrenal cortex of a nonheme iron protein and a flavoprotein functional as a reduced triphosphopyridine nucleotide-cytochrome P-450 reductase. *Archives of Biochemistry and Biophysics*, 117(3), 660–673. [https://doi.org/10.1016/0003-9861\(66\)90108-1](https://doi.org/10.1016/0003-9861(66)90108-1)

- Omura, Tsuneo, & Gotoh, O. (2017). Evolutionary origin of mitochondrial cytochrome P450. *The Journal of Biochemistry*, 161(5), 399–407. <https://doi.org/10.1093/jb/mvx011>
- Omura, Tsuneo, & Sato, R. (1962). A New Cytochrome in Liver Microsomes. *Journal of Biological Chemistry*, 237(4), PC1375–PC1376.
- Omura, Tsuneo, & Sato, R. (1964). The Carbon Monoxide-binding Pigment of Liver Microsomes II. SOLUBILIZATION, PURIFICATION, AND PROPERTIES. *Journal of Biological Chemistry*, 239(7), 2379–2385.
- Ortiz de Montellano, P. R. O. (2015). *Cytochrome P450* (P. R. Ortiz de Montellano, Ed.; 4th ed.). Springer International Publishing. <https://doi.org/10.1007/978-3-319-12108-6>
- Ost, T. W. B., Clark, J., Mowat, C. G., Miles, C. S., Walkinshaw, M. D., Reid, G. A., Chapman, S. K., & Daff, S. (2003). Oxygen Activation and Electron Transfer in Flavocytochrome P450 BM3. *Journal of the American Chemical Society*, 125(49), 15010–15020. <https://doi.org/10.1021/ja035731o>
- Packer, M. S., & Liu, D. R. (2015). Methods for the directed evolution of proteins. *Nature Reviews Genetics*, 16(7), 379–394. <https://doi.org/10.1038/nrg3927>
- Park, S.-Y., Yamane, K., Adachi, S., Shiro, Y., Weiss, K. E., Maves, S. A., & Sligar, S. G. (2002). Thermophilic cytochrome P450 (CYP119) from *Sulfolobus solfataricus*: High resolution structure and functional properties. *Journal of Inorganic Biochemistry*, 91(4), 491–501. [https://doi.org/10.1016/S0162-0134\(02\)00446-4](https://doi.org/10.1016/S0162-0134(02)00446-4)
- Parks Canada Agency, G. of C. (2017, September 20). *Natural Heritage—Mountain Pine Beetle—Home*. <https://www.pc.gc.ca/en/docs/v-g/dpp-mpb/index>
- Paulsen, M. D., Filipovic, D., Sligar, S. G., & Ornstein, R. L. (1993). Controlling the regioselectivity and coupling of cytochrome P450cam: T185F mutant increases coupling and abolishes 3-hydroxynorcamphor product. *Protein Science: A Publication of the Protein Society*, 2(3), 357–365.
- Phillips, M. A., & Croteau, R. B. (1999). Resin-based defenses in conifers. *Trends in Plant Science*, 4(5), 184–190. [https://doi.org/10.1016/S1360-1385\(99\)01401-6](https://doi.org/10.1016/S1360-1385(99)01401-6)
- Pikuleva, I. A. (2006). Cytochrome P450s and cholesterol homeostasis. *Pharmacology & Therapeutics*, 112(3), 761–773. <https://doi.org/10.1016/j.pharmthera.2006.05.014>
- Pitman, G. B., Vité, J. P., Kinzer, G. W., & Fentiman, A. F. (1968). Bark Beetle Attractants: Trans-verbenol isolated from *Dendroctonus*. *Nature*, 218(5137), 168–169. <https://doi.org/10.1038/218168a0>

- Pochapsky, S. S., Pochapsky, T. C., & Wei, J. W. (2003). A Model for Effector Activity in a Highly Specific Biological Electron Transfer Complex: The Cytochrome P450cam–Putidaredoxin Couple,. *Biochemistry*, *42*(19), 5649–5656. <https://doi.org/10.1021/bi034263s>
- Pochapsky, T. C., Kostic, M., Jain, N., & Pejchal, R. (2001). Redox-Dependent Conformational Selection in a Cys4Fe2S2 Ferredoxin. *Biochemistry*, *40*(19), 5602–5614. <https://doi.org/10.1021/bi0028845>
- Pochapsky, T. C., & Pochapsky, S. S. (2019). What Your Crystal Structure Will Not Tell You about Enzyme Function. *Accounts of Chemical Research*, *52*(5), 1409–1418. <https://doi.org/10.1021/acs.accounts.9b00066>
- Porter, T. D., & Kasper, C. B. (1986). NADPH-cytochrome P-450 oxidoreductase: Flavin mononucleotide and flavin adenine dinucleotide domains evolved from different flavoproteins. *Biochemistry*, *25*(7), 1682–1687. <https://doi.org/10.1021/bi00355a036>
- Poulos, T. L., Finzel, B. C., Gunsalus, I. C., Wagner, G. C., & Kraut, J. (1985). The 2.6-Å crystal structure of *Pseudomonas putida* cytochrome P-450. *Journal of Biological Chemistry*, *260*(30), 16122–16130.
- Poulos, T. L., Perez, M., & Wagner, G. C. (1982). Preliminary crystallographic data on cytochrome P-450CAM. *Journal of Biological Chemistry*, *257*(17), 10427–10429.
- Poulos, Thomas L. (2005). Structural biology of heme monooxygenases. *Biochemical and Biophysical Research Communications*, *338*(1), 337–345. <https://doi.org/10.1016/j.bbrc.2005.07.204>
- Poulos, Thomas L. (2014). Heme Enzyme Structure and Function. *Chemical Reviews*, *114*(7), 3919–3962. <https://doi.org/10.1021/cr400415k>
- Pozo, K., Harner, T., Shoeib, M., Urrutia, R., Barra, R., Parra, O., & Focardi, S. (2004). Passive-Sampler Derived Air Concentrations of Persistent Organic Pollutants on a North–South Transect in Chile. *Environmental Science & Technology*, *38*(24), 6529–6537. <https://doi.org/10.1021/es049065i>
- Pozo, K., Harner, T., Wania, F., Muir, D. C. G., Jones, K. C., & Barrie, L. A. (2006). Toward a Global Network for Persistent Organic Pollutants in Air: Results from the GAPS Study. *Environmental Science & Technology*, *40*(16), 4867–4873. <https://doi.org/10.1021/es060447t>
- Prasad, B. (2013). *The borneol cycle of cytochrome P450cam and evolution of the enzyme for new applications* [Thesis, Science: Department of Chemistry]. <https://summit.sfu.ca/item/12967>

- Prasad, B., Rojubbally, A., & Plettner, E. (2011). Identification of Camphor Oxidation and Reduction Products in *Pseudomonas putida*: New Activity of the Cytochrome P450cam System. *Journal of Chemical Ecology*, 37(6), 657–667. <https://doi.org/10.1007/s10886-011-9959-7>
- Primo, C. D., Sligar, S. G., Hoa, G. H. B., & Douzou, P. (1992). A critical role of protein-bound water in the catalytic cycle of cytochrome P-450 camphor. *FEBS Letters*, 312(2–3), 252–254. [https://doi.org/10.1016/0014-5793\(92\)80946-E](https://doi.org/10.1016/0014-5793(92)80946-E)
- Progar, R. A., Gillette, N., Fettig, C. J., & Hrinkevich, K. (2014). Applied Chemical Ecology of the Mountain Pine Beetle. *Forest Science*, 60(3), 414–433. <https://doi.org/10.5849/forsci.13-010>
- Puchkaev, A. V., & Ortiz de Montellano, P. R. (2005). The *Sulfolobus solfataricus* electron donor partners of thermophilic CYP119: An unusual non-NAD(P)H-dependent cytochrome P450 system. *Archives of Biochemistry and Biophysics*, 434(1), 169–177. <https://doi.org/10.1016/j.abb.2004.10.022>
- Queiroga, C. L., Ferracini, V. L., & Marsaioli, A. J. (1996). Three new oxygenated cadinanes from *Baccharis* species. *Phytochemistry*, 42(4), 1097–1103. [https://doi.org/10.1016/0031-9422\(95\)00977-9](https://doi.org/10.1016/0031-9422(95)00977-9)
- Rabe, K. S., Kiko, K., & Niemeyer, C. M. (2008). Characterization of the Peroxidase Activity of CYP119, a Thermostable P450 From *Sulfolobus acidocaldarius*. *ChemBioChem*, 9(3), 420–425. <https://doi.org/10.1002/cbic.200700450>
- Raucy, J. L., & Allen, S. W. (2001). Recent advances in P450 research. *The Pharmacogenomics Journal*, 1(3), 178–186. <https://doi.org/10.1038/sj.tpj.6500044>
- Ravichandran, K. G., Boddupalli, S. S., Hasermann, C. A., Peterson, J. A., & Deisenhofer, J. (1993). Crystal structure of hemoprotein domain of P450BM-3, a prototype for microsomal P450's. *Science*, 261(5122), 731–736. <https://doi.org/10.1126/science.8342039>
- Reed, N. R., & Koshlukova, S. (2014). Heptachlor. In P. Wexler (Ed.), *Encyclopedia of Toxicology (Third Edition)* (pp. 840–844). Academic Press. <https://doi.org/10.1016/B978-0-12-386454-3.00149-4>
- Rendic, S., & Guengerich, F. P. (2015). Survey of Human Oxidoreductases and Cytochrome P450 Enzymes Involved in the Metabolism of Xenobiotic and Natural Chemicals. *Chemical Research in Toxicology*, 28(1), 38–42. <https://doi.org/10.1021/tx500444e>
- Renwick, J. A., Hughes, P. R., & Krull, I. S. (1976). Selective production of cis- and trans-verbenol from (-)- and (+)-alpha by a bark beetle. *Science*, 191(4223), 199–201. <https://doi.org/10.1126/science.1246609>

- Rittle, J., & Green, M. T. (2010). Cytochrome P450 Compound I: Capture, Characterization, and C-H Bond Activation Kinetics. *Science*, 330(6006), 933–937. <https://doi.org/10.1126/science.1193478>
- Roberts, G. A., Çelik, A., Hunter, D. J. B., Ost, T. W. B., White, J. H., Chapman, S. K., Turner, N. J., & Flitsch, S. L. (2003). A Self-sufficient Cytochrome P450 with a Primary Structural Organization That Includes a Flavin Domain and a [2Fe-2S] Redox Center. *Journal of Biological Chemistry*, 278(49), 48914–48920. <https://doi.org/10.1074/jbc.M309630200>
- Roberts, G. A., Grogan, G., Greter, A., Flitsch, S. L., & Turner, N. J. (2002). Identification of a New Class of Cytochrome P450 from a Rhodococcus sp. *Journal of Bacteriology*, 184(14), 3898–3908. <https://doi.org/10.1128/JB.184.14.3898-3908.2002>
- Roberts, K., & Jones, J. (2010). Anilinic N-Oxides Support Cytochrome P450-Mediated N-Dealkylation through Hydrogen-Atom Transfer. *Chemistry*, 16(27), 8096–8107. <https://doi.org/10.1002/chem.201000185>
- Ruettinger, R. T., & Fulco, A. J. (1981). Epoxidation of unsaturated fatty acids by a soluble cytochrome P-450-dependent system from *Bacillus megaterium*. *Journal of Biological Chemistry*, 256(11), 5728–5734.
- Ruff, A. J., Kardashliev, T., Dennig, A., & Schwaneberg, U. (2014). The Sequence Saturation Mutagenesis (SeSaM) Method. In E. M. J. Gillam, J. N. Copp, & D. Ackerley (Eds.), *Directed Evolution Library Creation: Methods and Protocols* (pp. 45–68). Springer. https://doi.org/10.1007/978-1-4939-1053-3_4
- Rylott, E. L., Jackson, R. G., Edwards, J., Womack, G. L., Seth-Smith, H. M., Rathbone, D. A., Strand, S. E., & Bruce, N. C. (2006). An explosive-degrading cytochrome P450 activity and its targeted application for the phytoremediation of RDX. *Nature Biotechnology*, 24(2), 216–219. <https://doi.org/10.1038/nbt1184>
- Safranyik, L., Carroll, A. L., Régnière, J., Langor, D. W., Riel, W. G., Shore, T. L., Peter, B., Cooke, B. J., Nealis, V. G., & Taylor, S. W. (2010). Potential for Range Expansion of Mountain Pine Beetle into the Boreal Forest of North America. *The Canadian Entomologist*, 142(5), 415–442. <https://doi.org/10.4039/n08-CPA01>
- Saiyed, H., Dewan, A., Bhatnagar, V., Shenoy, U., Shenoy, R., Rajmohan, H., Patel, K., Kashyap, R., Kulkarni, P., Rajan, B., & Lakkad, B. (2003). Effect of endosulfan on male reproductive development. *Environmental Health Perspectives*, 111(16), 1958–1962. <https://doi.org/10.1289/ehp.6271>
- Sandstrom, P., Ginzel, M. D., Bearfield, J. C., Welch, W. H., Blomquist, G. J., & Tittiger, C. (2008). Myrcene Hydroxylases do not Determine Enantiomeric Composition of Pheromonal Ipsdienol in *Ips* spp. *Journal of Chemical Ecology*, 34(12), 1584–1592. <https://doi.org/10.1007/s10886-008-9563-7>

- Sandstrom, P., Welch, W. H., Blomquist, G. J., & Tittiger, C. (2006). Functional expression of a bark beetle cytochrome P450 that hydroxylates myrcene to ipsdienol. *Insect Biochemistry and Molecular Biology*, 36(11), 835–845. <https://doi.org/10.1016/j.ibmb.2006.08.004>
- Sauer, A. M., Crowe, W. E., Henderson, G., & Laine, R. a. (2009). An efficient and economic asymmetric synthesis of (+)-nootkatone, tetrahydronootkatone, and derivatives. *Organic Letters*, 11(16), 3530–3533. <https://doi.org/10.1021/ol8023709>
- Sauveplane, V., Kandel, S., Kastner, P.-E., Ehlting, J., Compagnon, V., Werck-Reichhart, D., & Pinot, F. (2009). Arabidopsis thaliana CYP77A4 is the first cytochrome P450 able to catalyze the epoxidation of free fatty acids in plants. *The FEBS Journal*, 276(3), 719–735. <https://doi.org/10.1111/j.1742-4658.2008.06819.x>
- Sawada, N., Sakaki, T., Yoneda, S., Kusudo, T., Shinkyo, R., Ohta, M., & Inouye, K. (2004). Conversion of vitamin D3 to $1\alpha,25$ -dihydroxyvitamin D3 by *Streptomyces griseolus* cytochrome P450SU-1. *Biochemical and Biophysical Research Communications*, 320(1), 156–164. <https://doi.org/10.1016/j.bbrc.2004.05.140>
- Schiffler, B., & Bernhardt, R. (2003). Bacterial (CYP101) and mitochondrial P450 systems—How comparable are they? *Biochemical and Biophysical Research Communications*, 312(1), 223–228. <https://doi.org/10.1016/j.bbrc.2003.09.214>
- Schlichting, I., Berendzen, J., Chu, K., Stock, A. M., Maves, S. A., Benson, D. E., Sweet, R. M., Ringe, D., Petsko, G. A., & Sligar, S. G. (2000). The Catalytic Pathway of Cytochrome P450cam at Atomic Resolution. *Science*, 287(5458), 1615–1622. <https://doi.org/10.1126/science.287.5458.1615>
- Schlichting, I., Jung, C., & Schulze, H. (1997). Crystal structure of cytochrome P-450cam complexed with the (1S)-camphor enantiomer. *FEBS Letters*, 415(3), 253–257. [https://doi.org/10.1016/S0014-5793\(97\)01135-6](https://doi.org/10.1016/S0014-5793(97)01135-6)
- Schmidt, J. O. (1999). Attractant or Pheromone: The Case of Nasonov Secretion and Honeybee Swarms. *Journal of Chemical Ecology*, 25(9), 2051–2056. <https://doi.org/10.1023/A:1021084706241>
- Schmidt, W. F., Bilboulia, S., Rice, C. P., Fetting, J. C., McConnell, L. L., & Hapeman, C. J. (2001). Thermodynamic, Spectroscopic, and Computational Evidence for the Irreversible Conversion of β - to α -Endosulfan. *Journal of Agricultural and Food Chemistry*, 49(11), 5372–5376. <https://doi.org/10.1021/jf0102214>
- Schmidt, W. F., Hapeman, C. J., Fetting, J. C., Rice, C. P., & Bilboulia, S. (1997). Structure and Asymmetry in the Isomeric Conversion of β - to α -Endosulfan. *Journal of Agricultural and Food Chemistry*, 45(4), 1023–1026. <https://doi.org/10.1021/jf970020t>

- Schuler, M. A. (2015). P450s in Plants, Insects, and Their Fungal Pathogens. In P. R. Ortiz de Montellano (Ed.), *Cytochrome P450: Structure, Mechanism, and Biochemistry* (pp. 409–449). Springer International Publishing. https://doi.org/10.1007/978-3-319-12108-6_7
- Schuler, M. A., & Werck-Reichhart, D. (2003). Functional Genomics of P450s. *Annual Review of Plant Biology*, 54(1), 629–667. <https://doi.org/10.1146/annurev.arplant.54.031902.134840>
- Scippo, M.-L., Argiris, C., Van De Weerd, C., Muller, M., Willemsen, P., Martial, J., & Maghuin-Rogister, G. (2004). Recombinant human estrogen, androgen and progesterone receptors for detection of potential endocrine disruptors. *Analytical and Bioanalytical Chemistry*, 378(3), 664–669. <https://doi.org/10.1007/s00216-003-2251-0>
- Seth-Smith, H. M. B., Rosser, S. J., Basran, A., Travis, E. R., Dabbs, E. R., Nicklin, S., & Bruce, N. C. (2002). Cloning, Sequencing, and Characterization of the Hexahydro-1,3,5-Trinitro-1,3,5-Triazine Degradation Gene Cluster from *Rhodococcus rhodochrous*. *Applied and Environmental Microbiology*, 68(10), 4764–4771. <https://doi.org/10.1128/AEM.68.10.4764-4771.2002>
- Sevrioukova, I. F., Garcia, C., Li, H., Bhaskar, B., & Poulos, T. L. (2003). Crystal Structure of Putidaredoxin, the [2Fe–2S] Component of the P450cam Monooxygenase System from *Pseudomonas putida*. *Journal of Molecular Biology*, 333(2), 377–392. <https://doi.org/10.1016/j.jmb.2003.08.028>
- Sevrioukova, I. F., Li, H., & Poulos, T. L. (2004). Crystal Structure of Putidaredoxin Reductase from *Pseudomonas putida*, the Final Structural Component of the Cytochrome P450cam Monooxygenase. *Journal of Molecular Biology*, 336(4), 889–902. <https://doi.org/10.1016/j.jmb.2003.12.067>
- Seybold, S. J., Quilici, D. R., Tillman, J. A., Vanderwel, D., Wood, D. L., & Blomquist, G. J. (1995). De novo biosynthesis of the aggregation pheromone components ipsenol and ipsdienol by the pine bark beetles *Ips paraconfusus* Lanier and *Ips pini* (Say) (Coleoptera: Scolytidae). *Proceedings of the National Academy of Sciences of the United States of America*, 92(18), 8393–8397.
- Shang, Y., & Huang, S. (2020). Engineering Plant Cytochrome P450s for Enhanced Synthesis of Natural Products: Past Achievements and Future Perspectives. *Plant Communications*, 1(1), 100012. <https://doi.org/10.1016/j.xplc.2019.100012>
- Shen, L., & Wania, F. (2005). Compilation, Evaluation, and Selection of Physical–Chemical Property Data for Organochlorine Pesticides. *Journal of Chemical & Engineering Data*, 50(3), 742–768. <https://doi.org/10.1021/jc049693f>
- Shen, L., Wania, F., Lei, Y. D., Teixeira, C., Muir, D. C. G., & Bidleman, T. F. (2005). Atmospheric Distribution and Long-Range Transport Behavior of Organochlorine Pesticides in North America. *Environmental Science & Technology*, 39(2), 409–420. <https://doi.org/10.1021/es049489c>

- Shibata, Y., Matsui, K., Kajiwara, T., & Hatanaka, A. (1995). Fatty Acid Hydroperoxide Lyase Is a Heme Protein. *Biochemical and Biophysical Research Communications*, 207(1), 438–443. <https://doi.org/10.1006/bbrc.1995.1207>
- Sibbesen, O., Zhang, Z., & Ortiz de Montellano, P. R. (1998). Cytochrome P450cam Substrate Specificity: Relationship between Structure and Catalytic Oxidation of Alkylbenzenes. *Archives of Biochemistry and Biophysics*, 353(2), 285–296. <https://doi.org/10.1006/abbi.1998.0632>
- Siddique, T., Okeke, B. C., Arshad, M., & Frankenberger, W. T. (2003). Enrichment and Isolation of Endosulfan-Degrading Microorganisms. *Journal of Environmental Quality*, 32(1), 47–54. <https://doi.org/10.2134/jeq2003.4700>
- Sigel, A., Sigel, H., & Sigel, R. K. O. (2007). *The ubiquitous roles of cytochrome P450 proteins / edited by Astrid Sigel, Helmut Sigel, and Roland K.O. Sigel*. John Wiley.
- Sligar, S. G. (1976). Coupling of spin, substrate, and redox equilibria in cytochrome P450. *Biochemistry*, 15(24), 5399–5406. <https://doi.org/10.1021/bi00669a029>
- Sligar, S. G. (2010). Glimpsing the Critical Intermediate in Cytochrome P450 Oxidations. *Science*, 330(6006), 924–925. <https://doi.org/10.1126/science.1197881>
- Smith, J. R. L., & Mortimer, D. N. (1985). Oxidative N-dealkylation of N,N-dimethylbenzylamines by metalloporphyrin-catalysed model systems for cytochrome P450 mono-oxygenases. *Journal of the Chemical Society, Chemical Communications*, 2, 64–65. <https://doi.org/10.1039/C39850000064>
- Soffer, M. D., & Jevnik, M. A. (1955a). SYNTHESIS The Synthesis of dl-Cryptone. *Journal of the American Chemical Society*, 77(3), 1003–1005.
- Soffer, M. D., & Jevnik, M. A. (1955b). SYNTHESIS The Synthesis of dl-Cryptone. *Journal of the American Chemical Society*, 77(3), 1003–1005.
- Song, M., Delaplain, P., Nguyen, T. T., Liu, X., Wickenberg, L., Jeffrey, C., Blomquist, G. J., & Tittiger, C. (2014). Exo-Brevicommin biosynthetic pathway enzymes from the Mountain Pine Beetle, *Dendroctonus ponderosae*. *Insect Biochemistry and Molecular Biology*, 53, 73–80. <https://doi.org/10.1016/j.ibmb.2014.08.002>
- Sono, M., Andersson, L. A., & Dawson, J. H. (1982). Sulfur donor ligand binding to ferric cytochrome P-450-CAM and myoglobin. Ultraviolet-visible absorption, magnetic circular dichroism, and electron paramagnetic resonance spectroscopic investigation of the complexes. *Journal of Biological Chemistry*, 257(14), 8308–8320.
- Sono, Masanori, Roach, M. P., Coulter, E. D., & Dawson, J. H. (1996). Heme-Containing Oxygenases. *Chemical Reviews*, 96(7), 2841–2888. <https://doi.org/10.1021/cr9500500>

- Sowden, R. J., Yasmin, S., Rees, N. H., Bell, S. G., & Wong, L.-L. (2005). Biotransformation of the sesquiterpene (+)-valencene by cytochrome P450cam and P450BM-3. *Organic & Biomolecular Chemistry*, 3(1), 57–64. <https://doi.org/10.1039/B413068E>
- Spolitak, T., Dawson, J. H., & Ballou, D. P. (2006). Rapid kinetics investigations of peracid oxidation of ferric cytochrome P450cam: Nature and possible function of compound ES. *Journal of Inorganic Biochemistry*, 100(12), 2034–2044. <https://doi.org/10.1016/j.jinorgbio.2006.09.026>
- Stanley, J., Sah, K., Jain, S. K., Bhatt, J. C., & Sushil, S. N. (2015). Evaluation of pesticide toxicity at their field recommended doses to honeybees, *Apis cerana* and *A. mellifera* through laboratory, semi-field and field studies. *Chemosphere*, 119, 668–674. <https://doi.org/10.1016/j.chemosphere.2014.07.039>
- Stevens, J. L., Snyder, M. J., Koener, J. F., & Feyereisen, R. (2000). Inducible P450s of the CYP9 family from larval *Manduca sexta* midgut. *Insect Biochemistry and Molecular Biology*, 30(7), 559–568. [https://doi.org/10.1016/S0965-1748\(00\)00024-2](https://doi.org/10.1016/S0965-1748(00)00024-2)
- Stevenson, J.-A., Bearpark, J. K., & Wong, L.-L. (1998). Engineering molecular recognition in alkane oxidation catalysed by cytochrome P450cam. *New Journal of Chemistry*, 22(6), 551–552. <https://doi.org/10.1039/A801637B>
- Stockholm Convention. (2011). *United Nations targets widely-used pesticide endosulfan for phase out*. <http://chm.pops.int/Implementation/PublicAwareness/PressReleases/COP5Geneva,3May2011Endosulfanphaseout/tabid/2216/Default.aspx>
- Stok, J. E., Hall, E. A., Stone, I. S. J., Noble, M. C., Wong, S. H., Bell, S. G., & De Voss, J. J. (2016). In vivo and in vitro hydroxylation of cineole and camphor by cytochromes P450CYP101A1, CYP101B1 and N242A CYP176A1. *Journal of Molecular Catalysis B: Enzymatic*, 128, 52–64. <https://doi.org/10.1016/j.molcatb.2016.03.004>
- Sutherland, T. D., Unnithan, G. C., & Feyereisen, R. (2000). Terpenoid ω -hydroxylase (CYP4C7) messenger RNA levels in the corpora allata: A marker for ovarian control of juvenile hormone synthesis in *Diploptera punctata*. *Journal of Insect Physiology*, 46(8), 1219–1227. [https://doi.org/10.1016/S0022-1910\(00\)00042-1](https://doi.org/10.1016/S0022-1910(00)00042-1)
- Sutherland, T., Horne, I., Harcourt, R. L., Russell, R. J., & Oakeshott, J. G. (2002). Isolation and characterization of a Mycobacterium strain that metabolizes the insecticide endosulfan. *Journal of Applied Microbiology*, 93(3), 380–389. <https://doi.org/10.1046/j.1365-2672.2002.01728.x>
- Sutherland, T., Horne, I., Lacey, M. J., Harcourt, R. L., Russell, R. J., & Oakeshott, J. G. (2000). Enrichment of an Endosulfan-Degrading Mixed Bacterial Culture. *Applied and Environmental Microbiology*, 66(7), 2822–2828.

- Sutherland, T., Horne, I., Russell, R. J., & Oakeshott, J. G. (2002). Gene Cloning and Molecular Characterization of a Two-Enzyme System Catalyzing the Oxidative Detoxification of β -Endosulfan. *Applied and Environmental Microbiology*, 68(12), 6237–6245. <https://doi.org/10.1128/AEM.68.12.6237-6245.2002>
- Sutherland, T., Weir, K. M., Lacey, M. J., Horne, I., Russell, R. J., & Oakeshott, J. G. (2002). Enrichment of a microbial culture capable of degrading endosulphate, the toxic metabolite of endosulfan. *Journal of Applied Microbiology*, 92(3), 541–548. <https://doi.org/10.1046/j.1365-2672.2002.01559.x>
- Sverko, E., Tomy, G. T., Reiner, E. J., Li, Y.-F., McCarry, B. E., Arnot, J. A., Law, R. J., & Hites, R. A. (2011). Dieldrin Plus and Related Compounds in the Environment: A Review. *Environmental Science & Technology*, 45(12), 5088–5098. <https://doi.org/10.1021/es2003028>
- Szuppa, T., Stolle, A., Ondruschka, B., & Hopfe, W. (2010). An alternative solvent-free synthesis of nopinone under ball-milling conditions: Investigation of reaction parameters. *ChemSusChem*, 3(10), 1181–1191. <https://doi.org/10.1002/cssc.201000122>
- Takaya, N., Suzuki, S., Kuwazaki, S., Shoun, H., Maruo, F., Yamaguchi, M., & Takeo, K. (1999). Cytochrome P450nor, a Novel Class of Mitochondrial Cytochrome P450 Involved in Nitrate Respiration in the Fungus *Fusarium oxysporum*. *Archives of Biochemistry and Biophysics*, 372(2), 340–346. <https://doi.org/10.1006/abbi.1999.1499>
- Taylor, M., Lamb, D. C., Cannell, R., Dawson, M., & Kelly, S. L. (1999). Cytochrome P450105D1 (CYP105D1) from *Streptomyces griseus*: Heterologous Expression, Activity, and Activation Effects of Multiple Xenobiotics. *Biochemical and Biophysical Research Communications*, 263(3), 838–842. <https://doi.org/10.1006/bbrc.1999.1427>
- Teklu, B. M., Retta, N., & Van den Brink, P. J. (2016). Sensitivity of Ethiopian aquatic macroinvertebrates to the pesticides endosulfan and diazinon, compared to literature data. *Ecotoxicology*, 25(6), 1226–1233. <https://doi.org/10.1007/s10646-016-1676-0>
- Tosha, T., Yoshioka, S., Ishimori, K., & Morishima, I. (2004). L358P Mutation on Cytochrome P450cam Simulates Structural Changes upon Putidaredoxin Binding THE STRUCTURAL CHANGES TRIGGER ELECTRON TRANSFER TO OXY-P450CAM FROM ELECTRON DONORS. *Journal of Biological Chemistry*, 279(41), 42836–42843. <https://doi.org/10.1074/jbc.M404216200>
- Tosha, T., Yoshioka, S., Takahashi, S., Ishimori, K., Shimada, H., & Morishima, I. (2003). NMR Study on the Structural Changes of Cytochrome P450cam upon the Complex Formation with Putidaredoxin FUNCTIONAL SIGNIFICANCE OF THE PUTIDAREDOXIN-INDUCED STRUCTURAL CHANGES. *Journal of Biological Chemistry*, 278(41), 39809–39821. <https://doi.org/10.1074/jbc.M304265200>

- Tripathi, S., Li, H., & Poulos, T. L. (2013). Structural Basis for Effector Control and Redox Partner Recognition in Cytochrome P450. *Science*, *340*(6137), 1227–1230. <https://doi.org/10.1126/science.1235797>
- Tyson, C. A., Lipscomb, J. D., & Gunsalus, I. C. (1972). The Roles of Putidaredoxin and P450cam in Methylene Hydroxylation. *Journal of Biological Chemistry*, *247*(18), 5777–5784.
- Ullah, A. J., Murray, R. I., Bhattacharyya, P. K., Wagner, G. C., & Gunsalus, I. C. (1990). Protein components of a cytochrome P-450 linalool 8-methyl hydroxylase. *Journal of Biological Chemistry*, *265*(3), 1345–1351.
- Unno, M., Christian, J. F., Benson, D. E., Gerber, N. C., Sligar, S. G., & Champion, P. M. (1997). Resonance Raman Investigations of Cytochrome P450cam Complexed with Putidaredoxin. *Journal of the American Chemical Society*, *119*(28), 6614–6620. <https://doi.org/10.1021/ja963785a>
- Unno, M., Shimada, H., Toba, Y., Makino, R., & Ishimura, Y. (1996). Role of Arg112 of Cytochrome P450cam in the Electron Transfer from Reduced Putidaredoxin ANALYSES WITH SITE-DIRECTED MUTANTS. *Journal of Biological Chemistry*, *271*(30), 17869–17874. <https://doi.org/10.1074/jbc.271.30.17869>
- Valterová, I., Unelius, C. R., Vrkoč, J., & Norin, T. (1992). Enantiomeric composition of monoterpene hydrocarbons from the liverwort *Conocephalum conicum*. *Phytochemistry*, *31*(9), 3121–3123. [http://dx.doi.org/10.1016/0031-9422\(92\)83457-A](http://dx.doi.org/10.1016/0031-9422(92)83457-A)
- Vandemeulebroucke, A., Aldag, C., Stiebritz, M. T., Reiher, M., & Hilvert, D. (2015). Kinetic Consequences of Introducing a Proximal Selenocysteine Ligand into Cytochrome P450cam. *Biochemistry*, *54*(44), 6692–6703. <https://doi.org/10.1021/acs.biochem.5b00939>
- Vidakovic, M., Sligar, S. G., Li, H., & Poulos, T. L. (1998). Understanding the Role of the Essential Asp251 in Cytochrome P450cam Using Site-Directed Mutagenesis, Crystallography, and Kinetic Solvent Isotope Effect. *Biochemistry*, *37*(26), 9211–9219. <https://doi.org/10.1021/bi980189f>
- Vijayan, V. A., Sathish Kumar, B. Y., Ganesh, K. N., Urmila, J., Fakoorziba, M. R., & Makkapati, A. K. (2007). Efficacy of piperonyl butoxide (PBO) as a synergist with deltamethrin on five species of mosquitoes. *Journal of Communicable Diseases*, *39*(3), 159–163.
- Vojinović, V., Azevedo, A. M., Martins, V. C. B., Cabral, J. M. S., Gibson, T. D., & Fonseca, L. P. (2004). Assay of H₂O₂ by HRP catalysed co-oxidation of phenol-4-sulphonic acid and 4-aminoantipyrine: Characterisation and optimisation. *Journal of Molecular Catalysis B: Enzymatic*, *28*(2), 129–135. <https://doi.org/10.1016/j.molcatb.2004.02.003>

- Volkamer, A., Griewel, A., Grombacher, T., & Rarey, M. (2010). Analyzing the Topology of Active Sites: On the Prediction of Pockets and Subpockets. *Journal of Chemical Information and Modeling*, 50(11), 2041–2052. <https://doi.org/10.1021/ci100241y>
- Wackett, L. P. (1995). Recruitment of Co-Metabolic Enzymes for Environmental Detoxification of Organohalides. *Environmental Health Perspectives*, 103, 45. <https://doi.org/10.2307/3432478>
- Wackett, L. P. (1998). Directed Evolution of New Enzymes and Pathways for Environmental Biocatalysis. *Annals of the New York Academy of Sciences*, 864(1), 142–152. <https://doi.org/10.1111/j.1749-6632.1998.tb10297.x>
- Wackett, L. P., Sadowsky, M. J., Newman, L. M., Hur, H.-G., & Li, S. (1994). Metabolism of polyhalogenated compounds by a genetically engineered bacterium. *Nature*, 368(6472), 627–629. <https://doi.org/10.1038/368627a0>
- Walse, S. S., Scott, G. I., & Ferry, J. L. (2003). Stereoselective degradation of aqueous endosulfan in modular estuarine mesocosms: Formation of endosulfan γ -hydroxycarboxylate. *Journal of Environmental Monitoring*, 5(3), 373–379. <https://doi.org/10.1039/B212165D>
- Walsh, M. E., Kyritsis, P., Eady, N. A. J., Allen, H., Hill, O., & Luet-Lok Wong. (2000). Catalytic reductive dehalogenation of hexachloroethane by molecular variants of cytochrome P450[subcam] (CYP101). *European Journal of Biochemistry*, 267(18), 5815. <https://doi.org/10.1046/j.1432-1327.2000.01666.x>
- WAN, M. T., KUO, J.-N., McPHERSON, B., & PASTERNAK, J. (2006). Agricultural Pesticide Residues in Farm Ditches of the Lower Fraser Valley, British Columbia, Canada. *Journal of Environmental Science and Health, Part B*, 41(5), 647–669. <https://doi.org/10.1080/03601230600701817>
- Wang, B., Li, C., Dubey, K. D., & Shaik, S. (2015). Quantum Mechanical/Molecular Mechanical Calculated Reactivity Networks Reveal How Cytochrome P450cam and Its T252A Mutant Select Their Oxidation Pathways. *Journal of the American Chemical Society*, 137(23), 7379–7390. <https://doi.org/10.1021/jacs.5b02800>
- Wang, D., Zheng, J., Shaik, S., & Thiel, W. (2008). Quantum and Molecular Mechanical Study of the First Proton Transfer in the Catalytic Cycle of Cytochrome P450cam and Its Mutant D251N. *The Journal of Physical Chemistry B*, 112(16), 5126–5138. <https://doi.org/10.1021/jp074958t>
- Wang, J., Ilie, A., & Reetz, M. T. (2017). Chemo- and Stereoselective Cytochrome P450-BM3-Catalyzed Sulfoxidation of 1-Thiochroman-4-ones Enabled by Directed Evolution. *Advanced Synthesis & Catalysis*, 359(12), 2056–2060. <https://doi.org/10.1002/adsc.201700414>

- Watanabe, Y., Iyanagi, T., & Oae, S. (1982). One electron transfer mechanism in the enzymatic oxygenation of sulfoxide to sulfone promoted by a reconstituted system with purified cytochrome p-450. *Tetrahedron Letters*, 23(5), 533–536. [https://doi.org/10.1016/S0040-4039\(00\)86881-1](https://doi.org/10.1016/S0040-4039(00)86881-1)
- Watanabe, Y., Oae, S., & Iyanagi, T. (1982). Mechanisms of Enzymatic S-Oxygenation of Thioanisole Derivatives and O-Demethylation of Anisole Derivatives Promoted by Both Microsomes and a Reconstituted System with Purified Cytochrome P-450. *Bulletin of the Chemical Society of Japan*, 55(1), 188–195. <https://doi.org/10.1246/bcsj.55.188>
- Weber, J., Halsall, C. J., Muir, D. C. G., Teixeira, C., Burniston, D. A., Strachan, W. M. J., Hung, H., Mackay, N., Arnold, D., & Kylin, H. (2006). Endosulfan and γ -HCH in the Arctic: An Assessment of Surface Seawater Concentrations and Air–Sea Exchange. *Environmental Science & Technology*, 40(24), 7570–7576. <https://doi.org/10.1021/es061591h>
- Weiss, M. J., McLeod, P., Schatz, B. G., & Hanson, B. K. (1991). Potential for Insecticidal Management of Flea Beetle (Coleoptera: Chrysomelidae) on Canola. *Journal of Economic Entomology*, 84(5), 1597–1603. <https://doi.org/10.1093/jee/84.5.1597>
- Wessel, N., Rousseau, S., Caisey, X., Quiniou, F., & Akcha, F. (2007). Investigating the relationship between embryotoxic and genotoxic effects of benzo[a]pyrene, 17 α -ethinylestradiol and endosulfan on *Crassostrea gigas* embryos. *Aquatic Toxicology*, 85(2), 133–142. <https://doi.org/10.1016/j.aquatox.2007.08.007>
- Whitehouse, C. J. C., Bell, S. G., & Wong, L.-L. (2008). Desaturation of Alkylbenzenes by Cytochrome P450BM3 (CYP102A1). *Chemistry – A European Journal*, 14(35), 10905–10908. <https://doi.org/10.1002/chem.200801927>
- Wojciechowski, M., & Lesyng, B. (2004). Generalized Born Model: Analysis, Refinement, and Applications to Proteins. *The Journal of Physical Chemistry B*, 108(47), 18368–18376. <https://doi.org/10.1021/jp046748b>
- Wong, L. L., Westlake, A. C. G., & Nickerson, D. P. (1997). Protein engineering of cytochrome P450cam. In H. A. O. Hill, P. J. Sadler, & A. J. Thomson (Eds.), *Metal Sites in Proteins and Models: Iron Centres* (pp. 175–207). Springer. https://doi.org/10.1007/3-540-62870-3_6
- Wong, T. S., Wu, N., Roccatano, D., Zacharias, M., & Schwaneberg, U. (2005). Sensitive Assay for Laboratory Evolution of Hydroxylases toward Aromatic and Heterocyclic Compounds. *Journal of Biomolecular Screening*, 10(3), 246–252. <https://doi.org/10.1177/1087057104273336>
- Wong, Tuck Seng, Tee, K. L., Hauer, B., & Schwaneberg, U. (2004). Sequence saturation mutagenesis (SeSaM): A novel method for directed evolution. *Nucleic Acids Research*, 32(3), e26. <https://doi.org/10.1093/nar/gnh028>

- Wong, Tuck Seng, Tee, K. L., Hauer, B., & Schwaneberg, U. (2005). Sequence saturation mutagenesis with tunable mutation frequencies. *Analytical Biochemistry*, *341*(1), 187–189. <https://doi.org/10.1016/j.ab.2005.03.023>
- Wood, D. L., Stark, R. W., Silverstein, R. M., & Rodin, J. O. (1967). Unique Synergistic Effects produced by the Principal Sex Attractant Compounds of *Ips confusus* (LeConte) (Coleoptera: Scolytidae). *Nature*, *215*(5097), 206–206. <https://doi.org/10.1038/215206a0>
- Wright, R. L., Harris, K., Solow, B., White, R. H., & Kennelly, P. J. (1996). Cloning of a potential cytochrome P450 from the Archaeon *Sulfolobus solfataricus*. *FEBS Letters*, *384*(3), 235–239. [https://doi.org/10.1016/0014-5793\(96\)00322-5](https://doi.org/10.1016/0014-5793(96)00322-5)
- Wu, K. K., & Liou, J.-Y. (2005). Cellular and molecular biology of prostacyclin synthase. *Biochemical and Biophysical Research Communications*, *338*(1), 45–52. <https://doi.org/10.1016/j.bbrc.2005.08.021>
- Yanagita, K., Sagami, I., & Shimizu, T. (1997). Distal Site and Surface Mutations of Cytochrome P450 1A2 Markedly Enhance Dehalogenation of Chlorinated Hydrocarbons. *Archives of Biochemistry and Biophysics*, *346*(2), 269–276. <https://doi.org/10.1006/abbi.1997.0301>
- Yano, J. K., Blasco, F., Li, H., Schmid, R. D., Henne, A., & Poulos, T. L. (2003). Preliminary Characterization and Crystal Structure of a Thermostable Cytochrome P450 from *Thermus thermophilus*. *Journal of Biological Chemistry*, *278*(1), 608–616. <https://doi.org/10.1074/jbc.M206568200>
- Yoshioka, S., Takahashi, S., Hori, H., Ishimori, K., & Morishima, I. (2001). Proximal cysteine residue is essential for the enzymatic activities of cytochrome P450cam. *European Journal of Biochemistry*, *268*(2), 252–259. <https://doi.org/10.1046/j.1432-1033.2001.01872.x>
- Yoshioka, S., Takahashi, S., Ishimori, K., & Morishima, I. (2000). Roles of the axial push effect in cytochrome P450cam studied with the site-directed mutagenesis at the heme proximal site. *Journal of Inorganic Biochemistry*, *81*(3), 141–151. [https://doi.org/10.1016/S0162-0134\(00\)00097-0](https://doi.org/10.1016/S0162-0134(00)00097-0)
- Zanger, U. M., & Schwab, M. (2013). Cytochrome P450 enzymes in drug metabolism: Regulation of gene expression, enzyme activities, and impact of genetic variation. *Pharmacology & Therapeutics*, *138*(1), 103–141. <https://doi.org/10.1016/j.pharmthera.2012.12.007>
- Zeng, Z., Tian, L., Li, Z., Jia, L., Zhang, X., Xia, M., & Hu, Y. (2015). Whole-cell method for phenol detection based on the color reaction of phenol with 4-aminoantipyrine catalyzed by CotA laccase on endospore surfaces. *Biosensors and Bioelectronics*, *69*, 162–166. <https://doi.org/10.1016/j.bios.2015.02.032>

- Zhang, J. L., Chen, L. A., Xu, R. B., Wang, C. F., Ruan, Y. P., Wang, A. E., & Huang, P. Q. (2013). Chiral imidazo[1,5-a]tetrahydroquinoline N-heterocyclic carbenes and their copper complexes for asymmetric catalysis. *Tetrahedron Asymmetry*, *24*(8), 492–498. <https://doi.org/10.1016/j.tetasy.2013.03.004>
- Zhang, P., Wang, Y., Bao, R., Luo, T., Yang, Z., & Tang, Y. (2012). Enantioselective Biomimetic Total Syntheses of Katsumadain and Katsumadain C. *Organic Letters*, *14*(1), 162–165. <https://doi.org/10.1021/ol2029433>
- Zhou, Y., Asplund, L., Yin, G., Athanassiadis, I., Wideqvist, U., Bignert, A., Qiu, Y., Zhu, Z., Zhao, J., & Bergman, Å. (2016). Extensive organohalogen contamination in wildlife from a site in the Yangtze River Delta. *Science of The Total Environment*, *554–555*, 320–328. <https://doi.org/10.1016/j.scitotenv.2016.02.176>

Appendix A. Chapter 3 supplementary information

Appendix A1. Mutations and primers designed

Mutant	Mutations	Primer sequence (5' to 3') forward primers only
ES2	F292S/A296V	GGAAGTACTCCGGCGC TCC TCGCTGGTT GTC GATGGCCGCATCCTCACC
	K314E/P321T	GGCGTGCAACTGAAG GAA GGTGACCAGATCCTGCTA ACG CAGATGCTGTCTGGCC
ES5	A296P	CCGGCGCTTCTCGCTGGTT CCC GATGGCCGCATCCTCACC
ES6	G120S	GGCCAACCAAGTGGTT AGC ATGCCGGTGGTGGATAAGCTGG
ES7	V247F	GGATGTGTGGCCTGTTACTG TTC GGCGGCCTGGATACGGTGG
	D297N	CCGGCGCTTCTCGCTGGTTGCC AAT GGCCGCATCCTCACCTCCG
	K314E	CGAGTTTCATGGCGTGCAACTGAAG GAA GGTGACCAGATCCTGCTACCGC
K314E	K314E	CGAGTTTCATGGCGTGCAACTGAAG GAA GGTGACCAGATCCTGCTACCGC
F292S/A296V	F292S/A296V	GGAAGTACTCCGGCGC TCC TCGCTGGTT GTC GATGGCCGCATCCTCACC

Appendix A2. Allosteric sigmoidal kinetics of ES diol (14) with different P450_{cam} mutants (crude lysate) and k_{cat} and K_M data analysis

Mutant Name	V_{max} ($\mu\text{M/s}$)	h	K' (K prime)	K_M (μM)	K_d (μM)	k_{cat} ($\mu\text{M/s}/\mu\text{M P450}$)
WT *	2.87			1024.6	4645	0.8 ± 0.0
IND1	10.50 ± 1.27	4.518	$3.69\text{E}+11$	363.3	$\sim 3.308\text{e}+017$	4.4 ± 0.5
ES1	18.51 ± 5.34	6.191	$1.16\text{E}+16$	393.2	657.3 ± 198.9	3.8 ± 1.1
ES2	25.61 ± 9.35	3.103	$9.54\text{E}+7$	372.8	705.8 ± 337.5	6.2 ± 2.3
ES3	14.95 ± 0.93	3.214	$3.22\text{E}+08$	443.8	601.5 ± 220.6	3.2 ± 0.2
ES4	12.01 ± 2.28	5.299	$1.84\text{E}+13$	318.6	414.9 ± 110.1	3.0 ± 0.6
ES5	20.25 ± 5.68	7.106	$1.82\text{E}+18$	371.3	675.9 ± 227.9	3.9 ± 1.1
ES6	10.56 ± 1.95	2.845	$2.32\text{E}+7$	387.8	537.8 ± 163.5	2.7 ± 0.5
ES7	15.30 ± 4.47	5.925	$8.71\text{E}+14$	332.3	554.1 ± 116.0	4.3 ± 1.2

* WT data from Lineweaver-Burk equation

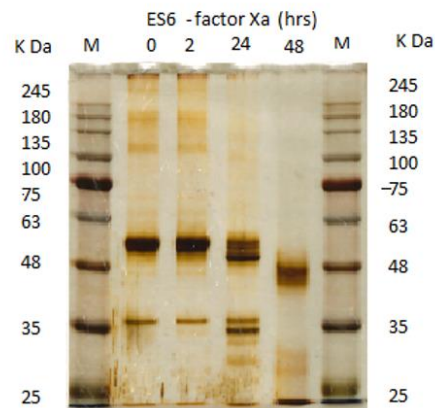
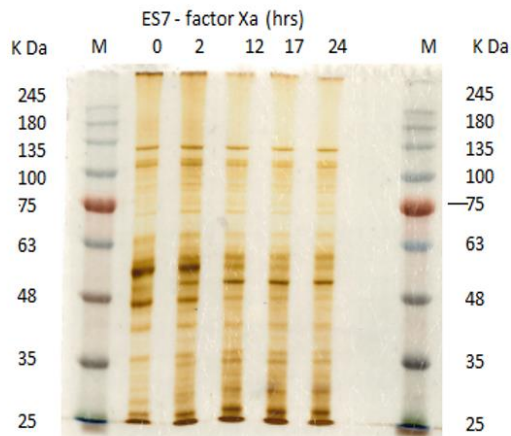
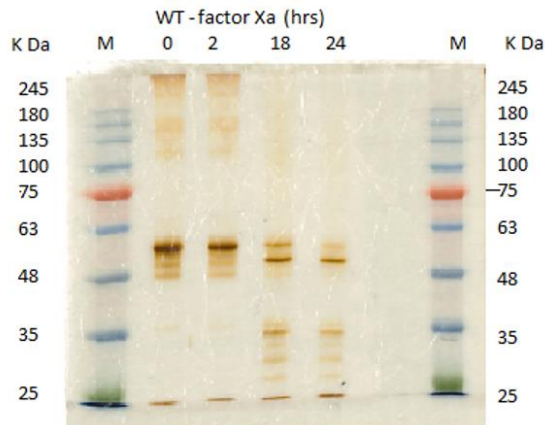
Note: Equation used by GraphPad Prism® for Allosteric sigmoidal kinetics ($Y=V_{max} \cdot X^h / (K' + X^h)$), K' is related to K_M and h is the Hill slope. When h = 1, this equation is identical to the standard Michaelis-Menten equation.

Appendix A3. Allosteric sigmoidal kinetics of ES diol (14) with purified WT P450_{cam} and mutants

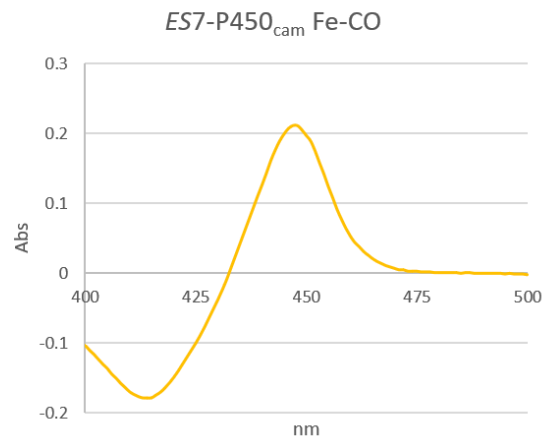
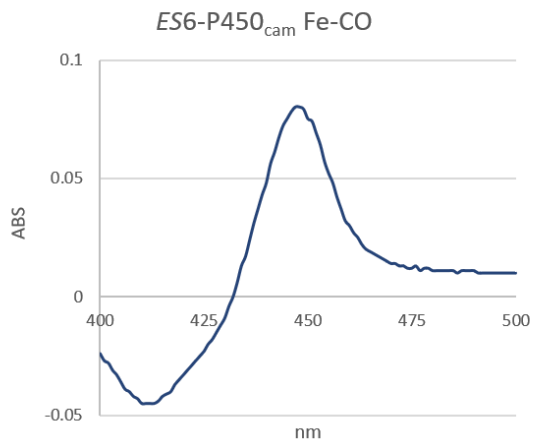
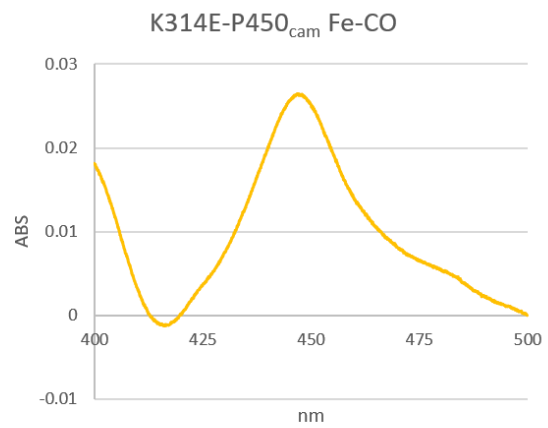
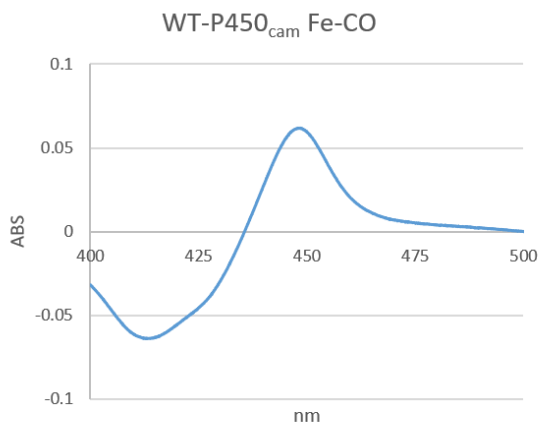
Mutant Name	V_{max} ($\mu\text{M/s}$)	h	K' (K prime)	K_M (μM)	k_{cat} ($\mu\text{M/s}/\mu\text{M P450}$)
WT ^a	0.15 ± 0.04	-	-	385	0.15 ± 0.04
ES2	n.d	n.d	n.d	n.d	n.d
ES5	n.d	n.d	n.d	n.d	n.d
K314E	3.8 ± 0.3	4.8	$8.59 \text{ E}+33$	370	3.8 ± 0.3
ES6	5.7 ± 0.3	7.4	$8.89 \text{ E}+18$	368	5.7 ± 0.3
ES7	12.6 ± 4.7	4.0	$3.75 \text{ E}+10$	394	12.6 ± 4.7

^a WT data from Lineweaver-Burk equation

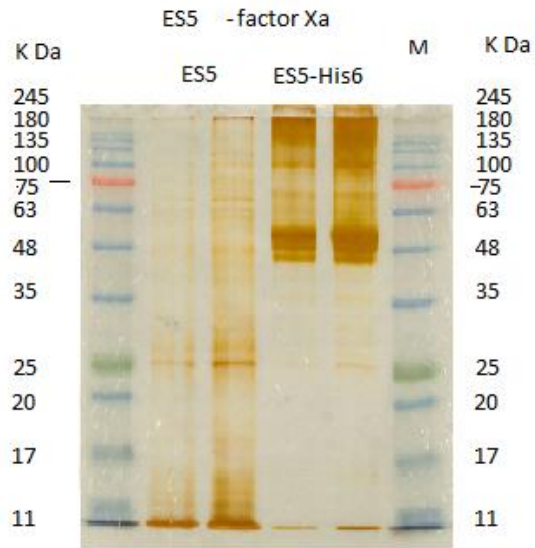
n.d = Not determined



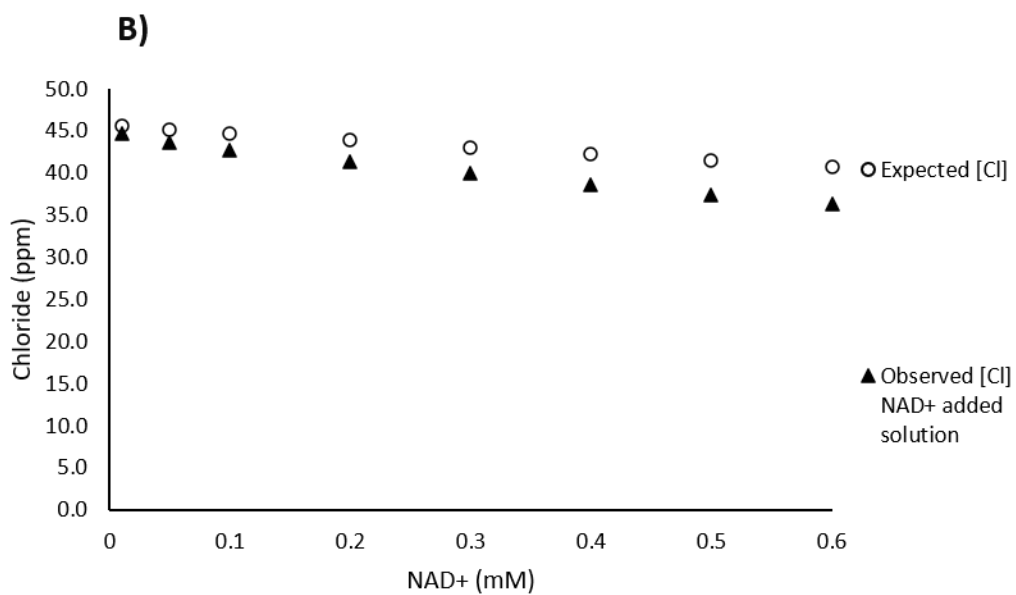
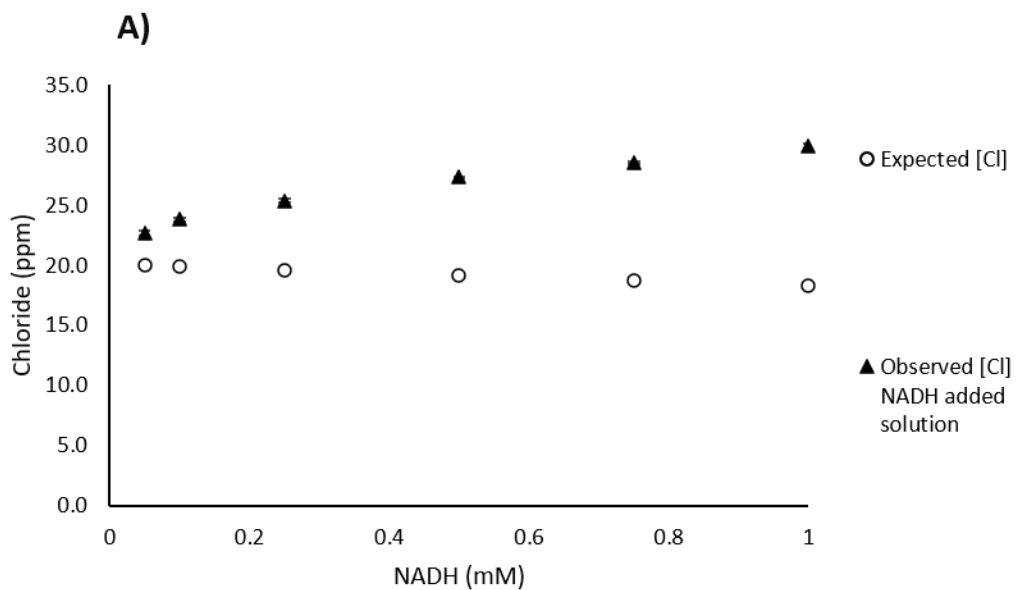
Appendix A4. SDS page of purified mutant and WT P450_{cam}, before and after Factor Xa (protease) cleavage (time in hours).



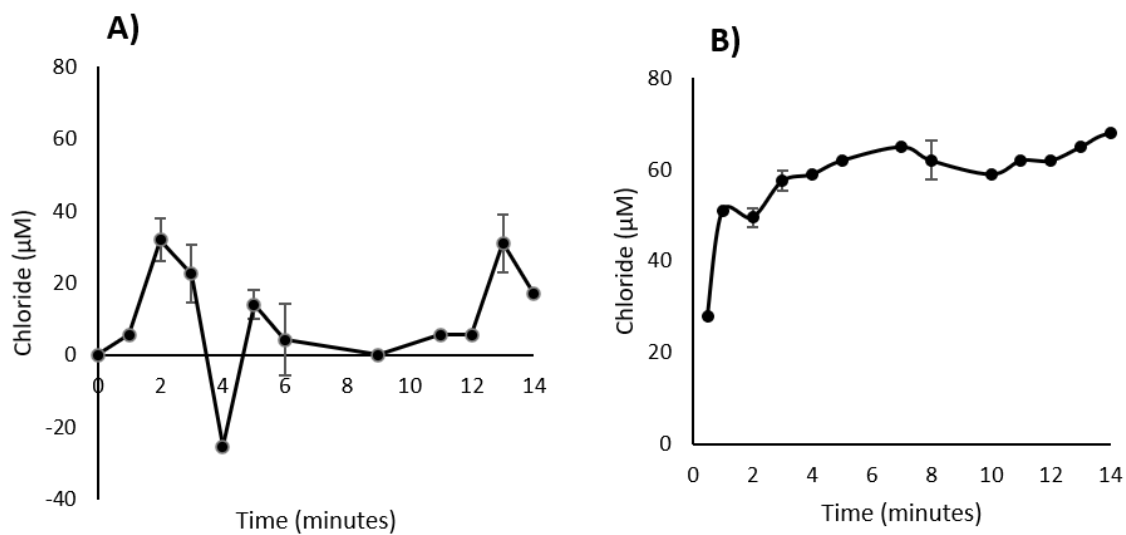
Appendix A5. Fe-CO spectra of WT P450_{cam} and mutants.



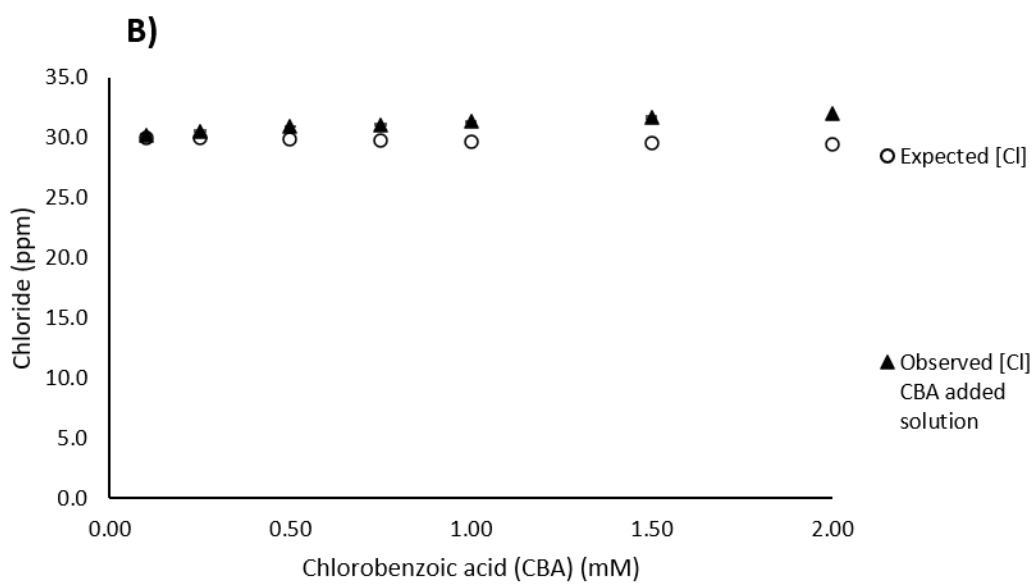
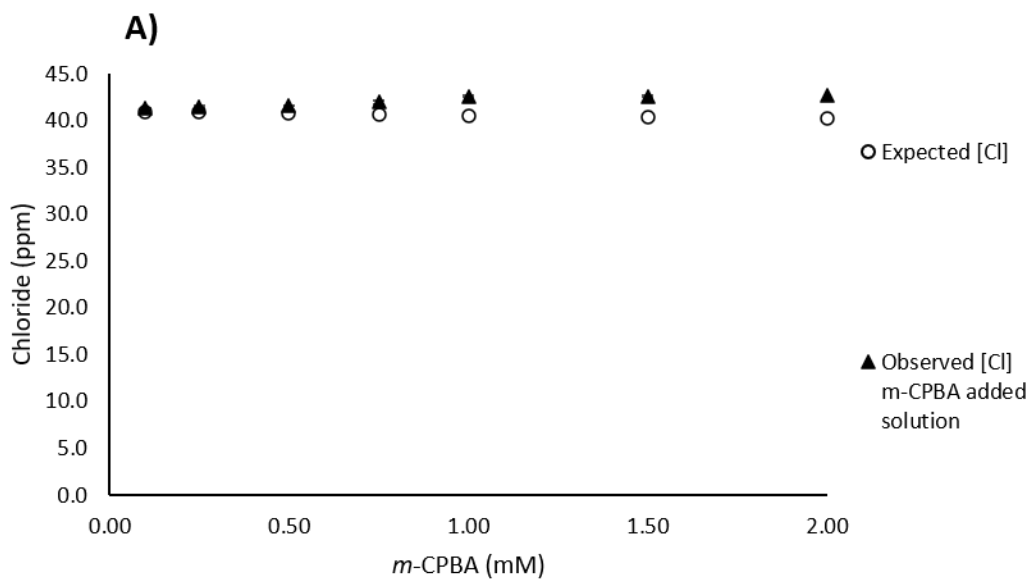
Appendix A6. SDS page of *ES5 P450_{cam}* before and after Factor Xa (protease) cleavage.



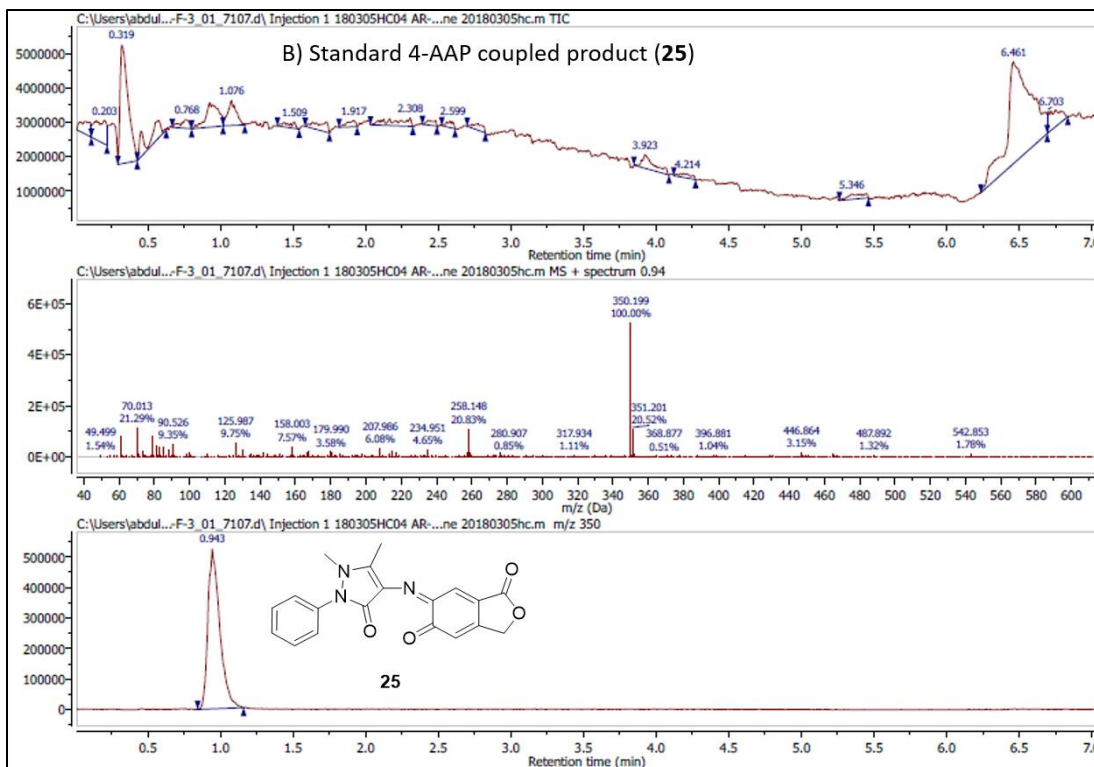
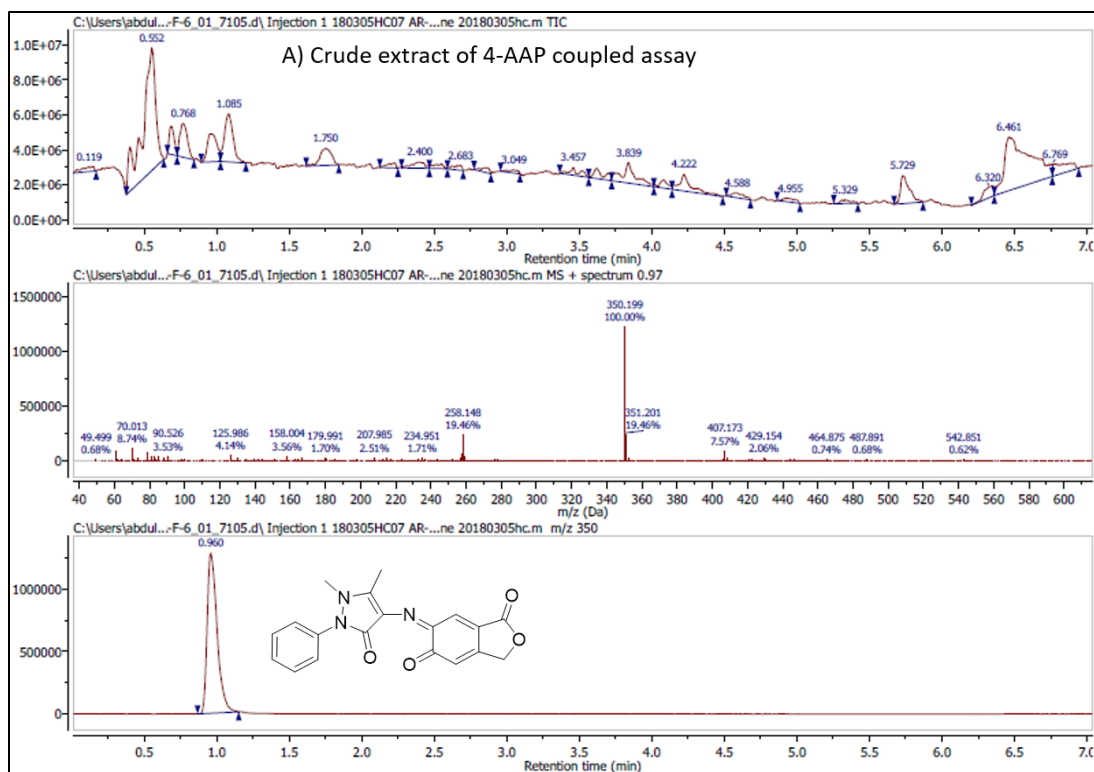
Appendix A7. Effects of NADH (A) and NAD⁺ (B) on Chloride ions reading by ion selective electrode.



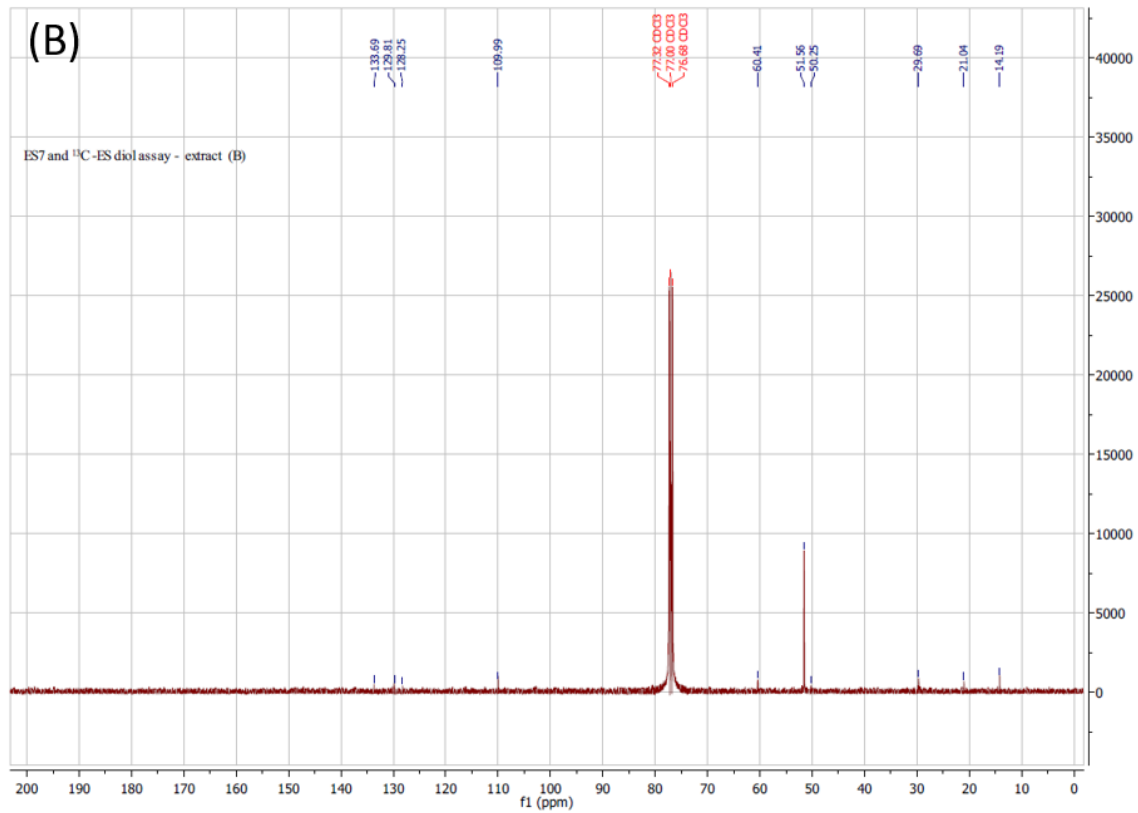
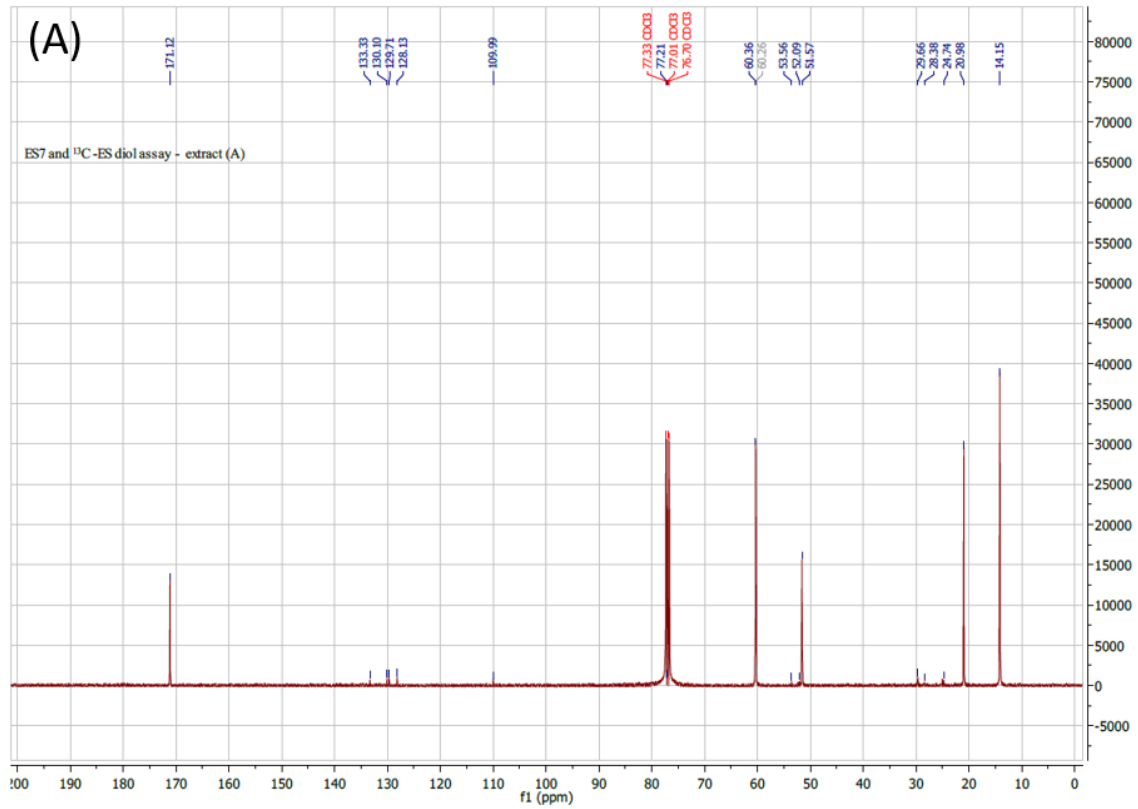
Appendix A8. Chloride release in *in vitro* assay of ES diol (14) using NADH regeneration by alcohol dehydrogenase, (A) WT-P450_{cam} (ES diol (14) 500 μM), (B) ES7 (ES diol (14) 300 μM).

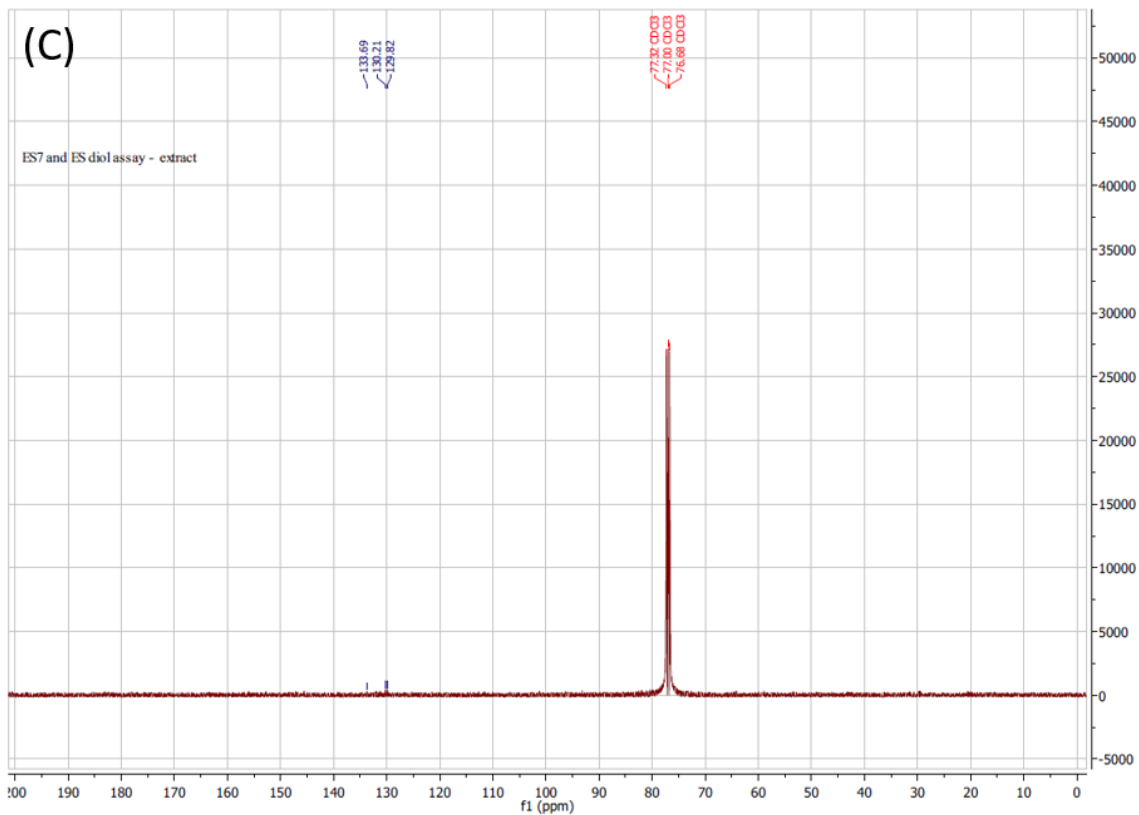


Appendix A9. Effects of *m*-CPBA (A) and chlorobenzoic acid (B) on Chloride ions reading by ion selective electrode.

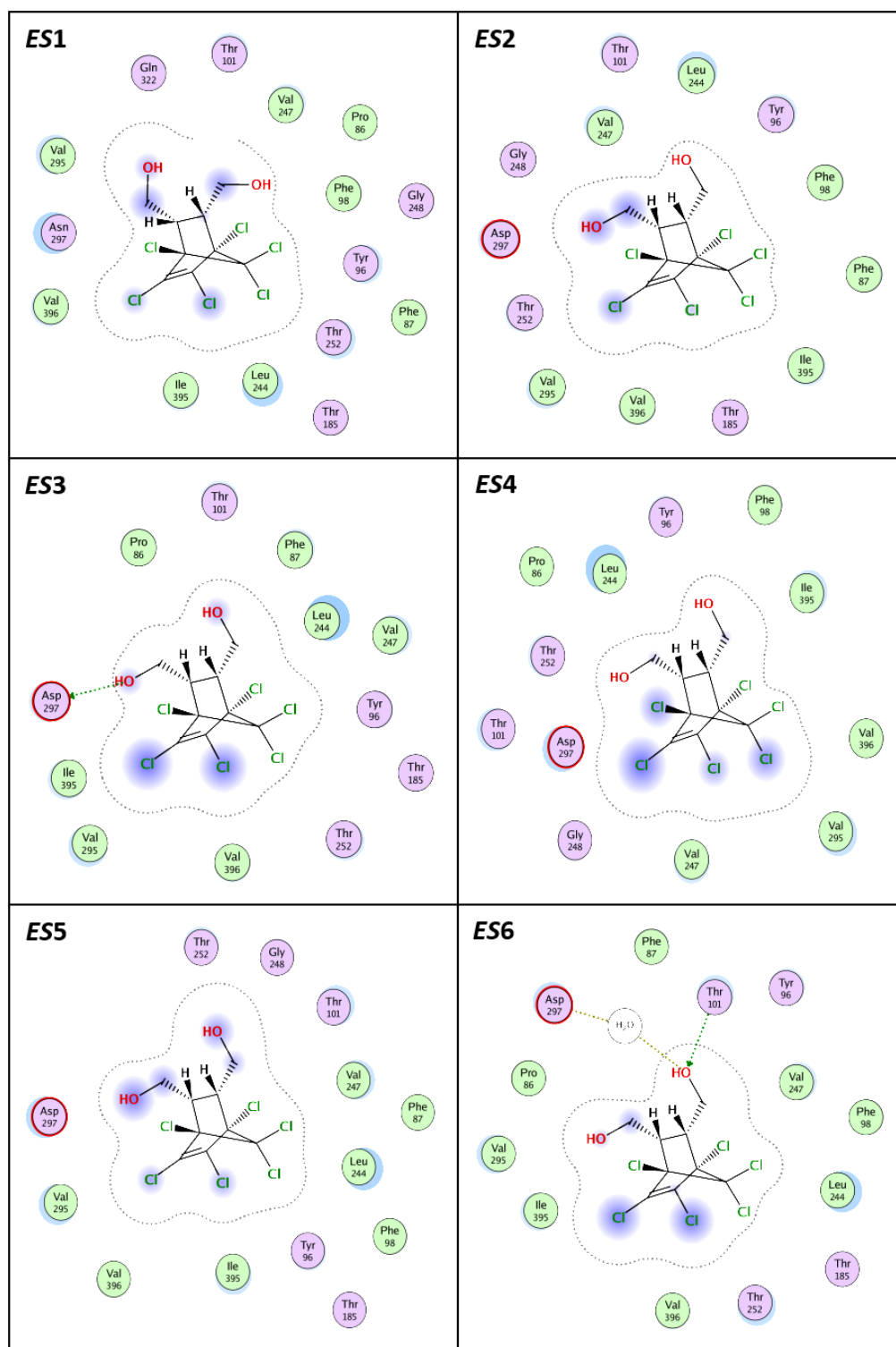


Appendix A10. LC-MS analysis of crude extract of 4-AAP coupled assay (A) and standard 4-AAP coupled product 25 (B), ($M+1$ 350.1, m/z 350 peak is extracted from the chromatogram).

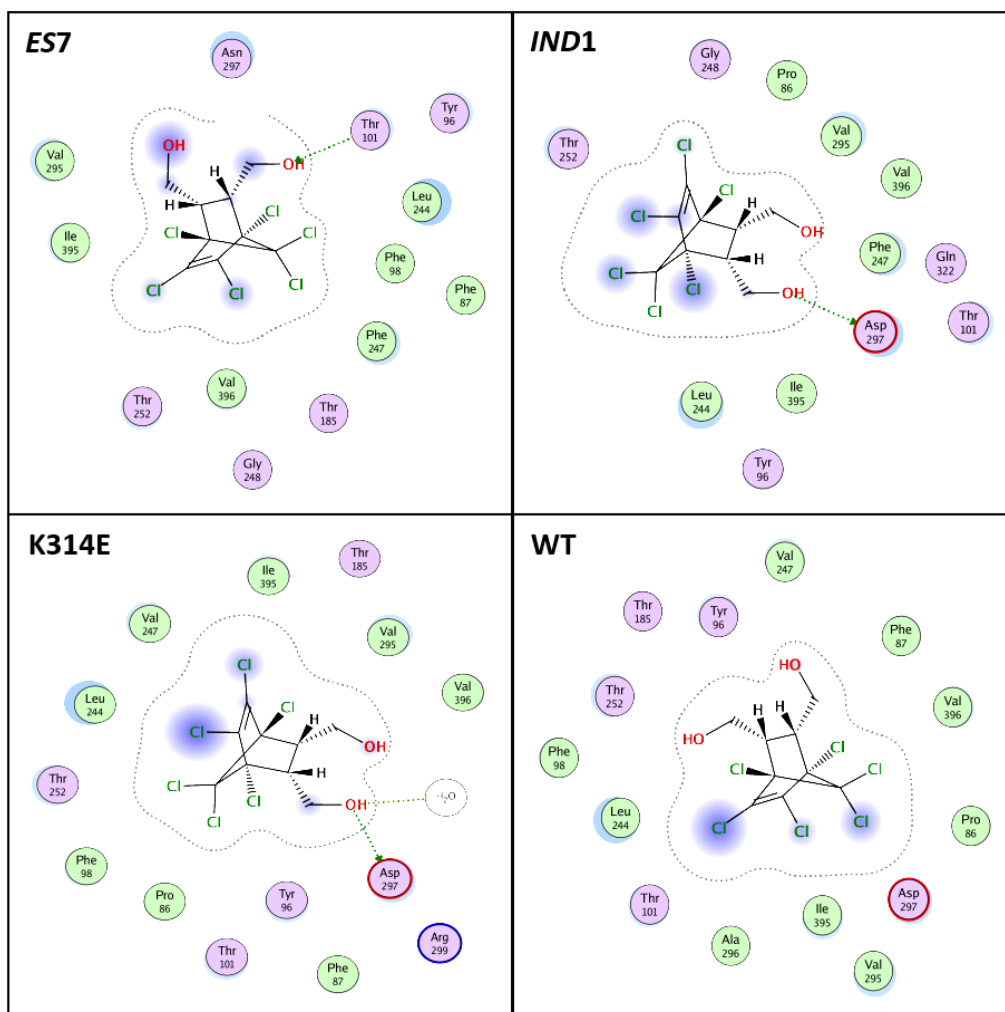




Appendix A11. ^{13}C NMR spectra of metabolites extracts from ^{13}C -ES diol (A and B) and ES diol (C) with ES7 (using *m*-CPBA).



Appendix A12. Map of protein-ligand interactions of the binding pocket residues in contact with of ES diol (14) in ES1, ES2, ES3, ES4, ES5, and ES6 P450_{cam} mutants. Residues shown in purple are polar while residues in green are nonpolar. Residues and ligand atoms with light blue clouds are exposed to the solvent environment.



Appendix A13. Map of protein-ligand interactions of the binding pocket residues in contact with of ES diol (14) in *ES7*, *IND1*, *K314E*, and *WT-P450_{cam}*. Residues in purple are polar while residues in green are nonpolar. Residues and ligand atoms with light blue clouds are exposed to the solvent environment.

```

A → 1 -----atgacgactgaaaccatacaaaagcaacgccaatcttgccctctgccaccccatgtgccagagca
B → 131 togaacgccagcacatggacagcccagatctgggtaccgggtgggtccggtattgagggtcgcatgacgactgaaaccatacaaaagcaacgccaatcttgccctctgccaccccatgtgccagagca
C → -----
66 cctggatttcgacttcgacatgtacaatccgtcgaatctgtctgccggcgtgcaggaggcctgggcagttctgcaagaatcaaacgtaccggatctgggtgtggactcgtgcaacggcggacactggatc
261 cctggatttcgacttcgacatgtacaatccgtcgaatctgtctgccggcgtgcaggaggcctgggcagttctgcaagaatcaaacgtaccggatctgggtgtggactcgtgcaacggcggacactggatc
-----
196 gccactcgcggccaactgatccgtgaggcctatgaagattaccgccactttccagcgagtgcccgttcatccctcgtgaagccggcgaagcctacgacttcattcccacctcgatggatccgcccagc
391 gccactcgcggccaactgatccgtgaggcctatgaagattaccgccactttccagcgagtgcccgttcatccctcgtgaagccggcgaagcctacgacttcattcccacctcgatggatccgcccagc
-----
326 agcgcagtttcgtgctgccaaccaagtgggtggcatgccgggtgggataagctggagaaccggatccaggagctggcctgctcgtgatcgagagcctgcgccgcaaggacagtgcaacttcac
521 agcgcagtttcgtgctgccaaccaagtgggtggcatgccgggtgggataagctggagaaccggatccaggagctggcctgctcgtgatcgagagcctgcgccgcaaggacagtgcaacttcac
-----
456 cgaggactacgccaacccctcccgatacgcattctcatgctgctcgcagggtctaccggaagaagatataccgcacttgaaatcacctaaccgatcagatgaccogtccggatggcagcatgaccttcgca
651 cgaggactacgccaacccctcccgatacgcattctcatgctgctcgcagggtctaccggaagaagatataccgcacttgaaatcacctaaccgatcagatgaccogtccggatggcagcatgaccttcgca
1 -----nncctggtnncangtattac-gnnnnnnnnntcccgcnntt-anaattcctnnnggatcagataaccnntctggatggcagcatgacnttcgca
586 gaggccaaggaggcgctctacgactatctgataccgatcatcgagcaacgcaggcagaagccgggaaccgcgctatcagcatcgttgccaacggccagggtcaatgggocgacgatcaccagtgcgaag
781 gaggccaaggaggcgctctacgactatctgataccgatcatcgagcaacgcaggcagaagccgggaaccgcgctatcagcatcgttgccaacggccagggtcaatgggocgacgatcaccagtgcgaag
91 gnggccaggaggcgctctnnnattatntgataccgatcatcgagcaacgcaggcagaagccgggaaccgcgctatcagcatcgttgccaacggccagggtcaatgggocgacgatcaccagtgcgaag
-----
716 ccaagaggatgtgtggcctgttactggctggcggcctggatacgggtggtaatttctcagcttcagcatggagttcctggccaaaagcccggagcatcgccaggagctgatcgagcgtcccagcgtat
911 ccaagaggatgtgtggcctgttactggctggcggcctggatacgggtggnt-----
221 ccaagaggatgtgtggcctgttactggctggcggcctggatacgggtggtaatttctcagcttcagcatggagttcctggccaaaagcccggagcatcgccaggagctgatcgagcgtcccagcgtat
-----
846 tcacgcccgttcgaggaactactccggcgcttctcgtcgttggcggatggccgcacccctcacctccgattacgagtttcatggcgtgcaactgaagaaagggtgaccagatcctgctaccgcagatgctg
351 tcacgcccgttcgaggaactactccggcgcttctcgtcgttggcggatggccgcacccctcacctccgattacgagtttcatggcgtgcaactgaagaaagggtgaccagatcctgctaccgcagatgctg
-----
976 tctggcctggatgagcgcgaaaaagcctgcccgatgacgctcagcttcagtcgccccaaaagggtttcacacaccaccttggccacggcagccatctgtgccttggccagcacctggcccgggaaatca
481 tctggcctggatgagcgcgaaaaagcctgcccgatgacgctcagcttcagtcgccccaaaagggtttcacacaccaccttggccacggcagccatctgtgccttggccagcacctggcccgggaaatca
-----
1106 tcgtcaccctcaaggaatggctgaccaggattcctgacttctccattgcccgggtgcccagatcagcacaagagcggcatcgtcagcggcgtgcaggcactccctctggtctgggatccggcgactac
611 tcgtcaccctcaaggaatggctgaccaggattcctgacttctccattgcccgggtgcccagatcagcacaagagcggcatcgtcagcggcgtgcaggcactccctctggtctgggatccggcgactac
-----
1236 caaagcggataa-----
741 caaagcggataaggctctaactctcctcgtgccatggcgatccggaattcagagctcgtcgcacaagccttgcggccgactcagacaccaccaccaccactgagatccggctgctaacaaa

```

Silent mutation (K178)

Appendix A14. DNA sequence analysis: A) WT-P450_{cam} DNA (CamC from *P. putida*), B) sequence of WT-P450_{cam} – His₆ with T7 forward primer, and C) sequence of WT-P450_{cam} – His₆ with T7 reverse primer.

A → 1 -----atgacgactgaaaccatacaaaagcaacgccaatcttgcccctctgccaccocatgtgccagag

B → 131 attcgaacgccagcacatggacagcccagatctgggtaccggtgggtgctccggtattgagggctgcatgacgactgaaaccatacaaaagcaacgccaatcttgcccctctgccaccocatgtgccagag

C → 1 -----ccccnnngncc-----

64 cacctggatttcgacttcgacatgtacaatccgtcgaatctgtctgccggcgtgcaggaggcctgggcagttcttgcagaatcaaacgtaccggatctggtgtggactcgtcgaacggcggacactgga

261 cacctggatttcgacttcgacatgtacaatccgtcgaatctgtctgccggcgtgcaggaggcctgggcagttcttgcagaatcaaacgtaccggatctggtgtggactcgtcgaacggcggacactgga

194 tcgccactcgcggccaactgatccgtgaggcctatgaagattaccgccacttttccagcagtgcccgttcacccctcgtgaagccggcgaagcctacgacttcattcccactcogatggatccgcccga

391 tcgccactcgcggccaactgatccgtgaggcctatgaagattaccgccacttttccagcagtgcccgttcacccctcgtgaagccggcgaagcctacgacttcattcccactcogatggatccgcccga

14 -----nnnnccnngggccc--tnnnnnnacnncnntttccangga-nnnccnntnnccntnnggaagcngggnnagcctnggnnttcattncnncttgngggatccgcccga

324 gcagcgcagatttctgctgctggccaaccaagtgggtggcatgccggtgggtgataagctggagaaccggatccaggagctggcctgctcgtgatcgaagacctgcccggcaaggacagtgaacttc

521 gcagcgcagatttctgctgctggccaaccaagtgggtggcatgccggtgggtgataagctggagaaccggatccaggagctggcctgctcgtgatcgaagacctgcccggcaaggacagtgaacttc

124 gcagnnccagttttnngcgtggccaaccaagtgggtggcatgccggt-gnggataagctggagaaccggatccaggagctggcctgctcgtgatcgaagacctgcccggcaaggacagtgaacttc

Silent mutation (K178)

454 accgaggactacgcogaacccttcccgatacgcatacttcatgctgctcgcagggtctaccggaagaagatatcccgcaacttgaaaatacctaaccggatcagatgaccctccggatggcagcatgaccttcg

651 accgaggactacgcogaacccttcccgatacgcatacttcatgctgctcgcagggtctaccggaagaagatatcccgcaacttgaaatacctaaccggatcagatgaccctccggatggcagcatgaccttcg

253 accgaggactacgcogaacccttcccgatacgcatacttcatgctgctcgcagggtctaccggaagaagatatcccgcaacttgaaatacctaaccggatcagatgaccctccggatggcagcatgaccttcg

584 cagaggccaaggaggcgctctacgactatctgataccgatcatcgagcaacgcaggcagaagccgggaaccgacgctatcagcatcgttgccaacggccagggtcaatgggacccgatcaccagtgaaga

781 cagaggccaaggaggcgctctacgactatctgataccgatcatcgagcaacgcaggcagaagccgggaaccgacgctatcagcatcgttgccaacggccagggtcaatgggacccgatcaccagtgaaga

383 cagaggccaaggaggcgctctacgactatctgataccgatcatcgagcaacgcaggcagaagccgggaaccgacgctatcagcatcgttgccaacggccagggtcaatgggacccgatcaccagtgaaga

714 agccaagaggatgtgtggcctgttactggctggcggcctggatacgggtgggtcaatttctcagcttcagcatggagttcctggccaaaagcccgagcatcgccaggagctgatcgaagctcccagcgt

911 agccaagaggatgtgtggcctgttactggctggcggcctggatacgggtgggtcaatttctcagcttcagcatggagttcctggccaaaagcccgagcatcgccaggagctgatcgaagctcccagcgt

513 agccaagaggatgtgtggcctgttactggctggcggcctggatacgggtgggtcaatttctcagcttcagcatggagttcctggccaaaagcccgagcatcgccaggagctgatcgaagctcccagcgt

844 attccagccgcttgcgaggaactactccggcgttctcgcctggttgcggatggccgcatacct-cacctccgattacgagtttcatggcgtgcaactgaaagaaaggtagaccagatcctgctaccgagatg

1039 attcc-nncnctgnnnnnaannntccgg-ncnncnnttggttinncaaggcnnnnncnncnctccaat-----nnn

643 attccagccgcttgcgaggaactactccggcgttctcgcctggttgcggatggccgcatacct-cacctccgattacgagtttcatggcgtgcaactgaaagaaaggtagaccagatcctgctaccgagatg

973 ctgtctggcctggatgagcgcgaaaacgcctgcccgatgcaactcagctcagtcgcaaaaaggtttcacacaccaccttggccacggcagccatctgtgccttggccagcacctggcccgcgggaaa

1113 nttncnggnnnnngnnnnang-----

772 ctgtctggcctggatgagcgcgaaaacgcctgcccgatgcaactcagctcagtcgcaaaaaggtttcacacaccaccttggccacggcagccatctgtgccttggccagcacctggcccgcgggaaa

1103 tcacgtcaccctcaaggaatggctgaccaggattcctgacttctccattgcccgggtgcccagatcagcacaagagcggcatcgtcagcggcgtgcaggcactcctctggtctgggatccggcgac

1133 -----aaggna-----ncaannngnna-----

902 tcacgtcaccctcaaggaatggctgaccaggattcctgacttctccattgcccgggtgcccagatcagcacaagagcggcatcgtcagcggcgtgcaggcactcctctggtctgggatccggcgac

1233 taccaaagcggataa-----

1032 taccaaagcggataaaggctcctaactctcctctggccatggcgatcggatccgaattcagagctccgtcgacaagcttgcggcgcactcagcagcaccaccaccaccactgagatccggctgctaac

Appendix A15. DNA sequence analysis: A) WT-P450_{cam} DNA (CamC from *P. putida*), B) sequence of ES2 – His₆ with T7 forward primer, and C) sequence of ES2 – His₆ with T7 reverse primer.

```

A → 1 -----atgacgactgaaaccatacaaagcaacgccaatcttgccoctctgccaccccatgtgccagag
B → 131 attogaacgccagcacatggacagccagatctgggtaccggtgggtgctccggtattgagggctgcatgacgactgaaaccatacaaagcaacgccaatcttgccoctctgccaccccatgtgccagag
C → -----

64 cacctggatttcgacttcgacatgtacaatccgtcgaatctgtctgccggcgtgcaggaggcctgggcagttctgcaagaatcaaacgtaccggatctggtgtggactcgtgcaacggcgggacactgga
261 cacctggatttcgacttcgacatgtacaatccgtcgaatctgtctgccggcgtgcaggaggcctgggcagttctgcaagaatcaaacgtaccggatctggtgtggactcgtgcaacggcgggacactgga
-----

194 tcgccaactcgcggccaactgatccgtgaggcctatgaagattaccgccactttccagcagtgcccgttcacccctcgtgaagccggcgaagcctacgacttcattcccacctcgatggatccgcccga
391 tcgccaactcgcggccaactgatccgtgaggcctatgaagattaccgccactttccagcagtgcccgttcacccctcgtgaagccggcgaagcctacgacttcattcccacctcgatggatccgcccga
1 -----cntnngnnttcattncncctnnaaggatccgcccga

324 gcagcgcaggtttcgtgctggccaaccaagtgttggcatgccggtggtggataagctggagaaccggatccaggagctggcctgctcgtgatcgagagcctgcgccgcaaggacagtgcaacttc
521 gcagcgcaggtttcgtgctggccaaccaagtgttggcatgccggtggtggataagctggagaaccggatccaggagctggcctgctcgtgatcgagagcctgcgccgcaaggacagtgcaacttc
38 gcaggnccagtttngnngctggccaaccaagtgttggcatgccggtggtggataagctggagaaccggatccaggagctggcctgctcgtgatcgagagcctgcgccgcaaggacagtgcaacttc

Silent mutation (K178)
454 accgaggactacgccaacccctcccgatacgcacttcatgctgctcgcaggtctaccggaagaagatataccgcacttgaaatacctaaccggatcagatgacccgtccggatggcagcatgaccttcg
651 accgaggactacgccaacccctcccgatacgcacttcatgctgctcgcaggtctaccggaagaagatataccgcacttgaaatacctaaccggatcagatgacccgtccggatggcagcatgaccttcg
168 accgaggactacgccaacccctcccgatacgcacttcatgctgctcgcaggtctaccggaagaagatataccgcacttgaaatacctaaccggatcagatgacccgtccggatggcagcatgaccttcg

584 cagaggccaaggaggcgctcctacgactatctgataccgatcctcagcaacgcagggcagaagccgggaaccgacgctatcagcatcgttgccaacggccagggtcaatgggogaccgatcaccagtgaaga
781 cagaggccaaggaggcgctcctacgactatctgataccgatcctcagcaacgcagggcagaagccgggaaccgacgctatcagcatcgttgccaacggccagggtcaatgggogaccgatcaccagtgaaga
298 cagaggccaaggaggcgctcctacgactatctgataccgatcctcagcaacgcagggcagaagccgggaaccgacgctatcagcatcgttgccaacggccagggtcaatgggogaccgatcaccagtgaaga

714 agccaagaggatgtgtggcctgttactggctggcggcctggatacgggtggtcaatctcctcagcttcagcatggagtctcctggccaaaagccgggagcatcgccaggagctgatcgagcgtcccagagcgt
911 agccaanaggatgtgtggcctgttactggctggcggcctggatacgggtggtcaatctcctcagcttcagcatggagtctcctggccaaaagccgggagcatcgccaggagctgatcgagcgtcccagagcgt
428 agccaagaggatgtgtggcctgttactggctggcggcctggatacgggtggtcaatctcctcagcttcagcatggagtctcctggccaaaagccgggagcatcgccaggagctgatcgagcgtcccagagcgt

844 attccagccgcttgcgaggaaactactccggcgcttctcgtggttgcggatggccgcatcctcacctccgattacgagtttcatggcgtgcaactgaagaaaggtgaccagatcctgctaccgcagatgc
A296P
041 attccagccgcttgcgaggaaactactccggnncttnc-ctggttccnhanggcc-catccnnnctccgantacaagttcnnngnnggaaactgaa-aaangnaccnna-----
558 attccagccgcttgcgaggaaactactccggcgcttctcgtggttcccgatggccgcatcctcacctccgattacgagtttcatggcgtgcaactgaagaaaggtgaccagatcctgctaccgcagatgc

974 tgtctggcctggatgagcgcgaaaacgcctgcccgatgcagctcgaacttcagtcgcaaaaaggtttcacacaccacctttggccacggcagccatctgtgccttggccagcactggcccgcgggaaat
-----

688 tgtctggcctggatgagcgcgaaaacgcctgcccgatgcagctcgaacttcagtcgcaaaaaggtttcacacaccacctttggccacggcagccatctgtgccttggccagcactggcccgcgggaaat

104 catcgtcacccctcaaggaatggctgaccaggattcctgacttctccattgcccgggtgcccagattcagcacaagagcggcatcgtcagcggcgtgcaggcactccctctggtctgggatccggcgact
150 -----annngnncnnaannnnnnng-----

818 catcgtcacccctcaaggaatggctgaccaggattcctgacttctccattgcccgggtgcccagattcagcacaagagcggcatcgtcagcggcgtgcaggcactccctctggtctgggatccggcgact

234 accaaagcggataa-----

948 accaaagcggataaaggctctaactctcctctggccatggcgatctcggatccgaattcagagctccgtcgacaagcttgcggccgcaactcagcagcaccaccaccaccactgagatccggctgctaaca

```

Appendix A16. DNA sequence analysis: A) WT-P450_{cam} DNA (CamC from *P. putida*), B) sequence of ES5 – His₆ with T7 forward primer, and C) sequence of ES5 – His₆ with T7 reverse primer.


```

A → 1 -----atgacgactgaaaccatacaaaagcaacgccaatcttgccacctgcccacccatgtgccaga
B → 131 aattcgaaagccagcacatggacagcccagatctgggtaccgggtggctccggattgagggctgcacatgacgactgaaaccatacaaaagcaacgccaatcttgccacctgcccacccatgtgccaga
C → 1 -----cngnaa-----ntttncnng

63 gca---cctggattcgcacttcgacatgtacaatccgtcgaaatctgtctgcccggcgtgcaggaggcctgggcagttctgcaagaatcaaacgtaccggatctggtgtggactcgcctgcaacggcggaca
261 gca---cctggattcgcacttcgacatgtacaatccgtcgaaatctgtctgcccggcgtgcaggaggcctgggcagttctgcaagaatcaaacgtaccggatctggtgtggactcgcctgcaacggcggaca
18 gcnnnnccnngcctt---tnccaaanna-----agt-----ccggatttggg-ngganncnnnna---nggggan

189 ctggatcgccactcggcccaactgatccgtgaggcctatgaagattaccgccactttccagcagtgcccgttccctcgtgaaagccggcgaagcctacgacttcattcccacctcgatggatccg
387 ctggatcgccactcggcccaactgatccgtgaggcctatgaagattaccgccactttccagcagtgcccgttccctcgtgaaagccggcgaagcctacgacttcattcccacctcgatggatccg
79 ctggannccc---tnngccaa-tgatccg-gnnnnntnnnaaga-taccgcn-ntttcca-nggnngcccgttnatccttng-gaagccngngaagcctangacttcattcccacctnganggatccg

319 ccgagcagcgcagttctcgtgcgctggccaaccaagtgggtggcatgcccgggtgggataagctggagaaccggatccaggagctggcctgctcgtgatcgagagcctgcgccgcaaggacagtgca
517 ccgagcagcgcagttctcgtgcgctggccaaccaagtgggttagcatgcccgggtgggataagctggagaaccggatccaggagctggcctgctcgtgatcgagagcctgcgccgcaaggacagtgca
200 ccgagcagcgcagttctcgtgcgctggccaaccaagtgggttagcatgcccgggtgggataagctggagaaccggatccaggagctggcctgctcgtgatcgagagcctgcgccgcaaggacagtgca
G120S
Silent mutation (K178)

449 acttcaccgaggactacgccgaacccttcccgatacgcattctcattgctgctgcaggtctaccggaagaagatatccgcacttgaaatacctaaccggatcagatgaccctgcggatggcagcatgac
647 acttcaccgaggactacgccgaacccttcccgatacgcattctcattgctgctgcaggtctaccggaagaagatatccgcacttgaaatacctaaccggatcagatgaccctgcggatggcagcatgac
330 acttcaccgaggactacgccgaacccttcccgatacgcattctcattgctgctgcaggtctaccggaagaagatatccgcacttgaaatacctaaccggatcagatgaccctgcggatggcagcatgac

579 cttcgcagagcccaaggaggcctctacgactatctgataccgatcatcgagcaaacgcaggcagaagccgggaaccgacgctatcagcatcgttgccaacggccagggtcaatggggcagccgatcaccagt
777 cttcgcagagcccaaggaggcctctacgactatctgataccgatcatcgagcaaacgcaggcagaagccgggaaccgacgctatcagcatcgttgccaacggccagggtcaatggggcagccgatcaccagt
460 cttcgcagagcccaaggaggcctctacgactatctgataccgatcatcgagcaaacgcaggcagaagccgggaaccgacgctatcagcatcgttgccaacggccagggtcaatggggcagccgatcaccagt

709 gacgaagccaagaggatgtgtggcctggtactggtcggcggcctggatacgggtggtaaatctcctcagcttcagcatggagtctcctggccaaaagcccggagcatcgccaggagctgatcgagcgtcccg
907 gacgaagccaagaggatgtgtggcctggtactggtcggcggcctggatacgggtggtaaatctcctcagcttcagcatggagtctcctggccaaaagcccgganacatcccaggagctgatcgagcgtcccg
590 gacgaagccaagaggatgtgtggcctggtactggtcggcggcctggatacgggtggtaaatctcctcagcttcagcatggagtctcctggccaaaagcccggagcatcgccaggagctgatcgagcgtcccg

839 agcgtattccagccgcttgagaggaactactccggccttctcgtggttgccgatggccgcacctcctcactccgattacaggtttcatggcgtgcaactgaagaaaggtgaccagatcctgctaccgca
037 agcgtattccagccgcttgcnngaactactccggnnntnnnnntgggtgcccgatggcnnatcctnncctcc-aatacaagt-tcctggcnngca-ctgaa-aangngacca----atcngnnnca
720 agcgtattccagccgcttgagaggaactactccggccttctcgtggttgccgatggccgcacctcctcactccgattacaggtttcatggcgtgcaactgaagaaaggtgaccagatcctgctaccgca

969 gatgctgtctggcctggatgagcgcgaaaaagcctgcccgatgcaactgcacttcagtcgcaaaaaggtttcacacaccacctttggccaacggcagccatctgtgccttggccagcacctggcccgcgg
159 -annnnntnggcc-ngannnc-cnaaaaccnncnannnnntnccnnntnnnnnccaaangntt---nnnnncccttggccngg-----cnnnngnaannnnnccn
850 gatgctgtctggcctggatgagcgcgaaaaagcctgcccgatgcaactgcacttcagtcgcaaaaaggtttcacacaccacctttggccaacggcagccatctgtgccttggccagcacctggcccgcgg

099 gaaatcatcgtcacctcaaggaatggctgaccaggattcctgacttctccattgcccgggtgcccagattcagcacaagagcggcatcgtcagcggcgtgcaggcactccctctggtctgggatccgg
244 -----nnnnntnggcttggcnnnccngg-----cnnnngnaannnnnccn
980 gaaatcatcgtcacctcaaggaatggctgaccaggattcctgacttctccattgcccgggtgcccagattcagcacaagagcggcatcgtcagcggcgtgcaggcactccctctggtctgggatccgg

229 cgactaccaaagcggataa-----
287 nna-----
110 cgactaccaaagcggataaagcctcctaactcctcctggccatggcgatccggatccgaattcagagctccgtcgacaagcctgcgccgacactcgagcaccaccaccaccactgagatccggcgtc

```

Appendix A17. DNA sequence analysis: A) WT-P450_{cam} DNA (CamC from *P. putida*), B) sequence of ES6 – His₆ with T7 forward primer, and C) sequence of ES6 – His₆ with T7 reverse primer.

A → 1 -----atgacgactgaaaccatacaaaagcaacgccaatcttgcccctctgccaccccatgtgcca
 B → 131 taaattogaacgccagcacatggacagcccagatctgggtaccgggtggctccggatttgagggctgcatgacgactgaaaccatacaaaagcaacgccaatcttgcccctctgccaccccatgtgcca
 C → -----

61 gagcacctggtattogacttgcacatgtacaatccgtcgaatctgtctgccggcgtgcaggaggcctgggcagttctgcaagaatcaaacgtaccggatctggtgtggactcgtgcaacggcgggacact
 261 gagcacctggtattogacttgcacatgtacaatccgtcgaatctgtctgccggcgtgcaggaggcctgggcagttctgcaagaatcaaacgtaccggatctggtgtggactcgtgcaacggcgggacact

191 ggatcgccactcgggccaactgatccgtgaggcctatgaagattaccgccactttccagcgagtgcccgttcacccctcgtgaagccggcgaagcctacgacttcattcccacctcgatggatccggc
 391 ggatcgccactcgggccaactgatccgtgaggcctatgaagattaccgccactttccagcgagtgcccgttcacccctcgtgaagccggcgaagcctacgacttcattcccacctcgatggatccggc

321 cgagcagcgcagtttcgtgcgctggccaaccaagtggttggcatgccgggtgggataagctggagaaccggatccaggagctggcctgctcgtgatcgagagcctgcgcccgaaggacagtgcAAC
 521 cgagcagcgcagtttcgtgcgctggccaaccaagtggttggcatgccgggtgggataagctggagaaccggatccaggagctggcctgctcgtgatcgagagcctgcgcccgaaggacagtgcAAC

451 ttaccggaggactacgcccgaacccttcccgatagcactctcatgctgctcgcagggtctaccggaagaagatatcccgcaacttgaaatcactaacggatcagatgaccgctccggatggcagcatgacct
 651 ttaccggaggactacgcccgaacccttcccgatagcactctcatgctgctcgcagggtctaccggaagaagatatcccgcaacttgaaatcactaacggatcagatgaccgctccggatggcagcatgacct

Silent mutation (K178)

581 tcgcagaggccaaggaggcgtctacgactatctgataccgatcatcgagcaacgcaggcagaagccgggaaccgacgctatcagcatcgttgccaacggccagggtcaatgggacaccgatcaccagtga
 781 tcgcagaggccaaggaggcgtctacgactatctgataccgatcatcgagcaacgcaggcagaagccgggaaccgacgctatcagcatcgttgccaacggccagggtcaatgggacaccgatcaccagtga
 1 -----cngatnccgatcctcgagcaacgcaggcagaagccgggaaccgacgctatcagcatcgttgccaacggccagggtcaatgggacaccgatcaccagtga

711 cgaagccaagaggatggtggtgcttactcgtcggcggcctggatacgggtggtcaatctcctcagcttcagcatggagtctcctggccaaaagccggagcatcgccaggagctgatcgagcgtcccgag
 911 cgaagccaagaggatggtggtgcttactcgtcggcggcctggatacgggtggtcaatctcctcagcttcagcatggagtctcctggccaaaagccggannatcnncaaga-----
 99 cgaagccaagaggatggtggtgcttactcgtcggcggcctggatacgggtggtcaatctcctcagcttcagcatggagtctcctggccaaaagccggagcatcgccaggagctgatcgagcgtcccgag

841 cgtattccagccgcttgcgaggaactactccggcgttctcgtggttgcagatggccgatcctcactccgattacgagtttcatggcgtgcaactgaagaaaggtgaccagatcctgctaccgcaga
 1022 -----aacnannannngt-----
 229 cgtattccagccgcttgcgaggaactactccggcgttctcgtggttgcagatggccgatcctcactccgattacgagtttcatggcgtgcaactgaagaaaggtgaccagatcctgctaccgcaga

971 tgctgtctggcctggatgagcgcgaaaacgcctgcccgatgcaogtcgacttcagtcgcaaaaaggtttcacacaccacctttggccacggcagccatctgtgccttggccagcactggcccgcggga
 1036 -----cccaannng-----
 359 tgctgtctggcctggatgagcgcgaaaacgcctgcccgatgcaogtcgacttcagtcgcaaaaaggtttcacacaccacctttggccacggcagccatctgtgccttggccagcactggcccgcggga

1101 aatcatogtcacccctcaaggaatggctgaccaggattcctgacttctccattgcccgggtgcccagatcagcacaagagcggcatcgtcagcggcgtgcaggcactccctctggtctgggatccggcg
 1044 -----annttca-----
 489 aatcatogtcacccctcaaggaatggctgaccaggattcctgacttctccattgcccgggtgcccagatcagcacaagagcggcatcgtcagcggcgtgcaggcactccctctggtctgggatccggcg

1231 actaccaaagcggataaa-----

 619 actaccaaagcggataaaggctctaactctcctctggccatgggatcggatccgaattcgagctccgtcgacaannnngggcggcactcgagcaccaccaccaccactgagatccggctgcta

Appendix A18. DNA sequence analysis: A) WT-P450_{cam} DNA (CamC from *P. putida*), B) sequence of *ES7* – His₆ with T7 forward primer, and C) sequence of *ES7* – His₆ with T7 reverse primer.

```

A → 1 -----atgacgactgaaaccatacaaaagcaacgccaatcttgcccocttgccaccccatgtgccaga
B → 131 aattcgaacgccagccatggacagcccagatctgggtaccgggtggctccggattgagggctgcgtgacgactgaaaccatacaaaagcaacgccaatcttgcccocttgccaccccatgtgccaga
C → -----
63 gcacctggatttcgacttcgacatgtacaatccgtcgaaatctgtctgcccggctgcaggaggcctgggcagttctgcaagaatcaaactgaccggatctgggtggactcgctgcaacggcgggacactgg
261 gcacctggatttcgacttcgacatgtacaatccgtcgaaatctgtctgcccggctgcaggaggcctgggcagttctgcaagaatcaaactgaccggatctgggtggactcgctgcaacggcgggacactgg
1 -----gggnnnnnnggnaangg-gggnnnnn
193 atcgccactcggcgccaactgatccgtgaggcctatgaagattaccgccaactttccagcagagtcccgttccatccctcgtgaagccggcgaagcctacgacttcatcccacctcgatggatccgccc
391 atcgccactcggcgccaactgatccgtgaggcctatgaagattaccgccaactttccagcagagtcccgttccatccctcgtgaagccggcgaagcctacgacttcatcccacctcgatggatccgccc
28 nnnnnnnnnnggccaanngatccngnngccttnnnnnnnntncncnntttccagggangggccgcttctcccttgggaaagccggggaagcctnngatttcatcccacct-ganggatccgccc
323 agcagcgccagtttctgctgctggccaaccaagtggttggcatgcccgggtgggataagctggagaacccggatccaggagctggcctgctcgtgatcgagagcctgcccggcaaggacagtgaactt
521 agcagcgccagtttctgctgctggccaaccaagtggttggcatgcccgggtgggataagctggagaacccggatccaggagctggcctgctcgtgatcgagagcctgcccggcaaggacagtgaactt
157 agcagnnncagtttctgctgctggccaaccaagtggttggcatgcccgggtgggataagctggagaacccggatccaggagctggcctgctcgtgatcgagagcctgcccggcaaggacagtgaactt
Silent mutation (K178)
453 caccgaggactacgcccgaacccttcccgatcgcacatcttcatgctgctcgcaggtctaccggaagaagatataccgcacttgaatacctaaccggatcagatgaccogtccggatggcagcatgacctt
651 caccgaggactacgcccgaacccttcccgatcgcacatcttcatgctgctcgcaggtctaccggaagaagatataccgcacttgaatacctaaccggatcagatgaccogtccggatggcagcatgacctt
287 caccgaggactacgcccgaacccttcccgatcgcacatcttcatgctgctcgcaggtctaccggaagaagatataccgcacttgaatacctaaccggatcagatgaccogtccggatggcagcatgacctt
583 gcagagggccaaggaggcgtctacgactatctgataccgatcatcgagcaacgcaggcagaagccgggaaccogacgctatcagcatcgttgccaacggccagggtcaatggggcgaaccgatcaccagtgaag
781 gcagagggccaaggaggcgtctacgactatctgataccgatcatcgagcaacgcaggcagaagccgggaaccogacgctatcagcatcgttgccaacggccagggtcaatggggcgaaccgatcaccagtgaag
417 gcagagggccaaggaggcgtctacgactatctgataccgatcatcgagcaacgcaggcagaagccgggaaccogacgctatcagcatcgttgccaacggccagggtcaatggggcgaaccgatcaccagtgaag
713 aagccaagaggatgtgtggcctgttactggtcggcggcctggatacgggtgggtcaatttccctcagcttcagcatggagttcctggccaaaagcccgagcatcggcaggagctgatcgagcgtcccagcgg
911 aagccaagaggatgtgtggcctgttactggtcggcggcctggatacgggtgggtcaatttccctcagcttcagcatggagttcctggccaaaagcccgagcatcggcaggagctgatcgagcgtcccagcgg
547 aagccaagaggatgtgtggcctgttactggtcggcggcctggatacgggtgggtcaatttccctcagcttcagcatggagttcctggccaaaagcccgagcatcggcaggagctgatcgagcgtcccagcgg
843 tattccagccgcttgcgaggaactactccggcgttctcgtggttgcgatggccgcacatcctcaccctccgattacgagtttcatggcgtgc--aact-gaagaaagggtgaccagatcctgcta--ccgca
1041 tattccagccgcttgcgaggaactactccggnnntnnngctggttgcenatggccnccatcctcaccnccgattacnngttcnnngngnnaantngaaggaaagggnaccaantccnnnnnccnca
677 tattccagccgcttgcgaggaactactccggcgttctcgtggttgcgatggccgcacatcctcaccctccgattacgagtttcatggcgtgc--aact-gaagaaagggtgaccagatcctgcta--ccgca
969 gatgctgtctggcctggatgagcggcaaaaagcctgcccgatgcaactgacttcagtcgcaaaaaggtttcacacaccaccttggccaacggcagccatctgtgcttggccagcacctggcccggcgg
1171 annnnnnnnnngncngnnnnnnnnnaaanccc-----
803 gatgctgtctggcctggatgagcggcaaaaagcctgcccgatgcaactgacttcagtcgcaaaaaggtttcacacaccaccttggccaacggcagccatctgtgcttggccagcacctggcccggcgg
1099 gaaatcatcgtcacccctcaaggaatggctgaccaggatctcctgacttctccattgcccgggtgcccagattcagcacaagagcggcatcgtcagcggcgtgacggcactcctctggtctgggatccgg
1205 -----ngncnnnnnnnnnnnnnnccnnaa-----
933 gaaatcatcgtcacccctcaaggaatggctgaccaggatctcctgacttctccattgcccgggtgcccagattcagcacaagagcggcatcgtcagcggcgtgacggcactcctctggtctgggatccgg
1229 cgactaccaaagcggataa-----
1063 cgactaccaaagcggataaaggtcttaactctcctctggccatggcgatatacggatccgaattcagactccgtcgacaagcttggggcggcactcagcaccacaccaccactgagatccggcgtgc

```

Appendix A19. DNA sequence analysis: A) WT-P450_{cam} DNA (CamC from *P. putida*), B) sequence of K314E – His₆ with T7 forward primer, and C) sequence of K314E – His₆ with T7 reverse primer.

```

A → 1 -----atgacgactgaaaccatacaaaagca-----acgccaatcttgcccctctgccaccca
B → 131 ttogaacgccagcacatggacagcccagatctgggtaccgggtgggtccgggtattgagggtcgcatgacgactgaaaccatacaaaagca-----acgccaatcttgcccctctgccaccca
C → 20 -----nnnnngtnnnnnngcannnganncannnnnnnnnaacnancantnnncnntcnnncnncnnnnn

54 tgtgccagagcacctggattcgaacttcgacatgtacaatccgtogaatctgtctgcccggcgtgacgaggcctgggcagttctgcaagaatcaaacgtaccggatctgggtggactcgctgcaacggc
250 tgtgccagagcacctggattcgaacttcgacatgtacaatccgtogaatctgtctgcccggcgtgacgaggcctgggcagttctgcaagaatcaaacgtaccggatctgggtggactcgctgcaacggc
84 nnagcc-----nccccnnnnnnnnnnnnnnnancnncnnaannttccnngcgnnnng--gnnccngcngnttc--nnnaannnaacnncocggnt----ngnnngnnnnnnnnnnngn

184 ggacactggatcgccactcgcggccaactgatccgtgaggcctatgaagattaccgccactttccacgagatgcccgttcatccctcgtgaagccggcgaagcctacgacttcattcccactcgatgg
380 ggacactggatcgccactcgcggccaactgatccgtgaggcctatgaagattaccgccactttccacgagatgcccgttcatccctcgtgaagccggcgaagcctacgacttcattcccactcgatgg
192 ngnnnnnnnannnc--cnnccnngcnaatnntccnnnngcctt----gannnacccgcnnttccacggnnnnnnccggttcctc--cttnngaagccgnggaagc--tnnnnttcattcccactcg--ngg

314 atccgccgagcagcgcagtttctgtgctggccaaccaagtgggtggcatgccggtgggtggataagctggagaaccggatccaggagctggcctgctcgtgatcgagagcctgcccgcgaaggaca
510 atccgccgagcagcgcagtttctgtgctggccaaccaagtgggtggcatgccggtgggtggataagctggagaaccggatccaggagctggcctgctcgtgatcgagagcctgcccgcgaaggaca
311 atccgccgagcagcgcagtttctgtgctggccaaccaagtgggtggcatgccggtgggtggataagctggagaaccggatccaggagctggcctgctcgtgatcgagagcctgcccgcgaaggaca
Silent mutation (K178)
444 gtgcaacttcaccgaggactacgcgaacccttcccgatacgcacatcttcatgctgctgcaggtctaccggaagaagatatacccgacttgaaatacctaaccggatcagatgaccgctccggatggcagc
640 nnncaacnncaccgagnnncacgcctaa-----
440 gtgcaacttcaccgaggactacgcgaacccttcccgatacgcacatcttcatgctgctgcaggtctaccggaagaagatatacccgacttgaaatacctaaccggatcagatgaccgctccggatggcagc

574 atgaccttcgagaggccaaggaggcgtctacgactatctgataccgatcatcgagcaacgcagggcagaagccgggaaccgacgctatcagcatcgttgccaacggccagggtcaatggggcagccgatca
570 atgaccttcgagaggccaaggaggcgtctacgactatctgataccgatcatcgagcaacgcagggcagaagccgggaaccgacgctatcagcatcgttgccaacggccagggtcaatggggcagccgatca

704 ccagtgcagcaagccaagaggatgtgtggcctgttactggctggcggcctggatacgggtggtaatttcctcagcttcagcatggagttcctggccaaaagccggagcatcgccaggagctgatcgagcg
700 ccagtgcagcaagccaagaggatgtgtggcctgttactggctggcggcctggatacgggtggtaatttcctcagcttcagcatggagttcctggccaaaagccggagcatcgccaggagctgatcgagcg

834 tcccgagcgtattccagccgcttgcgaggaactactccggcgttctcgtctggttgcgatggcgcacatcctcacctccgattacgagtttcatggcgtgcaactgaagaaagggtgaccagatcctgcta
830 tcccgagcgtattccagccgcttgcgaggaactactccggcgttctcgtctggttgcgatggcgcacatcctcacctccgattacgagtttcatggcgtgcaactgaagaaagggtgaccagatcctgcta

964 ccgcagatgctgtctggcctggatgagcgcgaaaaagcctgcccgatgacgctgcaacttcagtcgcaaaaagggtttcacacaccaccttggccacggcagccatctgtgcttggccagcacctggccc
960 ccgcagatgctgtctggcctggatgagcgcgaaaaagcctgcccgatgacgctgcaacttcagtcgcaaaaagggtttcacacaccaccttggccacggcagccatctgtgcttggccagcacctggccc

1094 gccgggaaatcatcgtcacctcaaggaatggctgaccaggatctcgtacttctccattgccccgggtgccagattcagcacaagagcggcatcgtcagggcgtgacggcactccctctggtctggga
1090 gccgggaaatcatcgtcacctcaaggaatggctgaccaggatctcgtacttctccattgccccgggtgccagattcagcacaagagcggcatcgtcagggcgtgacggcactccctctggtctggga

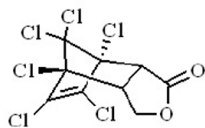
1224 tccggcgactaccaaagcggataaa-----
1220 tccggcgactaccaaagcggataaaggctctaactctcctctggccatggcgatattcgatccgaattcggagctcgtcgcacaagcttggcggcgcactcgagcaccaccaccaccactgagatccg

```

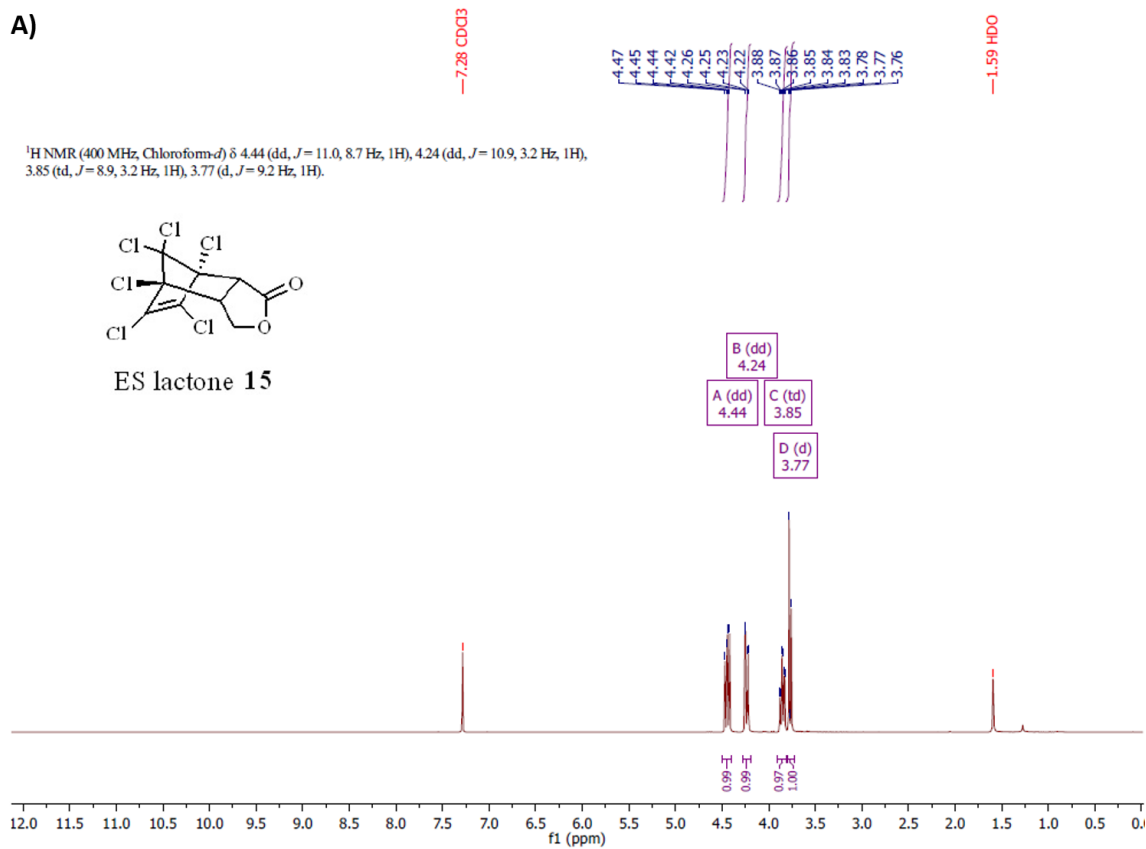
Appendix A20. DNA sequence analysis: A) WT-P450_{cam} DNA (CamC from *P. putida*), B) sequence of F292S/A296V – His₆ with T7 forward primer, and C) sequence of F292S/A296V – His₆ with T7 reverse primer.

A)

$^1\text{H NMR}$ (400 MHz, Chloroform-*d*) δ 4.44 (dd, $J=11.0, 8.7$ Hz, 1H), 4.24 (dd, $J=10.9, 3.2$ Hz, 1H), 3.85 (td, $J=8.9, 3.2$ Hz, 1H), 3.77 (d, $J=9.2$ Hz, 1H).

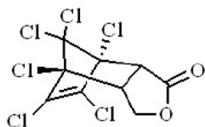


ES lactone **15**

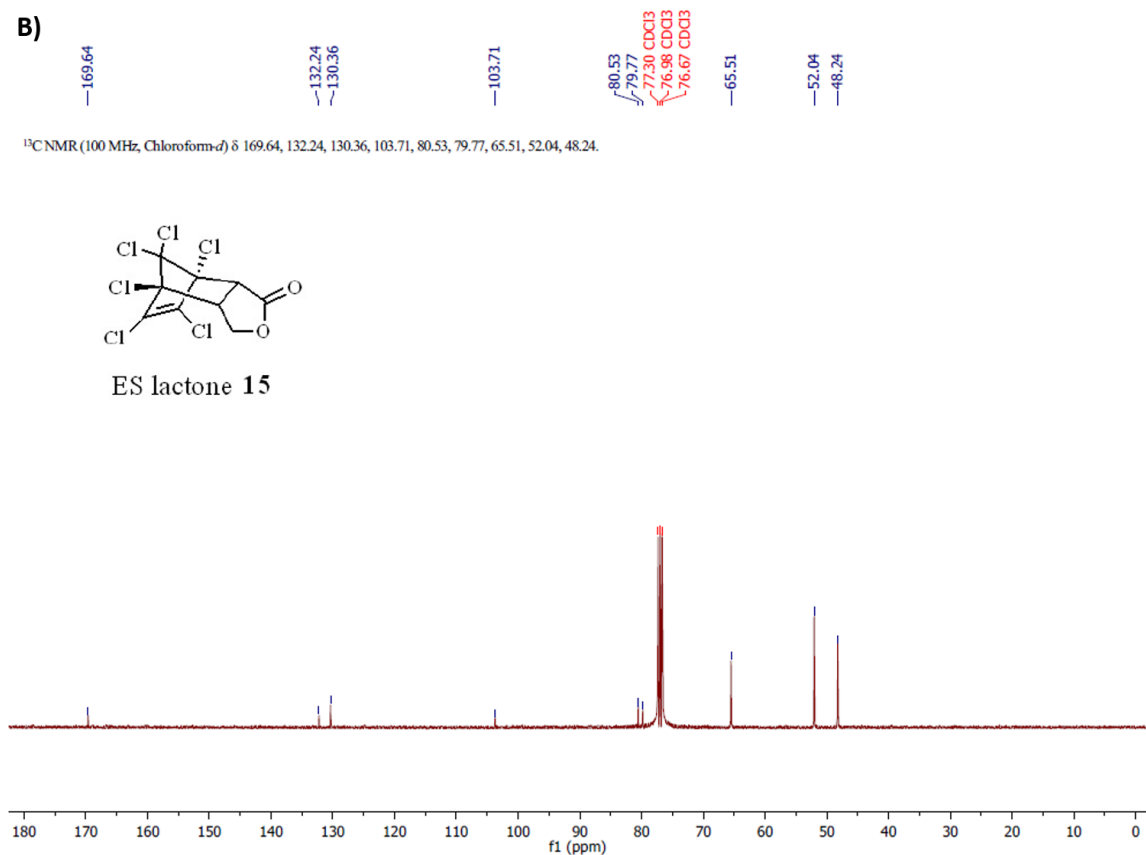


B)

$^{13}\text{C NMR}$ (100 MHz, Chloroform-*d*) δ 169.64, 132.24, 130.36, 103.71, 80.53, 79.77, 65.51, 52.04, 48.24.

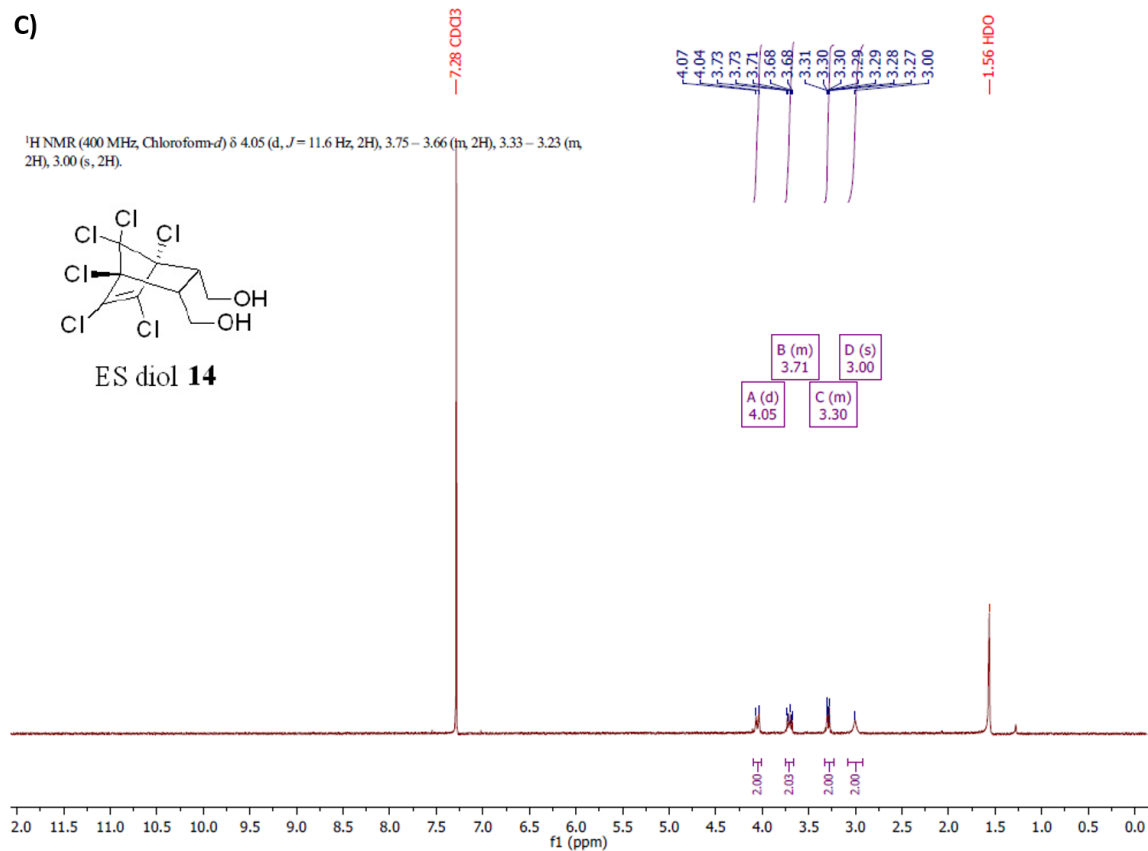
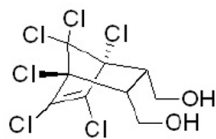


ES lactone **15**



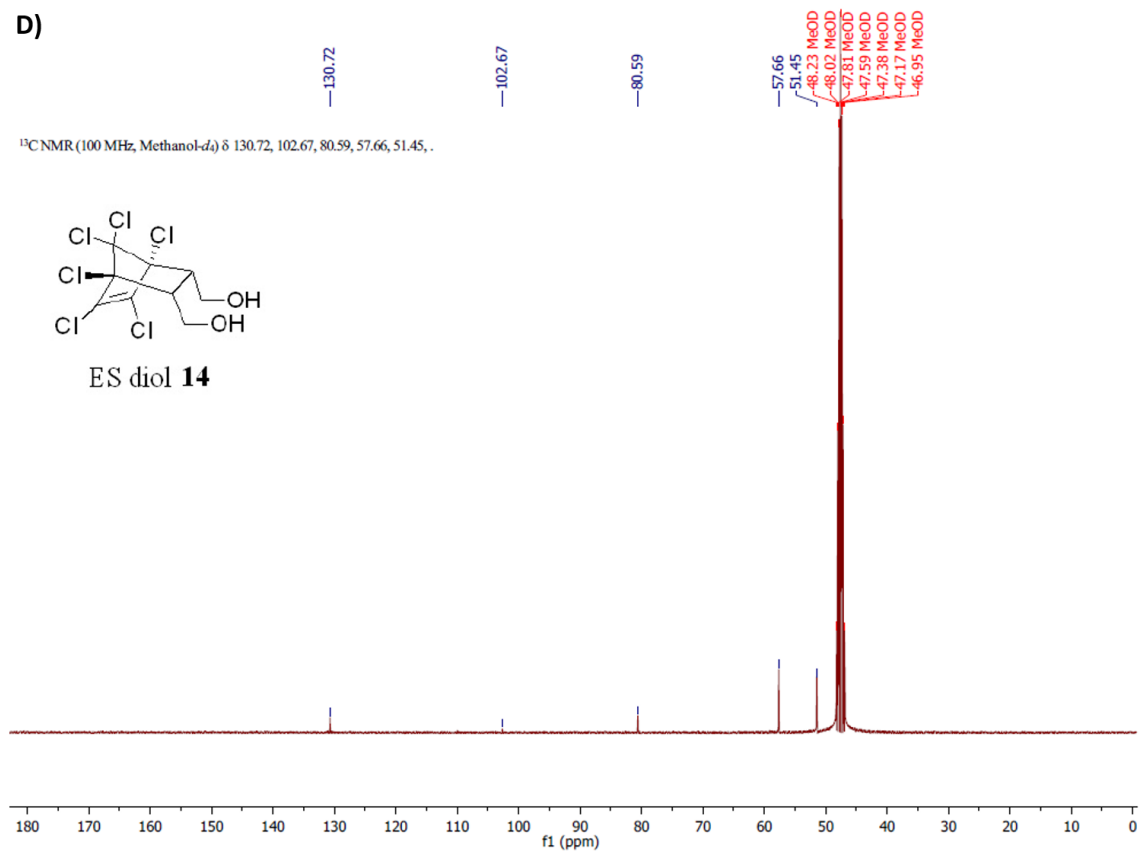
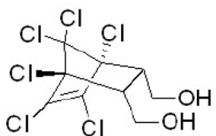
c)

¹H NMR (400 MHz, Chloroform-*d*) δ 4.05 (d, *J* = 11.6 Hz, 2H), 3.75 – 3.66 (m, 2H), 3.33 – 3.23 (m, 2H), 3.00 (s, 2H).



D)

¹³C NMR (100 MHz, Methanol-*d*₄) δ 130.72, 102.67, 80.59, 57.66, 51.45, .



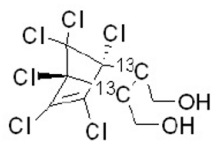
E)

^{13}C NMR (100 MHz, Chloroform-*d*) δ 51.61,

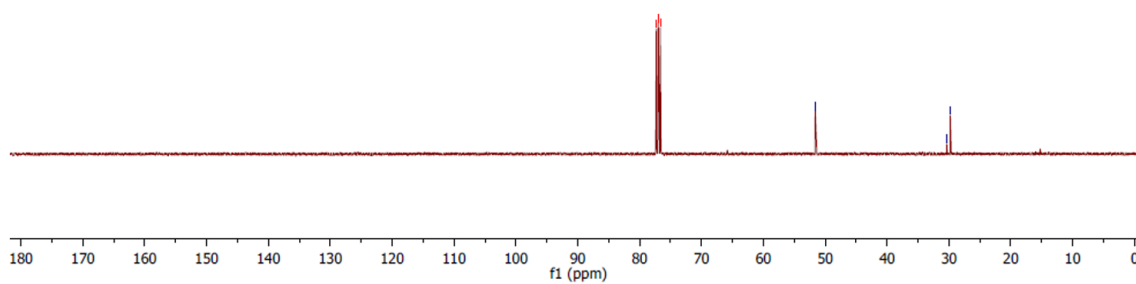
77.30 CDCl₃
76.98 CDCl₃
76.66 CDCl₃

— 51.61

30.33
29.77



^{13}C -ES diol



F)

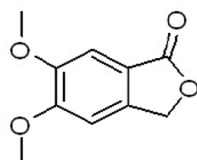
^1H NMR (400 MHz, Chloroform-*d*) δ 7.33 (s, 1H), 6.93 (s, 1H), 5.25 (s, 2H), 4.00 (s, 3H), 3.96 (s, 3H).

7.33
7.28 CDCl₃
6.93

— 5.25

4.00
3.96

— 1.61 H₂O



23

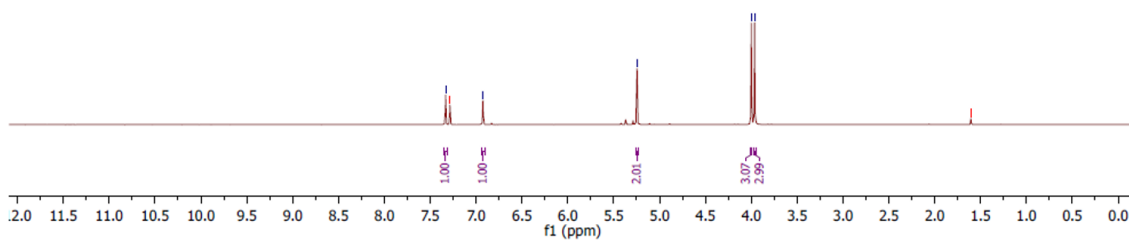
A (s)
7.33

B (s)
6.93

C (s)
5.25

D (s)
4.00

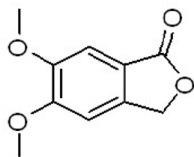
E (s)
3.96



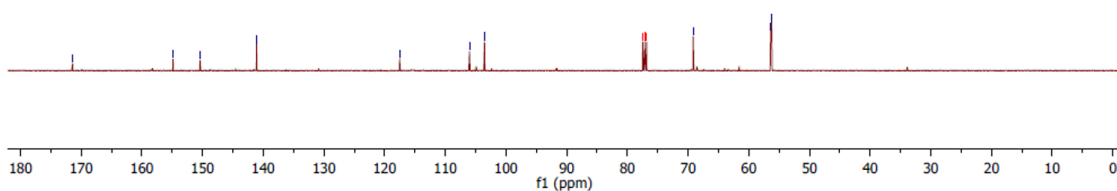
G)



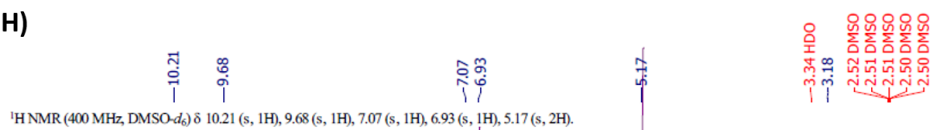
¹³C NMR (100 MHz, Chloroform-*d*) δ 171.39, 154.86, 150.40, 141.10, 117.52, 103.53, 69.15, 56.38, 56.23.



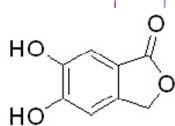
23



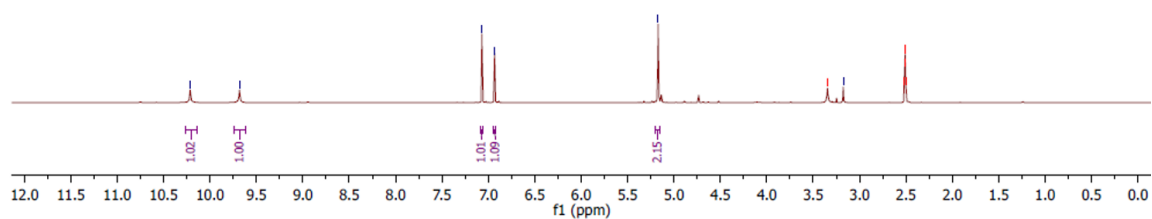
H)



¹H NMR (400 MHz, DMSO-*d*₆) δ 10.21 (s, 1H), 9.68 (s, 1H), 7.07 (s, 1H), 6.93 (s, 1H), 5.17 (s, 2H).



24



l)

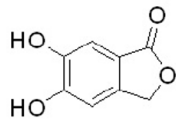
—171.33
—152.80
—147.17
—140.81

—115.87
—109.92
—108.66

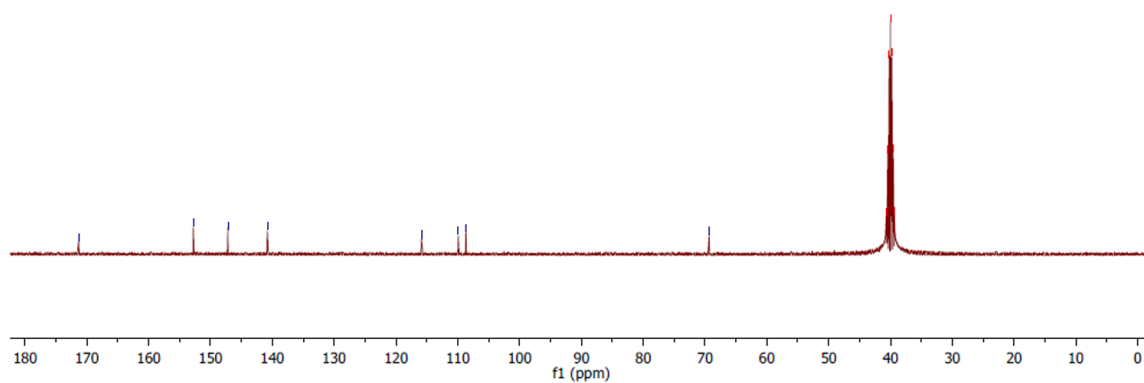
—69.34

40.62 DMSO
40.41 DMSO
40.21 DMSO
40.00 DMSO
39.79 DMSO
39.58 DMSO
39.37 DMSO

^{13}C NMR (100 MHz, $\text{DMSO-}d_6$) δ 69.34, 108.66, 109.92, 115.87, 140.81, 147.17, 152.80, 171.33.



24



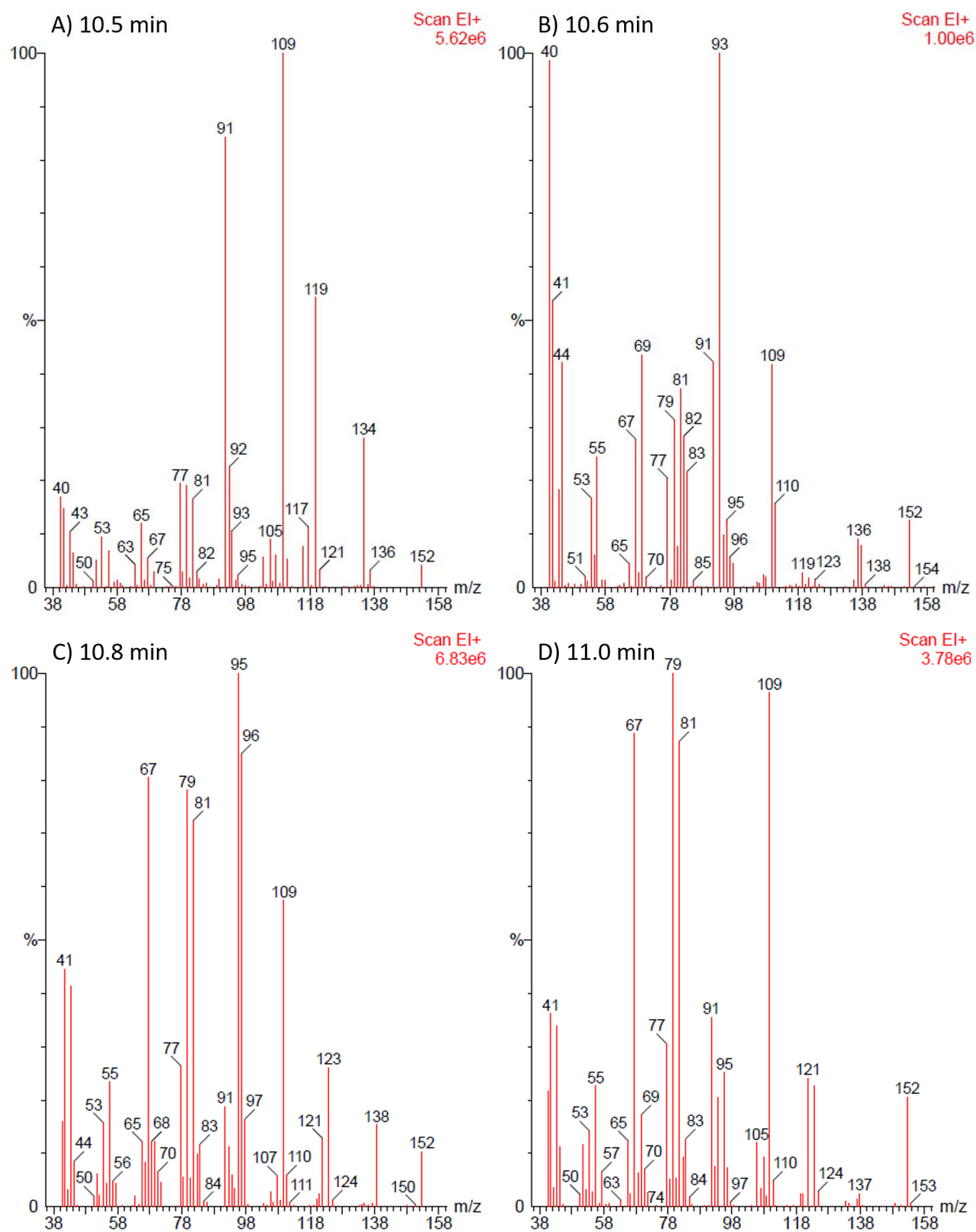
Appendix A21. NMR spectra of compounds synthesized in chapter 3.

Appendix B. Chapter 4 supplementary information

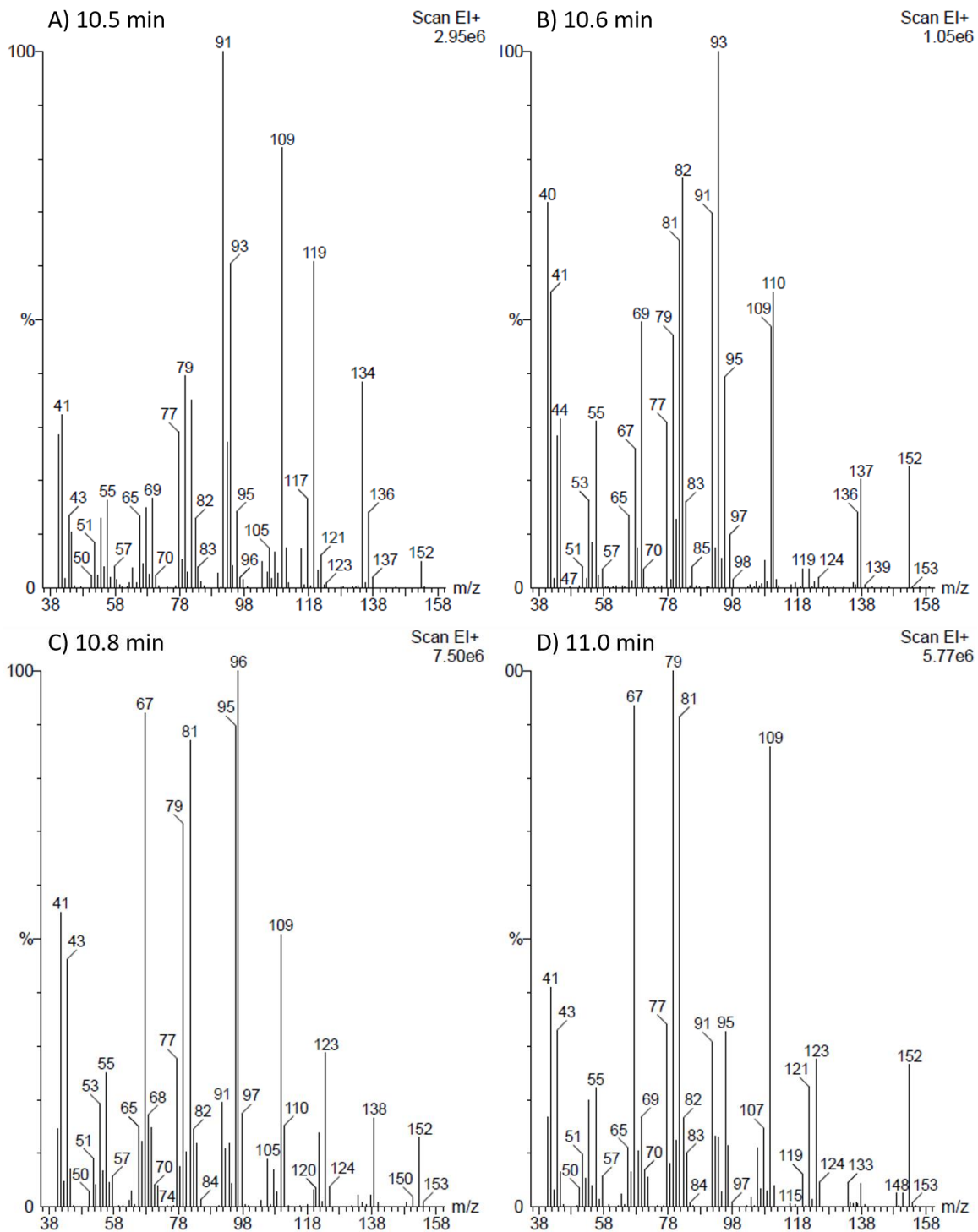
Oxidation of β -pinene to nopinone using KMnO_4

In general, oxidizing agent is added to a solution of β -pinene **21** (5.8 mmol) in mixture (100 ml) of CH_2Cl_2 and t-BuOH (9:1) or H_2O and t-BuOH (9:1). The mixture was stirred for 24 hours at room temperature. After 24 hours of stirring, 100 ml of water was added, and the mixture was filtered. The organic product was extracted using dichloromethane (3 \times 100 ml) and the organic layers was dried over Na_2SO_4 . The organic solvent was removed by distillation at 25 °C, giving an oily crude product as the residue. The crude product was purified using column chromatography (EtOAc: Hexanes 1:9), giving (+)-nopinone **27**.

In Table 4.1, for entry 1: KMnO_4 (4.4 g, 28 mmol) and alumina (17.6 g), entry 2: KMnO_4 (4.4 g, 28 mmol) and acidic alumina (17.6 g), and entry 3: NaIO_4 (5.1 g, 24 mmol) and KMnO_4 (0.2 g, 1.2 mmol) were used for oxidation of β -pinene **21**.



Appendix B1. Mass spectra of epoxidized products with peaks retention time: A) 10.5 min, B) 10.6 min, C) 10.8 min and D) 11.0 min from *in-vitro* assay of β -phellandrene oxidation using WT-P450_{cam} and *m*-CPBA.



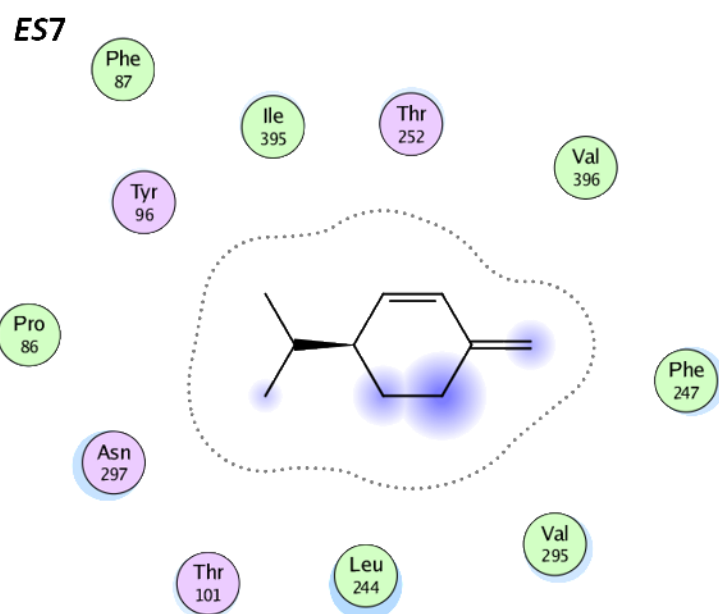
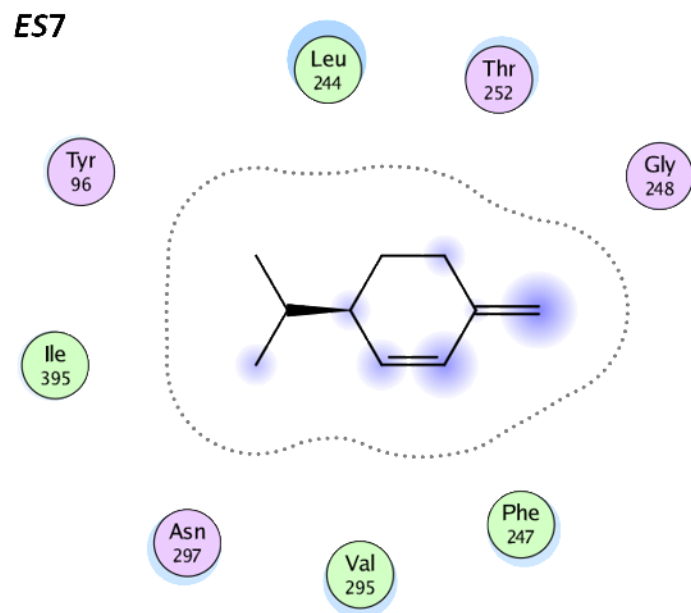
Appendix B2. Mass spectra of epoxidized products with peaks retention time: A) 10.5 min, B) 10.6 min, C) 10.8 min and D) 11.0 min from *in-vitro* assay of β -phellandrene oxidation using ES7-P450_{cam} and *m*-CPBA.

Appendix B3. Distance between heme-Fe to carbon atoms (C4, C5 and C6) from *in silico* docking of WT-P450_{cam} and β -phellandrene (22)

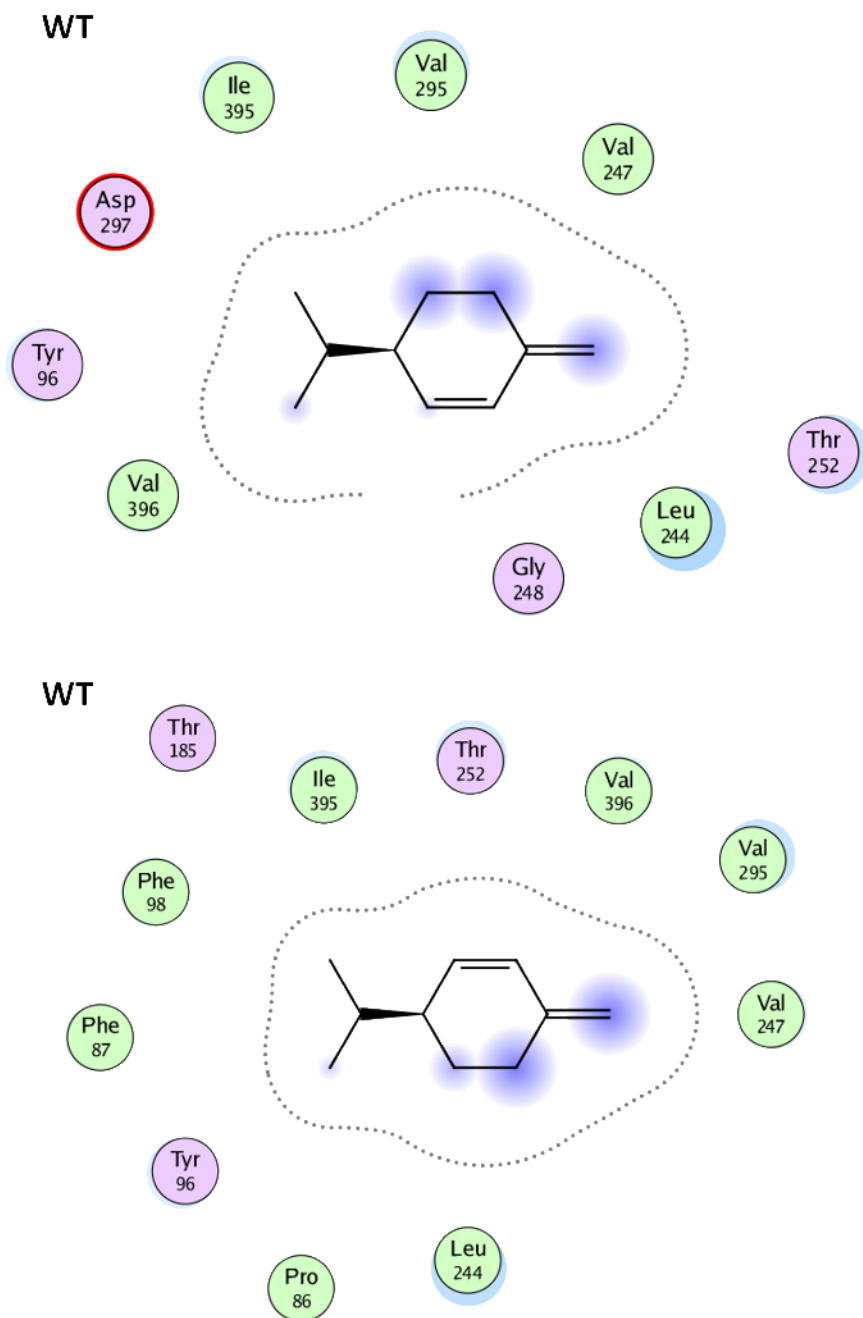
Distance (Å) between heme-Fe to (-)-R-22a				Distance (Å) between heme-Fe to (+)-S-22b			
Pose #	C4	C5	C6	Pose #	C4	C5	C6
1	8.26	7.67	6.72	18	7.87	6.80	7.15
2	7.49	7.84	8.28	19	8.58	7.05	6.72
3	6.25	6.44	7.82	20	5.44	6.89	7.64
4	8.43	7.25	5.98	21	8.45	6.93	6.79
5	8.45	8.00	6.92	22	8.66	7.16	6.54
6	9.31	7.92	7.61	23	6.65	7.78	7.61
7	8.95	8.07	8.10	24	9.58	8.66	7.18
8	4.99	6.42	7.42	25	8.62	7.31	7.88
9	8.42	8.08	7.25	26	8.74	8.64	7.57
10	9.34	7.91	7.57	27	8.84	7.65	6.34
11	8.06	6.78	6.40	28	9.29	7.83	7.07
12	8.93	7.57	7.92	29	8.81	8.42	7.35
13	8.79	7.39	7.79				
14	8.48	7.24	6.13				
15	8.26	7.19	6.03				
16	4.60	5.91	7.07				
17	8.75	7.71	6.27				
Ave.	7.99	7.38	7.13	Ave.	8.29	7.59	7.15
S.D.	1.40	0.65	0.76	S.D.	1.16	0.68	0.48
Min	4.60	5.91	5.98	Min	5.44	6.80	6.34
Max	9.34	8.08	8.28	Max	9.58	8.66	7.88

Appendix B4. Distance between heme-Fe to carbon atoms (C4, C5 and C6) from *in silico* docking of ES7 mutant P450_{cam} and β -phellandrene (22)

Distance (Å) between heme-Fe to (-)-R-22a				Distance (Å) between heme-Fe to (+)-S-22b			
Pose #	C4	C5	C6	Pose #	C4	C5	C6
1	7.63	6.3	5.78	11	8.43	7.21	5.92
2	8.07	6.57	6.57	12	6.70	7.21	7.73
3	5.21	6.19	7.52	13	5.64	6.22	7.61
4	4.77	6.21	7.19	14	4.68	5.80	6.87
5	8.71	7.65	6.58	15	7.77	6.48	6.23
6	4.91	6.28	7.39	16	8.20	6.73	6.17
7	7.52	6.4	5.43	17	5.50	6.32	7.08
8	5.87	7.02	7.02	18	5.11	5.71	6.56
9	4.36	5.81	6.08				
10	7.35	6.01	4.92				
Ave.	6.44	6.44	6.45	Ave.	6.50	6.46	6.77
S.D.	1.58	0.53	0.88	S.D.	1.48	0.57	0.67
Min	4.36	5.81	4.92	Min	4.68	5.71	5.92
Max	8.71	7.65	7.52	Max	8.43	7.21	7.73



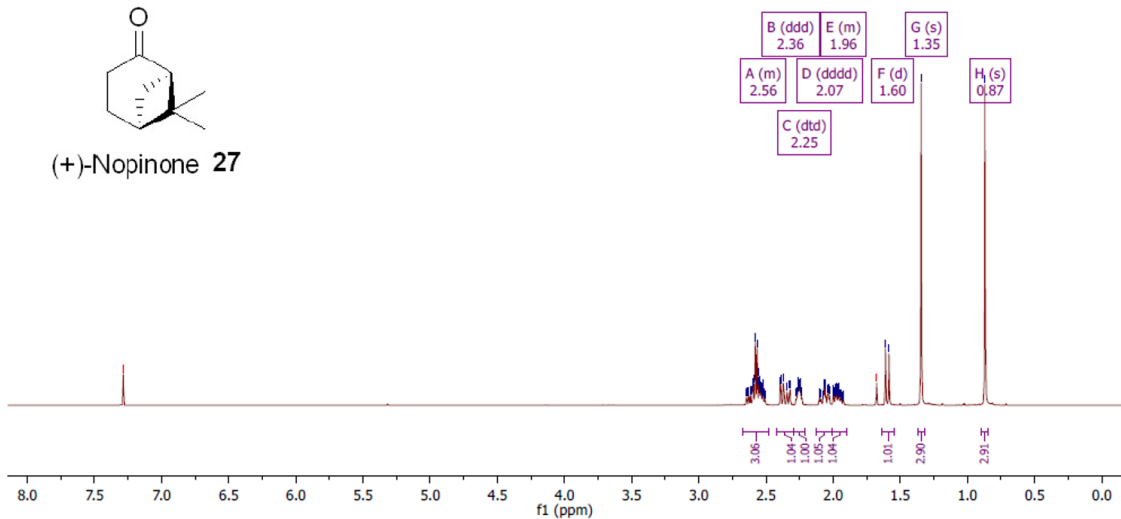
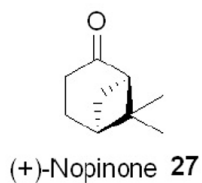
Appendix B5. Map of protein-ligand interactions of the binding pocket residues in contact with of (-)-*R*- β -phellandrene (22a, top) and (+)-*S*- β -phellandrene (22b, bottom) in *ES7*. Residues in purple are polar while residues in green are nonpolar, residues and ligand atoms with light blue clouds are exposed to the solvent environment.



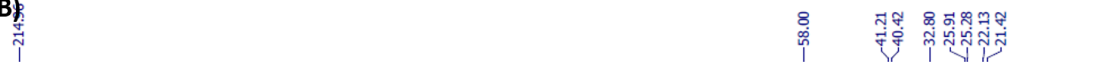
Appendix B6. Map of protein-ligand interactions of the binding pocket residues in contact with of (-)-*R*- β -phellandrene (22a, top) and (+)-*S*- β -phellandrene (22b, bottom) in WT-P450_{cam}. Residues in purple are polar while residues in green are nonpolar, residues and ligand atoms with light blue clouds are exposed to the solvent environment.



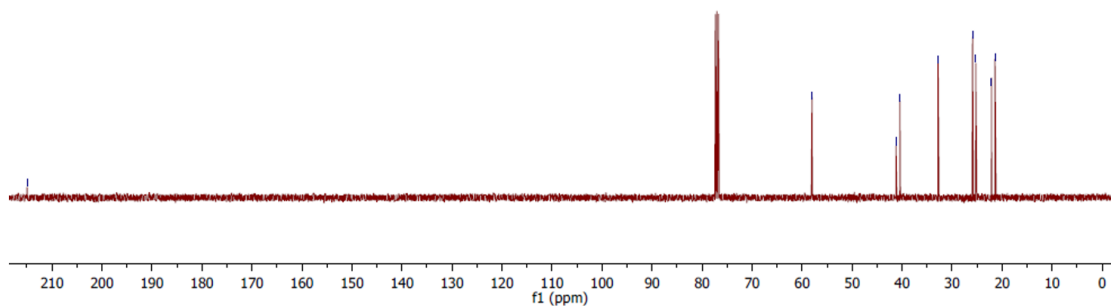
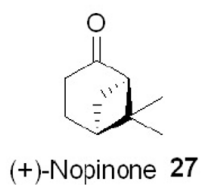
¹H NMR (400 MHz, Chloroform-*d*) δ 2.67–2.48 (m, 3H), 2.36 (ddd, *J* = 19.1, 9.1, 2.1 Hz, 1H), 2.25 (dtd, *J* = 6.2, 4.2, 2.1 Hz, 1H), 2.07 (dddd, *J* = 13.3, 11.1, 3.9, 2.1 Hz, 1H), 2.01–1.90 (m, 1H), 1.60 (d, *J* = 10.1 Hz, 1H), 1.35 (s, 3H), 0.87 (s, 3H).



B)

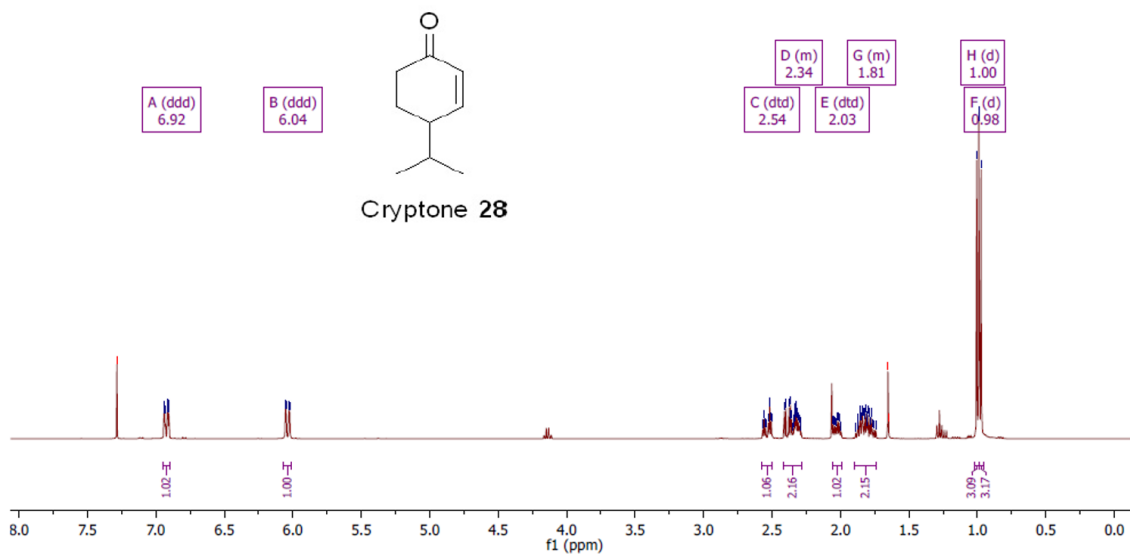


¹³C NMR (100 MHz, Chloroform-*d*) δ 214.96, 58.00, 41.21, 40.42, 32.80, 25.91, 25.28, 22.13, 21.42

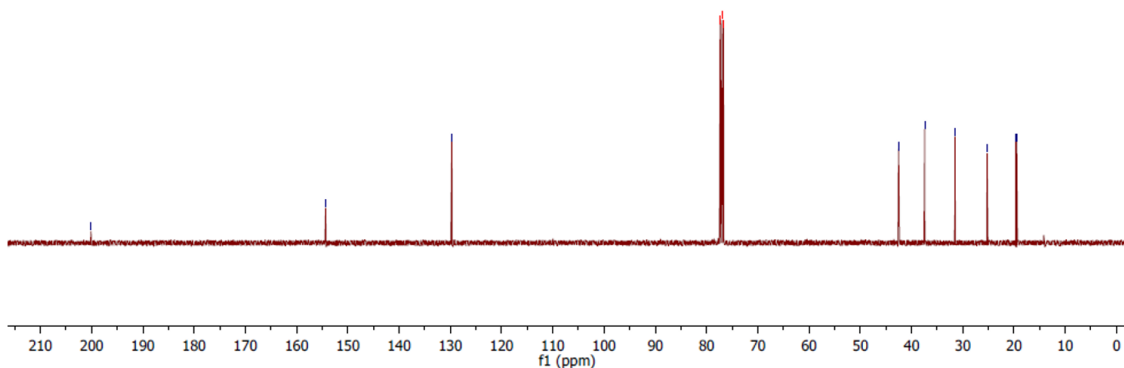
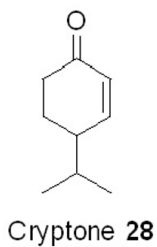


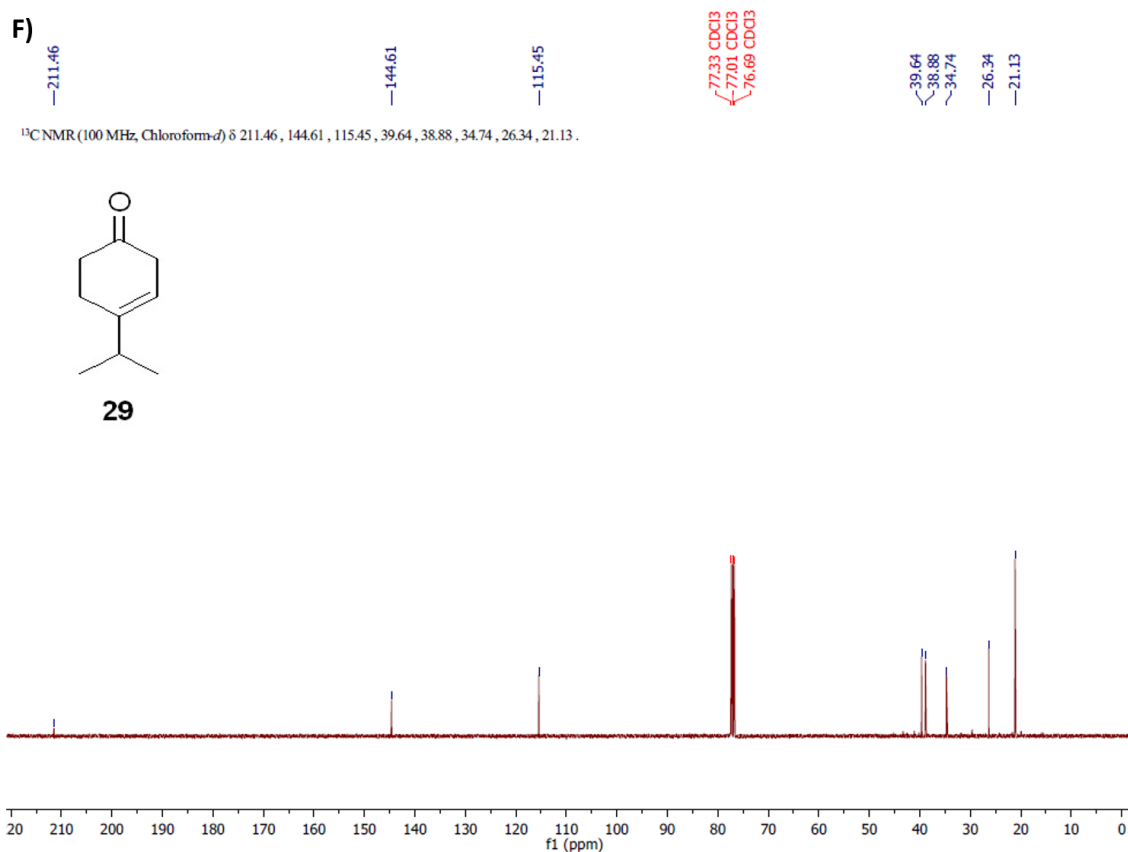
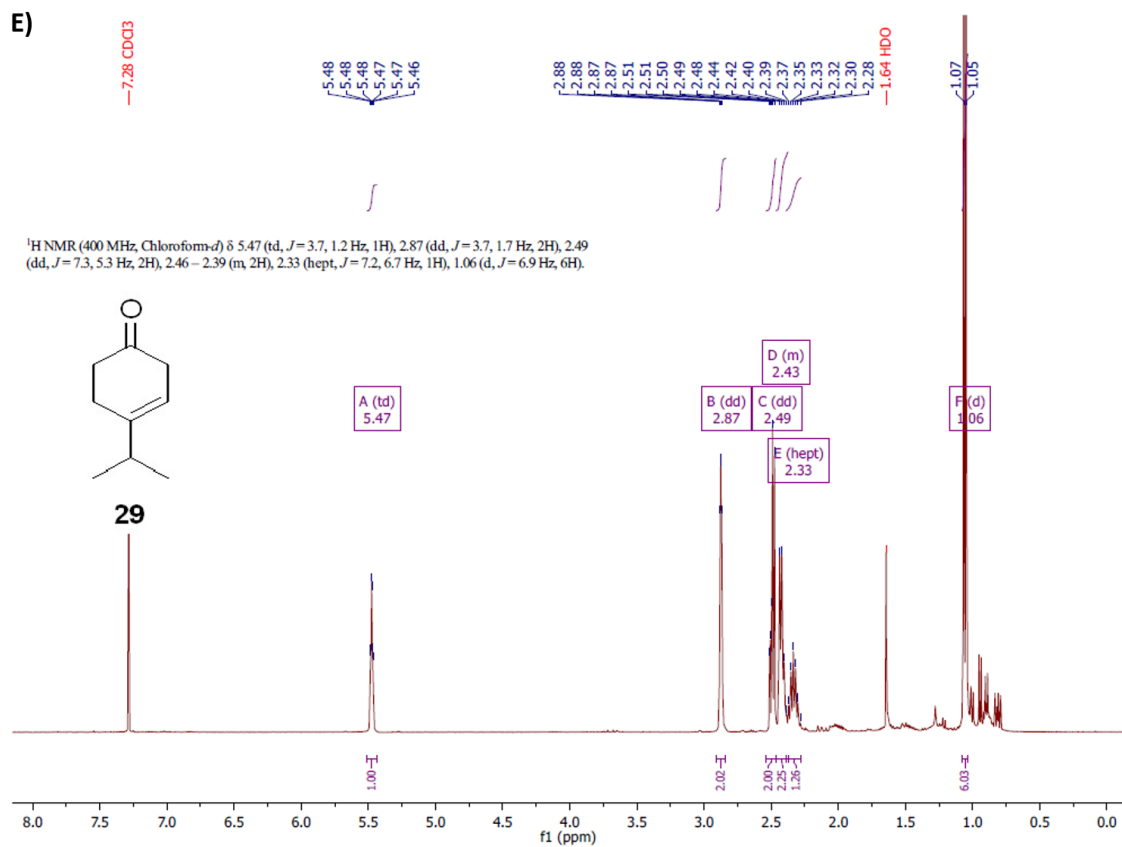


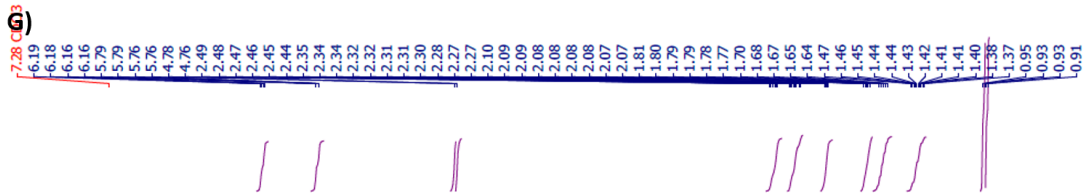
¹H NMR (400 MHz, Chloroform-*d*) δ 6.92 (ddd, *J* = 10.3, 2.4, 1.6 Hz, 1H), 6.04 (ddd, *J* = 10.3, 2.7, 1.0 Hz, 1H), 2.54 (dtd, *J* = 16.7, 4.3, 1.0 Hz, 1H), 2.42 – 2.28 (m, 2H), 2.03 (dtd, *J* = 13.7, 4.6, 1.6 Hz, 1H), 1.90 – 1.74 (m, 2H), 1.00 (d, *J* = 5.9 Hz, 3H), 0.98 (d, *J* = 5.9 Hz, 3H).



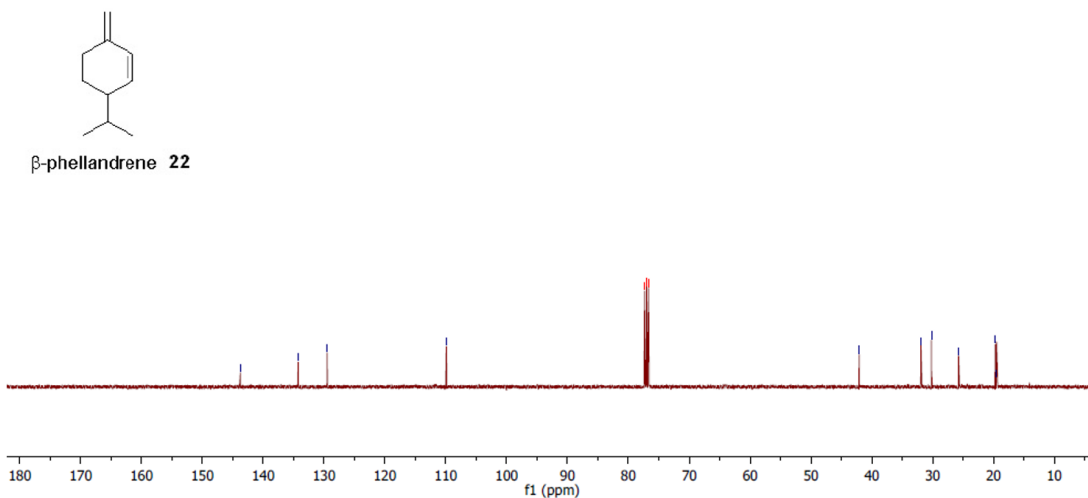
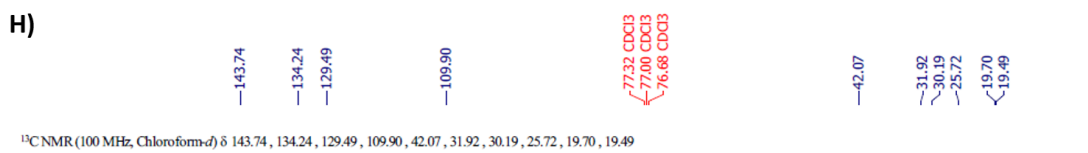
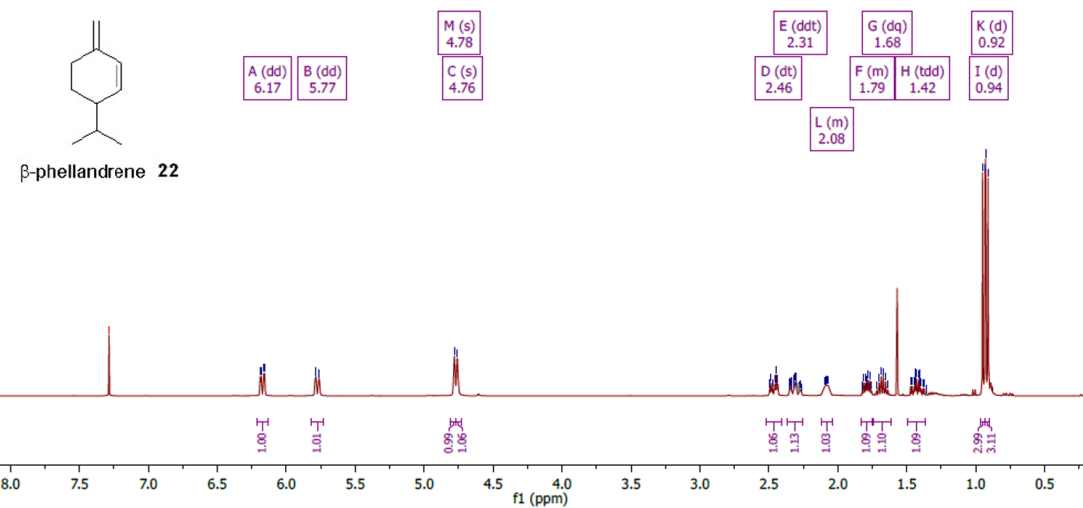
¹³C NMR (100 MHz, Chloroform-*d*) δ 200.11, 154.32, 129.70, 42.53, 37.42, 31.52, 25.27, 19.64, 19.48







¹H NMR (400 MHz, Chloroform-*d*) δ 0.92 (d, *J* = 6.8 Hz, 3H), 0.94 (d, *J* = 6.8 Hz, 3H), 1.42 (tdd, *J* = 12.6, 10.0, 3.8 Hz, 1H), 1.68 (dq, *J* = 13.7, 6.8 Hz, 1H), 1.75 – 1.83 (m, 1H), 2.04 – 2.12 (m, 1H), 2.31 (ddt, *J* = 17.0, 12.7, 2.1 Hz, 1H), 2.46 (dt, *J* = 15.0, 4.4 Hz, 1H), 4.76 (s, 1H), 4.78 (s, 1H), 5.77 (dd, *J* = 10.0, 1.3 Hz, 1H), 6.17 (dd, *J* = 10.0, 2.6 Hz, 1H).



Appendix B7. NMR spectra of compounds synthesized in chapter 4.